UTILIZATION OF BIO/ORGANIC PARTICLES TO PROBE

CELLULAR FUNCTION IN CANCER

By

RU WEN

(Under the Direction of Jin Xie)

ABSTRACT

The understanding of cellular function is essential to identify new targets for active cancer therapy. Natural and synthetic particles especially in nanoscale level have attracted immense interest for probing cellular mechanism and therapeutic intervention in cancer. A natural occurred biological nanoparticle–exosome–is a powerful tool to investigate the cellular function in cancer due to its unique biological properties. Exosomes are secreted from almost all cell types and play significant roles in cell-cell communication through translocation of incorporated components. Organic polymers have attracted great interest in synthetic particles due to the advantage of biodegradability, biocompatibility and controllable releasing payload. Biological and organic particles are used to investigate mechanistic pathways of protein acylation and cellular functions for cancer. Myristoylation promotes the encapsulation and translocation of oncogenic proteins (e.g., Src) through exosomes, which induces the apoptosis of recipient cells. Organic nanoparticles are able to induce the apoptosis of cancer cell by modulating the subcellular function. These findings provide new insights into design and development of nanoparticles for probing cellular function and identification of novel targets for cancer therapy.

INDEX WORDS: exosomes, nanoparticles, molecular mechanism, cellular function, cancer

UTILIZATION OF BIO/ORGANIC PARTICLES TO PROBE CELLULAR FUNCTION IN CANCER

By

RU WEN

B.E., Wuhan University, China, 2010

M.S., University of New South Wales, Australia, 2012

A Dissertation Submitted to the Graduate Faculty of The University of Georgia in Partial Fulfillment of the Requirements for the Degree

DOCTOR OF PHILOSOPHY

ATHENS, GEORGIA

2018

UTILIZATION OF BIO/ORGANIC PARTICLES TO PROBE CELLULAR FUNCTION IN CANCER

By

RU WEN

Approved:

Major Professor: Jin Xie

Committee: Houjian Cai
I. Jonathan Amster

Electronic version approved by:

Suzanne Barbour
Dean of Graduate School
The University of Georgia
May 2018

DEDICATION

To my family and friends

ACKNOWLEDGEMENTS

I strongly thank everyone, known and unknown, who offered me a hand during my pursuit of the Ph.D. degree in the last six years. I could not have gone through this program without the everyone's assistance. First, I would like to express my deepest appreciation to Dr. Houjian Cai who continuously provides me with tremendous academic support and wonderful chances to collaborate with other researchers. Without his guidance and persistent assistance, I would not be able to complete this dissertation.

I would like to thank Dr. Jin Xie for all the support and suggestions, for being my major professor when I came back to UGA as a graduate student and for providing me a chance to maintain my position. Profound gratitude goes to my committee member, Dr. Jon Amster, who has been a truly dedicated professor and helps me go through hardship in mentorship change and back to UGA as a graduate student, supporting my career goals.

I would also like to thank my previous advisors, Dr. Marcus Lay and Dr. Shanta Dhar, who provided the mentorship and professional guidance for two years or more. I thank previous committee member Dr. Tina Salguero who gave me a lot of constructive suggestions in the qualification exam. Special thanks are given to Dr. John Stickney who supported me so much with useful suggestions and advice when I got lost on the road.

I am grateful to all of those with whom I collaborate or work on research projects. I am hugely appreciative of Dr. Qianjin Li, Dr. Sunjin Kim, Dr. Yongjie Ma, Dr. Rakesh Pathak, Dr. Bhabatosh Banik, Dr. Basu Uttara. I also thank lab members Omar Awad Alsaidan, Maria Luisa Valle, Xiaohan Zhang, Junyi Li, Essilvo Sulejmani, and Xiaofei Tan and previous member Dr.

Huifeng Shen for their support and assistance. I especially thank Peter Lee who provided continuous assistance in grammar editing and revision. I would also thank Dr. Yutao Liu and Michelle Drewry from August University for characterization of exosomes, and thank July Nelson for helping in the flow cytometry.

I would like to thank my dear friends Dehui Kong, Yan Zhou, Yuan Wang, Wanying Li, Dr. Nhat Quach, Tong Zhang, Lige Zhao, Dr. Geoffrey Wang, Gusheng Zhang, who cheer and inspire me when I get frustrated and down in the mood, and who have generously offered me shelter during my transition, continuously support and encourage me in science. I thank Afoma Umeano very much for all of her support in my life, whether it be cheering me up emotionally, or assisting me with grammar editing, I learned a lot from her.

I would like to extend my gratefulness to the many people who generously assist me tremendously in the graduate studies. Special thanks go to Lauren Hutchison, Lauren Bowman, Dr. Gregory Robinson, Sevgi Ural, and Charles Lowman, they provided me great assistance during the administration processes. I also thank Kistie Manders, Kristie Huff, and Leslie Standridge. They provided great support and excellent professional assistance to me regarding lab/chemical orders and financial/accounting processing. I am grateful to Genet Kibreab who assisted me in the room booking for group or special meetings.

I am very grateful to the University of Georgia for allowing me to pursue the Ph.D. degree by providing wonderful resources and strong academic atmosphere in Athens.

Finally, I would like to especially thank my family for their continuously unbelievable support, and I dedicate this dissertation to them.

TABLE OF CONTENTS

LIST OF TABLES

LIST OF FIGURES

Figure 3.1 The enrichment of myristoylated proteins in exosomes. (A) The number of total proteins and myristoylated proteins in exosomes from 60 cancer cells and normal tissues including thymuc, breat milk, and urine [37-42]. There are 182 myristoylated proteins in a mammalian cell with about 20,000 of total proteins. The number of myristoylated proteins account for 0.9% of the mammalian genome. (B) Frequency of myristoylated proteins in 60 cancer cell lines[37]. The red line represents the 0.9% of myristoylated proteins in the mammalian genome. (C) The size, zeta potential and particle concentration of exosomes. DU145, PC-3, 22Rv1 and LNCaP cells were cultured in medium containing exosome-free FBS for 24 h at 37ºC in 5% CO_2. Exosomes were isolated in the conditioned medium by ultracentrifugation method (D) Expression levels of Src kinase, calnexin, GAPDH and CD9 in the exosomes (Exo) and total cell lysates (TCL) were determined by Western blot analysis. The same amount of protein (10 µg) from the exosomes (Exo) or total cell lysate (TCL) were loaded as determined by DC protein assay. The enrichment of Src protein was evaluated by the ratio of Src protein level

1. INTRODUCTION

Cancer is one of the leading causes of death in the world, and new cases of cancer have been diagnosed each year[1, 2]. With the development of various strategies including surgery, chemotherapy, immunotherapy, hormone therapy, radiotherapy or their combinations[3-6], patients with cancer are able to prolong their lifetime and improve the quality of life[7-9]. For example, the use of bevacizumab together with cisplatin–paclitaxel combination chemotherapy significantly improved the survival rate in advanced cervical cancer with about 3.7 months' improvement in patients[10].

The cytotoxic chemotherapy may cause the side effects to the body system. Doxorubicin has long been used in cancer therapy but it turns out to induce cardiomyopathy[11]. Cancer patients are found to be resistant to chemotherapy due to long-term exposure to drugs. Cisplatin is notably used in cancer therapy in the last four decades, and acquired cisplatin-resistance in cancer cells reduces the therapeutic efficacy and becomes a major barrier to combat cancer[12, 13]. The wide usage of tyrosine kinase inhibitors for patients with non–small cell lung cancers (NSCLCs) eventually leads to the development of acquired resistance within 1-2 year[14]. The development of novel strategies is necessary and targeted therapy has shown substantial improvement in cancer therapy[15]. To solve these issues, the understanding of cellular functions is essential by identifying new targets with fundamental mechanisms for active cancer therapy.

Natural and synthetic particles especially in nanoscale level have been attracted immense interest for probing cellular mechanism and therapeutic intervention in cancer. Nanosized particles are initially considered as particles with a size range of 1-100 nm, now it is

commonly defined as any size up to submicron (<1000 nm) [16, 17]. Nanoparticle has been widely used in the multiple fields spanning across physics, material science, engineering, biology, and chemistry. Specifically, nanoparticles have attracted great interest as delivery systems for therapeutics and imaging contrast agents in the biomedical field[18]. The types of nanoparticles can be of various formulations, including polymeric nanoparticles, liposomes, dendrimers, micelles, metal (e.g., Au) or metal oxide (e.g., CeO_2) nanoparticles, carbon nanotube, biological nanoparticles (e.g., exosomes) and viral nanoparticles[19]. Nanoparticles can also be made of both organic molecules (e.g., surrounding shells) and inorganic materials (e.g., core material)[20].

Nanoparticle-based therapeutics are designed to improve the therapeutic efficacy and minimize the side effect, and have shown clinical significance in these aspects[16]. Some nanoparticle systems have been approved for use in clinical settings, and a few nanoparticles are clinically approved to selectively target cancer cells[21]. Doxil is the first FDA-approved nanoparticle drug system for cancer therapy, and it mitigates cardiotoxicity and associated sequelae caused from free agent, doxorubicin [22].

Nanoparticles can be used to selectively image tumors and associated surrounding metastases when conjugated with targeting moieties[23]. Iodine-131-doped CuS nanoparticles (CuS/[131I]I) were modified with polyethylene glycol (PEG) for radiotherapy (RT) and photothermal therapy (PTT) by taking advantage of doped 131I-radioactivity and high near-infrared absorbance, respectively. The combination therapy of CuS/[131I]I-PEG nanoparticles showed remarkable synergistic therapeutic effects for treatment of tumors as well as providing tumor imaging guide for surgical resection of primary tumors[24]. Nanoparticles also find their applications in diagnosis of cancer. Magnetic nanoparticles are a major class of nanomaterials used for magnetic

resonance imaging (MRI) for cancer diagnosis in addition to drug delivery and hyperthermia due to their unique physical/chemical/magnetic properties and biocompatibility[25]. Targeted superparamagnetic iron oxide (SPIO) nanoparticles constructed by incorporation with anti-EGFR monoclonal antibody showed synergistically enhanced therapeutic effects for lung cancer with the capacity to noninvasively monitor the therapeutic efficacy in rat models simultaneously[26]. Gd-metallofullerene (Gd/C80) nanoparticles were successfully used for noninvasive MRI detection of tumor in a mouse model at a low concentration when conjugated with cytokine interleukin-13 for effective targeting glioblastoma multiforme (GBM) cells[27].

1.1 THE USE OF EXOSOMES TO PROBE CELLULAR MECHANISM

A few studies have been conducted on the utilization of nanotechnology tools for investigating the molecular mechanism in cancer. Exosome, a biological nanoparticle, is of particular interest in this aspect due to its unique properties in cell-cell communication. Exosomes derived from pancreatic lesions are reported to prime liver pre-metastatic niche formation and metastasis. The exosomal migration inhibitory factor (MIF) is responsible for this initiation by promoting the generation of transforming growth factor β (TGFβ), which induces fibronectin (FN) providing the niche for accumulation of bone marrow-derived macrophages and neutrophils. MIF is reported to be highly expressed in serum exosomes derived from pancreatic cancer implanted mouse model or pancreatic ductal adenocarcinomas patients with progressed post-diagnosis, and knockdown of MIF significantly prevented the pre-metastatic niche formation and metastasis in a mouse model[28]. The RNAs in tumor exosomes are demonstrated to promote lung pre-metastatic niche formation through activating Toll-like receptor 3 (TLR3) pathway for subsequent chemokine secretion induction and neutrophil recruitment in the lung. When the lung tumor exosomes were incubated with AT-II and MLE-12 cells, the expression of Tlr3 and

chemokine gene were significantly upregulated, and chemokines expression were dramatically decreased when depleting Tlr3 in cells[29]. More details about exosomes regarding their biogenesis, uptake and biomarker application will be illustrated in chapter 2.

1.2 THE APPLICATION OF ORGANIC NANOPARTICLES

Organic nanoparticles, such as liposomes and polymeric nanoparticles, have been widely used as delivery systems and have shown great therapeutic potential for cancer. Both biodegradable and non-degradable polymers can be used to construct nanoparticle systems. Biodegradable polymers are attracted great interest due to its biocompatibility, biodegradability, non-toxicity and bioactivity with controllable payload release after degradation in the human body's system. The commonly used biodegradable polymers are polyethylene glycol (PEG), polylactic acid (PLA), and poly(D,L-lactic-co-glycolic acid) (PLGA), poly (ε-caprolactone) (PCL), which are well-known FDA approved polymers and can be metabolically degraded in the physiological environment[30].

PLGA is a copolymer constructed by PLA and poly glycolic acid (PGA) and is widely used as delivery system due to high performance and bioactivity[31]. The solubility of PLGA in aqueous solution can be modified by tuning nature properties, such as composition (e.g., ratio of PLA: PGA), and molecular weight;, and introduction of external components (e.g., such as PEG) or modifiers (e.g., like antacids) [32]. Chitosan-modified PLGA (C-PLGA) nanoparticles are reported to deliver paclitaxel (PTX) for enhanced cellular uptake and effective therapeutic intervention. The enhanced cellular uptake was confirmed by strong fluorescence intensity with coumarin 6 as a probe in A549 cells and CT-26 cells, and tumor tissues through electrostatic interaction of nanoparticles-cellular membranes. The PTX loaded C-PLGA nanoparticles were

much more toxic at acidic lower pH (pH 6) physiological environment compared to higher pH (pH 7-8) microenvironment[33].

PEG is a hydrophilic polymer with the capability to prevent the particle aggregation and decrease the interaction with opsonin to avoid rapid reticuloendothelial system (RES) clearance. Low molar mass PEG (20-50 kDa) is usually used for the deliver small molecules, oligonucleotides, and siRNA by conjugation. PEG with a molecular mass of 1-5 kDa can be used to deliver large drugs such as antibodies[34]. PEGylation is commonly used to enhance the properties of other biopolymers in terms of achieving long circulation, reducing nanoparticle aggregation, RES/kidney clearance and proteolytic degradation, enhancing retention time and stability of therapeutics and solubility in body system[35, 36]. The di-block copolymer PLGA–PEG is developed by taking advantage of unique properties of individual PLGA and PEG polymers, and has been widely used as delivery carriers. Doxorubicin (DOX) was chemically attached to PLGA-PEG through amine group. The polymeric DOX-PLGA-PEG micelles demonstrated more sustainable DOX release profile with high loading and encapsulation efficiency compared to PEG–PLGA micelles with DOX physically incorporated. *In vitro* studies showed that DOX-PLGA-PEG micelles had higher cellular uptake and were more toxic to HepG2 cells than free doxorubicin[37]. PLGA-PEG nanoparticles were prepared by a nanoprecipitation method, of which drug–polymer organic solution (water miscible) was added into water and self-assembled nanoparticles were recovered by centrifuge-wash steps. Nanoparticles with a size of 100-200 nm could be made by controlling the experimental parameters such as organic solvents (e.g., acetone, acetonitrile), ratio of organic solvent: water, concentration of polymers or drugs, and purification step[38].

However, PEGylation may block cellular uptake and prevent endosomal escape. Several approaches have been proposed to overcome this issue. Active targeting is one of such strategies to improve the selectivity, binding and uptake of the polymeric nanoparticles. The PEGylated nanoparticles can be modified by ligands such as proteins, antibodies or its fragments, aptamers or receptors. DNA aptamer AS1411 (Ap) is reported as targeting ligand to facilitate the delivery paclitaxel (PTX) in PEG–PLGA nanoparticles. The incorporation of Ap significantly enhanced cellular uptake of nanoparticles by C6 glioma cells through Ap-nucleolin interaction. The Ap-PTX-PLGA-PEG nanoparticle (Ap-PTX-NP) was in uniform size of ~150 nm with a negative zeta potential of −30 mV, and significantly enhanced its cytotoxicity of PTX at low concentration. *In vivo* studies in mouse bearing C6 glioma xenografts demonstrated the prolonged circulation and enhanced delivery of PTX to tumor site, attributing to greater tumor inhibition compared to PTX-NP and/or Taxol[39]. Copolymer PEG-PLA is able to encapsulate salinomycin (SAL), a selective agent that could both target and eradicate cancer cells, for pancreatic cancer and PEG-PLA micelles did not affect cytotoxicity to normal and tumor cells[40].

Targeted polymeric nanoparticles can be constructed with targeting moieties specifically to cancer tissues, cells, or cellular organelles to deliver chemotherapies with enhanced delivery efficiency and improved therapeutic efficacy in a low concentration by reducing the side effects[41]. Organelle-specific targeting has been attracted great interest since therapeutics directly acts at organelles to modify their function through precise localization with targeting moieties. The nucleus is critical for cellular function and metabolism, and it controls gene expression and replication. Nucleus is recognized as one of the important targets for cancer. N-(2-hydroxypropyl) methacrylamide (HPMA) copolymer is reported to deliver therapeutic

compound H1 peptide into nucleus through conjugating with nuclear transport subunits by a glycylphenylalanylleucylglycine linker. Targeting peptide R8NLS was also incorporated to facilitate cellular penetration and internalization. The targeted HPMA showed dramatically higher drug accumulation (e.g., 50-fold more) in nucleus compared to non-targeted conjugates in both *in vitro* and *in vivo*[42]. The mitochondrion is known as cellular power house of cells due to its vital role in generating ATP; mitochondria play significant roles in cellular hemostasis and metabolism[43-45]. Lipophilic cations such as triphenylphosphonium (TPP) can be used to deliver therapeutics to mitochondria through an electrochemical gradient provided by a large mitochondrial membrane potential (-150-180 mV)[46]. The copolymer PLGA-PEG is capable of precisely targeting cancer mitochondria for drug delivery when conjugated with TPP cation.

In this dissertation, two sets of nanoparticles will be discussed in detail regarding their potential in probing molecular mechanism in cancer and possible therapeutic intervention. The biological nanoparticle exosomes will be discussed in Chapter 2 and 3, in which Chapter 2 will summarize the biogenesis and uptake mechanism of exosomes, as well as experimental techniques regarding their isolation, purification and characterization, and finally, their potential application as biomarkers for cancer diagnosis and prognosis will also be evaluated. Chapter 3 reveals the mechanistic pathway of oncogenic Src protein accumulation into secreted exosomes and its translocation from tumor cells to recipient cells by exosome causing apoptotic signaling. Chapter 4 studies the cellular mechanism of anticancer drug α-tocopheryl succinate (α-TOS) for inducing apoptosis of cancer cells when delivered in a polymeric nanoparticle formulation. Polymeric nanoparticles are formulated with biocompatible and biodegradable PLGA-*b*-PEG copolymers and modified with a targeting ligand triphenylphosphonium (TPP) cation recognizing the mitochondria in cancer cells by taking advantage of negative membrane potential.

The α-TOS loaded polymeric nanoparticles show significant therapeutic efficacy *in vitro* and mechanistic studies indicate that targeted α-TOS nanoparticles upregulated the complex V activity in mitochondria to induce the apoptosis of cancer cells. Finally, future directions will be discussed regarding to development of nanoparticles as probing tools to reveal mechanistic pathways in cancer development and therapies.

1.3 REFERENCES

1. Siegel, R.L., K.D. Miller, and A. Jemal, Cancer statistics, 2016. CA Cancer J Clin, 2016. 66(1): p. 7-30.
2. Chen, W., R. Zheng, P.D. Baade, S. Zhang, H. Zeng, F. Bray, A. Jemal, X.Q. Yu, and J. He, Cancer statistics in China, 2015. CA Cancer J Clin, 2016. 66(2): p. 115-132.
3. Wen, R. and S. Dhar, Turn up the cellular power generator with vitamin E analogue formulation. Chem Sci, 2016. 7(8): p. 5559-5567.
4. Park, E.J., M.S. Cho, S.J. Baek, H. Hur, B.S. Min, S.H. Baik, K.Y. Lee, and N.K. Kim, Long-term oncologic outcomes of robotic low anterior resection for rectal cancer: a comparative study with laparoscopic surgery. Annals of surgery, 2015. 261(1): p. 129-137.
5. Lutkenhaus, L.J., J. Visser, R. de Jong, M.C. Hulshof, and A. Bel, Evaluation of delivered dose for a clinical daily adaptive plan selection strategy for bladder cancer radiotherapy. Radiother Oncol, 2015. 116(1): p. 51-56.
6. Nicholas, G.A., J.R. Goffin, S.A. Laurie, A.G. Robinson, G.D. Goss, M.N. Reaume, M. Mates, P. Wheatley-Price, P.M. Ellis, and R.A. Juergens, A phase Ib study of selumetinib in patients (pts) with previously untreated metastatic Non-Small Cell Lung Cancer (NSCLC) receiving standard chemotherapy: NCIC Clinical Trials Group IND. 215. NCT01783197. 2015, American Society of Clinical Oncology.
7. Miller, K.D., R.L. Siegel, C.C. Lin, A.B. Mariotto, J.L. Kramer, J.H. Rowland, K.D. Stein, R. Alteri, and A. Jemal, Cancer treatment and survivorship statistics, 2016. CA Cancer J Clin, 2016. 66(4): p. 271-289.
8. Eggermont, A.M., V. Chiarion-Sileni, J.-J. Grob, R. Dummer, J.D. Wolchok, H. Schmidt, O. Hamid, C. Robert, P.A. Ascierto, and J.M. Richards, Prolonged survival in stage III melanoma with ipilimumab adjuvant therapy. N Engl J Med, 2016. 375(19): p. 1845-1855.
9. Li, X., M.A. Truty, Y.a. Kang, X. Chopin-Laly, R. Zhang, D. Roife, D. Chatterjee, E. Lin, R.M. Thomas, and H. Wang, Extracellular lumican inhibits pancreatic cancer cell growth and is associated with prolonged survival after surgery. Clinical Cancer Research, 2014. 20(24): p. 6529-6540.
10. Tewari, K.S., M.W. Sill, H.J. Long III, R.T. Penson, H. Huang, L.M. Ramondetta, L.M. Landrum, A. Oaknin, T.J. Reid, and M.M. Leitao, Improved survival with bevacizumab in advanced cervical cancer. N Engl J Med, 2014. 370(8): p. 734-743.
11. Chatterjee, K., J. Zhang, N. Honbo, and J.S. Karliner, Doxorubicin cardiomyopathy. Cardiology, 2010. 115(2): p. 155-162.
12. Galluzzi, L., I. Vitale, J. Michels, C. Brenner, G. Szabadkai, A. Harel-Bellan, M. Castedo, and G. Kroemer, Systems biology of cisplatin resistance: past, present and future. Cell Death Dis, 2014. 5(5): p. e1257.
13. Amable, L., Cisplatin resistance and opportunities for precision medicine. Pharmacol Res, 2016. 106: p. 27-36.
14. Crystal, A.S., A.T. Shaw, L.V. Sequist, L. Friboulet, M.J. Niederst, E.L. Lockerman, R.L. Frias, J.F. Gainor, A. Amzallag, and P. Greninger, Patient-derived models of acquired resistance can identify effective drug combinations for cancer. Science, 2014. 346(6216): p. 1480-1486.

15. Hirsch, F.R., K. Suda, J. Wiens, and P.A. Bunn Jr, New and emerging targeted treatments in advanced non-small-cell lung cancer. The Lancet, 2016. 388(10048): p. 1012-1024.
16. Davis, M.E. and D.M. Shin, Nanoparticle therapeutics: an emerging treatment modality for cancer. Nat Rev Drug Discov, 2008. 7(9): p. 771-782.
17. Brigger, I., C. Dubernet, and P. Couvreur, Nanoparticles in cancer therapy and diagnosis. Adv Drug Deliver Rev, 2002. 54(5): p. 631-651.
18. Ferrari, M., Cancer nanotechnology: opportunities and challenges. Nat Rev Cancer, 2005. 5(3): p. 161-171.
19. Byrne, J.D., T. Betancourt, and L. Brannon-Peppas, Active targeting schemes for nanoparticle systems in cancer therapeutics. Adv Drug Deliver Rev, 2008. 60(15): p. 1615-1626.
20. Haley, B. and E. Frenkel. Nanoparticles for drug delivery in cancer treatment. in Urologic Oncology: Seminars and original investigations. 2008. Elsevier.
21. Peer, D., J.M. Karp, S. Hong, O.C. Farokhzad, R. Margalit, and R. Langer, Nanocarriers as an emerging platform for cancer therapy. Nat Nanotechnol, 2007. 2(12): p. 751-760.
22. Barenholz, Y.C., Doxil®—the first FDA-approved nano-drug: lessons learned. J Control Rel, 2012. 160(2): p. 117-134.
23. Yezhelyev, M.V., X. Gao, Y. Xing, A. Al-Hajj, S. Nie, and R.M. O'Regan, Emerging use of nanoparticles in diagnosis and treatment of breast cancer. Lancet Oncol, 2006. 7(8): p. 657-667.
24. Yi, X., K. Yang, C. Liang, X. Zhong, P. Ning, G. Song, D. Wang, C. Ge, C. Chen, and Z. Chai, Imaging-Guided Combined Photothermal and Radiotherapy to Treat Subcutaneous and Metastatic Tumors Using Iodine-131-Doped Copper Sulfide Nanoparticles. Adv Funct Mater, 2015. 25(29): p. 4689-4699.
25. Lima-Tenório, M.K., E.A.G. Pineda, N.M. Ahmad, H. Fessi, and A. Elaissari, Magnetic nanoparticles: In vivo cancer diagnosis and therapy. Int J Pharm, 2015. 493(1-2): p. 313-327.
26. Wang, Z., R. Qiao, N. Tang, Z. Lu, H. Wang, Z. Zhang, X. Xue, Z. Huang, S. Zhang, and G. Zhang, Active targeting theranostic iron oxide nanoparticles for MRI and magnetic resonance-guided focused ultrasound ablation of lung cancer. Biomaterials, 2017. 127: p. 25-35.
27. Li, T., S. Murphy, B. Kiselev, K.S. Bakshi, J. Zhang, A. Eltahir, Y. Zhang, Y. Chen, J. Zhu, and R.M. Davis, A new interleukin-13 amino-coated gadolinium metallofullerene nanoparticle for targeted MRI detection of glioblastoma tumor cells. J Am Chem Soc, 2015. 137(24): p. 7881-7888.
28. Costa-Silva, B., N.M. Aiello, A.J. Ocean, S. Singh, H. Zhang, B.K. Thakur, A. Becker, A. Hoshino, M.T. Mark, and H. Molina, Pancreatic cancer exosomes initiate pre-metastatic niche formation in the liver. Nat Cell Biol, 2015. 17(6): p. 816.
29. Liu, Y., Y. Gu, Y. Han, Q. Zhang, Z. Jiang, X. Zhang, B. Huang, X. Xu, J. Zheng, and X. Cao, Tumor exosomal RNAs promote lung pre-metastatic niche formation by activating alveolar epithelial TLR3 to recruit neutrophils. Cancer cell, 2016. 30(2): p. 243-256.
30. Mansour, H.M., M. Sohn, A. Al-Ghananeem, and P.P. DeLuca, Materials for pharmaceutical dosage forms: molecular pharmaceutics and controlled release drug delivery aspects. Int J Mol Sci, 2010. 11(9): p. 3298-3322.
31. Makadia, H.K. and S.J. Siegel, Poly lactic-co-glycolic acid (PLGA) as biodegradable controlled drug delivery carrier. Polymers, 2011. 3(3): p. 1377-1397.

32. Taluja, A., Y.S. Youn, and Y.H. Bae, Novel approaches in microparticulate PLGA delivery systems encapsulating proteins. J Mater Chem, 2007. 17(38): p. 4002-4014.
33. Yang, R., W.-S. Shim, F.-D. Cui, G. Cheng, X. Han, Q.-R. Jin, D.-D. Kim, S.-J. Chung, and C.-K. Shim, Enhanced electrostatic interaction between chitosan-modified PLGA nanoparticle and tumor. Int J Pharm, 2009. 371(1-2): p. 142-147.
34. Knop, K., R. Hoogenboom, D. Fischer, and U.S. Schubert, Poly (ethylene glycol) in drug delivery: pros and cons as well as potential alternatives. Angew Chem Int Ed, 2010. 49(36): p. 6288-6308.
35. Hatakeyama, H., H. Akita, and H. Harashima, The polyethyleneglycol dilemma: advantage and disadvantage of PEGylation of liposomes for systemic genes and nucleic acids delivery to tumors. Biol Pharm Bull, 2013. 36(6): p. 892-899.
36. Mishra, P., B. Nayak, and R. Dey, PEGylation in anti-cancer therapy: An overview. Asian J Pharm, 2016. 11(3): p. 337-348.
37. Yoo, H.S. and T.G. Park, Biodegradable polymeric micelles composed of doxorubicin conjugated PLGA–PEG block copolymer. J Control Rel, 2001. 70(1-2): p. 63-70.
38. Cheng, J., B.A. Teply, I. Sherifi, J. Sung, G. Luther, F.X. Gu, E. Levy-Nissenbaum, A.F. Radovic-Moreno, R. Langer, and O.C. Farokhzad, Formulation of functionalized PLGA–PEG nanoparticles for in vivo targeted drug delivery. Biomaterials, 2007. 28(5): p. 869-876.
39. Guo, J., X. Gao, L. Su, H. Xia, G. Gu, Z. Pang, X. Jiang, L. Yao, J. Chen, and H. Chen, Aptamer-functionalized PEG–PLGA nanoparticles for enhanced anti-glioma drug delivery. Biomaterials, 2011. 32(31): p. 8010-8020.
40. Daman, Z., H. Montazeri, M. Azizi, F. Rezaie, S.N. Ostad, M. Amini, and K. Gilani, Polymeric micelles of PEG-PLA copolymer as a carrier for salinomycin against gemcitabine-resistant pancreatic cancer. Pharm Res, 2015. 32(11): p. 3756-3767.
41. Chan, J.M., P.M. Valencia, L. Zhang, R. Langer, and O.C. Farokhzad, Polymeric nanoparticles for drug delivery, in Cancer Nanotechnology. 2010, Springer. p. 163-175.
42. Zhong, J., L. Li, X. Zhu, S. Guan, Q. Yang, Z. Zhou, Z. Zhang, and Y. Huang, A smart polymeric platform for multistage nucleus-targeted anticancer drug delivery. Biomaterials, 2015. 65: p. 43-55.
43. Wen, R., B. Banik, R.K. Pathak, A. Kumar, N. Kolishetti, and S. Dhar, Nanotechnology inspired tools for mitochondrial dysfunction related diseases. Adv Drug Deliver Rev, 2016. 99: p. 52-69.
44. Wen, R., A.C. Umeano, and S. Dhar, Accessing Mitochondrial Targets Using NanoCargos, in Intracellular Delivery III. 2016, Springer. p. 229-254.
45. Wen, R., A.C. Umeano, L. Francis, N. Sharma, S. Tundup, and S. Dhar, Mitochondrion: a promising target for nanoparticle-based vaccine delivery systems. Vaccines, 2016. 4(2): p. 18.
46. Murphy, M.P., Targeting lipophilic cations to mitochondria. BBA-Bioenergetics, 2008. 1777(7-8): p. 1028-1031.

2. EXOSOME BIOGENESIS, CHARACTERRIZATION AND BIOMARKER APPLICATION FOR CANCER DIAGNOSIS*

*Wen, R.; Xie, J.; Cai, H.; To be submitted to *Front Psychol.*

ABSTRACT

Exosomes are membrane-bound vesicles that are secreted by almost all cell types. The secretion of exosomes can be modulated by various pathways or factors, such as calcium, p53 protein, and Rab35. Exosomes are selectively enriched with proteins, lipid, and coding/non-coding RNAs from its original derived cell types. Exosomes are critical in cell-to-cell communication with neighboring or distant cells through diffusion or systemic transport to neighboring or distant sites for signal transduction. The identification and discrimination of exosome from normal cells to pathological cells in biological fluids have attracted growing interests. Here, I will focus the biogenesis of exosomes and their uptake mechanism into recipient cells, recent progress of exosome isolation, composition and characterization techniques, and potential application as biomarkers for cancer diagnosis.

2.1 INTRODUCTION

Exosomes are membrane-bound vesicles with a diameter of 30-150 nm and a density of 1.10-1.21 g/mL that are secreted into extracellular space by almost all types of cells[1-4]. Exosomes were first identified via studies related to transferrin receptors in 1983 and were termed "exosomes" in 1987[5, 6]. The releasing of exosomes was first found during maturation of sheep reticulocytes and is then recognized as nanoscale vesicles from nearly all kinds of cell[5].

Many proteins from the plasma membrane get reduced or disappeared. Meanwhile, lysosomal and endosomal components are found to be lost or altered. Originating from the fusion of MVBs with plasma membrane, exosomes are selectively enriched with plasma membrane proteins, lipid, coding and non-coding RNAs[2]. DNA is found in the exosomes as well even though secretory process is rarely associated with nuclear compartment[7]. Double-stranded genomic DNA was detected in both exosomes derived from pancreatic cancer cells and serum exosomes from patients with pancreatic cancer[8]. Exosomes derived from astrocytes and glioblastoma cells are reported to contain mitochondrial DNA but not nuclear DNA[9]. Exosomes contain adhesion molecules, including intercellular adhesion molecule-1, CD11, CD18, CD53, CD146, CD166, CD326, LFA-3 ,mac-1, ALCAM, tetraspanins, integrin α chain, EGF factor VIII[10, 11], and heat-shock proteins such as Hsp70 and Hsp90, which regulate cellular homeostasis and enhance cell survival in response to external stimulation such as stress[12]. Tetraspanins including CD9, CD63, CD81, and CD82 can be used as markers for exosome[13]. Proteins such as Alix and thioredoxin peroxidase II involved in apoptosis are also found in exosomes[14]. Some proteins like immunoglobulin-supergene family proteins such as MHC I, II, CD86/B7.2, and CD54/ICAM-1 are cell-specifically existed in exosome[15]. Lipids are also present in the exosome, such as cholesterol, diglycerides, stomatin, and sphingolipids[11].

Initially, exosomes were thought of vesicles for removal of unwanted components from cells, later on, the discovery of cellular communication mediated by exosomes has sparked great interest in exosome biology[16]. Exosomes play significant roles in intercellular communication with neighboring cells or distal cells. Information exchange is possible by exosome-mediated regulation [17]. The secreted exosome can diffuse to neighboring cells or systemic transport to distant sites for signal transduction or information exchange. Exosomes have been used as drug delivery system for various diseases[18]. Exosomes derived from pluripotent stem cells are reported to deliver cardioprotective miRNAs to combat ischemic myocardium[19]. Exosomes released from cardiomyocyte progenitor cells could induce the migration of endothelial cells[20]. Cancer cell exosomes can trigger the differentiation of fibroblasts to myofibroblasts with upregulating of α-smooth muscle actin expression and other associated changes[21]. Prostate cancer exosomes induced the differentiation process through TGFβ1 dependent pathway, where heparan sulfate molecules directed TGFβ communication between exosomes and stromal cell[22]. Tumor-derived exosomes transport oncogenic molecules and pathogenic proteins such as EGFRvIII, RNA, and DNA fragments, to normal cells, which can induce malignant transformation and tumor progression[23-25]. Exosomes from cancer cells are enriched in biological fluids and are potential biomarkers for cancer diagnosis[26].

The discovery and identification of exosome upon significant function and dynamic information attract considerable interests in the research field. Hence, it is necessary to be understand the biogenesis and uptake into target cells, as well as be acquainted with basic techniques in collecting exosomes for relative biological investigation. Here, we will illustrate the biogenesis of exosomes and its uptake mechanisms into recipient cells. Furthermore, isolation/purification techniques for exosome as well as exosome composition and

characterization will be discussed. Finally, exosome application as a biomarker will be potentiated for cancer diagnosis.

2.2 EXOSOME SECRETION AND BIOGENESIS

Exosome secretion is involved in the formation of intraluminal vesicles (ILVs) within the endosome and fusion of multivesicular bodies (MVBs) with cell membrane(Figure 2.1)[27]. The late endosomes contain multiple ILVs, inward budding of limiting membrane into late endosomes' lumen, and thus are also called MVBs or multivesicular endosomes (MVEs), which can be directly fused with the plasma membrane for subsequent releasing of included vesicles to extracellular space as of exosomes [28]. Alternatively, MVBs can be fused with lysosome for degradation, and thus the proteins in late endosomes can be recycled to the plasma membrane, secreted into exosomes or degraded through lysosomes participating in cellular processes.

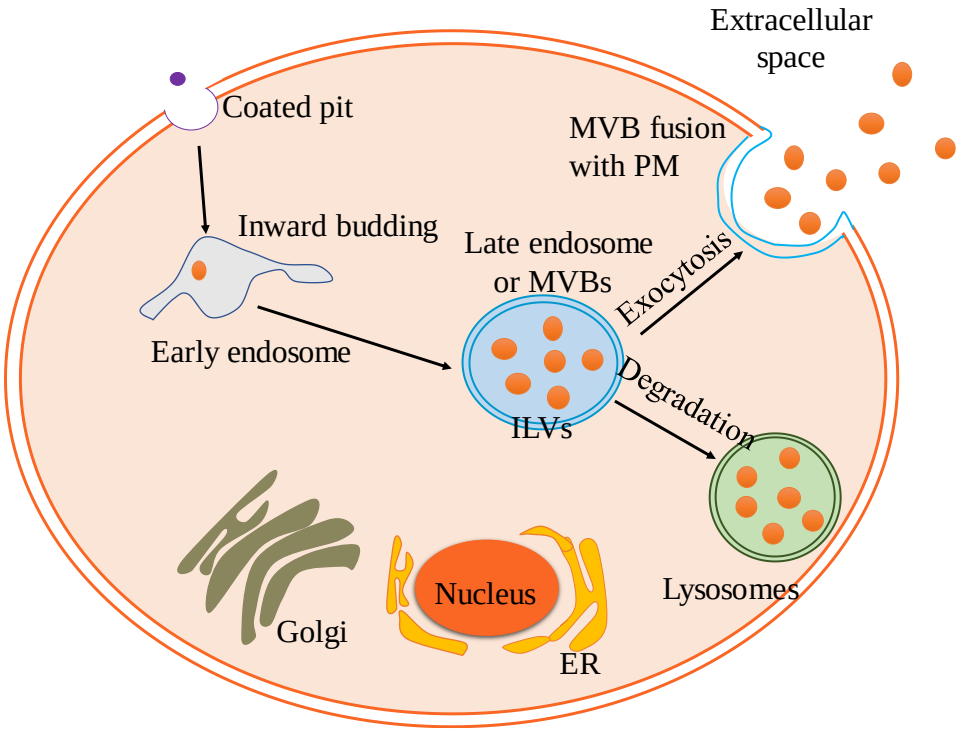

Figure 2.1 Secretory pathway of exosome in cellular environment. MVBs-multivesicular bodies, ILVs-intraluminal vesicles, PM-plasma membrane, ER-endoplasmic reticulum.

The secretion of exosomes can be modulated by various factors, such as Rab, syntenin, syndecan, calcium, and p53 protein[29-31]. Many efforts have been made to understand the fundamental science of exosome secretion and biogenesis. Several pathways have been proposed to sort proteins into exosomes, such as endosomal sorting complex required for transport (ESCRT) and lipid-raft machinery. The mechanisms of exosome secretion are not fully discovered, and more studies are still necessary to reveal the comprehensive pathways and influential factors. Here I summarize the current understanding of protein sorting pathways and/or influential factors for exosome secretion.

Rab family members

Rab proteins are members of GTPases family and are critical for intracellular membrane trafficking and exosome production[32-34]. Figure 2.2 describes the Rab protein regulating the exosome biogenesis. Rab superfamily of small GTPases are situated in membrane-bound compartments, Rab8 and Rab11 are limited to the recycling endosome and can move proteins via exocytic trafficking to the plasma membrane[35]. Rab6 is situated in the Golgi and associated with membrane docking[36]. Rab domain is not statically remained, and can be disassembled and reassembled to remodel membranes. The interaction of class C VPS/HOPS complex with Rab5 induces the conversion of Rab5 to Rab7 during cargo encapsulation between early and late endosomes[37].

Various Rab proteins were observed in exosomes with Rab35 as the most abundance in oligodendroglial cell lines. Rab35 depletion reduced the secretion of exosome by inhibiting the docking/tethering to plasma membrane from endosomal compartments. Rab GTPase-activating protein (GAP) TBC1D10A–C modulates exosome's release in a similar manner[30]. Rab11 protein is associated with the transferrin recycling from the pericentriolar endocytic recycling system to cell membrane. When transfected with Rab11 wild-type protein in K562 cells, the

exosome secretion was lightly enhanced, and the secretion could be significantly inhibited by transfection with dominant-negative mutant Rab11S25N. Possibly, the protein got reduced from MVB formation and also subsequent fusion process with membrane[38]. Later, Rab 11 was confirmed to favor the docking/tethering and fusion of MVBs with the plasma membrane. The overexpression of Rab 11 in RAW macrophages significantly enhanced the exosome secretion. The monensin or ionophore A23187 treatment stimulated the secretion of exosomes by upregulating cytosolic calcium level in cells (K562 and RAW macrophages) transfected with Rab11 Wild-Type or its mutants through escaping the Rab11 protein mediated restriction[39].

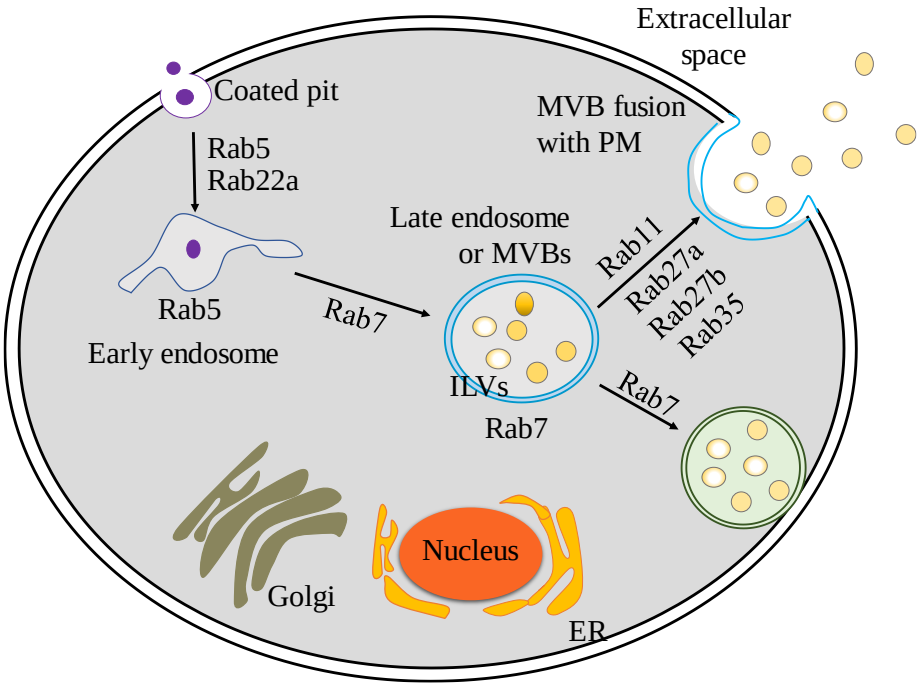

Figure 2.2 The role of Rab family proteins in exosome secretion

The Rab27a and Rab27b proteins are reported to boost the exosome secretion in HeLa cells. The knockdown of Rab27a and Rab27b disturbed the fusion of MVBs with the plasma membrane. Specifically, Rab27a knockdown increased the size of multivesicular endosomes (MVEs), and the reducing of Rab27b redistributed MVEs to perinuclear center instead of docking at the plasma membrane[40]. Rab5 protein is reported to modulate the intra-endosomal

trafficking in early endosomes. The overexpression of $Rab5^{Q79L}$ mutant enlarged the structure of early endosomes compared to normal controls, enhanced the HRP uptake and inhibited transferrin recycling. The recycling of transferrin was faster by overexpression of wild-type Rab5 compared to the mutant Rab5 S34N which induced very small endocytic vesicles[41]. The Rab7 is a downstream of Rab5 and modulates the membrane transport from early to late endosomes and/or from late endosome to lysosomes[42, 43]. The overexpression of mutants Rab7N125I and Rab7T22N inhibited the membrane transport to late endosomes as evidenced by the accumulation of VSV-G protein (a transport marker) in early endosomes, and significantly decreased the late endosomal cleavage of SV5 HN compared to mock-transfected or Rab7 wild-type overexpressing cells[43]. The knockdown of Rab7 is reported to enlarge endosomes and dramatically reduce the release of exosome[44].

Syntenin-syndecan associated pathway

Syntenin is a cytosolic protein containing two PSD95/Dlg/zonula occludens 1 (ZO-1) (PDZ) domains, a C-terminal and an N-terminal region. The PDZ domains provide the binding site for high-affinity interaction with syndecan involving membrane docking[45, 46]. The interaction of syntenin with phosphatidylinositol 4,5-bisphosphate (PIP2) via PDZ domains modulates the endocytic recycling of syndecans or its associated complexes such as fibroblast growth factors(FGF)/FGF receptor (FGFR)[47, 48]. Syntenin can interact with Alix through three LYPXnL motifs in N-terminus region[44, 49]. Syndecans are cell membrane proteins linked with heparan sulfate chains, which consist of various ligands, such as adhesion molecules and growth factors (e.g., fibronectin and FGFs)[50]. Syntenin and syndecans play important roles in exosome biogenesis (Figure 2.3).

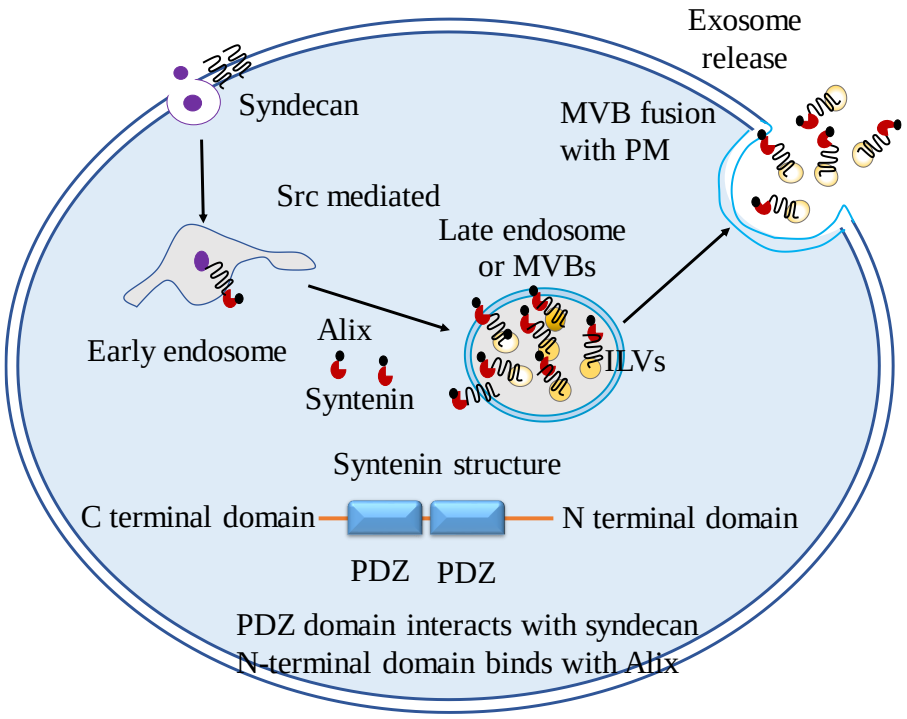

Figure 2.3 The role of syntenin-syndecan in exosome secretion, PDZ: PSD95/Dlg/zonula occludens 1 (ZO-1).

Situated in the endosome and cell surface membrane, ADP ribosylation factor 6 (ARF6) plays an critical role in vesicular trafficking and membrane transport/remodeling by modulating late endosomal events of ILVs budding and can also degrade the MVBs through epidermal growth factor receptor regulation[51-53]. Syntenin-Alix modulates the budding of ILVs into MVBs through ARF6 and its effector phospholipase D2. Syntenin regulates the sorting and secretion of exosomes through direct binding of PDZ domains to membrane receptors like syndecans. ARF6 modulates endocytic recycling of syntenin. ARF6 depletion and overexpression had no significant effects on the cellular level of syntenin, Alix or syndecan-1 C-terminal fragment (SDC1CTF), but it significantly decreased or increased the level of syntenin, Alix, CD63, and SDC1CTF, respectively[53]. Alix can modulate the budding and abscission processes, while syndecan regulates the post-receptor trafficking. The formation of syntenin requires the syndecan cleavage in endosomal domains to form syntenin-syndecan binding for stabilizing the membrane

budding process. Syndecan with a cytoplasmic domain can bind cytosolic factors like PDZ scaffolding syntenin protein. The syndecan, syntenin and Alix can form complexes through interaction of syndecan with syntenin at PDZ domain, and linking of N-terminal domain of syntenin to V-domain of Alix. Syndecan-syntenin-Alix complex modulates the secretory pathway of exosomes regarding membrane trafficking, formation of ILVs, budding process and exosome generation. The depletion of syntenin significantly decreased the size of endosomes, and reduced the exosomal syntenin, Alix, CD63 and HSP70, but has no effect on expression level of Flotillin-1 in exosome[44]. The enzyme heparanase can modulate the syndecan-syntenin pathway by promoting endosomal membrane budding and cleaving heparan sulfate chains of syndecans to biologically active fragments. The heparanase enhances the sorting of syntenin-1, syndecan and other exosomal proteins like CD63, but has no effects on the secretion of CD9, CD81, and flotillin-1. The capacity of heparanase to stimulate exosome production depends on syntenin-Alix interaction, and knockdown of heparanase reduced the expression of syndecan-1 and syndecan-1 CTF in exosomes[49].

The oncogenic Src kinase is reported to mediate syntenin-syndecans endosomal budding through acting at upstream of ARNO/ARF6/PLD2 and direct phosphorylating syndecan DEGSY motif cytosolic domain and tyrosine 46 of syntenin. The Src phosphorylation provides the tyrosine residues for syndecans-syntenin and enhances the endosomal budding. The promigratory effects of Src-contained exosomes are dependent on syntenin. The inhibition or depletion of Src in cells reduced the secretion of exosomes and decreased the expression of syntenin, syndecan-1 C-terminal fragment (SDC1 CTF), ALIX, and CD63 in exosomes. The overexpressed Src wild-type or constitutively active mutant Src(Y527F) increased the level of exosomal proteins involved in syntenin pathway to support the budding process at endosomal

membranes. The syntenin is a prerequisite for Src effects and Src-present exosomes derived from syntenin-depleted tumor cells did not stimulate the migration of HUVEC cells[54].

Endosomal sorting complex required for transport pathway

The most common pathway of exosome secretion and biogenesis is regulated through endosomal sorting complex required for transport (ESCRT)[55, 56]. The ESCRT family composed of ESCRT-0, -I, -II and -III, Vps4 and associated proteins[57, 58]. ESCRT-0, I and -II are involved in intraluminal sorting of ubiquitinated cargo into ILVs through ubiquitin and lipid binding[59]. ESCRT-III regulates the final sequestration for cargo and exosome formation, ATPase Vps4 is essential for ESCRT-III recycling and membrane remodeling(Figure 2.4)[60].

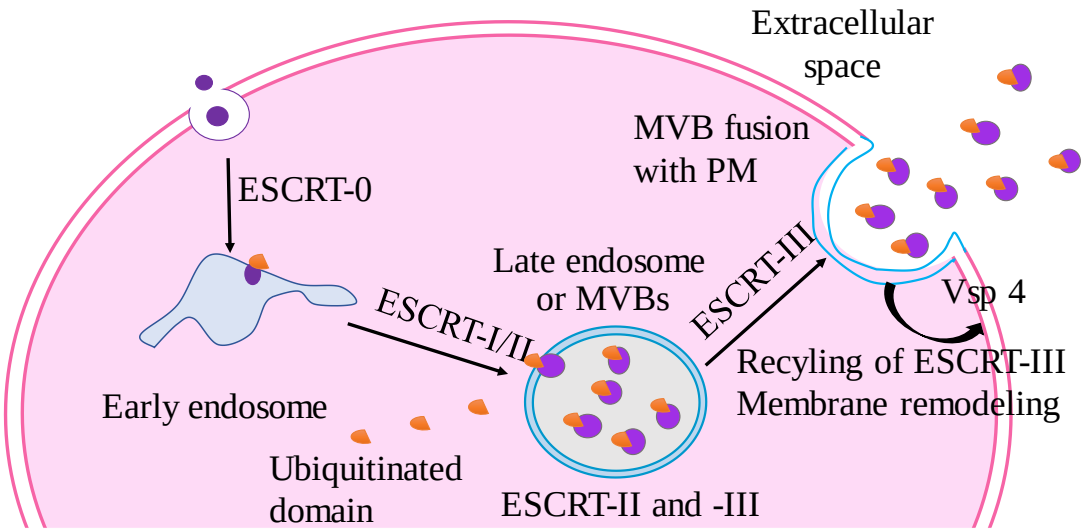

Figure 2.4 The ESCRT pathway of protein sorting in exosome secretion

ESCRT-0 complex consists of two proteins Hrs and STAM with 1:1 formulation and initiates the clustering of cargo proteins during MVB biogenesis[61]. The ESCRT-0 can bind ubiquitinylated cargos as many as eight ubiquitin moieties through ubiquitin-binding motifs[62]. It also participates in cargo sorting by interacting with clathrin vesicles within endosome through clathrin-binding motif of Vps27/Hrs[57]. ESCRT-0 binds with ubiquitinated proteins through the interaction with VHS (Vps27, Hrs, and STAM) and UIM motifs, and human ESCRT-0 binds

polyubiquitin e.g., Lys63-linked tetraubiquitin (50-fold) much tighter than monoubiquitin[63]. ESCRT-0 protein Hrs, is reported to promote the secretion of exosomes from dendritic cells (DCs). The secreted level of exosome was significantly reduced in Hrs-depleted DCs compared to normal DCs and could not recovered with ovalbumin or by Ca^{2+} ionophore A23187 stimulation[64].

ESCRT-I is a rod-shaped complex with high molecular weight of ~350 kDa that consists of many proteins such as TSG101, Vps23, Vps28, Vps37, UBAP1 and hMvb12[61, 65]. TSG101, Vps23, hMvb12 and their corresponding homologs facilitate the sorting of ubiquitinated cargo through regulating the binding activity of ubiquitin[57, 66]. Vps23 recognizes ubiquitinated cargoes for their inclusion in MVBs[67]. Vps37b facilitates the release of the HIV-1 virus by regulating TSG101/ESCRT-I activity. TSG101 interacts with HIV-1 Gag protein, and the mutant of TSG101 prevents HIV-1 budding through inhibiting PTAP or Vps28 binding activity[68]. ESCRT-I physically binds to Vps27 on endosome to recruit the ubiquitinated cargoes and activates the MVB pathway whereas Vps27 interacts with phosphatidylinositol 3-phosphate and ubiquitin via FYVE domains[69]. ESCRT-I links ESCRT-0 together with ESCRT-II, and stabilizes the ESCRT-III through Alix or ESCRT-II connection[70-72].

ESCRT-II is a Y-shaped ~155 kDa protein complex composed of class E Vps proteins with one copy of Vps22 and Vps36, and two copies of Vps25, and is critical in regulating downstream of ESCRT-I and initiation of ESCRT-III[73, 74]. ESCRT-II strongly interacts with ESCRT-III through direct binding Vps25 in ESCRT-II to helix α1 of Vps20 in ESCRT-III, which activates Vps20 for subsequent assembly and oligomerization of Snf7[59, 75]. ESCRT-III is composed of four core subunits (Vps2, Vps20, and Vps24, Snf7/Vps32) and modulates the final sorting of proteins to MVBs, and vesicle formation and scission[76, 77]. Unlike ESCRT-I and -II, there has

not yet been observed any ubiquitin-binding subunits in ESCRT-III[78]. The ESCRT-II is essential for the localization of ESCRT-III and it associated protein (e.g., Vps20p) can induce the binding of ESCRT-II to lipid[75]. Snf7 is a key regulator of the size of MVBs. Larger and heterogeneous Snf7 oligomers can create fewer, but larger and heterogeneous MVBs[59]. Alix and histidine-domain protein tyrosine phosphatase (HD-PTP) are essential in the recruiting specific cargo and connecting to ESCRT-III[76, 79]. Alix recruits ESCRT-III complex proteins for ILV formation during endosomal sorting and budding of exosomes[80]. ESCRT-III associated protein CHMP6 modulates endosomal cargo sorting by interacting with EAP20 of ESCRT-II[81]. The assembly of ESCRT-III is dependent on the activity of ATPase Vps4, and Vps2 subunit containing Vps-4 binding MIM1 motif is responsible for this process. The Vps4 plays an important role in the recycling of ESCRT-III after scission and additional budding from the cell surface[82]. The protein-protein interaction between ESCRT-III and Vps4 proteins allows protein sorting and vesicle formation through releasing membrane-associated proteins[83].

Lipid raft-mediated pathway

Lipid rafts are nanoscale structured microdomain enriched in cholesterol and sphingolipids and related proteins for membrane signaling and trafficking[84]. The lipid domains are associated with protein sorting, endosomal recycling, and ILV formation and construction[85]. The lipid raft contains various components such as cholesterol, glycolipids, Src tyrosine kinases, i.e., Lyn, and proteins with prohibitin-domain, i.e., stomatin, GPI-associated proteins, i.e., AChE[67]. The components of lipid raft in the endosomal system can be sorted into ILVs of MVBs. Exosomes are reported to be enriched in lipid components and lipid-raft associated proteins in proteomic lipidomic studies[86, 87]. The proteins with low lateral diffusion properties in lipid microdomain slow down the recycling of GPI-related proteins to the plasma membrane, which provides the capability of protein sorting into ILVs, on the other hand, fast recycling

molecules can easily escape from MVB budding[67]. The oligomerization of low-affinity raft can generate and stabilize the raft domain through lipid-lipid, lipid-protein or protein-protein interactions like phosphorylation-nucleotide binding[88-90].

The sphingolipid ceramide is an important regulator of exosome biogenesis and secretion. Ceramide is a lipid in the membrane and can combine small microdomains into large raft domains for promoting the domain-induced ILVs formation and budding[91, 92]. Exogenous C_6-ceramide can induce vesicles formation and increase the size of late endosomes[93]. Ceramide is produced by the hydrolysis of sphingomyelin through sphingomyelinase catalyzing. The exosomes were enriched of ceramide, and the release of exosomes was significantly reduced when the activity of sphingomyelinase was inhibited by GW4869, spiroepoxide or glutathione[93]. The inhibition of ESCRT machinery by knockdown of Hrs, Alix or Tsg101 did not affect the inward budding of proteolipid protein[91]. A later investigation indicated that exosomal level of TSG101, Alix and CD9 was significantly reduced upon inhibition of sphingomyelinases[94]. The release of chemokine-containing exosomes is reported to be dependent on lipid-raft machinery. Heat stress increased the ATP release as well as calcium level, through which chemokines like CCL2, CCL3, CCL4, CCL5, and CCL20 were accumulated into cholesterol-rich lipid rafts for subsequent exosome release. The use of ATP inhibitor (e.g., apryase and suramin), and calcium inhibitor (e.g., EDTA, verapamil, BAPTA) decreased the chemokines release in exosomes[95]. The reduction of cholesterol enhanced the vesicle release from prostate cancer cells. The cellular cholesterol level was decreased by both cholesterol-depleting agent methyl-β-cyclodextrin (methyl-β-cyclodextrin) or lovastatin inhibiting the enzyme for cholesterol biogenesis, and the protein profile was similar to control vesicles but with

a different expression level, given that caveolin-1 and LAMP-1 were significantly overexpressed in vesicles derived from PC-3 cells treated by cholesterol disrupting agents[96].

Heat shock protein-associated pathway

The heat shock proteins (HSPs) are intracellular proteins that participate in cellular processes responding to the stressful condition of heat[97]. The release of HSP into exosomes is distinct from common secretory pathways like endoplasmic reticulum(ER)-Golgi pathway[98]. The understanding of HSP biogenesis is controversial [99]. Hunter-Lavin et al. reported that HSP70 was released by a non-classical pathway possibly depending on lysosomal lipid rafts. The release of HSP70 from peripheral blood mononuclear cells (PBMCs) was inhibited by methyl-β-cyclodextrin, monensin, and methylamine, but not affected by Brefeldin A inhibiting protein transport through ER-Golgi [100]. Broquet et al. indicated that lipid rafts might be the responsible cellular pathway for release of HSPs. Cellular conditions like heat shock or drugs involving protein trafficking could increase the expression of HSP, and translocate them into lipid raft and undergo subsequent release[101]. On the other hand, Lancaster et al. demonstrated that HSP70 release was independent of the lipid raft pathway. The treatment by Brefeldin A and methyl-β-cyclodextrin, a lipid-raft disrupting agent, did not inhibit the HSP70 release from PBMCs. Instead, methyl-β-cyclodextrin treatment enhanced the release of HSP70, which was likely through disrupting the plasma membrane integrity for the subsequent leaking of HSP70 protein into the extracellular space[12]. The association of HSP70 with lipids such as phospholipid bis(monoacylglycero)phosphate is through electrostatic interaction[99]. Vega et al. reported that HSP70 protein was inserted and localized into plasma membrane before releasing into extracellular space in membrane-associated formulations through exocytosis or membrane shedding[102].

Tetraspanin-associated proteins

Tetraspanins are a family of four-transmembrane proteins with a molecular weight at 25-50 kD[103]. Tetraspanins can interact with various transmembrane and cytosolic proteins, such as CD9/pro-TGF-α, CD82/EGFR, or CD151/integrins[104]. The involvement of tetraspanins with lipids and transmembrane proteins constructs the tetraspanin-enriched microdomains (TEMs), which are physically and functionally different from lipid-raft microdomains and can regulate the vesicular fusion and/or fission [105, 106]. Tetraspanins play important roles in the function of growth factor signaling proteins (e.g., pro-TGFα, pro-HB-EGF, and pro-amphiregulin) and integrins (e.g., α3β1, α6β1, α4). Tetraspanins are highly enriched in the exosome and can regulate the protein trafficking, and stabilize/prevent activities of associated molecules[107, 108].

Tetraspanin Tspan8 is reported to recruit selective proteins and mRNAs into exosomes. Differential mRNA analysis showed that AS-Tspan8 exosomes were enriched more than three-fold of 285 transcripts compared to AS exosomes. The MycN, Spi-C, FGFBP1, TCEB-1, and GDF3 transcription factors and corresponding proteins were both increased in AS-Tspan8 exosomes compared to AS exosomes by RT-PCR and western blot analysis. The CD49d and CD49e proteins were selectively recruited to exosomes by Tspan8. Besides, high expression level of various proteins like MCM7, CD106/ VCAM-1, laminin receptor 1, Mac2BP (galactoside-binding protein-3), and major VAULT proteins were detected in AS-Tspan8 exosomes as well[109]. CD63 is localized both in the endosomal system and at the plasma membrane. The incorporation of CD63 into ILVs is independent on ESCRT, but is affected by ceramide[91], and CD63 can be recycled back to the cell surface when endocytic vesicles were fused with plasma membrane[110].

High-order oligomerized membrane complex

High-order oligomerization of membrane complexes can drive the proteins into exosomes. Various plasma membrane anchors are reported to target oligomeric and cytoplasmic proteins like TyA-GFP to exosomes. The plasma membrane association by myristoylation tag and PIP2-binding domain showed the highest vesicle budding efficiency for TyA-GFP protein, and prenylation/palmitoylation tag induced less TyA-GFP encapsulation in exosomes. Endosome membrane anchor phosphatidylinositol-(3,4,5)-trisphosphate (PIP3) binding domain and integral plasma membrane protein CD43 were weakly sorted proteins into exosomes[111].

Miscellaneous factors

The intracellular calcium level is related to secretion of exosomes by mediating plasma membrane fusion process. Monensin stimulates exosome releasing through altering the proton gradient of vesicle membrane facilitating Ca^{2+} movement into the cytosol[29]. Vacuolar-type H^{+}-ATPase mediates the budding of MVBs and their fusion events with plasma membrane[112]. The exosomes are increasingly generated when p53 protein is activated in response to stress[31]. Neurons exosome production can be regulated by synaptic glutamatergic activity[113]. The autophagy process inhibits exosome secretion by modulating fusion. Autophagy participates in a way by fusion of MVBs with autophagic vacuoles instead of plasma membrane[114]. The soluble N-ethylmaleimide-sensitive factor attachment protein receptors (SNAREs) (SNARE) are critical in modulating the recognition and fusion of homotypic fusion of MVBs or heterotypic fusion of late endosomes with lysosomes or plasma membranes[115]. The SNARE complex can be built up by syntaxins (e.g., syntaxin 4, 7, 8), Vti1b, synaptobrevin and vesicle-associated membrane protein (VAMP) (e.g., VAMP-2, -7, -8)[115, 116]. The SNARE protein SNAP-23 was situated in lipid raft microdomains, while only a small amount of syntaxin 4 or VAMP-2 was found in lipid-raft in rat basophilic leukemia cells. The overexpression of poorly raft-

associated SNAP-23 family member could inhibit the vesicle exocytotic process[116]. The v-SNARE protein VAMP3 is proposed to participate in the early and recycling endosomes, which is essential for the fusion of MVBs with autophagosomes. VAMP7 is involved in the fusion process of MVBs-plasma membrane for the release of exosomes[117]. Serglycin regulates the protein sorting and secretion of exosomes derived from tumor cells. The knockdown of serglycin dramatically reduced the number of proteins in exosomes compared to gerglycin-expressing cells and serglycin-depleted exosomes were less efficient in triggering cellular response to tumors and/or host cells[118].

2.3 THE UPTAKE OF EXOSOMES INTO RECIPIENT CELLS

Prior to uptake into recipient cells, exosomes were first bound to the cells through exosome-cell interactions. The surface overexpression proteins such as tetraspanin of the exosomes or target cells play essentials roles in the interaction of exosomes with cells. The exosomes can be internalized to target cells through endocytosis or membrane fusion pathways[119]. The exosomes can gain access into cells either through mainly one route or via multiple mechanisms. For certain type of cells, exosome uptake pathway is dependent on cell types. For instance, macrophages always take up the exosomes through phagocytosis[120, 121]. The mechanistic routes of exosome uptake can be determined or visualized by various techniques, such as flow cytometry and confocal microscopy, when using different inhibitors to block specific pathways[122].

Protein interaction

Adhesion molecules are involved in the exosome binding to recipient cells. Protein-protein interactions between exosomes and recipient cells is of particular interest and essential for the attachment of exosomes to cells for further uptake. The interaction is often investigated by either blocking the surface receptors or ligands with specific antibodies, overexpression, or knockdown

of surface proteins by cell transfection. The exosome uptake into cells can be modulated by interaction of exosomal proteins such as milk fat globule (MFG)–E8/lactadherin, phosphatidylserine or tetraspanins (CD9) with the cell surface molecules, e.g., integrin, CD11a or CD54[123].

Heparan sulfate proteoglycans (HSPGs) are a type of glycoproteins that are modified by sulfation and covalently bound with heparan sulfate (HS) chains. HSPGs are present in both cell membranes (e.g., syndecans, and GPI-linked proteins) and secreted exosomes (e.g., serglycin)[124]. The HSPG-associated functional uptake pathway is reported for cancer cell-derived exosomes. The properties of HS such as structure and negative charge are critical in modulating exosome uptake. When treated with α-difluoromethylornithine to trigger structural changes of HS, the uptake efficiency of exosome into GBM cells was significantly enhanced. Heparin modulates the exosome uptake in a dose-dependent manner, with 55% reduction at a concentration of 10 μg/mL. HS-6 treatment caused more inhibition of exosome uptake than HS-2[125].

Tetraspanins or associated complexes such as tetraspanin-integrin complexes provide another entry pathway for exosome binding and subsequent uptake to target cells. Tetraspanin-complex is maintained in exosomes during internalization and is involved in the endosomal assembly. The Tspan8 internalization is much faster than CD9 and Tspan8 can be recovered in the early endosomes[126]. Tumor-derived exosomes enriched with Tspan8–CD49d complex propensely bind to endothelial cells and induce angiogenesis[126]. The exosomal Tspan8-integrin complexes are reported for recipient cell selection both *in* vitro and *in vivo*. The exosomes were derived from rat pancreatic adenocarcinoma lines BSp73AS (AS) or the related mutated cells. *In vitro* studies indicate that AS- and AS-Tspan8/CD9n-exosomes were selectively taken up by

$CD44^+$ leukocytes, and endothelial cells (ECs), bone marrow cells and lymph node cells. AS-Tspan8-β4-exosomes preferentially bound fibroblast cells and LN cells. Exosomes were demonstrated to be effectively taken up by solid organs *in vivo*. AS-Tspan8-exosomes were mainly found in pancreas and lung, and AS-Tspan8-β4-exosomes were preferentially localized in kidney, lung, and gut. More specifically, exosomes were distinctly internalized into cells of organs in a cell-specific dependent manner. AS-Tspan8-exosomes were mainly internalized into EC, but AS-exosomes were mostly taken up by pericytes[127]. CD29/CD81 complexes can be formulated as a strategy to increase the cellular uptake of exosomes. The radiation treatment greatly enhanced the exosome uptake into target cells upon 6 h exposure in various combinations of exosomes and recipient cells (e.g., human bone marrow-derived mesenchymal stem cells (MSCs), and rat small intestinal epithelial cells IEC6). The radiation regulates the exosome-cell binding through modifying the cell membrane surface molecules with the formation of CD29/CD81 complexes[128].

Situated on the outer membrane of exosomes, Bcl-xL substrate can be cleaved by caspase-3 to facilitate the L88-derived exosomes uptake into plasma myeloma cells (e.g., OPM2 and RPMI 8226) and lymphoma cells (e.g., B cell and T cells). The inhibition of caspase activity by Q-VD-OPh reduced the uptake of L88 stroma cell-derived exosomes in target cells like RPMI 8226 and OPM2 cells. When exosomes were preincubated with Bcl-2/Bcl-xL BH3 mimetic inhibitor ABT737, or using D61A and D76A Bcl-xL mutant-L88 cells derived exosomes, the exosomes was significantly blocked to be internalized into OPM2 or RPMI 8226 cells[129].

Endocytosis

Endocytosis is one of the most common pathways for cellular uptake of exosome and is composed of several subtypes, such as clathrin-mediated endocytosis, caveolae-mediated endocytosis, macropinocytosis, and phagocytosis[130]. Exosomes can be internalized into target

cells by endocytosis, in which the exosomes are surrounded and enwrapped by a small part of plasma membrane, and then get inside the cell in the form of a vesicle to undergo endosomal trafficking, ending by lysosomal degradation, or directed back to plasma membrane via recycling process[131, 132]. The specific exosome uptake pathway is associated with exosome origin and recipient cell types.

Trophoblast-derived exosomes and serum-derived exosomes from pregnant women are reported to be taken up by BeWo cells through endocytosis via syncytin-1 and syncytin-2 dependent pathway. The expression level of syncytin-2 was much less in serum-derived exosomes from pregnant women with preeclampsia than normal pregnant women. The downregulation of syncytin-1 or syncytin-2 inhibited the uptake of exosomes[133]. Exosomes derived from glioblastoma (GBM) cells are demonstrated to be internalized through lipid-raft dependent endocytosis rather than membrane fusion at the plasma membrane. The lipid raft-associated protein caveolin-1 (CAV1) and ERK1/2 phosphorylation are negatively associated with exosome uptake. Cholesterol depletion by MβCD inhibited the exosome uptake into human umbilical vein endothelial cells (HUVECs) and U87 MG cells, and the attenuated intracellular exosome transport by microtubule disruption with nocodazole eliminated the membrane fusion entry pathway[120]. Oligodendroglia-derived exosomes were imported into microglia cells through micropinocytosis pathway, which accounted for eventual clearance of exosomes involving the degradation of oligodendroglial membrane[134].

Ovarian carcinoma SKOV3 cell derived exosomes is reported to get into the same type of SKOV3 cells through endocytic pathway. The uptake capacity was significantly decreased at 4°C, suggesting energy-dependent endocytosis. The exosome uptake was inhibited when treated with chlorpromazine, an inhibitor of clathrin-mediated endocytosis, indicating the clathrin-

dependent endocytosis. Other endocytic pathways were confirmed uptake inhibition treatment by 5-ethyl-N-isopropyl amiloride (micropinocytosis inhibitor), cytochalasin D (phagocytosis inhibitor) and MβCD (lipid-raft endocytosis inhibitor)[135]. PC12 cell-derived exosomes are reported to access into bone marrow-derived mesenchymal stromal cells through clathrin-mediated endocytosis and micropinocytosis pathways. The K^+ depletion and CPZ compound treatment significantly inhibited the exosome uptake, suggesting the clathrin-mediated endocytosis of exosome internalization. The uptake process could also be interrupted by EIPA and LY294002 blocking micropinocytosis. Further inhibition treatment indicated that PC12 exosomes internalization did not rely on caveolae-mediated endocytosis and phagocytosis pathways [130].

Macropinocytosis pathway of exosome uptake can be induced by cancer-related receptors, such as epidermal growth factor receptor (EGFR). The HeLa exosomes were greatly internalized into A431 human epidermoid carcinoma cells by stimulation of EGFR with EGF treatment in a macropinocytotic pathway, and MIA PaCa-2 cells had greater uptake capacity compared to BxPC-3 cells due to intensive Ras-mediated macropinocytosis[136].

Exosomes from K562 or MT4 cells are reported to enter the macrophages through actin and PI3-kinase (PI3K)-dependent phagocytosis pathway. The K562 and MT4 were effectively internalized into phagocytic cells including U937, THP-1, J774A.1 cells RAW 264.7 macrophages, whereas only a small part could be taken up by non-phagocytic cells such as NIH 3T3 cells with mostly exosomes surfaced attached. The internalized exosomes were then sorted into phagolysosomes upon the evidence from colocalized observation with phagolysosomal markers. The down expression of dynamin2 (phagocytosis modulator) extensively inhibited exosome uptake, and treatment by EIPA, macropiocytosis inhibitor, did not influence the

exosome uptake into phagocytic cells, excluding the micropinocytosis pathway for the internalization behavior[121].

Membrane fusion

Membrane fusion is a merging process with plasma membrane of the cell[132]. Besides classic endocytosis, exosomes can also be internalized into recipient cells via membrane fusion. The uptake of BMDC exosomes to dendritic cells (DCs) is reported to undergo a fusion process of exosomes with plasma membrane upon protein-protein binding interaction. The inhibition of CD51, CD61, CD11a and CD54, or CD9 and CD81 blockage by antibodies significantly decreased the BMDCs exosome uptake into DCs. The uptake of exosomes was much higher in immature DCs than DCs attributed to CD86 molecule interactions. *In vivo* studies indicated that the exosomes were taken up by splenic DCs and hepatic Kupffer cells[123]. The microenvironmental pH plays a significant role in the fusion and trafficking of exosomes in target cells. The exosomes were derived from melanoma cells cultured in either acidic (pH 6.0) (Mel1ac) or buffered (pH 7.4) (Mel1). The colocalization of exosome with Rab 5b and Lamp-1 indicated the specific interaction of internalized exosomes with acidic cytoplasmic vesicles in melanoma cells. A fusion assay indicated that exosomes were able to fuse with parental-producing cells. The fusion of exosome was mainly dependent on temperature with active efficiency at physiological temperature and of weak calcium-dependent. The lipids in the membrane directly participated in membrane/membrane fusion process and filipin treatment remarkably attenuated the exosomes' uptake in both acidic and buffered conditions[137].

Miscellaneous pathways

Human bladder cancer exosomes were taken up by SW780 bladder cancer cells primarily through receptor-mediated endocytosis and partially by HSPGs expressed on recipient cells. Heparin partially decreased the uptake of exosomes, and exosomes were observed to bind cells

through cell-surface receptors for subsequently internalization[122]. Smaller sized exosomes collected from Exoquick(EQ) method are reported to preferentially be internalized to elicit effective cellular response compared to larger exosomes prepared by ultracentrifuge method. EQ prepared exosomes derived from both glioma associated stem cells (GASC) and human glioblastoma A172 cells showed similar trend of short time (e.g., 3h) internalization into A172 cells[138]. The capacity of exosomes uptake varies in different cell and exosome types. PC-3 cell-derived exosomes and prostasomes showed much higher uptake into benign CRL2221 cells than malignant PC3 cells, and PC-derived exosomes were internalized faster than prostasomes. The uptake ability was attenuated by BafA1, V-ATPs inhibitor, and 2-deoxyglucose, glycolysis inhibitor, suggesting the energy-dependent pathway from the glycolytic flux and ATP production[139].

2.4 ISOLATION AND PURIFICATION OF EXOSOMES

The cultured cell exosomes are commonly collected after 24 h or 48 h incubation at a 15-cm dish or 175 cm^2 flask, or multiple (e.g., 10) small flasks (e.g., 75 cm^2) or dishes (e.g. 10-cm), with ~1-50 μg of protein separated from cell culture media [140-142]. Fetal Bovine serum (FBS) contains significant amount of exosomes, and thus it is favorable to use exosome-free FBS in culture condition. Exosome depletion can be achieved by ultracentrifuge (UC) method, in which exosomes were removed by centrifugation for a long time (e.g., 15-18 hours) at high speed (e.g., 120,000×g)[143-145]. The low percentage of FBS (e.g., 2%) in complete medium and serum-free medium have also been reported in exosome isolation and purification[21, 146, 147]. However, there should be cautious when using serum-free medium since serum-free culture might alter the quantity and quality of secreted exosomes[148].

The type of isolation method plays significant roles in generating function-specific exosomes. The isolation of exosomes in biological fluids, such as cell culture medium, plasma, urine, milk, and saliva, can be mainly classified as ultracentrifuge (UC), ultrafiltration (UF), size-exclusion chromatography (SEC), immunoaffinity capture, and field flow fractionation[149]. Besides, a combination of these methods or incorporating of a new approach, such as field flow fractionation with in-line ultraviolet absorbance, high-pressure liquid chromatography-gel exclusion chromatography, or multi-angle light scattering, is also possible in the separation of high purity exosomes[150]. The comparison of various isolation methods for exosomes is summarized in Table 2.1.

The most commonly used method is UC technique, which is widely used as of simple, low cost and easy to operation. However, UC method is lengthy with limited samples processed at a time and is difficult to scale up. Serial steps of centrifugation before ultracentrifugation are usually used to remove the live, apoptotic or dead cells, and cellular debris. Ultracentrifuge over 100,000 ×g is generally used to pellet the exosome from biological fluids. The type of rotor affects the yield, composition and purity exosomes. For example, SW rotor pelleted more protein, but less RNA compared to the FA rotor when using same centrifuge force and time (118,000 ×g, 70 min). The RNA level using SW rotor could be increasingly recovered with prolonged centrifugation period (114 min). The pellets were enriched with a size of exosomes over 100 nm or less than 50 nm when prolonging the centrifugation process, which greatly enhanced the yields of exosomal RNA and protein[151]. A filtration process can be introduced before the ultracentrifugation to remove cellular debris to replace the medium centrifuge step at medium speed (e.g., 10,000 ×g)[152]. When sucrose is involved in the UC method, a density gradient is created, which facilitates the purification of exosomes regarding size, density, and compositions.

Proteins precipitate as pellets, while lipid-containing vesicles float into equilibrium buoyant density upon sucrose gradient[16]. Exosomes are reported to have an equilibrium buoyant density of 1.10–1.21 g/mL in a linear sucrose gradient[153, 154]. Density gradient method is more efficient in exosome extraction than UC method, but it is more costly due to high requirement of equipment and time-consuming issue[155].

UF is another powerful tool for separating exosomes. UF tool usually uses a pressure-driven concentrator, with which exosomes are bound and concentrated, and then get recovered from the membrane. UF is an easy, simple and time-saving method. However, some exosomes may adhere to membranes and can hardly be removed. The yield of exosome is significantly low compared to centrifuge concentrating technique. Besides, the pressure applied in UF may cause deformation and damage of exosome and result in low-quality exosomes with less protein or RNA.

Exosome isolation reagents are used in exosome separation from blood samples and cell culture medium[156]. The introduction of reagents can eliminate the ultracentrifuge process over 100,000 ×g. Commercially available methods take advantage of reagents with either polymers or magnetic beads to precipitate or capture the exosomes. ExoQuick (EQ)™ precipitation and Exo-spin™ (ES) method are such commercial available reagent-based methods to isolate exosome from biological fluids, such as cell culture medium, urine, saliva, and plasma. In EQ method, upon removing the biological fluids samples from cells and cellular debris, exosome isolation reagents are used to precipitate the exosomes and a centrifuge process at 10,000 ×g will be used to pellet the exosomes. EQ method is suitable for small-scale exosome collection, such as five mL of plasma samples. ES method introduces a column to post purify the pelleted exosomes. ES precipitation is less expensive than EQ method and can be used to isolate exosomes from cell

culture medium with large volume (e.g., 500 mL). ES-derived exosomes are suitable for RNA and protein analysis, and functional purpose. Both ES and EQ methods are costly when compared to UC method. It is reported that EQ method is superior to UC method in collecting exosome from urine, given that EQ produces more exosomal particles, a higher level of exosomal mRNA and miRNA, and requires less in-hand time[157]. With modifications to standard EQ method, exosome yield could be highly enhanced (e.g., five-fold). The introduction of filtration step decreased the yield of exosome[157].

Deun et al. compared four different isolation methods for the separation of exosome from cell culture medium (CCM) of Rab27B-expressing MCF-7 cell line regarding recovery, size, morphology, protein, and RNA level[158]. Precipitation solution-based method EQ and Total Exosome Isolation (TEI) method generated higher protein yield of exosome but had a lower level of exosomal marker proteins Alix, HSP90α, CD63, and TSG101 compared to centrifuge-based UC and OptiPrep™ density gradient ultracentrifugation (ODG) method. The higher levels of proteins from EQ and TEI methods were attributed to the existence of contamination from non-exosomal proteins serum albumin and apolipoprotein E. Exosomes prepared from ODG were heterogeneous with a size of 35-100 nm and of CD63-positive, and enriched with genes related to translation and ribosome. Exosomes were easily clumped/aggregated by UC, EQ and TEI methods[158]. Lobb et al. reported the quantity and qualification evaluation of particle separated from cell culture medium and plasma using SEC, UC, and UF methods. As for cell culture medium, Centricon (Centrifuge-based) method prepared a 3-fold higher yield than Stirred Cell (pressure-driven) method. The UF method produced particles with similar size distribution profile and exosomal protein level to UC, but UF recovered more particles and required less time. The repeated UC cycle could reduce the particle recovery. EQ and ES methods produced a

higher yield of small vesicles (<100 nm) than ODG method. The exosomes from EQ method were less pure compared to ES preparation, both of which were superseded by ODG method. When considering the isolation of plasma samples, SEC using qEV columns had the lowest recovery but the highest purity of exosomal vesicles. High contamination of other proteins was present in exosomes prepared by EQ and ES methods[159]. Recently, Helwa et al. assessed the exosome separation by UC and commercial methods from human serum [160]. The commercial kits miRCURY, EQ, and TEI recovered more than 40-fold of particles than UC method. The exosomes prepared from all four methods were of a similar size range of 40-150 nm, presence of exosomal proteins and with high quality of exRNA.

Recently, exosome total isolation chip (ExoTIC) is reported to efficiently isolate exosomes with high yield and quality from both culture media and human plasma[161]. ExoTIC used nanoporous membrane to separate and purify intact exosomes with a size of 30-200 nm. ExoTIC obtained a much higher yield of exosomes compared to UC and polyethylene glycol (PEG)-based precipitation methods, and exosomes prepared by ExoTIC had similar microRNA profile, but a higher number of proteins compared to UC method[161]. Another study integrated two acoustofluidic modules (acoustics and microfluidics) onto a single chip to remove the blood components and isolate the exosomes directly from whole blood. The acoustofluidic-based chip successfully generated exosomes with a size of 110 nm and a high yield of ~99%[162].

Table 2.1 A comparison of various methods for exosome isolation

Methods	Advantages	Disadvantage	Comments
Ultracentrifuge (UC)	Simple, easy to perform, good for protein, low cost for separation once installed the equipment	Lengthy, limited samples can be processed at a time, scalability issue, poor exosome quality, costly at installation	Widely used methods.
Ultrafiltration (UF)	Fast, simple	Expensive, low yield, may cause damage or	Filters through a semipermeable

		deformation, unwanted sample lose	membrane
Field flow fractionation (FFF)	High purity, high separation selectivity	Costly at installation	Has been modified or combined with other methods such as isoelectric focusing and asymmetrical flow FFF
Size-exclusion chromatography (SEC)	High purity, precise separation	Costly at installation, time-consuming, limited samples run at a time	Modified SEC method can dramatically enhanced isolation efficiency, sepharose CL-2B SEC isolation takes <20 minutes[149].
Immunoaffinity capture (IAC)	Allows selective isolation	not good for large sample volumes, may lose functionality	Usually uses antibody-coating to selective bind to exosome.
Reagent-based method	Fast, no sample limitation, high throughput, mild effect	Expensive, high cost	Some commercially available methods are using this method, such as ExoQuick™ (EQ) and Exo-spin™ (ES) method, good for small volume samples
Sieving method	Fast, high purity	Low yield	Rarely used
Chip method	fast, good repeatability, minimum human bias, convenient for analysis, high efficient for small sample volume.	Complicated, expensive	The on-chip technology is only recently reported and have not yet commercialized.

2.5 EXOSOME COMPOSITION, IDENTFICATION AND CHARACTERIZATION

The level of exosome released is associated with cell types. The rapid proliferating cells tend to release more exosomes than slowly growing cells[163]. The quantity of exosomes is reported to be 0.2-0.5 μg protein per 10^6 of dendritic cells after 24h incubation[164], and 0.5-2 μg protein per 10^6 of most murine tumor cell lines[140]. Epithelial associated cancer cells produce slightly fewer exosomes. It is reported that epithelial ovarian cancer (EOC) cells release 0.01-0.3 μg protein per 10^6 cells in 48 h, and non-malignant immortalized ovarian surface epithelium (IOSE) control cells also secrete the exosomes in the same range with 0.2 μg protein per 10^6 cells in 2 days[141]. It is reported that stage III advanced ovarian cancer-derived human plasma had higher exosome content than early stage I[165]. A comparison of exosome level in urine from healthy donors and prostate cancer (PCa) derived patients did not show significant difference[166]. Table 2.2 summarizes the exosome secretion from *in vitro* cells or biological fluids.

Table 2.2 The secretion level of exosome from various cells or in biological fluids

Categories	Exosome quantity	Condition	Comments	References
Ovarian cancer patient-derived human plasma	70-125 μg/mL	-	Stage I is ~70 μg/mL, Stage III is ~125 μg/mL	[165]
Prostate cancer-patient-derived urine	30-2200 ng/mL	-	Health donors show a similar range 50-900 ng/mL, no much difference was observed in healthy men and advanced diseased patients	[166]
Dendritic cells	0.2 ± 0.1 μg/10^6 mature cells, 0.5 ± 0.1 μg/million immature cells	24 h	Mature exosomes had 2-3 fold more MHC II molecules than immature exosomes	[164, 167]
Epithelial MODE K cell line	0.5 μg/10^6 cells	48 h	IFN-γ stimulated cells secreted exosomes containing A33 antigen	[168]
B16BL6	1.1 μg/10^6 cells	24h	80% confluency was	[140]

murine melanoma cells			reached after cells plating in a 15-cm dish	
RAW264.7 murine macrophages	5 µg/10^6 cells			
C2C12 murine myoblast cells	1.9 µg/10^6 cells			
MAEC murine aortic endothelial cells	0.5 µg/10^6 cells			
NIH3T3 murine fibroblasts cells	1.8 µg/10^6 cells			
Epithelial ovarian cancer (EOC) cells	0.01-0.3 µg/10^6 cells	48 h	EOC-derived exosomes promote cancer invasion through CD44 transfer, which mediates MMP-9 secretion	[141]
non-malignant immortalized ovarian surface epithelium (IOSE) normal cells	0.2 µg/10^6 cells	48 h		

Exosome composition

The exosomes are mainly composed of proteins, lipids, DNAs, RNAs, such as mRNAs and microRNAs (Figure 2.5). The exosome database, Exocarta increasingly identifies the exosomal protein, RNA, and lipid and current version includes 41,860 proteins, over 7540 RNA and 1116 lipids in exosomes collected from 286 exosomal studies, with almost a quarter of human proteins are recognized in exosomes[169]. Although the full protein library is various in exosomes from different cell types, all exosomes share some common proteins, which could serve as markers for exosome identification. For example, SW80 cell-derived exosomes consisted of 941 proteins, 628 proteins were confirmed in SW620 colon cancer cell-derived exosomes as well, including common proteins TSG101, Alix, and CD9[170]. The common proteins shared by most of the exosomes are described in Table 2.3. Positive exosomal markers consist of tetraspanin, CD9,

CD63, CD81, CD81, Alix, TSG101. Negative controls such as endoplasmic reticulum calnexin are usually used to confirm the purify of exosomes.

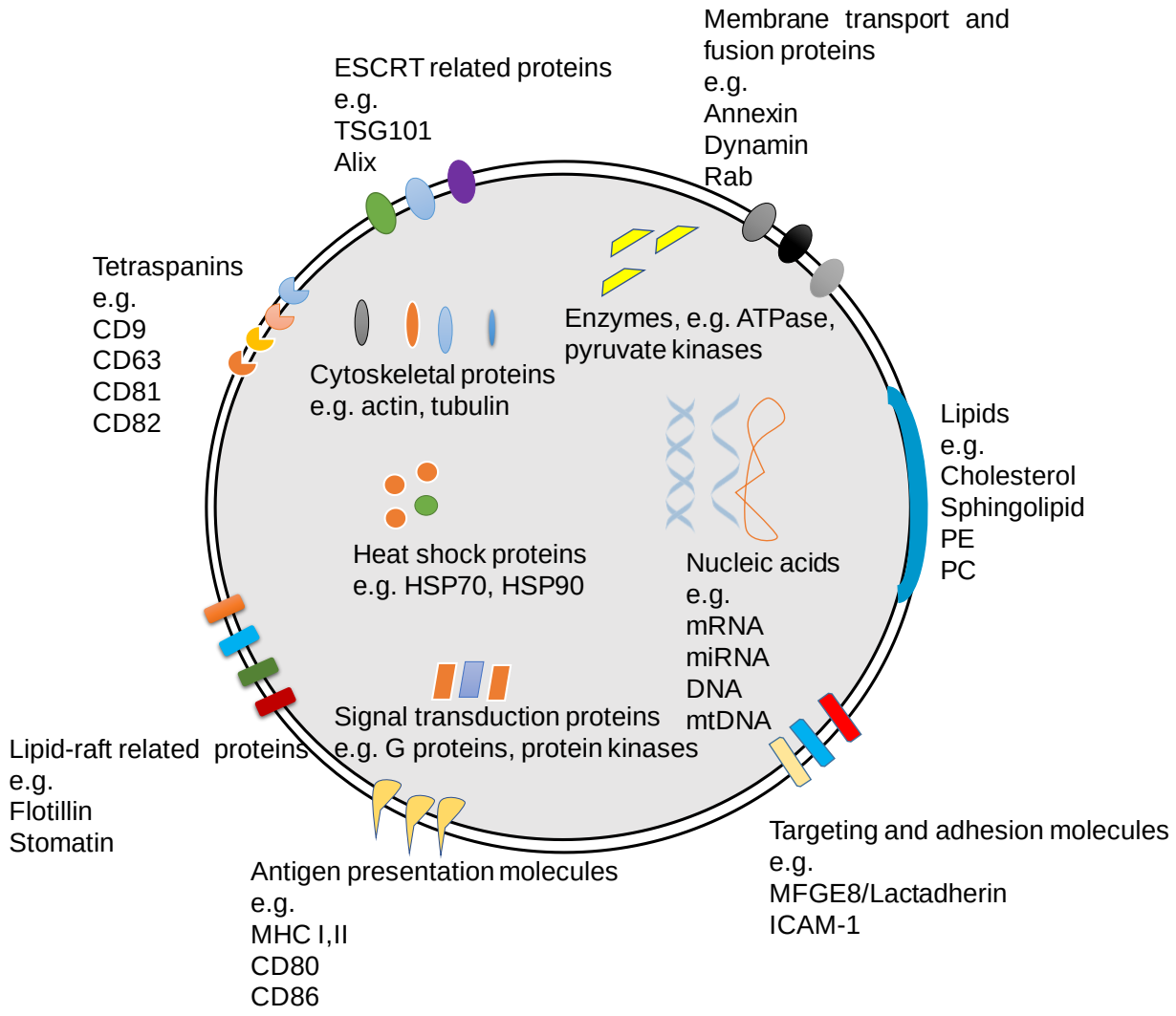

Figure 2.5 Schematic composition diagram of exosomes

The proteins of exosomes mainly originate from plasma membrane, endocytic pathway, and cytosol. Membrane-associated proteins such as tetraspanins CD9, CD63 are enriched in exosomes[171]. The highly abundant properties of tetraspanins make them commonly used as exosomal markers. Tetraspanins interact with many transmembrane and cytosolic proteins, facilitating protein sorting and vesicle fusion/fission[172]. Tetraspanins may be associated with mRNA, miRNA, and cholesterol enrichment toward exosomes as well[105, 173]. Exosomes

enriched in tetraspanin Tspan8 are reported to undergo rapid uptake by endothelial and pancreas cells with CD54 as the major targeting ligand[127]. Tetraspanin-driven pathway suggests their potential for therapeutic agents loading and/or serving as targeting moieties in nanocarrier system. Endosomal sorting complex required for transport (ESCRT) associated proteins such as Alix and TSG101 are usually detected in exosomes[27]. ESCRT traffics cargo via membrane budding process [174]. Alix facilitates intraluminal budding of vesicles in endosomes by directly interacting with syntenin through LYPX(n)L motifs, in which syndecan plays an indirect role through interacting with syntenin[44].

Exosomes have a similar lipid profile to plasma membrane, and the enriched lipid provides an alternative path for protein sorting into exosomes[172]. Similar to ESCRT, lipid raft domains undergo exosomal protein sorting in a ubiquitin-dependent platform[67]. Lipid-raft associated proteins such as flotillin, stomatin, CD55 are screted into exosome through clustering of proteins into lipid rafts due to the presence of lipid-raft like domain, or affinity properties associated with lipid-raft domains[175]. Heat shock proteins (e.g., HSP70, HSP90) are also found in exosomes [174]. Heat shock proteins are overexpressed in cancers involving in cancer cell proliferation, differentiation, invasion, and death[176]. The proteins from other organelles such as endoplasmic reticulum, mitochondria or nucleus are usually not detected in exosomes.

Table 2.3 Protein composition in exosomes

Proteins category	Proteins	Function	Cells	Comments	Ref.
Tetraspanin	CD9	Signal transduction, cell adhesion and spreading	Most cells	Commonly used as exosomal markers, interact with many proteins, associated with cancer	[24][110, 177, 178]
	CD81	Immune regulation, monocyte fusion			
	CD82	Cell adhesion,			

		migration, apoptosis, and morphogenesis.			
	CD63	Influences activity and stability of integrin, regulation of other proteins in tumor development, cell survival and apoptosis			
Antigen presentation molecules	MHC I, II	Stimulates T lymphocytes for immune response	Dendritic cells, B lymphocytes, epithelium	Cell-specific proteins	[179, 180]
ESCRT associated proteins	Alix	Involved in apoptosis	Most cells	Exosomal marker	[181]
	TSG101	Ubiquitin recognition, cell cycle, and growth, mediates other proteins (e.g., connexin)	Most cells	Exosomal marker	[182-184]
Membrane transport and fusion	Rab	Regulates exosome secretion	Many cells, e.g., Hela	Rab27a and -27b control different steps in exosome secretion pathway	[34, 40, 174]
	Annexin	Mediates membrane cytoskeleton dynamics and membrane fusion	Many cells	Annexin-V binding is Ca^{2+} dependent	[185, 186]
Heat shock protein	HSP70	Protein loading and folding, regulates immune response, tumor cells survival	Most cells	Tumor-derived exosomes/cells have higher level than normal control	[15, 187, 188]
	HSP90	Protein loading and folding, signal	Most cells	the level in cancer cells is 2-10 fold higher than normal	[189, 190]

		transduction		cell	
Lipid-raft associated proteins	Flotillin	Protein sorting, signaling, interacts with cytoskeleton	Many cells, e.g., HeLa, N2a cells	Flotillin-1 has been used as exosomal marker	[191, 192]
	Stomatin	Mediates ion channels and transporters, associated with cell fusion	Many cells, e.g., red blood cells	Localizes to the membrane	[185, 193-196]
Cytoskeletal proteins	Actin	Interacts with proteins, mediates cell motility, maintains cell shape and polarity	Many cells	Cellular actin involved in exosome uptake, exosomes have lower expression level than cells.	[14, 141, 197, 198]
	Tubulin	Involves in cell division and cellular function	Many cells	Tubulin was confirmed in exosomes derived from 23 amniotic fluids	[14, 199, 200]

ESCRT-endosomal sorting complex required for transport, MHC-major histocompatibility complex.

The exosomes are biologically and functionally distinguished in various types of cells attributed to cell-specific proteins. B lymphocytes and dendritic cells (DCs) derived exosomes contain antigen proteins major histocompatibility complex (MHC) class-I and -II[180]. LNCaP cancer cell-derived exosomes expressing Fas ligand trigger the apoptotic cascade of T cells to inhibit the cell proliferation[201]. Some tumor-derived exosomes are associated with tumorigenesis and metastasis via transfer of adhesion molecules, metalloproteinases, miRNA, and tissue-specific proteins to surrounding normal cells/tissues[202].

The exosome is a double layer vesicle and enriched with lipids including cholesterol, sphingolipids, phosphatidylethanolamine, phosphatidylcholine, and glycerophospholipids, originating from cellular lipids[203]. Cholesterol is abundant in cells and has high affinity with

associated proteins, such as tetraspannins[86, 171, 204]. Lysobisphosphatidic acid (LBPA) regulates the formation of intraluminal membranes within late endosomes[205, 206].

Exosomes contain nucleic acids including DNA and RNA. Exosomes can exchange the genetic information in cells by transferring nucleic acids such as mRNA, miRNA or DNA [7, 207, 208]. The miRNA is non-coding RNA involved in cell differentiation, replication, and regeneration[209]. It mediates messenger RNA (mRNA) or protein levels through degrading mRNA and/or blocking translation of protein[210]. The aberrant miRNA level is associated with physiological and pathological changes in many diseases. The miRNA-1 and miRNA-133 are reported to be significantly enhanced in serum exosomes derived from patients with cardiovascular disease, indicating pathological alterations of myocardium[211]. Double-stranded DNA (dsDNA) is commonly present in cancer-derived exosomes, including melanoma, chronic myeloid leukemia, lung, colon, pancreatic, breast and prostate cancers[7].

In addition to mitochondrial DNA (mtDNA) and single-stranded DNA (ssDNA) [74,75], tumor exosomes have also been shown to contain double-stranded DNA (dsDNA). Recently, Thakur and colleagues identified dsDNA of mutated KRAS and p53 within exosomes derived from pancreatic cancer cells, and these mutations were the most frequent mutations in human pancreatic cancer [39]. The exosomal DNA has been demonstrated to be associated with mutational status of parent mutation cells both *in vitro* and *in vivo*, in which EGFR mutation was detected in H292 (WT), H1975, H1650 and PC-9 cells, and BRAF(V600E) mutation were found in plasma exosomes derived from melanoma-bearing mice[7].

Size, density and surface properties

It is important to characterize exosomes collected from various biological fluids. The size of exosomes can be measured by nanoparticle tracking analysis (NTA) or dynamic light scattering (DLS) instruments. Both NTA and DLS visualize the particle size by measuring Brownian

motion of particles in the liquid, in which Stokes-Einstein equation obtains the hydrodynamic size distribution from velocity, Boltzmann's constant, diffusion constant, and absolute temperature[212-214]. NTA can measure more dilute samples (e.g., 1000 times) and has higher resolution, and DLS has a wider non-diluted concentration window detection, and is faster in evaluating mean size and polydispersity. Transmission electron microscopy (TEM) is a common technique used to analyze the size and morphology of exosomes. The negative staining TEM characterizes exosomes in a cup or spherical shape with a diameter of 50-150 nm[215].

Zeta potential (ζ) is a commonly used to characterize the surface charge of particles in suspension reflecting particle stability. It determines the electrical potential of interfacial double layer at the location in slipping/shear plane from particle surface[216]. Zeta potential can be measured by Zetasizer, electrophoretic light scattering (ELS), or other Zeta Potential Analyzers. Exosomes usually have negatively charged surface due to the presence of anionic phospholipid in the vesicle membrane. The Calu-3 exosomes had a zeta potential of −31.0 ± 1.1 mV[217]. B16-BL6-derived exosomes were characterized with a size of 66 ± 11 nm and zeta potential of −44.9 ± 1.5 mV[218]. Charoenviriyakul et al. reported exosomes with a size of 100-120 nm and zeta potential of -35 to -45 mV originated from multiple murine cell lines[140].

Varies techniques may vary in characterizing the same particles. A comparison of techniques used for exosome characterization is illustrated in Table 2.4. Pol et al. compared four techniques, namely, TEM, NTA, flow cytometry and resistive pulse sensing (RPS) in obtaining the size and concentration of urine vesicles, which was varied in size distribution and concentration[219]. The minimum detectable size of NTA was 70–90 nm, which was similar to RPS method of 70–100 nm. The vesicles at a size of 150–190 nm were determined by dedicated flow cytometry, and submicron size of 270–600 nm was measured when using conventional flow cytometry. TEM

had the highest resolution with the vesicle size down to 1 nm. NTA and RPS showed a concentration of ~10^{10} particles/mL for urine vesicles, much higher than TEM method (10^9 particles/mL) and flow cytometry (10^7-10^8 particles/mL). The density of exosomes (1.10-1.21 g/mL) can be obtained by characterizing fractions of suspension with exosomes floating in a sucrose density gradient[220].

Table 2.4 Comparison of various techniques used for exosome characterization

Methods	Advantages	Disadvantage	Measurement
NTA	Can visualize the particle movement, high resolution	Less repeatable than DLS	Size
DLS	wide non-diluted concentration window, high reproducibility	Low resolution, may suffer from multiple light scattering	Size
AFM	Provides 3D surface profile, high resolution	Slow, single scan image size, image artifacts	Size, morphology
TEM	High resolution	Only provides 2D image, complicated sample preparation, high cost	Size, morphology
Western blot	High sensitivity and specificity	Time-consuming, limited sample number at a time	Proteins
ELISA	Quick, convenient, high sensitivity, strong specificity	Cross-reactivity, non-specific antigen immobilization	Proteins
Mass spectrometry	Small sample size, fast	Limited analysis of molecules with similarly fragmented ions, need pure sample	Lipid, protein
Gel electrophoresis	Simple, low cost, reliable	semi-quantitative, limited sample analysis	Protein
BCA assay	Simple, fast	Low sensitivity	Total protein amount

Flow cytometry	Accurate, fast	Expensive, require live cells	Size, protein
RT-qPCR	Effective, less contamination, convenient	Low sensitivity and specificity, less reproducibility	RNA

Mass spectrometry-based method

Mass spectrometry (MS) is increasingly involved in biological applications, including complex protein samples. The protein is analyzed by sorting ionized species based on mass-to-charge ratio. Proteomics and lipidomics are a large-scale analysis of proteins and lipid profiles in a biological system, respectively[221, 222]. The MS technique makes it possible to profile and interpret the function of exosomes at both protein and lipid level. Incorporating with another method such as liquid chromatography (LC) or gas chromatography (GC) into MS is possible to synergistically enhance the capabilities of individual methods. Pisitkun et al. identified 295 unique proteins in urinal exosomes, including 73 proteins related to membrane trafficking by LC-MS/MS method[223]. Most of identified proteins were associated with cytoplasm and plasma membrane origin. In contrast, few proteins were found to be related to mitochondria, nucleus, Golgi apparatus or endoplasmic reticulum. The total lipids of exosomes can be extracted by Bligh and Dyer's method based on liquid−liquid phase extraction for lipidomic analysis[224]. Other lipid extraction method may also be used, such as Soxhlet, Roese-Gottlieb, or modified Bligh and Dyer[225, 226]. The lipidomic profile of prostate cancer cell PC-3 derived exosomes was achieved by MS method[227]. The PC-3 derived exosomes were characterized of 217 lipid species, with 190 species as common as PC cells. The PC-3 derived exosomes consisted of a higher proportion of PS than their parent cells[227].

Antibody-based method

Western blot is widely used in specific protein identification in biological fields. Exosomes are enriched of many proteins such as tetraspanin including CD9, CD81, CD82, CD83, and CD63, Alix and TGS101. These enriched proteins are used as common markers in Western blot to identify exosomes[228, 229]. Calnexin is a chaperone involving in protein folding, assembly, and retaining[230], and is always used as a negative marker since it is endoplasmic reticulum marker and only exists in cells rather than exosomes[231]. Nuceoporin is also reported as a negative marker[232]. The enzyme-linked immunosorbent assay (ELISA) is not commonly used, but could also be a technique to detect and/quantify species such as protein in exosomes. Exosomes derived from dendric cells are reported to play significant roles in anti-inflammatory and immune response[233, 234]. The immature bone marrow dendritic cells (BMDC)-derived exosomes were demonstrated to contain high level of MHC-I and -II antigens by ELISA method[235].

Exosome labeling and tracking

The exosomes are critical in cell-to-cell communication, and it is important to track exosomes in microenvironment for studies in *in vitro* and *in vivo*. The fluorescent probe can be used to label the exosomes, and a summary of currently used exosome labeling probe is made in Table 2.5. A membrane-bound lipophilic fluorescent probe such as PKH26 and PKH67 can be used to label exosome through interaction with membrane. The PKH26 labeled K562-exosomes demonstrated the internalization of exosomes in perinuclear region of HUVECs and cytoplasm of CCD-27Sk cells. When mixing the HUVECs from treatment with either PKH26 or PKH67 labelled exosomes, both the red and green exosomes were observed in cells within the tubular network after 4 h, suggesting the exosome transfer between neighbor cells[236].

It is possible to label exosomes by exosomal markers tagged with fluorescent protein such as green fluorescent protein (GFP) and/or red fluorescent protein (RFP). Suetsugu et al. reported a GFP-CD63 probe to label exosomes by anchoring the enriched CD63 proteins both in *in vitro* and *in vivo*. Indirectly labeling of exosomes is possible by transfecting the cells with plasmids overexpressing fluorescent proteins. Fluorescent proteins can be sorted into exosomes through tagging with membrane proteins. The N-Rh-PE-labeled Jurkat T-cells are reported to secrete fluorescent exosomes when using a myristoyl tag and/or PIP2- binding domain[111].

Chemoluminescence probe such as luciferase can be used for exosome probe as well. The Gaussia luciferase and a truncated lactadherin, gLuc-lactadherin (gLuc-LA) have been used for *in vivo* tracking of exosomes[218]. The gLuc-LA was introduced into the B16-BL6 cells by transfection with plasmid overexpressing gLuc-LA. The released exosomes showed strong luciferase activity as luminescence and were injected into mice at a dose of 1×10^{10} RLU (~5 μg protein)/shot for biodistribution studies. The gLuc activity indicated that exosomes were mainly in liver and lung. Exosomes labeled with PKH26 showed a similar biodistribution pattern with most of exosomes detected in liver, spleen, and lung. These exosomes had a short half-life in *in vivo* administration[218].

Table 2.5 Exosome labeling methods

Categories	Labelling Probes	Examples	Comments	Reference
Fluorescent labeling	PKH26	PKH26 labeled exosomes were used for internalization and communication tracking in HUVECs cells and *in vivo* mice injection at a dose of 2 μg/shot	Red fluorescence, widely used, very stable	[236, 237]
	PKH67	The PKH67-labelled exosomes accessed into HBMVEC cells	Green fluorescence, widely used, moderate stable	[47]

	DiI	B16 melanoma exosomes were labeled with 1.0 μmol/L DiI or DiR	Lipophilic dye, Excitation 549 nm/Emission 565 nm	[238]
	DiR		Lipophilic dye, Excitation 750 nm/ Emission 780, Melanoma exosomes preferably homed to ipsilateral sentinel lymph nodes after 48 h from footpad injection	
	DiD and TAMRA-NHS	PC12 derived exosomes were dual labeled with DiD and TAMRA-NHS	Labeled exosomes were achieved by 10 min incubation with DiD and 1 h incubation with TAMRA-NHS.	[198]
Exosomal marker labeling	GFP tagged CD63	GFP-exosomes entered RFP labeled breast cancer cells. MDA-MB-231-RFP/GFP-exosomes were injected in mice, and newly secreted exosomes from lung mainly went to tumor-surrounding tissue	GFP or RFP fused exosomal protein markers could be used to track exosomes	[239]
Transfection labeling	N-Rh-PE	Fluorescent-labeled Jurkat T-cells were able to secrete fluorescent exosomes	N-Rh-PE labeling was used as a control for evaluation of GFP labeled protein	[111]
	GFP	Jurkat T cells were transfected with expressing MusD-GFP, AcylMusD-GFP, TyA-GFP-2xFYVE, CD43-TyA-GFP, GFP-SYN, AKT-GFP	Myristoyl tag and/or PIP2-binding domain Acylation Tag could target proteins to exosomes	
	gLuc-LA	The gLuc-LA exosomes were tail vein injected into mice at a dose of 5 μg/200 μl/shot.	Chemiluminescent probe, Labeled by gLuc-LA-expressing plasmid vectors with polyethylenimine matrix	[140, 218]

2.6 EXOSOME AS BIOMARKER FOR CANCER

The unique properties of exosomes make them potential biomarkers for many diseases, such as cancer, neurological disorder, and cardiovascular disease[94, 240, 241]. The exosomal components, such as miRNA and/or proteins, are associated with pathological diseases and can act as critical biomarkers for diagnosis, as well as prognosis of therapeutic effects during the treatment.

Exosome quantity

The elevated exosomes in biological fluid such as plasma are reported as diagnostic markers for some types of cancer[242, 243]. The exosome level is associated with the stage of cancer; more exosomes are reported to be released in advanced stage than early stage. Taylor et. al. reported that stage III of ovarian cancer patients had a plasma exosome level of 0.995 ± 0.084 mg protein/mL, which was higher than stage II level of 0.640 ± 0.053 mg/ml, and this was further increased to 1.42 ± 0.228 mg/mL at stage IV, all of which were much higher than patients with benign ovarian disease (0.149 ± 0.065 mg/mL)[244]. However, the exosome level is not a universal diagnosis marker for all biological fluids. Mitchell et al. reported that the quantity of urinary exosome was highly variable in patients and could not be used as a biomarker in clinical diagnosis for PCa, since the level of exosomes derived from patients could not be discriminated from heathy donors[166].

Exosomal lipids

Exosomes are enriched in lipids such as lysophosphatidylcholine (LPC)[245], and lipid species are potential biomarkers for cancer. For example, Skotland et al. demonstrated urinary exosome as prostate cancer (PCa) biomarker by comparing nine different lipid species of exosomes derived from 15 PCa patients and 13 healthy donors. The patients-derived urinary

exosomes always showed higher levels of hexosylceramide and lactosylceramide than healthy controls. The phosphatidylserine was less in patient-derived exosomes than healthy controls[246].

Exosomal RNA

Circular RNAs (circRNAs) are noncoding RNAs with cell type-specific properties that can modulate gene expression[247]. The circRNAs are commonly enriched in exosomes derived from various cancer cells. The expression level of exosomal circRNAs was confirmed to be much higher (> 2-fold) than those in producer cells by RNA-seq and quantitative PCR analysis. A *in vivo* xenograft mouse model study demonstrated that tumor-derived exo-circRNA was detectable in serum and was correlated with tumor mass, suggesting a potential role as a biomarker for cancer detection. A further investigation of exo-circRNA from cancer patients indicated different profile of exo-circRNAs with 67 species missing and 257 new species in healthy donors and upregulated expression of circ-KLDHC10 in cancer serum[248].

Another type of noncoding RNA, microRNA (miRNA) modulating the translation of mRNAs has been associated with various cancers and attracted intensive interest as potential biomarkers[244, 249, 250]. Exosomal miRNA is reported to be detected only in ovarian cancer patients but not normal controls, enhanced miRNA level was observed in patients with stage I, II, III ovarian cancer than benign disease[244]. Twelve tumor-associated specific miRNAs in cells including hsa-miR-17-3p, hsa-miR-21, hsa-miR-106a, hsa-miR-146, hsa-miR-155, hsa-miR-191, hsa-miR-192, hsa-miR-203, hsa-miR-205, hsa-miR-210, hsa-miR-212, and hsa-miR-214 were correlated to exosome encapsulation, which was enhanced in non-small cell lung cancer (NSCLC) compared to non-detectable normal controls[251]. Two miRNAs (miR-1290 and miR-375) are reported as prognostic biomarkers for prostate cancer. High levels of exosomal miR-1290 and miR-375 in serum were correlated with a high mortality rate (~80%) in patients with prostate cancer[252]. *In vitro* studies showed significantly higher levels of miRNAs including

miR-23a, miR-1229, miR-1246, miR-150, miR-21, miR-223, and let-7a in exosomes derived from colon cancer cells than normal controls, and serum-derived exosomes also showed much higher expression level of these miRNAs in colorectal cancer (CRC) patients compared to healthy controls, which was greatly reduced by surgical removal of tumors[253].

Serum exosomal miR-19a may be a potential biomarker of prognosis for CRC. Exosomal miR-17-92a cluster in serum is reported to be involved in the recurrence of CRC. The expression level of serum-derived exosomal miRNAs such as miR-19a (situated at miR-17-92a locus) was significantly enhanced in CRC patients when compared with healthy donors[254]. Serum exosomal miR-21 is reported as a potential biomarker for the early detection of hepatocellular carcinoma (HCC). The expression of serum exosomal miR-21 was positively related to cirrhosis and tumor stage but did not correlate with other clinical parameters such as age, gender, and HBV infection. Upregulated expression of exosomal miR-21 in serum was observed in HCC patients compared to healthy controls[255]. The serum exosomal miR-21 is also demonstrated as a clinical biomarker for poor prognostic esophageal cancer, which is common in non-Western countries and mainly caused by smoking and alcohol consumption. The serum miR-21 in the Esophageal squamous cell carcinoma (ESCC) group was significantly upregulated compared to control group[250]. The expression level of serum exosomal miR-373 was demonstrated to be higher in triple negative breast cancer patients than luminal breast cancer and healthy women. The miR-373 showed no influence on cell proliferation but could inhibit the stimulated apoptosis of cells[256]. Expression profiles determined by qRT-PCR indicated that serum miR-19b-3p and miR-106a-5p were significantly enhanced in the exosomes of gastric cancer patients, and the combination of these two miRNAs was a potential signature for gastric cancer detection[257].

Exosomal DNA

The DNA in exosomes reflects the genomic DNA in parental producing cells and the mutation in exosomal DNA can be used to identify the gene mutations in parental cells. Serum exosomal DNA is reported to be detectable in patients with pancreatic cancer regarding $KRAS^{G12D}$ and $TP53^{R273H}$ mutation. Patients with pancreas-associated pathologies showed a higher frequency of $KRAS^{G12D}$ and $TP53^{R273H}$ mutations in serum exosomes than healthy controls[258]. Double-stranded dsDNA is reported to be the major exosomal DNA in various cell lines (e.g., leukemia, lung and breast cancer cells). The mutated parental cells secreted the exosomes with detectable mutations, such as EGFR and BRAF(V600E) mutation, in DNA as well. *In vivo* animal model of melanoma (SK-MEL-28) showed the BRAF(V600E) mutation in exosomal DNA in serum samples by AS-PCR[7]. Hence, the exosomal DNA might be a potential biomarker for the diagnosis and prognosis of cancer and its metastasis.

Exosomal proteins

Transcript factors such as ATF3 and WT-1, and Fetuin-A protein in urine exosome are reported as biomarkers for acute kidney injury[259, 260]. The exosomal protein survivin is more stable and efficient biomarker than prostate-specific antigen (PSA) for diagnosis of early staged PCa[261]. Li. Et al. reported different expression level of leucine-rich α-2-glycoprotein (LRG1) protein in urinary exosome in NSCLC patients and healthy controls[262]. The presence of LRG1 was detected in urine exosomes by MS/MS, and confirmed by Western blots with six-fold increasing of LRG1 expression level in NSCLC patients than controls, and immunohistochemistry indicated 65% of NSCLC samples were stained positive while 10% stained positive was found in controls[262]. To combine proteins and miRNA as biomarkers is likely to synergistically enhance the sensitivity and specificity of diagnosis and prognosis than individual biomarker. Madhavan et al. demonstrated the significantly improved sensitivity of

pancreatic cancer diagnosis by detecting pancreatic cancer-initiating cell (PaCIC) markers including CD44v6, Tspan8, EpCAM, MET and CD104, and miRNA in serum exosomes[263]. The screening of PaCIC markers showed that normal cell exosomes expressed CD9, CD24, CD63 and CD151 markers but had low or undetectable interaction with marker panel of -CD104, -Tspan8, -EpCAM, -MET, -CD44v6, which were all found in exosomes derived from both pancreatic cancer (PaCa) cells and patient serum. The quantity of miRNA was different in cell-derived exosomes (499 miRNAs) compared to patient-derived exosomes (201 miRNAs), of which four miRNAs, namely miR-1246, miR-4644, miR-3976, miR-4306, were enriched in both patient serum and *in vitro* cell supernatants, and this enrichment was also observed in exosome depleted PaCa. Microarray analysis indicated that individual miRNA could not determine false-positives or -negatives, and high reactivity was observed in the late stage of PaCa. The combination of PaCaCIC markers which was superior in early detection and miRNA that was reliable in tumor progression indicated that a significantly improved sensitivity of 1.0 with a specificity of 0.8 in patients with PaCa[263].

2.7 CONCLUSIONS

Exosomes are critical in regulating the intracellular communication and cellular function. The secretion of exosomes is mainly through endosome-mediated pathway. Beside the common ESCRT pathway responsible for ESCRT-associated proteins, other pathways such as lipid-raft pathway, syntenin-syndecan interactions, Rab family protein also participate in the exosomal protein sorting and secretion. The internalization of exosomes into recipient cells includes three steps: 1) the floating and approaching of exosomes to cells, 2) the interaction of proteins in the surface of exosomes and cells, 3) the internalization process and subsequent cellular trafficking inside the recipient cells. The exosomes can be internalized into cells through several

mechanisms, in which endocytosis is the major route. The uptake routes are dependent on the properties of both exosome and recipient cells. Membrane fusion is a less common pathway for exosome uptake but also an alternative mechanistic path for specific type of cells, e.g., DCs. Despite the effects, extensive investigations are still in need to fully understand the mechanism of exosomes' uptake. For example, there might be different pathways for uptake of the same type of exosomes into either tumor recipient or normal recipient cells due to different cell surface molecules.

Exosomes consist of lipids, nucleic acids, metabolites, and proteins and exosomal components, e.g., miRNA, reflect the biological status of their parental cell types, and some of them have been recognized as biomarker diagnosis for cancer. Particularly, the presence of exosomal miRNA is identified in various cancers and provides diagnosis and prognosis of therapeutic intervention during treatment. Given the success of exosomes isolation, characterization and discrimination of pathological diseases from normal controls in cell culture medium as well as in bodily fluids such as urine and plasma, it is worthwhile to harness exosomes as useful and efficient biomarkers for cancer diagnosis in the clinical field. However, these studies are still in their infantile phase, and further investigation is necessary to broaden exosome' application as biomarker in clinical settings as an alternative or addition to conventional biomarkers.

2.8 REFERENCES

1. Chairoungdua, A., D.L. Smith, P. Pochard, M. Hull, and M.J. Caplan, Exosome release of β-catenin: a novel mechanism that antagonizes Wnt signaling. J Cell Biol, 2010: p. jcb. 201002049.
2. Zhang, J., S. Li, L. Li, M. Li, C. Guo, J. Yao, and S. Mi, Exosome and Exosomal MicroRNA: Trafficking, Sorting, and Function. Genomics Proteomics Bioinformatics, 2015. 13(1): p. 17-24.
3. Yamashita, T., Y. Takahashi, M. Nishikawa, and Y. Takakura, Effect of exosome isolation methods on physicochemical properties of exosomes and clearance of exosomes from the blood circulation. Eur J Pharm Biopharm, 2016. 98: p. 1-8.
4. Wolfers, J., A. Lozier, G. Raposo, A. Regnault, C. Théry, C. Masurier, C. Flament, S. Pouzieux, F. Faure, and T. Tursz, Tumor-derived exosomes are a source of shared tumor rejection antigens for CTL cross-priming. Nat Med, 2001. 7(3): p. 297-303.
5. Pan, B.-T. and R.M. Johnstone, Fate of the transferrin receptor during maturation of sheep reticulocytes in vitro: selective externalization of the receptor. Cell, 1983. 33(3): p. 967-978.
6. Johnstone, R.M., M. Adam, J. Hammond, L. Orr, and C. Turbide, Vesicle formation during reticulocyte maturation. Association of plasma membrane activities with released vesicles (exosomes). J Biol Chem, 1987. 262(19): p. 9412-9420.
7. Thakur, B.K., H. Zhang, A. Becker, I. Matei, Y. Huang, B. Costa-Silva, Y. Zheng, A. Hoshino, H. Brazier, and J. Xiang, Double-stranded DNA in exosomes: a novel biomarker in cancer detection. Cell Res, 2014. 24(6): p. 766-769.
8. Kahlert, C., S.A. Melo, A. Protopopov, J. Tang, S. Seth, M. Koch, J. Zhang, J. Weitz, L. Chin, and A. Futreal, Identification of double-stranded genomic DNA spanning all chromosomes with mutated KRAS and p53 DNA in the serum exosomes of patients with pancreatic cancer. J Biol Chem, 2014. 289(7): p. 3869-3875.
9. Guescini, M., S. Genedani, V. Stocchi, and L.F. Agnati, Astrocytes and Glioblastoma cells release exosomes carrying mtDNA. J Neural Transm, 2010. 117(1): p. 1.
10. Schorey, J.S. and S. Bhatnagar, Exosome function: from tumor immunology to pathogen biology. Traffic, 2008. 9(6): p. 871-881.
11. Frydrychowicz, M., A. Kolecka-Bednarczyk, M. Madejczyk, S. Yasar, and G. Dworacki, Exosomes–Structure, Biogenesis and Biological Role in Non-Small-Cell Lung Cancer. Scand J Immunol, 2015. 81(1): p. 2-10.
12. Lancaster, G.I. and M.A. Febbraio, Exosome-dependent trafficking of HSP70 A novel secretory pathway for cellular stress proteins. J Biol Chem, 2005. 280(24): p. 23349-23355.
13. Raimondo, F., L. Morosi, C. Chinello, F. Magni, and M. Pitto, Advances in membranous vesicle and exosome proteomics improving biological understanding and biomarker discovery. Proteomics, 2011. 11(4): p. 709-720.
14. Théry, C., M. Boussac, P. Véron, P. Ricciardi-Castagnoli, G. Raposo, J. Garin, and S. Amigorena, Proteomic analysis of dendritic cell-derived exosomes: a secreted subcellular compartment distinct from apoptotic vesicles. J Immunol, 2001. 166(12): p. 7309-7318.
15. Denzer, K., M.J. Kleijmeer, H. Heijnen, W. Stoorvogel, and H.J. Geuze, Exosome: from internal vesicle of the multivesicular body to intercellular signaling device. J Cell Sci, 2000. 113(19): p. 3365-3374.

16. Colombo, M., G. Raposo, and C. Théry, Biogenesis, secretion, and intercellular interactions of exosomes and other extracellular vesicles. Annu Rev Cell Dev Biol, 2014. 30: p. 255-289.
17. Keller, S., M.P. Sanderson, A. Stoeck, and P. Altevogt, Exosomes: From biogenesis and secretion to biological function. Immunol Lett, 2006. 107(2): p. 102-108.
18. Lai, R.C., T.S. Chen, and S.K. Lim, Mesenchymal stem cell exosome: a novel stem cell-based therapy for cardiovascular disease. Regen Med, 2011. 6(4): p. 481-492.
19. Wang, Y., L. Zhang, Y. Li, L. Chen, X. Wang, W. Guo, X. Zhang, G. Qin, S.-h. He, and A. Zimmerman, Exosomes/microvesicles from induced pluripotent stem cells deliver cardioprotective miRNAs and prevent cardiomyocyte apoptosis in the ischemic myocardium. Int J Cardiol, 2015. 192: p. 61-69.
20. Vrijsen, K., J. Sluijter, M. Schuchardt, B. Van Balkom, W. Noort, S. Chamuleau, and P. Doevendans, Cardiomyocyte progenitor cell-derived exosomes stimulate migration of endothelial cells. J Cell Mol Med, 2010. 14(5): p. 1064-1070.
21. Webber, J., R. Steadman, M.D. Mason, Z. Tabi, and A. Clayton, Cancer exosomes trigger fibroblast to myofibroblast differentiation. Cancer Res, 2010. 70(23): p. 9621-9630.
22. Webber, J.P., L.K. Spary, A.J. Sanders, R. Chowdhury, W.G. Jiang, R. Steadman, J. Wymant, A.T. Jones, H. Kynaston, and M.D. Mason, Differentiation of tumour-promoting stromal myofibroblasts by cancer exosomes. Oncogene, 2015. 34(3): p. 290-302.
23. Syn, N., L. Wang, G. Sethi, J.-P. Thiery, and B.-C. Goh, Exosome-Mediated Metastasis: From Epithelial–Mesenchymal Transition to Escape from Immunosurveillance. Trends Pharmacol Sci, 2016. 37(7): p. 606-617.
24. Hoshino, A., B. Costa-Silva, T.-L. Shen, G. Rodrigues, A. Hashimoto, M.T. Mark, H. Molina, S. Kohsaka, A. Di Giannatale, and S. Ceder, Tumour exosome integrins determine organotropic metastasis. Nature, 2015. 527(7578): p. 329-335.
25. Al-Nedawi, K., B. Meehan, J. Micallef, V. Lhotak, L. May, A. Guha, and J. Rak, Intercellular transfer of the oncogenic receptor EGFRvIII by microvesicles derived from tumour cells. Nat Cell Biol, 2008. 10(5): p. 619-624.
26. Duijvesz, D., T. Luider, C.H. Bangma, and G. Jenster, Exosomes as Biomarker Treasure Chests for Prostate Cancer. Eur Urol, 2011. 59(5): p. 823-831.
27. Simons, M. and G. Raposo, Exosomes–vesicular carriers for intercellular communication. Curr Opin Cell Biol, 2009. 21(4): p. 575-581.
28. Thery, C., L. Zitvogel, and S. Amigorena, Exosomes: composition, biogenesis and function. Nat Rev Immunol, 2002. 2(8): p. 569-579.
29. Savina, A., M. Furlán, M. Vidal, and M.I. Colombo, Exosome release is regulated by a calcium-dependent mechanism in K562 cells. J Biol Chem, 2003. 278(22): p. 20083-20090.
30. Hsu, C., Y. Morohashi, S.-i. Yoshimura, N. Manrique-Hoyos, S. Jung, M.A. Lauterbach, M. Bakhti, M. Grønborg, W. Möbius, and J. Rhee, Regulation of exosome secretion by Rab35 and its GTPase-activating proteins TBC1D10A–C. J Cell Biol, 2010. 189(2): p. 223-232.
31. Yu, X., S.L. Harris, and A.J. Levine, The regulation of exosome secretion: a novel function of the p53 protein. Cancer Res, 2006. 66(9): p. 4795-4801.
32. Stenmark, H., Rab GTPases as coordinators of vesicle traffic. Nat Rev Mol Cell Biol, 2009. 10(8): p. 513-525.

33. Chavrier, P. and B. Goud, The role of ARF and Rab GTPases in membrane transport. Curr Opin Cell Biol, 1999. 11(4): p. 466-475.
34. Grosshans, B.L., D. Ortiz, and P. Novick, Rabs and their effectors: achieving specificity in membrane traffic. Proc Natl Acad Sci, 2006. 103(32): p. 11821-11827.
35. Rowe, R.K., J.W. Suszko, and A. Pekosz, Roles for the recycling endosome, Rab8, and Rab11 in hantavirus release from epithelial cells. Virology, 2008. 382(2): p. 239-249.
36. Hutagalung, A.H. and P.J. Novick, Role of Rab GTPases in membrane traffic and cell physiology. Physiol Rev, 2011. 91(1): p. 119-149.
37. Rink, J., E. Ghigo, Y. Kalaidzidis, and M. Zerial, Rab conversion as a mechanism of progression from early to late endosomes. Cell, 2005. 122(5): p. 735-749.
38. Savina, A., M. Vidal, and M.I. Colombo, The exosome pathway in K562 cells is regulated by Rab11. J Cell Sci, 2002. 115(12): p. 2505-2515.
39. Savina, A., C.M. Fader, M.T. Damiani, and M.I. Colombo, Rab11 promotes docking and fusion of multivesicular bodies in a calcium-dependent manner. Traffic, 2005. 6(2): p. 131-143.
40. Ostrowski, M., N.B. Carmo, S. Krumeich, I. Fanget, G. Raposo, A. Savina, C.F. Moita, K. Schauer, A.N. Hume, and R.P. Freitas, Rab27a and Rab27b control different steps of the exosome secretion pathway. Nat Cell Biol, 2010. 12(1): p. 19-30.
41. Stenmark, H., R.G. Parton, O. Steele-Mortimer, A. Lütcke, J. Gruenberg, and M. Zerial, Inhibition of rab5 GTPase activity stimulates membrane fusion in endocytosis. EMBO J, 1994. 13(6): p. 1287.
42. Hurley, J.H. and G. Odorizzi, Get on the exosome bus with ALIX. Nat Cell Biol, 2012. 14(7): p. 654-655.
43. Feng, Y., B. Press, and A. Wandinger-Ness, Rab 7: an important regulator of late endocytic membrane traffic. J Cell Biol, 1995. 131(6): p. 1435-1452.
44. Baietti, M.F., Z. Zhang, E. Mortier, A. Melchior, G. Degeest, A. Geeraerts, Y. Ivarsson, F. Depoortere, C. Coomans, and E. Vermeiren, Syndecan-syntenin-ALIX regulates the biogenesis of exosomes. Nat Cell Biol, 2012. 14(7): p. 677-685.
45. Grootjans, J.J., G. Reekmans, H. Ceulemans, and G. David, Syntenin-syndecan binding requires syndecan-synteny and the co-operation of both PDZ domains of syntenin. J Biol Chem, 2000. 275(26): p. 19933-19941.
46. Grootjans, J.J., P. Zimmermann, G. Reekmans, A. Smets, G. Degeest, J. Dürr, and G. David, Syntenin, a PDZ protein that binds syndecan cytoplasmic domains. Proc Natl Acad Sci, 1997. 94(25): p. 13683-13688.
47. Zimmermann, P., K. Meerschaert, G. Reekmans, I. Leenaerts, J.V. Small, J. Vandekerckhove, G. David, and J. Gettemans, PIP 2-PDZ domain binding controls the association of syntenin with the plasma membrane. Mol Cell, 2002. 9(6): p. 1215-1225.
48. Zimmermann, P., Z. Zhang, G. Degeest, E. Mortier, I. Leenaerts, C. Coomans, J. Schulz, F. N'Kuli, P.J. Courtoy, and G. David, Syndecan Recyling Is Controlled by Syntenin-PIP 2 Interaction and Arf6. Dev Cell, 2005. 9(3): p. 377-388.
49. Roucourt, B., S. Meeussen, J. Bao, P. Zimmermann, and G. David, Heparanase activates the syndecan-syntenin-ALIX exosome pathway. Cell Res, 2015. 25(4): p. 412-428.
50. Friand, V., G. David, and P. Zimmermann, Syntenin and syndecan in the biogenesis of exosomes. Biol Cell, 2015. 107(10): p. 331-341.
51. D'Souza-Schorey, C. and P. Chavrier, ARF proteins: roles in membrane traffic and beyond. Nat Rev Mol Cell Biol, 2006. 7(5): p. 347-358.

52. D'Souza-Schorey, C., E. van Donselaar, V.W. Hsu, C. Yang, P.D. Stahl, and P.J. Peters, ARF6 targets recycling vesicles to the plasma membrane: insights from an ultrastructural investigation. J Cell Biol, 1998. 140(3): p. 603-616.
53. Ghossoub, R., F. Lembo, A. Rubio, C.B. Gaillard, J. Bouchet, N. Vitale, J. Slavík, M. Machala, and P. Zimmermann, Syntenin-ALIX exosome biogenesis and budding into multivesicular bodies are controlled by ARF6 and PLD2. Nat Commun, 2014. 5: p. ncomms4477.
54. Imjeti, N.S., K. Menck, A.L. Egea-Jimenez, C. Lecointre, F. Lembo, H. Bouguenina, A. Badache, R. Ghossoub, G. David, and S. Roche, Syntenin mediates SRC function in exosomal cell-to-cell communication. Proc Natl Acad Sci, 2017. 114(47): p. 12495-12500.
55. Colombo, M., C. Moita, G. van Niel, J. Kowal, J. Vigneron, P. Benaroch, N. Manel, L.F. Moita, C. Théry, and G. Raposo, Analysis of ESCRT functions in exosome biogenesis, composition and secretion highlights the heterogeneity of extracellular vesicles. J Cell Sci, 2013. 126(24): p. 5553-5565.
56. Raiborg, C. and H. Stenmark, The ESCRT machinery in endosomal sorting of ubiquitylated membrane proteins. Nature, 2009. 458(7237): p. 445-452.
57. Henne, W.M., N.J. Buchkovich, and S.D. Emr, The ESCRT pathway. Dev Cell, 2011. 21(1): p. 77-91.
58. Hurley, J.H., ESCRT complexes and the biogenesis of multivesicular bodies. Curr Opin Cell Biol, 2008. 20(1): p. 4-11.
59. Teis, D., S. Saksena, B.L. Judson, and S.D. Emr, ESCRT-II coordinates the assembly of ESCRT-III filaments for cargo sorting and multivesicular body vesicle formation. EMBO J, 2010. 29(5): p. 871-883.
60. Tang, S., N.J. Buchkovich, W.M. Henne, S. Banjade, Y.J. Kim, and S.D. Emr, ESCRT-III activation by parallel action of ESCRT-I/II and ESCRT-0/Bro1 during MVB biogenesis. Elife, 2016. 5: p. e15507.
61. Gingras, M.-C., J.M. Kazan, and A. Pause, Role of ESCRT component HD-PTP/PTPN23 in cancer. Biochem Soc Trans, 2017. 45(3): p. 845-854.
62. Mayers, J.R., I. Fyfe, A.L. Schuh, E.R. Chapman, J.M. Edwardson, and A. Audhya, ESCRT-0 assembles as a heterotetrameric complex on membranes and binds multiple ubiquitinylated cargoes simultaneously. J Biol Chem, 2011. 286(11): p. 9636-9645.
63. Ren, X. and J.H. Hurley, VHS domains of ESCRT-0 cooperate in high-avidity binding to polyubiquitinated cargo. EMBO J, 2010. 29(6): p. 1045-1054.
64. Tamai, K., N. Tanaka, T. Nakano, E. Kakazu, Y. Kondo, J. Inoue, M. Shiina, K. Fukushima, T. Hoshino, and K. Sano, Exosome secretion of dendritic cells is regulated by Hrs, an ESCRT-0 protein. Biophys Res Commun, 2010. 399(3): p. 384-390.
65. Demirov, D.G., A. Ono, J.M. Orenstein, and E.O. Freed, Overexpression of the N-terminal domain of TSG101 inhibits HIV-1 budding by blocking late domain function. Proc Natl Acad Sci, 2002. 99(2): p. 955-960.
66. Lu, Q., L.W. Hope, M. Brasch, C. Reinhard, and S.N. Cohen, TSG101 interaction with HRS mediates endosomal trafficking and receptor down-regulation. Proc Natl Acad Sci, 2003. 100(13): p. 7626-7631.
67. de Gassart, A., C. Géminard, B. Février, G. Raposo, and M. Vidal, Lipid raft-associated protein sorting in exosomes. Blood, 2003. 102(13): p. 4336-4344.

68. Stuchell, M.D., J.E. Garrus, B. Müller, K.M. Stray, S. Ghaffarian, R. McKinnon, H.-G. Kräusslich, S.G. Morham, and W.I. Sundquist, The human endosomal sorting complex required for transport (ESCRT-I) and its role in HIV-1 budding. J Biol Chem, 2004. 279(34): p. 36059-36071.
69. Katzmann, D.J., C.J. Stefan, M. Babst, and S.D. Emr, Vps27 recruits ESCRT machinery to endosomes during MVB sorting. J Cell Biol, 2003. 162(3): p. 413-423.
70. Hurley, J.H. and P.I. Hanson, Membrane budding and scission by the ESCRT machinery: it's all in the neck. Nat Rev Mol Cell Biol, 2010. 11(8): p. 556-566.
71. Williams, R.L. and S. Urbé, The emerging shape of the ESCRT machinery. Nat Rev Mol Cell Biol, 2007. 8(5): p. 355-368.
72. Wollert, T. and J.H. Hurley, Molecular mechanism of multivesicular body biogenesis by ESCRT complexes. Nature, 2010. 464(7290): p. 864-869.
73. Babst, M., D.J. Katzmann, W.B. Snyder, B. Wendland, and S.D. Emr, Endosome-associated complex, ESCRT-II, recruits transport machinery for protein sorting at the multivesicular body. Dev Cell, 2002. 3(2): p. 283-289.
74. Hierro, A., J. Sun, A.S. Rusnak, J. Kim, G. Prag, S.D. Emr, and J.H. Hurley, Structure of the ESCRT-II endosomal trafficking complex. Nature, 2004. 431(7005): p. 221-225.
75. Teo, H., O. Perisic, B. González, and R.L. Williams, ESCRT-II, an Endosome-Associated Complex Required for Protein Sorting: Crystal Structure and Interactions with ESCRT-III and Membranes. Dev Cell, 2004. 7(4): p. 559-569.
76. Parkinson, M.D., S.C. Piper, N.A. Bright, J.L. Evans, J.M. Boname, K. Bowers, P.J. Lehner, and J.P. Luzio, A non-canonical ESCRT pathway, including histidine domain phosphotyrosine phosphatase (HD-PTP), is used for down-regulation of virally ubiquitinated MHC class I. Biochem J, 2015. 471(1): p. 79-88.
77. Babst, M., D.J. Katzmann, E.J. Estepa-Sabal, T. Meerloo, and S.D. Emr, Escrt-III: an endosome-associated heterooligomeric protein complex required for mvb sorting. Dev Cell, 2002. 3(2): p. 271-282.
78. Slagsvold, T., K. Pattni, L. Malerød, and H. Stenmark, Endosomal and non-endosomal functions of ESCRT proteins. Trends in cell biology, 2006. 16(6): p. 317-326.
79. Gahloth, D., C. Levy, G. Heaven, F. Stefani, L. Wunderley, P. Mould, M.J. Cliff, J. Bella, A.J. Fielding, and P. Woodman, Structural basis for selective interaction between the ESCRT regulator HD-PTP and UBAP1. Structure, 2016. 24(12): p. 2115-2126.
80. Pires, R., B. Hartlieb, L. Signor, G. Schoehn, S. Lata, M. Roessle, C. Moriscot, S. Popov, A. Hinz, and M. Jamin, A crescent-shaped ALIX dimer targets ESCRT-III CHMP4 filaments. Structure, 2009. 17(6): p. 843-856.
81. Yorikawa, C., H. Shibata, S. Waguri, K. Hatta, M. Horii, K. Katoh, T. Kobayashi, Y. Uchiyama, and M. Masatoshi, Human CHMP6, a myristoylated ESCRT-III protein, interacts directly with an ESCRT-II component EAP20 and regulates endosomal cargo sorting. Biochem J, 2005. 387(1): p. 17-26.
82. Wollert, T., C. Wunder, J. Lippincott-Schwartz, and J.H. Hurley, Membrane scission by the ESCRT-III complex. Nature, 2009. 458(7235): p. 172-177.
83. Scott, A., J. Gaspar, M.D. Stuchell-Brereton, S.L. Alam, J.J. Skalicky, and W.I. Sundquist, Structure and ESCRT-III protein interactions of the MIT domain of human VPS4A. Proc Natl Acad Sci, 2005. 102(39): p. 13813-13818.
84. Lingwood, D. and K. Simons, Lipid rafts as a membrane-organizing principle. Science, 2010. 327(5961): p. 46-50.

85. Staubach, S. and F.-G. Hanisch, Lipid rafts: signaling and sorting platforms of cells and their roles in cancer. Expert Rev Proteomics, 2011. 8(2): p. 263-277.
86. Wubbolts, R., R.S. Leckie, P.T. Veenhuizen, G. Schwarzmann, W. Möbius, J. Hoernschemeyer, J.-W. Slot, H.J. Geuze, and W. Stoorvogel, Proteomic and biochemical analyses of human B cell-derived exosomes Potential implications for their function and multivesicular body formation. J Biol Chem, 2003. 278(13): p. 10963-10972.
87. Staubach, S., H. Razawi, and F.G. Hanisch, Proteomics of MUC1-containing lipid rafts from plasma membranes and exosomes of human breast carcinoma cells MCF-7. Proteomics, 2009. 9(10): p. 2820-2835.
88. Helms, J.B. and C. Zurzolo, Lipids as targeting signals: lipid rafts and intracellular trafficking. Traffic, 2004. 5(4): p. 247-254.
89. Murata, M., J. Peränen, R. Schreiner, F. Wieland, T.V. Kurzchalia, and K. Simons, VIP21/caveolin is a cholesterol-binding protein. Proc Natl Acad Sci, 1995. 92(22): p. 10339-10343.
90. Allen, J.A., R.A. Halverson-Tamboli, and M.M. Rasenick, Lipid raft microdomains and neurotransmitter signalling. Nature Rev Neurosci, 2007. 8(2): p. 128-140.
91. Trajkovic, K., C. Hsu, S. Chiantia, L. Rajendran, D. Wenzel, F. Wieland, P. Schwille, B. Brügger, and M. Simons, Ceramide triggers budding of exosome vesicles into multivesicular endosomes. Science, 2008. 319(5867): p. 1244-1247.
92. London, E., Ceramide selectively displaces cholesterol from ordered lipid domains (rafts) implications for lipid raft structure and function. J Biol Chem, 2004. 279(11): p. 9997-10004.
93. Li, R., E.J. Blanchette-Mackie, and S. Ladisch, Induction of endocytic vesicles by exogenous C6-ceramide. J Biol Chem, 1999. 274(30): p. 21121-21127.
94. Lau, C., Y. Kim, D. Chia, N. Spielmann, G. Eibl, D. Elashoff, F. Wei, Y.-L. Lin, A. Moro, and T. Grogan, Role of pancreatic cancer-derived exosomes in salivary biomarker development. J Biol Chem, 2013. 288(37): p. 26888-26897.
95. Chen, T., J. Guo, M. Yang, X. Zhu, and X. Cao, Chemokine-containing exosomes are released from heat-stressed tumor cells via lipid raft-dependent pathway and act as efficient tumor vaccine. J Immunol, 2011. 186(4): p. 2219-2228.
96. Llorente, A., B. van Deurs, and K. Sandvig, Cholesterol regulates prostasome release from secretory lysosomes in PC-3 human prostate cancer cells. Eur J Cell Biol, 2007. 86(7): p. 405-415.
97. Lindquist, S. and E. Craig, The heat-shock proteins. Annu Rev Genet, 1988. 22(1): p. 631-677.
98. De Maio, A., Extracellular Hsp70: export and function. Curr Protein Pept Sci, 2014. 15(3): p. 225-231.
99. De Maio, A. and D. Vazquez, Extracellular heat shock proteins: a new location, a new function. Shock, 2013. 40(4): p. 239.
100. Hunter-Lavin, C., E.L. Davies, M.M. Bacelar, M.J. Marshall, S.M. Andrew, and J.H. Williams, Hsp70 release from peripheral blood mononuclear cells. Biochem Biophys Res Commun, 2004. 324(2): p. 511-517.
101. Broquet, A.H., G. Thomas, J. Masliah, G. Trugnan, and M. Bachelet, Expression of the molecular chaperone Hsp70 in detergent-resistant microdomains correlates with its membrane delivery and release. J Biol Chem, 2003. 278(24): p. 21601-21606.

102. Vega, V.L., M. Rodríguez-Silva, T. Frey, M. Gehrmann, J.C. Diaz, C. Steinem, G. Multhoff, N. Arispe, and A. De Maio, Hsp70 translocates into the plasma membrane after stress and is released into the extracellular environment in a membrane-associated form that activates macrophages. J Immunol, 2008. 180(6): p. 4299-4307.
103. Hemler, M.E., Specific tetraspanin functions. J Cell Biol, 2001. 155(7): p. 1103-1108.
104. Hu, C.-C.A., F.-X. Liang, G. Zhou, L. Tu, C.-H.A. Tang, J. Zhou, G. Kreibich, and T.-T. Sun, Assembly of urothelial plaques: tetraspanin function in membrane protein trafficking. Mol Biol Cell, 2005. 16(9): p. 3937-3950.
105. Perez-Hernandez, D., C. Gutiérrez-Vázquez, I. Jorge, S. López-Martín, A. Ursa, F. Sánchez-Madrid, J. Vázquez, and M. Yáñez-Mó, The intracellular interactome of tetraspanin-enriched microdomains reveals their function as sorting machineries toward exosomes. J Biol Chem, 2013. 288(17): p. 11649-11661.
106. Hemler, M.E., Tetraspanin proteins mediate cellular penetration, invasion, and fusion events and define a novel type of membrane microdomain. Annu Rev Cell Dev Biol, 2003. 19(1): p. 397-422.
107. Rana, S. and M. Zöller, Exosome target cell selection and the importance of exosomal tetraspanins: a hypothesis. Biochem Soc Trans, 2011. 39(2): p. 559-562.
108. Odintsova, E. and F. Berditchevski, Tetraspanins as Regulators of Protein Trafficking, in Tetraspanins. 2013, Springer. p. 109-130.
109. Nazarenko, I., S. Rana, A. Baumann, J. McAlear, A. Hellwig, M. Trendelenburg, G. Lochnit, K.T. Preissner, and M. Zöller, Cell surface tetraspanin Tspan8 contributes to molecular pathways of exosome-induced endothelial cell activation. Cancer Res, 2010. 70(4): p. 1668-1678.
110. Pols, M.S. and J. Klumperman, Trafficking and function of the tetraspanin CD63. Exp Cell Res, 2009. 315(9): p. 1584-1592.
111. Shen, B., N. Wu, J.-M. Yang, and S.J. Gould, Protein targeting to exosomes/microvesicles by plasma membrane anchors. J Biol Chem, 2011. 286(16): p. 14383-14395.
112. Marshansky, V. and M. Futai, The V-type H+-ATPase in vesicular trafficking: targeting, regulation and function. Curr Opin Cell Biol, 2008. 20(4): p. 415-426.
113. Lachenal, G., K. Pernet-Gallay, M. Chivet, F.J. Hemming, A. Belly, G. Bodon, B. Blot, G. Haase, Y. Goldberg, and R. Sadoul, Release of exosomes from differentiated neurons and its regulation by synaptic glutamatergic activity. Mol Cell Neurosci, 2011. 46(2): p. 409-418.
114. Fader, C.M., D. Sánchez, M. Furlán, and M.I. Colombo, Induction of autophagy promotes fusion of multivesicular bodies with autophagic vacuoles in k562 cells. Traffic, 2008. 9(2): p. 230-250.
115. Fader, C.M., A. Savina, D. Sánchez, and M.I. Colombo, Exosome secretion and red cell maturation: Exploring molecular components involved in the docking and fusion of multivesicular bodies in K562 cells. Blood Cells Mol Dis, 2005. 35(2): p. 153-157.
116. Puri, N. and P.A. Roche, Ternary SNARE complexes are enriched in lipid rafts during mast cell exocytosis. Traffic, 2006. 7(11): p. 1482-1494.
117. Fader, C.M., D.G. Sánchez, M.B. Mestre, and M.I. Colombo, TI-VAMP/VAMP7 and VAMP3/cellubrevin: two v-SNARE proteins involved in specific steps of the autophagy/multivesicular body pathways. BBA Mol Cell Res, 2009. 1793(12): p. 1901-1916.

118. Purushothaman, A., S.K. Bandari, D.S. Chandrashekar, R.J. Jones, H.C. Lee, D.M. Weber, and R.Z. Orlowski, Chondroitin sulfate proteoglycan serglycin influences protein cargo loading and functions of tumor-derived exosomes. Oncotarget, 2017. 8(43): p. 73723.
119. Mulcahy, L.A., R.C. Pink, and D.R.F. Carter, Routes and mechanisms of extracellular vesicle uptake. J Extracell Vesicles, 2014. 3(1): p. 24641.
120. Svensson, K.J., H.C. Christianson, A. Wittrup, E. Bourseau-Guilmain, E. Lindqvist, L.M. Svensson, M. Mörgelin, and M. Belting, Exosome uptake depends on ERK1/2-heat shock protein 27 signaling and lipid Raft-mediated endocytosis negatively regulated by caveolin-1. J Biol Chem, 2013. 288(24): p. 17713-17724.
121. Feng, D., W.L. Zhao, Y.Y. Ye, X.C. Bai, R.Q. Liu, L.F. Chang, Q. Zhou, and S.F. Sui, Cellular internalization of exosomes occurs through phagocytosis. Traffic, 2010. 11(5): p. 675-687.
122. Franzen, C.A., P.E. Simms, A.F. Van Huis, K.E. Foreman, P.C. Kuo, and G.N. Gupta, Characterization of uptake and internalization of exosomes by bladder cancer cells. BioMed Res Int, 2014. 2014.
123. Morelli, A.E., A.T. Larregina, W.J. Shufesky, M.L. Sullivan, D.B. Stolz, G.D. Papworth, A.F. Zahorchak, A.J. Logar, Z. Wang, and S.C. Watkins, Endocytosis, intracellular sorting, and processing of exosomes by dendritic cells. Blood, 2004. 104(10): p. 3257-3266.
124. Sarrazin, S., W.C. Lamanna, and J.D. Esko, Heparan sulfate proteoglycans. Cold Spring Harb Perspect, 2011. 3(7): p. a004952.
125. Christianson, H.C., K.J. Svensson, T.H. van Kuppevelt, J.-P. Li, and M. Belting, Cancer cell exosomes depend on cell-surface heparan sulfate proteoglycans for their internalization and functional activity. Proc Natl Acad Sci, 2013. 110(43): p. 17380-17385.
126. Rana, S., C. Claas, C.C. Kretz, I. Nazarenko, and M. Zoeller, Activation-induced internalization differs for the tetraspanins CD9 and Tspan8: Impact on tumor cell motility. Int J Biochem Cell Biol, 2011. 43(1): p. 106-119.
127. Rana, S., S. Yue, D. Stadel, and M. Zöller, Toward tailored exosomes: The exosomal tetraspanin web contributes to target cell selection. Int J Biochem Cell Biol, 2012. 44(9): p. 1574-1584.
128. Hazawa, M., K. Tomiyama, A. Saotome-Nakamura, C. Obara, T. Yasuda, T. Gotoh, I. Tanaka, H. Yakumaru, H. Ishihara, and K. Tajima, Radiation increases the cellular uptake of exosomes through CD29/CD81 complex formation. Biochem Biophys Res Commun, 2014. 446(4): p. 1165-1171.
129. Vardaki, I., C. Sanchez, P. Fonseca, M. Olsson, D. Chioureas, G. Rassidakis, A. Ullén, B. Zhivotovsky, M. Björkholm, and T. Panaretakis, Caspase-3–dependent cleavage of Bcl-xL in the stroma exosomes is required for their uptake by hematological malignant cells. Blood, 2016. 128(23): p. 2655-2665.
130. Tian, T., Y.-L. Zhu, Y.-Y. Zhou, G.-F. Liang, Y.-Y. Wang, F.-H. Hu, and Z.-D. Xiao, Exosome uptake through clathrin-mediated endocytosis and macropinocytosis and mediating miR-21 delivery. J Biol Chem, 2014. 289(32): p. 22258-22267.
131. Cooper, G.M., The Cell: A Molecular Approach. 2nd edition. 2000, Sunderland (MA): Sinauer Associates.

132. McKelvey, K.J., K.L. Powell, A.W. Ashton, J.M. Morris, and S.A. McCracken, Exosomes: mechanisms of uptake. J Circ Biomark, 2015. 4: p. 7.
133. Vargas, A., S. Zhou, M. Éthier-Chiasson, D. Flipo, J. Lafond, C. Gilbert, and B. Barbeau, Syncytin proteins incorporated in placenta exosomes are important for cell uptake and show variation in abundance in serum exosomes from patients with preeclampsia. The FASEB Journal, 2014. 28(8): p. 3703-3719.
134. Fitzner, D., M. Schnaars, D. van Rossum, G. Krishnamoorthy, P. Dibaj, M. Bakhti, T. Regen, U.-K. Hanisch, and M. Simons, Selective transfer of exosomes from oligodendrocytes to microglia by macropinocytosis. J Cell Sci, 2011. 124(3): p. 447-458.
135. Escrevente, C., S. Keller, P. Altevogt, and J. Costa, Interaction and uptake of exosomes by ovarian cancer cells. BMC cancer, 2011. 11(1): p. 108.
136. Nakase, I., N.B. Kobayashi, T. Takatani-Nakase, and T. Yoshida, Active macropinocytosis induction by stimulation of epidermal growth factor receptor and oncogenic Ras expression potentiates cellular uptake efficacy of exosomes. Sci Rep, 2015. 5.
137. Parolini, I., C. Federici, C. Raggi, L. Lugini, S. Palleschi, A. De Milito, C. Coscia, E. Iessi, M. Logozzi, and A. Molinari, Microenvironmental pH is a key factor for exosome traffic in tumor cells. J Biol Chem, 2009. 284(49): p. 34211-34222.
138. Caponnetto, F., I. Manini, M. Skrap, T. Palmai-Pallag, C. Di Loreto, A.P. Beltrami, D. Cesselli, and E. Ferrari, Size-dependent cellular uptake of exosomes. Nanomed Nanotech Biol Med, 2017. 13(3): p. 1011-1020.
139. Ronquist, K.G., C. Sanchez, L. Dubois, D. Chioureas, P. Fonseca, A. Larsson, A. Ullén, J. Yachnin, G. Ronquist, and T. Panaretakis, Energy-requiring uptake of prostasomes and PC3 cell-derived exosomes into non-malignant and malignant cells. J Extracell Vesicles, 2016. 5(1): p. 29877.
140. Charoenviriyakul, C., Y. Takahashi, M. Morishita, A. Matsumoto, M. Nishikawa, and Y. Takakura, Cell type-specific and common characteristics of exosomes derived from mouse cell lines: Yield, physicochemical properties, and pharmacokinetics. Eur J Pharm Sci, 2017. 96: p. 316-322.
141. Nakamura, K., K. Sawada, Y. Kinose, A. Yoshimura, A. Toda, E. Nakatsuka, K. Hashimoto, S. Mabuchi, K.-i. Morishige, and H. Kurachi, Exosomes promote ovarian cancer cell invasion through transfer of CD44 to peritoneal mesothelial cells. Mol Cancer Res, 2016: p. molcanres. 0191.2016.
142. Corcoran, C., S. Rani, K. O'Brien, A. O'Neill, M. Prencipe, R. Sheikh, G. Webb, R. McDermott, W. Watson, and J. Crown, Docetaxel-resistance in prostate cancer: evaluating associated phenotypic changes and potential for resistance transfer via exosomes. PLoS One, 2012. 7(12): p. e50999.
143. Shelke, G.V., C. Lässer, Y.S. Gho, and J. Lötvall, Importance of exosome depletion protocols to eliminate functional and RNA-containing extracellular vesicles from fetal bovine serum. J Extracell Vesicles, 2014. 3.
144. Lee, C., S.A. Mitsialis, M. Aslam, S.H. Vitali, E. Vergadi, G. Konstantinou, K. Sdrimas, A. Fernandez-Gonzalez, and S. Kourembanas, Exosomes mediate the cytoprotective action of mesenchymal stromal cells on hypoxia-induced pulmonary hypertension. Circulation, 2012: p. CIRCULATIONAHA. 112.114173.

145. Atay, S., C. Gercel-Taylor, and D.D. Taylor, Human Trophoblast-Derived Exosomal Fibronectin Induces Pro-Inflammatory Il-1β Production by Macrophages. Am J Reprod Immunol, 2011. 66(4): p. 259-269.
146. Lehmann, B.D., M.S. Paine, A.M. Brooks, J.A. McCubrey, R.H. Renegar, R. Wang, and D.M. Terrian, Senescence-associated exosome release from human prostate cancer cells. Cancer Res, 2008. 68(19): p. 7864-7871.
147. Chen, L., Y. Wang, Y. Pan, L. Zhang, C. Shen, G. Qin, M. Ashraf, N. Weintraub, G. Ma, and Y. Tang, Cardiac progenitor-derived exosomes protect ischemic myocardium from acute ischemia/reperfusion injury. Biochem Biophys Res Commun, 2013. 431(3): p. 566-571.
148. Li, J., Y. Lee, H.J. Johansson, I. Mäger, P. Vader, J.Z. Nordin, O.P. Wiklander, J. Lehtiö, M.J. Wood, and S.E. Andaloussi, Serum-free culture alters the quantity and protein composition of neuroblastoma-derived extracellular vesicles. J Extracell Vesicles, 2015. 4.
149. Böing, A.N., E. Van Der Pol, A.E. Grootemaat, F.A. Coumans, A. Sturk, and R. Nieuwland, Single-step isolation of extracellular vesicles by size-exclusion chromatography. J Extracell Vesicles, 2014. 3.
150. Petersen, K.E., E. Manangon, J.L. Hood, S.A. Wickline, D.P. Fernandez, W.P. Johnson, and B.K. Gale, A review of exosome separation techniques and characterization of B16-F10 mouse melanoma exosomes with AF4-UV-MALS-DLS-TEM. Anal Bioanal Chem, 2014. 406(30): p. 7855-7866.
151. Cvjetkovic, A., J. Lötvall, and C. Lässer, The influence of rotor type and centrifugation time on the yield and purity of extracellular vesicles. J Extracell Vesicles, 2014. 3.
152. Skog, J., T. Würdinger, S. Van Rijn, D.H. Meijer, L. Gainche, W.T. Curry, B.S. Carter, A.M. Krichevsky, and X.O. Breakefield, Glioblastoma microvesicles transport RNA and proteins that promote tumour growth and provide diagnostic biomarkers. Nat Cell Biol, 2008. 10(12): p. 1470-1476.
153. Kleijmeer, M.J., W. Stoorvogel, J.M. Griffith, O. Yoshie, and H.J. Geuze, Selective enrichment of tetraspan proteins on the internal vesicles of multivesicular endosomes and on exosomes secreted by human B-lymphocytes. J Biol Chem, 1998. 273(32): p. 20121-20127.
154. Andre, F., B. Escudier, E. Angevin, T. Tursz, and L. Zitvogel, Exosomes for cancer immunotherapy. Ann Oncol, 2004. 15(4): p. 141-144.
155. Zhang, Z., C. Wang, T. Li, Z. Liu, and L. Li, Comparison of ultracentrifugation and density gradient separation methods for isolating Tca8113 human tongue cancer cell line ‐derived exosomes. Oncol Lett, 2014. 8(4): p. 1701-1706.
156. Li, M., A.J. Rai, G. Joel DeCastro, E. Zeringer, T. Barta, S. Magdaleno, R. Setterquist, and A.V. Vlassov, An optimized procedure for exosome isolation and analysis using serum samples: Application to cancer biomarker discovery. Methods, 2015. 87: p. 26-30.
157. Rekker, K., M. Saare, A.M. Roost, A.-L. Kubo, N. Zarovni, A. Chiesi, A. Salumets, and M. Peters, Comparison of serum exosome isolation methods for microRNA profiling. Clin Biochem, 2014. 47(1–2): p. 135-138.
158. Van Deun, J., P. Mestdagh, R. Sormunen, V. Cocquyt, K. Vermaelen, J. Vandesompele, M. Bracke, O. De Wever, and A. Hendrix, The impact of disparate isolation methods for extracellular vesicles on downstream RNA profiling. J Extracell Vesicles, 2014. 3.

159. Lobb, R.J., M. Becker, S.W. Wen, C.S. Wong, A.P. Wiegmans, A. Leimgruber, and A. Möller, Optimized exosome isolation protocol for cell culture supernatant and human plasma. J Extracell Vesicles, 2015. 4.
160. Helwa, I., J. Cai, M.D. Drewry, A. Zimmerman, M.B. Dinkins, M.L. Khaled, M. Seremwe, W.M. Dismuke, E. Bieberich, W.D. Stamer, M.W. Hamrick, and Y. Liu, A Comparative Study of Serum Exosome Isolation Using Differential Ultracentrifugation and Three Commercial Reagents. PLoS One, 2017. 12(1): p. e0170628.
161. Liu, F., O. Vermesh, V. Mani, T.J. Ge, S.J. Madsen, A. Sabour, E.-C. Hsu, G. Gowrishankar, M. Kanada, and J.V. Jokerst, The Exosome Total Isolation Chip. ACS nano, 2017. 11(11): p. 10712-10723.
162. Wu, M., Y. Ouyang, Z. Wang, R. Zhang, P.-H. Huang, C. Chen, H. Li, P. Li, D. Quinn, and M. Dao, Isolation of exosomes from whole blood by integrating acoustics and microfluidics. Proc Natl Acad Sci, 2017: p. 201709210.
163. Ratajczak, J., M. Wysoczynski, F. Hayek, A. Janowska-Wieczorek, and M. Ratajczak, Membrane-derived microvesicles: important and underappreciated mediators of cell-to-cell communication. Leukemia, 2006. 20(9): p. 1487-1495.
164. Théry, C., S. Amigorena, G. Raposo, and A. Clayton, Isolation and characterization of exosomes from cell culture supernatants and biological fluids. Curr Protoc Cell Biol, 2006: p. 3.22. 1-3.22. 29.
165. Szajnik, M., M. Derbis, M. Lach, P. Patalas, M. Michalak, H. Drzewiecka, D. Szpurek, A. Nowakowski, M. Spaczynski, and W. Baranowski, Exosomes in plasma of patients with ovarian carcinoma: potential biomarkers of tumor progression and response to therapy. Gynecol Obstet, 2013: p. 003.
166. Mitchell, P.J., J. Welton, J. Staffurth, M.D. Mason, Z. Tabi, and A. Clayton, Can urinary exosomes act as treatment response markers in prostate cancer? J Transl Med, 2009. 7(1): p. 4.
167. Segura, E., C. Nicco, B. Lombard, P. Véron, G. Raposo, F. Batteux, S. Amigorena, and C. Théry, ICAM-1 on exosomes from mature dendritic cells is critical for efficient naive T-cell priming. Blood, 2005. 106(1): p. 216-223.
168. Van Niel, G., J. Mallegol, C. Bevilacqua, C. Candalh, S. Brugière, E. Tomaskovic-Crook, J.K. Heath, N. Cerf-Bensussan, and M. Heyman, Intestinal epithelial exosomes carry MHC class II/peptides able to inform the immune system in mice. Gut, 2003. 52(12): p. 1690-1697.
169. Keerthikumar, S., D. Chisanga, D. Ariyaratne, H. Al Saffar, S. Anand, K. Zhao, M. Samuel, M. Pathan, M. Jois, and N. Chilamkurti, ExoCarta: a web-based compendium of exosomal cargo. J Mol Biol, 2016. 428(4): p. 688-692.
170. Ji, H., D.W. Greening, T.W. Barnes, J.W. Lim, B.J. Tauro, A. Rai, R. Xu, C. Adda, S. Mathivanan, and W. Zhao, Proteome profiling of exosomes derived from human primary and metastatic colorectal cancer cells reveal differential expression of key metastatic factors and signal transduction components. Proteomics, 2013. 13(10-11): p. 1672-1686.
171. Van Niel, G., I. Porto-Carreiro, S. Simoes, and G. Raposo, Exosomes: a common pathway for a specialized function. J Biochem, 2006. 140(1): p. 13-21.
172. Villarroya-Beltri, C., F. Baixauli, C. Gutiérrez-Vázquez, F. Sánchez-Madrid, and M. Mittelbrunn, Sorting it out: Regulation of exosome loading. Semin Cancer Biol, 2014. 28: p. 3-13.

173. Charrin, S., S. Manié, C. Thiele, M. Billard, D. Gerlier, C. Boucheix, and E. Rubinstein, A physical and functional link between cholesterol and tetraspanins. Eur J Immunol, 2003. 33(9): p. 2479-2489.
174. Kowal, J., M. Tkach, and C. Théry, Biogenesis and secretion of exosomes. Curr Opin Cell Biol, 2014. 29: p. 116-125.
175. Vella, L.J., R.A. Sharples, R.M. Nisbet, R. Cappai, and A.F. Hill, The role of exosomes in the processing of proteins associated with neurodegenerative diseases. Eur Biophys J, 2008. 37(3): p. 323-332.
176. Ciocca, D.R. and S.K. Calderwood, Heat shock proteins in cancer: diagnostic, prognostic, predictive, and treatment implications. Cell Stress Chaperon, 2005. 10(2): p. 86-103.
177. Longhurst, C. and L. Jennings, Integrin-mediated signal transduction. Cell Mol Life Sci, 1998. 54(6): p. 514-526.
178. Hemler, M.E., Tetraspanin functions and associated microdomains. Nat Rev Mol Cell Biol, 2005. 6(10): p. 801-811.
179. Buschow, S.I., B.W. Van Balkom, M. Aalberts, A.J. Heck, M. Wauben, and W. Stoorvogel, MHC class II-associated proteins in B-cell exosomes and potential functional implications for exosome biogenesis. Immunol Cell Biol, 2010. 88(8): p. 851-856.
180. Denzer, K., M. van Eijk, M.J. Kleijmeer, E. Jakobson, C. de Groot, and H.J. Geuze, Follicular dendritic cells carry MHC class II-expressing microvesicles at their surface. J Immunol, 2000. 165(3): p. 1259-1265.
181. Chatellard-Causse, C., B. Blot, N. Cristina, S. Torch, M. Missotten, and R. Sadoul, Alix (ALG-2-interacting protein X), a protein involved in apoptosis, binds to endophilins and induces cytoplasmic vacuolization. J Biol Chem, 2002. 277(32): p. 29108-29115.
182. Sundquist, W.I., H.L. Schubert, B.N. Kelly, G.C. Hill, J.M. Holton, and C.P. Hill, Ubiquitin recognition by the human TSG101 protein. Mol Cell, 2004. 13(6): p. 783-789.
183. Zhu, G., R. Gilchrist, N. Borley, H.W. Chng, M. Morgan, J.F. Marshall, R.S. Camplejohn, G.H. Muir, and I.R. Hart, Reduction of TSG101 protein has a negative impact on tumor cell growth. Int J Cancer, 2004. 109(4): p. 541-547.
184. Auth, T., S. Schlüter, S. Urschel, P. Kussmann, S. Sonntag, T. Höher, M.M. Kreuzberg, R. Dobrowolski, and K. Willecke, The TSG101 protein binds to connexins and is involved in connexin degradation. Exp Cell Res, 2009. 315(6): p. 1053-1062.
185. Février, B. and G. Raposo, Exosomes: endosomal-derived vesicles shipping extracellular messages. Curr Opin Cell Biol, 2004. 16(4): p. 415-421.
186. Heijnen, H.F., A.E. Schiel, R. Fijnheer, H.J. Geuze, and J.J. Sixma, Activated Platelets Release Two Types of Membrane Vesicles: Microvesicles by Surface Shedding and Exosomes Derived From Exocytosis of Multivesicular Bodies and Granules. Blood, 1999. 94(11): p. 3791-3799.
187. Cho, J.-a., Y.-S. Lee, S.-H. Kim, J.-K. Ko, and C.-W. Kim, MHC independent anti-tumor immune responses induced by Hsp70-enriched exosomes generate tumor regression in murine models. Cancer Lett, 2009. 275(2): p. 256-265.
188. Multhoff, G., Heat shock protein 70 (Hsp70): Membrane location, export and immunological relevance. Methods, 2007. 43(3): p. 229-237.
189. Te, J., L. Jia, J. Rogers, A. Miller, and S.D. Hartson, Novel subunits of the mammalian Hsp90 signal transduction chaperone. J Proteome Res, 2007. 6(5): p. 1963-1973.

190. Li, W., F. Tsen, D. Sahu, A. Bhatia, M. Chen, G. Multhoff, and D.T. Woodley, Extracellular Hsp90 (eHsp90) as the actual target in clinical trials: intentionally or unintentionally. Int Rev Cell Mol Biol, 2013. 303: p. 203.
191. Rajendran, L., M. Honsho, T.R. Zahn, P. Keller, K.D. Geiger, P. Verkade, and K. Simons, Alzheimer's disease β-amyloid peptides are released in association with exosomes. Proc Natl Acad Sci, 2006. 103(30): p. 11172-11177.
192. Otto, G.P. and B.J. Nichols, The roles of flotillin microdomains–endocytosis and beyond. J Cell Sci, 2011. 124(23): p. 3933-3940.
193. Price, M.P., R.J. Thompson, J.O. Eshcol, J.A. Wemmie, and C.J. Benson, Stomatin modulates gating of acid-sensing ion channels. J Biol Chem, 2004. 279(51): p. 53886-53891.
194. Salzer, U. and R. Prohaska, Stomatin, flotillin-1, and flotillin-2 are major integral proteins of erythrocyte lipid rafts. Blood, 2001. 97(4): p. 1141-1143.
195. Sedensky, M.M., J. Siefker, and P.G. Morgan, Model Organisms: New Insights Into Ion Channel and Transporter Function. Stomatin homologues interact inCaenorhabditis elegans. Am J Physiol Cell Physiol, 2001. 280(5): p. C1340-C1348.
196. Lee, J.-H., C.-F. Hsieh, H.-W. Liu, C.-Y. Chen, S.-C. Wu, T.-W. Chen, C.-S. Hsu, Y.-H. Liao, C.-Y. Yang, and J.-F. Shyu, Lipid raft–associated stomatin enhances cell fusion. FASEB J, 2017. 31(1): p. 47-59.
197. Dominguez, R. and K.C. Holmes, Actin structure and function. Annu Rev Biophys, 2011. 40: p. 169-186.
198. Tian, T., Y. Wang, H. Wang, Z. Zhu, and Z. Xiao, Visualizing of the cellular uptake and intracellular trafficking of exosomes by live-cell microscopy. J Cell Biochem, 2010. 111(2): p. 488-496.
199. Asea, A., C. Jean-Pierre, P. Kaur, P. Rao, I.M. Linhares, D. Skupski, and S.S. Witkin, Heat shock protein-containing exosomes in mid-trimester amniotic fluids. J Reprod Immunol, 2008. 79(1): p. 12-17.
200. Pellegrini, F. and D.R. Budman, Review: tubulin function, action of antitubulin drugs, and new drug development. Cancer Invest, 2005. 23(3): p. 264-273.
201. Abusamra, A.J., Z. Zhong, X. Zheng, M. Li, T.E. Ichim, J.L. Chin, and W.-P. Min, Tumor exosomes expressing Fas ligand mediate CD8+ T-cell apoptosis. Blood Cells Mol Dis, 2005. 35(2): p. 169-173.
202. Melo, S.A., H. Sugimoto, J.T. O'Connell, N. Kato, A. Villanueva, A. Vidal, L. Qiu, E. Vitkin, L.T. Perelman, and C.A. Melo, Cancer exosomes perform cell-independent microRNA biogenesis and promote tumorigenesis. Cancer Cell, 2014. 26(5): p. 707-721.
203. Subra, C., K. Laulagnier, B. Perret, and M. Record, Exosome lipidomics unravels lipid sorting at the level of multivesicular bodies. Biochimie, 2007. 89(2): p. 205-212.
204. Record, M., C. Subra, S. Silvente-Poirot, and M. Poirot, Exosomes as intercellular signalosomes and pharmacological effectors. Biochem Pharmacol, 2011. 81(10): p. 1171-1182.
205. Matsuo, H., J. Chevallier, N. Mayran, I. Le Blanc, C. Ferguson, J. Fauré, N.S. Blanc, S. Matile, J. Dubochet, and R. Sadoul, Role of LBPA and Alix in multivesicular liposome formation and endosome organization. Science, 2004. 303(5657): p. 531-534.
206. Falguières, T., P.-P. Luyet, and J. Gruenberg, Molecular assemblies and membrane domains in multivesicular endosome dynamics. Exp Cell Res, 2009. 315(9): p. 1567-1573.

207. van Hoof, A., P.A. Frischmeyer, H.C. Dietz, and R. Parker, Exosome-mediated recognition and degradation of mRNAs lacking a termination codon. Science, 2002. 295(5563): p. 2262-2264.
208. Valadi, H., K. Ekström, A. Bossios, M. Sjöstrand, J.J. Lee, and J.O. Lötvall, Exosome-mediated transfer of mRNAs and microRNAs is a novel mechanism of genetic exchange between cells. Nat Cell Biol, 2007. 9(6): p. 654-659.
209. Etheridge, A., I. Lee, L. Hood, D. Galas, and K. Wang, Extracellular microRNA: A new source of biomarkers. Mutat Res Fund Mol Mech Mut, 2011. 717(1–2): p. 85-90.
210. Brase, J.C., D. Wuttig, R. Kuner, and H. Sültmann, Serum microRNAs as non-invasive biomarkers for cancer. Mol Cancer, 2010. 9(1): p. 306.
211. Kuwabara, Y., K. Ono, T. Horie, H. Nishi, K. Nagao, M. Kinoshita, S. Watanabe, O. Baba, Y. Kojima, and S. Shizuta, Increased microRNA-1 and microRNA-133a levels in serum of patients with cardiovascular disease indicate the existence of myocardial damage. Circ Cardiovasc Genet, 2011: p. CIRCGENETICS. 110.958975.
212. He, F., G.W. Becker, J.R. Litowski, L.O. Narhi, D.N. Brems, and V.I. Razinkov, High-throughput dynamic light scattering method for measuring viscosity of concentrated protein solutions. Anal Biochem, 2010. 399(1): p. 141-143.
213. Gallego-Urrea, J.A., J. Tuoriniemi, and M. Hassellöv, Applications of particle-tracking analysis to the determination of size distributions and concentrations of nanoparticles in environmental, biological and food samples. Trends Anal Chem, 2011. 30(3): p. 473-483.
214. Boyd, R.D., S.K. Pichaimuthu, and A. Cuenat, New approach to inter-technique comparisons for nanoparticle size measurements; using atomic force microscopy, nanoparticle tracking analysis and dynamic light scattering. Colloids Surf A Physicochem Eng Asp, 2011. 387(1–3): p. 35-42.
215. Le, M., C. Fernandez-Palomo, F.E. McNeill, C.B. Seymour, A.J. Rainbow, and C.E. Mothersill, Exosomes are released by bystander cells exposed to radiation-induced biophoton signals: Reconciling the mechanisms mediating the bystander effect. PLoS One, 2017. 12(3): p. e0173685.
216. Xu, R., Progress in nanoparticles characterization: Sizing and zeta potential measurement. Particuology, 2008. 6(2): p. 112-115.
217. Kesimer, M. and R. Gupta, Physical characterization and profiling of airway epithelial derived exosomes using light scattering. Methods, 2015. 87: p. 59-63.
218. Takahashi, Y., M. Nishikawa, H. Shinotsuka, Y. Matsui, S. Ohara, T. Imai, and Y. Takakura, Visualization and in vivo tracking of the exosomes of murine melanoma B16-BL6 cells in mice after intravenous injection. J Biotech, 2013. 165(2): p. 77-84.
219. Pol, E., F. Coumans, A. Grootemaat, C. Gardiner, I. Sargent, P. Harrison, A. Sturk, T. Leeuwen, and R. Nieuwland, Particle size distribution of exosomes and microvesicles determined by transmission electron microscopy, flow cytometry, nanoparticle tracking analysis, and resistive pulse sensing. J Thromb Haemost, 2014. 12(7): p. 1182-1192.
220. Atay, S., C. Gercel-Taylor, M. Kesimer, and D.D. Taylor, Morphologic and proteomic characterization of exosomes released by cultured extravillous trophoblast cells. Exp Cell Res, 2011. 317(8): p. 1192-1202.
221. Aebersold, R. and M. Mann, Mass spectrometry-based proteomics. Nature, 2003. 422(6928): p. 198-207.
222. Griffiths, W.J. and Y. Wang, Mass spectrometry: from proteomics to metabolomics and lipidomics. Chem Soc Rev, 2009. 38(7): p. 1882-1896.

223. Pisitkun, T., R.-F. Shen, and M.A. Knepper, Identification and proteomic profiling of exosomes in human urine. Proc Natl Acad Sci, 2004. 101(36): p. 13368-13373.
224. Bligh, E.G. and W.J. Dyer, A rapid method of total lipid extraction and purification. Can J Biochem Physiol, 1959. 37(8): p. 911-917.
225. Iverson, S.J., S.L. Lang, and M.H. Cooper, Comparison of the Bligh and Dyer and Folch methods for total lipid determination in a broad range of marine tissue. Lipids, 2001. 36(11): p. 1283-1287.
226. Manirakiza, P., A. Covaci, and P. Schepens, Comparative study on total lipid determination using Soxhlet, Roese-Gottlieb, Bligh & Dyer, and modified Bligh & Dyer extraction methods. J Food Comp Anal, 2001. 14(1): p. 93-100.
227. Llorente, A., T. Skotland, T. Sylvänne, D. Kauhanen, T. Róg, A. Orłowski, I. Vattulainen, K. Ekroos, and K. Sandvig, Molecular lipidomics of exosomes released by PC-3 prostate cancer cells. BBA-Mol Cell Biol Lipids, 2013. 1831(7): p. 1302-1309.
228. Fauré, J., G. Lachenal, M. Court, J. Hirrlinger, C. Chatellard-Causse, B. Blot, J. Grange, G. Schoehn, Y. Goldberg, V. Boyer, F. Kirchhoff, G. Raposo, J. Garin, and R. Sadoul, Exosomes are released by cultured cortical neurones. Mol Cell Neurosci, 2006. 31(4): p. 642-648.
229. Pedersen, K., B. Kierulf, I. Manger, M. Oksvold, M. Li, V. Alexander, N. Roos, A. Kullmann, and A. Neurauter, Direct Isolation of Exosomes from Cell Culture: Simplifying Methods for Exosome Enrichment and Analysis. Transl Biomed, 2015.
230. Knee, R., I. Ahsan, N. Mesaeli, R.J. Kaufman, and M. Michalak, Compromised calnexin function in calreticulin-deficient cells. Biochem Biophys Res Commun, 2003. 304(4): p. 661-666.
231. Lonnerdal, B., X. Du, Y. Liao, and J. Li, Human milk exosomes resist digestion in vitro and are internalized by human intestinal cells. FASEB J, 2015. 29(1 Supplement): p. 121.3.
232. Properzi, F., M. Logozzi, H. Abdel-Haq, C. Federici, L. Lugini, T. Azzarito, I. Cristofaro, D. di Sevo, E. Ferroni, and F. Cardone, Detection of exosomal prions in blood by immunochemistry techniques. J Gen Virol, 2015. 96(7): p. 1969-1974.
233. Bobrie, A., M. Colombo, G. Raposo, and C. Théry, Exosome secretion: molecular mechanisms and roles in immune responses. Traffic, 2011. 12(12): p. 1659-1668.
234. Kim, S.H., N. Bianco, R. Menon, E.R. Lechman, W.J. Shufesky, A.E. Morelli, and P.D. Robbins, Exosomes derived from genetically modified DC expressing FasL are anti-inflammatory and immunosuppressive. Mol Ther, 2006. 13(2): p. 289-300.
235. Colino, J. and C.M. Snapper, Exosomes from bone marrow dendritic cells pulsed with diphtheria toxoid preferentially induce type 1 antigen-specific IgG responses in naive recipients in the absence of free antigen. J Immunol, 2006. 177(6): p. 3757-3762.
236. Mineo, M., S.H. Garfield, S. Taverna, A. Flugy, G. De Leo, R. Alessandro, and E.C. Kohn, Exosomes released by K562 chronic myeloid leukemia cells promote angiogenesis in a Src-dependent fashion. Angiogenesis, 2012. 15(1): p. 33-45.
237. Imai, T., Y. Takahashi, M. Nishikawa, K. Kato, M. Morishita, T. Yamashita, A. Matsumoto, C. Charoenviriyakul, and Y. Takakura, Macrophage-dependent clearance of systemically administered B16BL6-derived exosomes from the blood circulation in mice. J Extracell Vesicles, 2015. 4.
238. Hood, J.L., R.S. San, and S.A. Wickline, Exosomes released by melanoma cells prepare sentinel lymph nodes for tumor metastasis. Cancer Res, 2011. 71(11): p. 3792-3801.

239. Suetsugu, A., K. Honma, S. Saji, H. Moriwaki, T. Ochiya, and R.M. Hoffman, Imaging exosome transfer from breast cancer cells to stroma at metastatic sites in orthotopic nude-mouse models. Adv Drug Deliver Rev, 2013. 65(3): p. 383-390.
240. Tijsen, A.J., Y.M. Pinto, and E.E. Creemers, Circulating microRNAs as diagnostic biomarkers for cardiovascular diseases. Am J Physiol Heart Circ Physiol, 2012. 303(9): p. H1085-H1095.
241. Van Giau, V. and S.S.A. An, Emergence of exosomal miRNAs as a diagnostic biomarker for Alzheimer's disease. J Neurol Sci, 2016. 360: p. 141-152.
242. Matsumoto, Y., M. Kano, Y. Akutsu, N. Hanari, I. Hoshino, K. Murakami, A. Usui, H. Suito, M. Takahashi, and R. Otsuka, Quantification of plasma exosome is a potential prognostic marker for esophageal squamous cell carcinoma. Oncol Rep, 2016. 36(5): p. 2535.
243. Camussi, G., M.-C. Deregibus, S. Bruno, C. Grange, V. Fonsato, and C. Tetta, Exosome/microvesicle-mediated epigenetic reprogramming of cells. Am J Cancer Res, 2011. 1(1): p. 98-110.
244. Taylor, D.D. and C. Gercel-Taylor, MicroRNA signatures of tumor-derived exosomes as diagnostic biomarkers of ovarian cancer. Gynecol Oncol, 2008. 110(1): p. 13-21.
245. Record, M., Exosomal lipids in cell–cell communication, in Emerging Concepts of Tumor Exosome–Mediated Cell-Cell Communication. 2013, Springer. p. 47-68.
246. Skotland, T., K. Ekroos, D. Kauhanen, H. Simolin, T. Seierstad, V. Berge, K. Sandvig, and A. Llorente, Molecular lipid species in urinary exosomes as potential prostate cancer biomarkers. Eur J Cancer, 2017. 70: p. 122-132.
247. Memczak, S., M. Jens, A. Elefsinioti, F. Torti, J. Krueger, A. Rybak, L. Maier, S.D. Mackowiak, L.H. Gregersen, and M. Munschauer, Circular RNAs are a large class of animal RNAs with regulatory potency. Nature, 2013. 495(7441): p. 333-338.
248. Li, Y., Q. Zheng, C. Bao, S. Li, W. Guo, J. Zhao, D. Chen, J. Gu, X. He, and S. Huang, Circular RNA is enriched and stable in exosomes: a promising biomarker for cancer diagnosis. Cell Res, 2015. 25(8): p. 981.
249. Reid, G., M.B. Kirschner, and N. van Zandwijk, Circulating microRNAs: Association with disease and potential use as biomarkers. Crit Rev Oncol Hematol, 2011. 80(2): p. 193-208.
250. Tanaka, Y., H. Kamohara, K. Kinoshita, J. Kurashige, T. Ishimoto, M. Iwatsuki, M. Watanabe, and H. Baba, Clinical impact of serum exosomal microRNA-21 as a clinical biomarker in human esophageal squamous cell carcinoma. Cancer, 2013. 119(6): p. 1159-1167.
251. Rabinowits, G., C. Gerçel-Taylor, J.M. Day, D.D. Taylor, and G.H. Kloecker, Exosomal microRNA: a diagnostic marker for lung cancer. Clin Lung Cancer, 2009. 10(1): p. 42-46.
252. Huang, X., T. Yuan, M. Liang, M. Du, S. Xia, R. Dittmar, D. Wang, W. See, B.A. Costello, and F. Quevedo, Exosomal miR-1290 and miR-375 as prognostic markers in castration-resistant prostate cancer. Eur Urol, 2015. 67(1): p. 33-41.
253. Ogata-Kawata, H., M. Izumiya, D. Kurioka, Y. Honma, Y. Yamada, K. Furuta, T. Gunji, H. Ohta, H. Okamoto, and H. Sonoda, Circulating exosomal microRNAs as biomarkers of colon cancer. PloS one, 2014. 9(4): p. e92921.
254. Matsumura, T., K. Sugimachi, H. Iinuma, Y. Takahashi, J. Kurashige, G. Sawada, M. Ueda, R. Uchi, H. Ueo, and Y. Takano, Exosomal microRNA in serum is a novel

biomarker of recurrence in human colorectal cancer. Br J Cancer, 2015. 113(2): p. 275-281.
255. Wang, H., L. Hou, A. Li, Y. Duan, H. Gao, and X. Song, Expression of serum exosomal microRNA-21 in human hepatocellular carcinoma. BioMed Res Int, 2014. 2014.
256. Eichelser, C., I. Stückrath, V. Müller, K. Milde-Langosch, H. Wikman, K. Pantel, and H. Schwarzenbach, Increased serum levels of circulating exosomal microRNA-373 in receptor-negative breast cancer patients. Oncotarget, 2014. 5(20): p. 9650.
257. Wang, N., L. Wang, Y. Yang, L. Gong, B. Xiao, and X. Liu, A serum exosomal microRNA panel as a potential biomarker test for gastric cancer. Biochem Biophys Res Commun, 2017. 493(3): p. 1322-1328.
258. Yang, S., S.P. Che, P. Kurywchak, J.L. Tavormina, L.B. Gansmo, P. Correa de Sampaio, M. Tachezy, M. Bockhorn, F. Gebauer, and A.R. Haltom, Detection of mutant KRAS and TP53 DNA in circulating exosomes from healthy individuals and patients with pancreatic cancer. Cancer Biol Ther, 2017. 18(3): p. 158-165.
259. Zhou, H., A. Cheruvanky, X. Hu, T. Matsumoto, N. Hiramatsu, M.E. Cho, A. Berger, A. Leelahavanichkul, K. Doi, and L.S. Chawla, Urinary exosomal transcription factors, a new class of biomarkers for renal disease. Kidney Int, 2008. 74(5): p. 613-621.
260. Zhou, H., T. Pisitkun, A. Aponte, P.S. Yuen, J.D. Hoffert, H. Yasuda, X. Hu, L. Chawla, R.-F. Shen, and M.A. Knepper, Exosomal Fetuin-A identified by proteomics: a novel urinary biomarker for detecting acute kidney injury. Kidney Int, 2006. 70(10): p. 1847-1857.
261. Khan, S., J.M. Jutzy, M.M.A. Valenzuela, D. Turay, J.R. Aspe, A. Ashok, S. Mirshahidi, D. Mercola, M.B. Lilly, and N.R. Wall, Plasma-derived exosomal survivin, a plausible biomarker for early detection of prostate cancer. PLoS One, 2012. 7(10): p. e46737.
262. Dear, J.W., J.M. Street, and M.A. Bailey, Urinary exosomes: a reservoir for biomarker discovery and potential mediators of intrarenal signalling. Proteomics, 2013. 13(10-11): p. 1572-1580.
263. Madhavan, B., S. Yue, U. Galli, S. Rana, W. Gross, M. Müller, N.A. Giese, H. Kalthoff, T. Becker, and M.W. Büchler, Combined evaluation of a panel of protein and miRNA serum-exosome biomarkers for pancreatic cancer diagnosis increases sensitivity and specificity. Int J Cancer, 2015. 136(11): p. 2616-2627.

3. MYRISTOYLATION PROMOTES THE ENCAPSULATION OF SRC FAMILY KINASES INTO EXOSOMES*

*Wen, R.; Li, Q.; Kim, S.; Ma, Y.; Xie, J.; Cai, H.; To be submitted to *J Cell Biol*.

ABSTRACT

Exosomes mediate intercellular communication through transfer of proteins, mRNA, microRNAs, and other exosomal substances. How oncogenic proteins are selectively encapsulated into exosomes remains unclear. Here, we demonstrated that Src kinase, an oncogenic protein aberrantly expressed and activated in various cells including prostate cancer cells, was highly enriched in exosomes. Myristoylation promoted the sorting of Src kinase in exosomes whereas palmitoylation inhibited this encapsulation process. Loss of myristoylation inhibited the expression levels of Src kinase in exosomes. The encapsulation of Src protein into exosomes was involved in classic endosomal sorting complexes required for transport (ESCRT) machinery as decrease of Src incorporation into exosomes was observed in TSG101-knockdown cells. Exosomes derived from xenograft tumors induced apoptosis of recipient cells via induction of caspase pathway. Additionally, while exosomes from cancer cells expressing Src(Y529F) further promoted apoptotic process, loss of myristoylation inhibited the process. *In vivo* studies showed that DU145 overexpressing Src(Y529F) exhibited significantly higher expression level of Src protein in the serum exosomes compared to vector and Src(Y529/G2A) transduced DU145 controls, confirming the role of myristoylation in facilitating Src protein encapsulation into exosomes. These findings provide new insights on Src kinase sorting mechanism into exosomes and therapeutic approaches by inhibiting oncogenic proteins' translocation through targeting the protein myristoylation process.

3.1 INTRODUCTION

Exosomes are nanovesicles with a diameter of 30-150 nm secreted from almost all cell types[1]. They are generated through cell exocytosis originated from the fusion of multivesicular bodies (MVBs) with the plasma membrane[2-4], and mediate the cell-to-cell communication by exchanging exosomal contents such as RNAs between cells [5, 6]. Exosomes may transfer oncogenic components between cells in the microenvironment and generate communication networks facilitating the dissemination of disease like cancer[7]. Tumor-derived exosomes promote tumorigenesis through transferring active tumor proteins, mRNA and microRNAs (miRNAs), and/or escaping immune system by disrupting immune cells, e.g., T cells[8, 9].

Src family kinases (SFKs) are a group of non-receptor tyrosine kinases that are fundamental regulators of signal transduction involving cellular differentiation, adhesion, cell-cycle progression, invasion and migration [10-12]. All SFKs are composed of an N-terminal Src Homology (SH) 4 domain controlling membrane association, SH3, SH2, and tyrosine kinase SH1 domains bearing autophosphorylation site (e.g., Tyrosine 416 in Src in chicken), and a short C-terminal tail containing autoinhibitory phosphorylation site (e.g., Tyrosine 527 in Src in chicken)[13-15]. Elevated SFK activity is clinically associated with prostate cancer in patients with short life expectancy and a high probability of distant metastasis [16]. The Src plays oncogenic roles in tumor growth, progression, and metastasis of human cancers such as colon, breast, and prostate cancer[17]. Src is overexpressed in various cancers including prostate cancer[18, 19], and inhibition of Src kinase is identified as a potential therapeutic strategy for cancer through suppressing the proliferation, invasion, and migration of cancer cells [20-22].

Protein lipidation by myristoylation or palmitoylation is associated with diverse biological functions such as cell signaling, protein localization, and cell-cell communication [23, 24].

Myristoylation is lipid modification of protein when N-terminal glycine attached with a myristoyl group, 14-carbon saturated fatty acid [25]. Most of SFKs, such as Fyn and Lyn, are dual acylated by palmitic and myristic acids, Src and Blk kinases are only myristoylated due to the absence of N-terminal cysteine residues[26-28]. Many proteins lipidated by myristoylation and palmitoylation are involved in membrane microdomain localizations such as lipid raft, which are essential for signal transduction [29, 30]. Dual acylation is reported to enhance the membrane affinity of SFKs, and palmitoylation is preferable for caveolae localization in NIH 3T3 fibroblasts and cervical Hela cells [31, 32].

Previous studies have demonstrated that myristoylation mediates high-fat diet associated tumor progression through Src-mediated pathway both *in vitro* and *in vivo*[33]. The exogenous myristate enhanced the localization of Src protein into membrane fraction for oncogenic activity. The high-fat (45%-60%) diets dramatically enhanced the tumor growth in PC-3 Src(Y529F) xenografts compared to 10% low-fat diet, which was correlated to the elevated activity of Src kinase and the associated downstream signaling (e.g., pAKT and pErk). The loss of myristoylation in Src(Y529F/G2A) mutant inhibited the tumor growth in mice fed with both low and high fat diets[33]. A further study suggests that the suppression of myristoylation by N-myristoyltransferase NMT1 prevented tumorigenic activity of Src kinase by inhibiting cell proliferation, invasion and malignant migration of prostate cancer cells[34]. A few studies demonstrate that oncogenic Src protein could be enriched in exosomes derived from cancer cells such as PC-3 cells[35], however, there are not yet reports revealing the mechanistic pathway on how Src is encapsulated into exosomes for secretion and dissemination.

Here, we evaluate the role of myristoylation in the encapsulation of Src kinase into exosomes. We demonstrate that myristoylation could promote the accumulation of Src kinase in exosomes

both *in vitro* and *in vivo*. Loss of myristoylation in the Src(G2A) mutant, or gain of palmitoyl site in the Src(S3C/S6C) mutant significantly decreased Src expresson levels in exosomes. The removal of palmitoylation in the Fyn(C3S/C6S) mutant significantly enhanced expression levels of Fyn mutant protein in exosomes. Mechanistically, exosomal Src encapsulation was dependent on the endosomal sorting complexes required for transport (ESCRT) machinery but not lipid-raft pathway. Myristoylation of phosphorylated Src was preferably encapsulated into exosomes and could mediate the syntenin trafficking and secretion in exosomes. *In vivo* studies showed that Src(Y529F) had significantly elevated Src expression levels in the serum exosomes compared to vector and Src(Y529F/G2A). The myristoylation facilitated the transfer of exosomal Src kinase into recipient fibroblast cells and induced apoptotic signals. This process was inhibited by loss of myritoylation in the Src(Y529F/G2A) mutant.

3.2 EXPERIMENTAL SECTION

Cell line and cell culture

Human prostate cancer cells DU145, PC-3, 22RV1 and LNCaP were purchased from American Type Culture Collection (ATCC). Mycoplasma detection were made to examine any contamination periodically (Figure S3.1).

Plasmid construct

Lentiviral vectors Src(WT), Src(G2A), Src(Y529F), Src(Y529F/G2A), Src(S3C/S6C), Fyn(WT), Fyn (G2A), Fyn (C3S/C6S) were cloned using the FUCRW parental vector as previously reported[34, 36]. The cells were used up to 20 passages.

Isolation of exosomes from the conditioned medium through ultra-centrifugation

Tested cells were grown in ATCC recommended medium in a 150-mm petri-dish. After reached 90% confluence, the medium was replaced with 5% exosome-free FBS (Life Technology Inc.), and grown in 5% CO_2 37 ºC incubator for another 24 h. The conditioned

medium was collected for the exosomes isolation. Specifically, the conditioned medium went through a series of centrifugations at 300 ×*g* at 4 ºC for 10 min., 2,000 ×*g* at 4 ºC for 10 min, and 10,000 ×*g* at 4 ºC for 30 min to remove live cells, dead cells, and cell debris, respectively. The supernatant of the medium was further ultra-centrifugated with 100,000 ×*g* at 4 ºC for 90 min. The exosome pellet was re-suspended in 1X PBS to wash out the residue medium, and re-ultracentrifuged at 100,000 ×*g* at 4 ºC for 90 min. The pelleted exosomes were re-suspended either in RIPA for protein analysis or 1X PBS for DLS measurement.

Characterization of exosomes

The size, zeta potential, and concentration of exosomes were measured by nanoparticle tracking analysis (NTA, Particle Metrix, Germany) with ZetaView software for data record and analysis.

Detergent compatible protein assay

The protein concentration of exosomes and cell lysates was determined by detergent compatible (DC) protein assay (Bio-Rad Laboratories). The total cell lysates (TCL) and exosomes were dissolved in radioimmunoprecipitation assay lysis buffer (RIPA) [50 mM Tris-base (pH 7.4), 1% NP-40, 0.50% sodium deoxycholate, 0.1% SDS, 150 mM NaCl, 2 mM EDTA and protease inhibitor (1X)]. Standards and samples (5 μL) were added into 96-well plate, followed by a mixture of Reagent A and S in a ratio of 50:1 (25 μL) and Reagent C (200 μL). The absorbance at 750 nm was detected after 15 min incubation at room temperature. The concentration of sample was calculated based on the calibration curve constructed by the standard.

Western blotting anlaysis

The cells and exosomes were dissolved in radioimmunoprecipitation assay (RIPA) buffer. The denatured proteins were subjected to SDS-PAGE gel, and transferred into nitrocellulose

membrane. The membrane was incubated with the primary antibody (dilution factor depending on an antibody) at 4 ºC overnight. After multiple washing steps with TBST, secondary antibody was added to the membrane at room temperature for 1 h. The blot was imaged with enhanced chemiluminescence (ECL). The bands of interest in the blot were quantified by Image J software. Rabbit antibodies anti-Src (catalog No. 2109), rabbit mAb anti-calnexin (catalog No. 2679), rabbit mAb anti-CD-9 (catalog No. 13403 for human species, catalog No. 2118 for mouse species), rabbit mAb anti-GAPDH (catalog No. 13403), rabbit Fyn(catalog No. 4023) and rabbit mAb anti-FAK(catalog No. 13009), rabbit mAb CD81 (catalog No. 10037), mouse mAb caspase-9 antibody (catalog No. 9508), caspase-7 antibody (catalog No. 9492), rabbit cleaved caspase-3 antibody (catalog No. 9661), and rabbit cleaved PARP mAb antibody (catalog No. 5625) were purchased from Cell Signaling Technology. Rabbit anti-RFP Antibody (catalog No. 600-401-379, Rockland Inc), rabbit anti-AR Antibody (catalog No. sc-816, Santa Cruz Biotechnology), and secondary antibody anti-rabbit IgG HRP-linked Antibody (7074, Cell Signaling Technology) were used according to manufactory's recommended dilution.

Determination of myristoylated Src kinase in exosomes by click chemistry reaction

Tested cells such as DU145 cells expressing Src kinase were plated at 150 mm petri dish and grown until 90% confluence in the EMEM medium with 5% PBS. The medium was replaced with the EMEM medium containing exosome-free FBS and 50 μM of myristic acid-azide (an analog of myristic acid). The cells were grown for another 24 h. The conditioned medium was collected and used for exosome isolation by ultracentrifuge method. The cells or exosomes were lysed in the M-PER buffer (Thermo Scientific) containing protease inhibitors and phosphatase inhibitors. The cell lysates or exosomes lysate (10 μg protein) were added into a working solution containing biotin-alkyne (0.1 mM), $CuSO_4$ (1 mM), TCEP (1 mM) and TBTA (0.1 mM) and incubated at room temperature for 1 h. After the Click reaction, the samples were mixed with

loading dye and boiled at 95 ^{o}C for 5 min. The lysates were subjected to SDS-PAGE gel, transferred into nitrocellulose membrane. After blocked with 5% milk overnight, the membrane was incubated with High Sensitivity Streptavidin-HRP (catalog No. 21130, ThermoFisher Scientific) at room temperature for 1 h. Myristoylated proteins (e.g., myristoylated Src kinase) were detected by ECL.

Exosomes uptake studies

SYF1 cells were grown in 8-well μ-slides (catalog No. 80826, ibidi) overnight. The labeled exosomes were added and incubated for various times (0-120 h). At each time point, the cells were imaged under a fluorescence microscope to record the cellular uptake of exosomes.

Parallelly, SYF1 and/or NIH 3T3 cells were grown in a 12-well plate overnight. The medium was replaced with fresh medium containing exosomes (20 μg/mL), and cells were incubated at 37^{o}C in 5% CO_2 for another 24 h. The cells were washed with PBS (1X) and lysed in the RIPA buffer (100 μL) for western blot analysis.

Lipid raft disrupting

PC-3 and DU145 cells were grown in 15-cm petri dish overnight. The medium was replaced the same growth medium but containing exosome-free FBS with DMSO (the control) or filipin III (0-1 μM) to disrupt the lipid raft for 24 h. The exosomes were collected from the conditioned medium. The exosomes and cells were lysed with the RIPA buffer for immunoblotting analysis.

Haemotoxylin and Eosin (H&E) staining

The tissue samples were fixed with PBS buffered 10% formaldehyde. The samples were further paraffin-embedded, and sectioned in Leica RM2235 Rotary Microtomy to 4 μm thickness and mounted on microscope slides (catalog No. 12-550-15, Fisher Scientific). Paraffin embedded sections were immerged through a series of solvents including 100% xylene to de-paraffin for 5 min (3X), 100% ethanol to rehydrate for 2 min (2X), 95% ethanol for 2 min (2X), 75% ethanol

for 2 min (2X), and then rinsed thoroughly by distilled water (3X). The sections were stained in Ehrlich's Hematoxylin for 5 min and washed with distilled water (3X), followed by 5-6 quick dips in acid alcohol (0.3%) to differentiate and wash thoroughly with distilled water (3X). The tissue sections were dipped into Scott's Tap Solution for 2 min and rinsed thoroughly with distilled water (3X). Counterstain in Eosin solution for 2 min and washed with distilled water (3X), followed by dehydration in 95% alcohol for 5 dips (2X) and 100% alcohol for 5 dips (2X). After xylene clearing for 1 min (3X), tissue sections were mounted with a coverslip in the mounting medium.

Immunohistochemistry (IHC) staining

4 µm thickness of tissue section on a microscope slide was baked for 60 min at 65 ^{o}C, and de-paraffined in 100% xylene for 5 min (2X), dehydrated in 100% ethanol for 5 min (2X), 95% ethanol for 5 min (2X), 70% ethanol for 5 min. After washed with PBS for 10 min (3X), the tissue slides were cooked in 0.01 M citrate buffer (pH 6.0) in a steamer cooker at a microwave with 60% power for 15 min and 10% power for 15 min. After cooling, tissue slides were washed with PBS for 10 min (2X). The tissues were circled with a PAP Pen liquid blocker (Part # 6505, Newcomer Supply). 300 µL of 0.3% H_2O_2 in distilled water was added into each tissue spot for 5-10 min and then washed with PBS for 10 min (3X). The tissues were blocked in 2.5% goat serum in PBS for 1 h at room temperature, and then incubated with primary antibody (Src 1:250, RFP 1:250, cleaved caspase 3 1:200 and cleaved PARP 1:200) in PBST overnight at 4 ^{o}C. The tissue slides were washed with PBST for 10 min (3X), and then incubated with secondary antibody (Cat: M7401) in PBST at room temperature for 1 h. After washing steps with PBS for 10 min (3X), the tissues slides were incubated with DAB solution (catalog No. SK-4100) for development. As soon as brown color was appeared under a microscope, the reaction was stopped by dipping the slide into distilled water. The time to develop for control and treatment

was kept the same. The tissue slides were stained in Hematoxylin for 1 min and washed with distilled water (3X), then immersed in $NaHCO_3$ solution for 3 min and washed with distilled water (3 X). The tissue slides were again dehydrated by treating samples in a series of alcohol solutions (75%, 95%, 100% ethanol for 5 min ×2), and then air dry for 10 min. After treated with xylene for 5 min (2X), the tissue sections were air-dried for 10 min, and mounted with the mounting medium and coverslip.

Exosomes isolation and characterization from plasma

The supernatant was collected after centrifugation of blood samples collected from mice at 2,000 ×*g* for 10 min. The exosomes were isolated from plasma by the Exoquick kit (catalog No. EXOQ5A-1, System Biosciences). ExoQuick Reagent (63 μL) was added to serum samples (250 μL) and incubated at 4 ºC for 30 min. The pellet exosomes were collected by centrifugation at 1500 ×*g* for 30 min and re-suspended in RIPA or PBS buffer. The exosomes re-suspended in PBS buffer were used for the characterization of size and zeta potential of exosomes by dynamic light scattering (DLS) with zetasizer (Malvern, USA). The lysed exosome in the RIPA buffer was used for western blot analysis.

Animal studies

All animal studies had access to diet and water throughout the experiments, and were approved by the Institutional Animal Care and Use Committee (IACUC) of University of Georgia. Male SCID mice with age of 8–10 weeks were randomly divided into 4 groups (n = 3). DU145 cells expressing Src(Y529F), Src(Y529F/G2A), or control (10,000 cells/mice) were implanted sub-renal of mice. The mice were routinely examined and euthanized after a 5-week study.

Statistical analysis

The data were presented as mean ± S.E.M (standard error of the mean). All the data with more than two groups were analyzed by one-way ANOVA with a *post hoc* Tukey test in GraphPad Prism software, and two values were compared by an unpaired student *t*-test. * $p < 0.05$; ** $p < 0.01$; *** $p < 0.001$; ns, non-significant.

Data sources and analysis

The Uniprot database was accessed and searched using the keyword “myristate” and the filters “Reviewed” and “Homo Sapiens”. 194 results were recovered and downloaded for further analysis. The sequences of proteins were analyzed and any protein sequences lacking a glycine at the second position were removed from the list. The remaining 182 proteins were checked together with the exosome data provided from the NCI-60 cell lines, and grouped by the number of times when each protein appeared in the exosomes , with 60 being the highest and 0 being the lowest[37-39].

Literature review focusing on the proteomic analysis of exosomes uncovered three studies on thymic, breast milk, and urine exosomes published in these three articles with the titles of “Characterization of human thymic exosomes”, “Comprehensive Proteomic Analysis of Human Milk-derived Extracellular Vesicles Unveils a Novel Functional Proteome Distinct from Other Milk Components”, and “Proteomic analysis of urine exosomes by multidimensional protein identification technology (MudPIT)”[40-42]. The 182 proteins taken from the Uniprot database were checked against the exosome data from each of the three studies, and their appearances in each of the three studies were recorded.

3.3 RESULTS

Enrichment of myristoylated proteins in exosome.

Given 20,000 proteins in a mammalian cell, 182 proteins were found to be myristoylated. We then investigated the number of myristoylated proteins enriched in exosomes in comparison with that in total cell lysate based on the available literature data sets. The proteomics study show that among 6071 proteins identified in exosomes, 98 myristoylated proteins were found in the exosomes in a study on 60 cancer cell lines. The myristoylated proteins represented 1.6-2.5% of total identified exosomal proteins (Figure 3.1A, Table S3.1) [37-39]. The frequency of myristoylated proteins was significantly higher in exosomes in all 60 cell lines in comparison with 0.9% of myristoylated proteins in the cells (Figure 3.1B)[37].

Additionally, the enrichment of myristoylated protein in the exosomes was also observed in three normal tissues. Specifically, 48, 41, and 59 myristoylated proteins were detected from 1853 exosomal proteins in Thymus, 1963 in breast milk, and 3280 in urine, respectively. The myristoylated proteins represented 2.6%, 2.1%, and 1.8% of total identified proteins in the exosomes (Figure 3.1A, Table S3.2, S3.3, S3.4) [40-42]. Collectively, the data suggest that myristoylated proteins are significantly enriched in the exosomes.

Enrichment of Src family kinases in prostate cancer cells

Our previous studies and others have demonstrated that Src family kinases (SFKs) are myristoylated, and/or palmitoylated. To examine the role of myristoylation and palmitoylation for protein enrichment in exosomes, the expression levels of SFKs in exosomes were compared with those in the cell lysate. The exosomes derived from four prostate cancer cell lines were characterized by a size of ~140 nm and zeta potential of ~-30 mV to ~-60 mV (Figure 3.1C, Figure S3.2). DU145-derived exosomes showed significantly higher concentration regarding the total number of particles compared to PC-3, 22Rv1 and LNCaP-derived exosomes (Figure 3.1C).

To explore enrichment of Src family kinases in exosomes, we investigated two members, Src which is only myristoylated, and Fyn which is dual acylated (myristoylated and palmitoylated), in four prostate cancer cell lines (DU145, PC-3, 22Rv1, LNCaP). Src kinase was mostly enriched in DU145 exosomes (Exo) with three-fold higher than DU145 total cell lysates (TCL), and 2-fold enrichment was observed in PC cells. The expression level of Src kinase was similar to that of total cell lysates in both 22Rv1 and LNCaP cells. Interestingly, the expression levels of Fyn kinase were under the detection limit in exosomes of all four cell lines (Figure 3.1D). The marker tetraspanin CD9 confirmed the existence of exosomes and the absence of calnexin suggested that isolated exosomes were of high purity (Figure 3.1D).

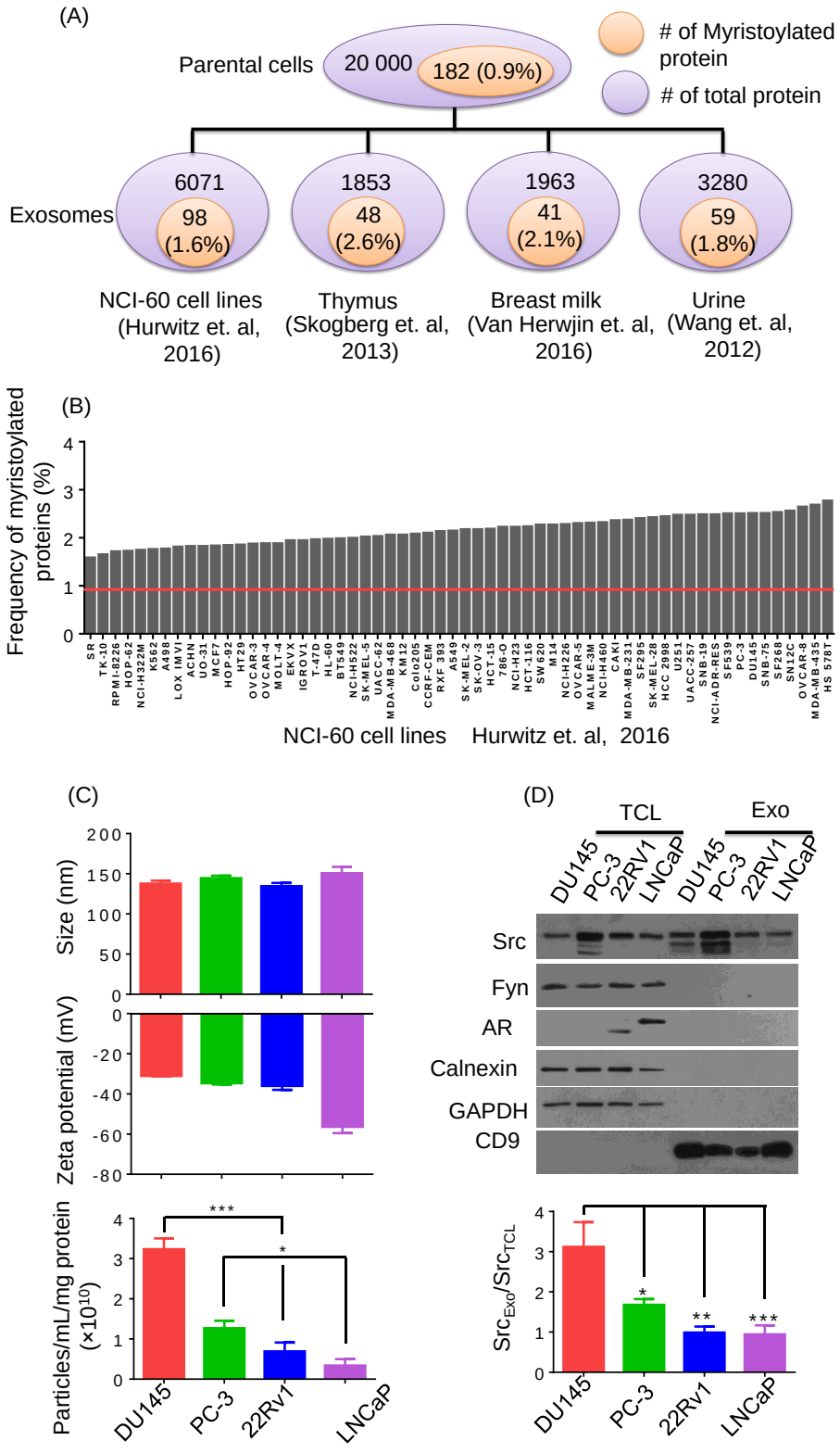

Figure 3.1 The enrichment of myristoylated proteins in exosomes. (A) The number of total proteins and myristoylated proteins in exosomes from 60 cancer cells and normal tissues including thymuc, breat milk, and urine [37-42]. There are 182 myristoylated proteins in a

mammalian cell with about 20,000 of total proteins. The number of myristoylated proteins account for 0.9% of the mammalian genome. (B) Frequency of myristoylated proteins in 60 cancer cell lines[37]. The red line represents the 0.9% of myristoylated proteins in the mammalian genome. (C) The size, zeta potential and particle concentration of exosomes. DU145, PC-3, 22Rv1 and LNCaP cells were cultured in medium containing exosome-free FBS for 24 h at 37ºC in 5% CO_2. Exosomes were isolated in the conditioned medium by ultracentrifugation method (D) Expression levels of Src kinase, calnexin, GAPDH and CD9 in the exosomes (Exo) and total cell lysates (TCL) were determined by Western blot analysis. The same amount of protein (10 µg) from the exosomes (Exo) or total cell lysate (TCL) were loaded as determined by DC protein assay. The enrichment of Src protein was evaluated by the ratio of Src protein level in Exo relative to that in TCL. Data were expressed as mean±S.E.M, * $p < 0.05$; ** $p < 0.01$; *** $p < 0.001$.

Myristoylation promotes encapsulation of Src kinase into exosomes

The enrichment of exosomal Src kinase prompted us to explore the role of myristoylation in encapsulation of Src kinase. Four cell lines including DU145, 22Rv1, NIH 3T3 and SYF1 cells were transfected with Src(WT) and Src(G2A) (loss of myristoylation) mutant by lentiviral infection(Figure 3.2A). The ratio of the expression levels of Src kinase in exosomes vesus total cell lysate were significantly inhibited in all four types of cells expressing Src(WT) in comparison with those expressing Src(G2A). The data suggest that myristoylation is essential for the encapsulation of Src kinase into exosomes (Figure 3.2B and 3.2C).

Myristoylation is initiated through the glycine site of the N-terminus in the Src kinase. We further studied if other regions of Src kinase may also contribute to its encapsulation. To do that, lenviral vector expressing a modified RFP gene was created. In this modified RFP protein, the N-terminus of Src kinase containing the sequence of MGSNKSKP was fused with RFP, designated as mRFP(WT). Additionally, MASNKSKP was also fused with RFP, designated as mRFP(G2A), which led to the loss of site for myristoylation. DU145 cells were overexpressed with mRFP(WT) or mRFP(G2A) by lentiviral infection. The RFP was highly enriched in exosomes derived from DU145 overexpressing mRFP(WT), but not mRFP(G2A) mutant (Figure

3.2D). These results further indicated that myristoylation, particularly the glycine site, is critical for myristoylated proteins to be encapsulated into exosomes.

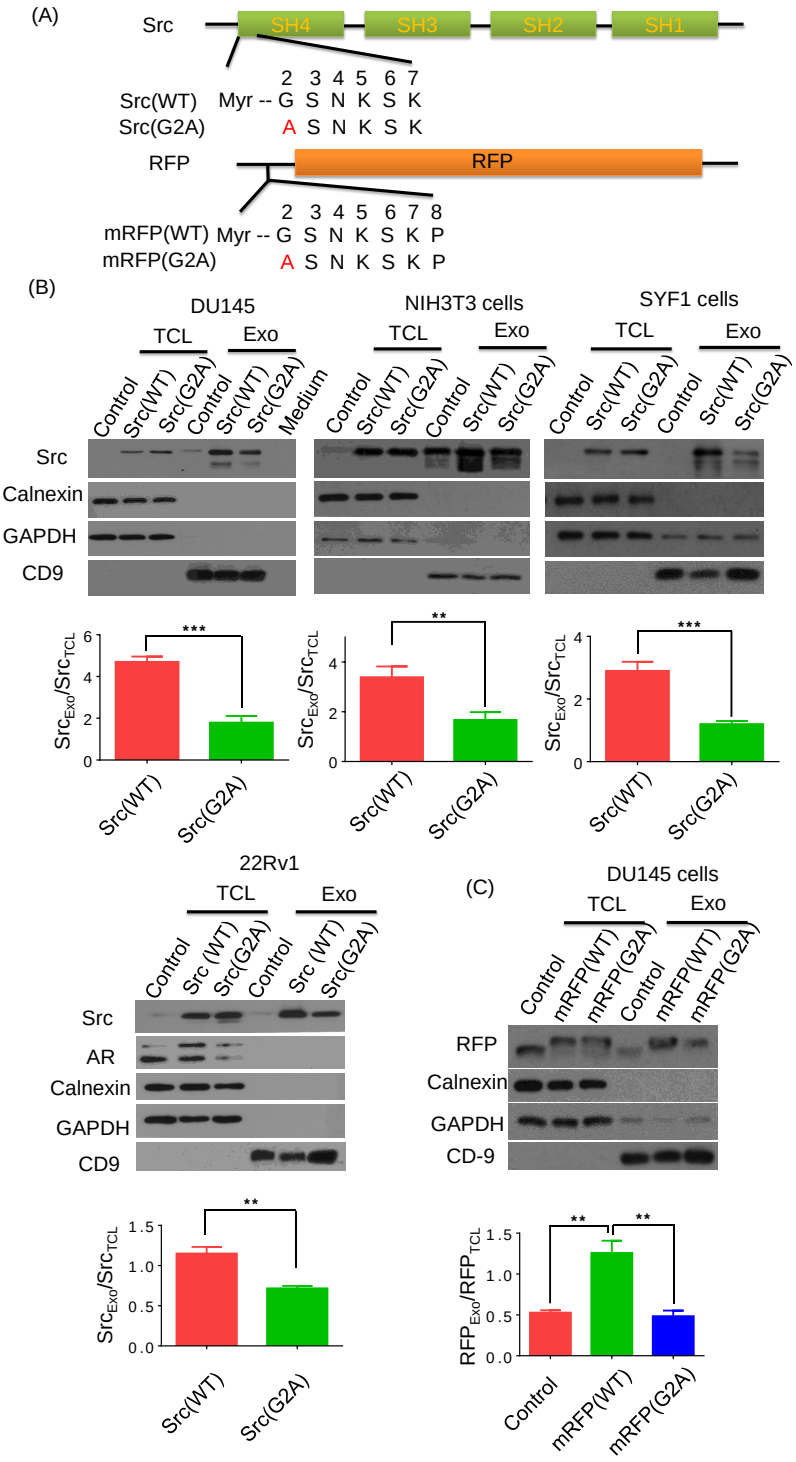

Figure 3.2 Loss of myristoylation inhibits Src protein encapsulation into exosomes. (A) Schematic diagram of Src(WT) and Src(G2A) constructs. (B) DU145, NIH3T3, SYF1,

22Rv1cells were transduced with Src(WT) or Src(G2A) by lentiviral infection. The transfected cells were grown in exosome-free FBS medium at 37ºC in 5% CO_2 and exosomes were collected from cell culture medium by ultracentrifugation method. Expression levels of Src in various types of Exo and TCL were evaluated by Western blot analysis. 10 μg of exosomes (Exo) or total cell lysates (TCL) were loaded. (C) Two lentiviral vector were constructed. One expresses a myristoylated red fluorescence protein (mRFP) containing eight amino acids (MGSNKSKP) derived from the N-terminus of Src kinase. The other expresses the RFP gene fused MASNKSKP in the N-terminus, which glycine is replaced by alanine, designated with mRFP(G2A). DU145 cells were transduced with the mRFP(WT) or mRFP(G2A) by lentiviral infection, and the transfected cells were grown in exosome-free medium. Exosomes were collected by ultracentrifugation method. The expression levels of RFP, Calnexin, GAPDH, and CD9 were analyzed by Western blotting. The Src protein was quantified by Image J software regarding the ratio of Src protein level in Exo relative to its level in TCL. Data were expressed as mean±S.E.M, ** $p < 0.01$; *** $p < 0.001$.

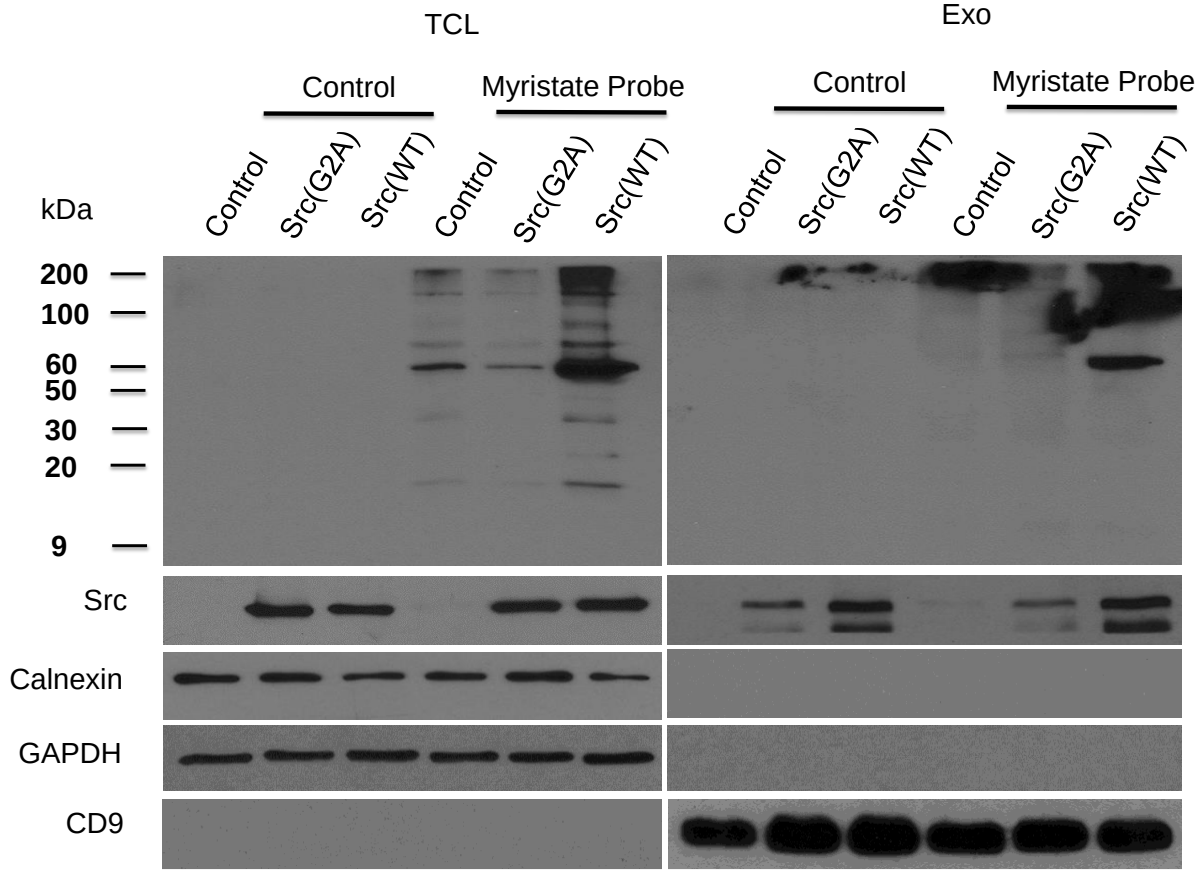

Figure 3.3 Loss of myristoylation inhibits Src encapsulation in exosomes. DU145 cells were transduced with Src(WT) and Src(G2A) by lentiviral infection. The transduced cells were incubated with 50 μM myristic acid-azide (an analog of myristic acid) for 24 h in exosome-free FBS medium at 37ºC in 5% CO_2. The exosomes were isolated from the conditioned medium by ultracentrifuge method. The myristoylated proteins from either exosome (Exo) and total cell lysates (TCL) were detected using Click Chemistry reaction, by which myristoylated proteins react with alkyne-biotin through azide-alkyne interaction. Expression levels of Src, calnexin,

GAPDH and CD9 was also measured by Western blot analysis. Ten μg of proteins from exosomes or total cell lysates was loaded.

Determination of myristoylated protein

To confirm if the exosomal Src protein was myristylated, DU145 expressing control/vector, Src(WT), or Src(G2A) cells were cultured in the medium containing myristic acid-azide. Expression levels of Src protein were similar in DU145 cells expressing Src(WT) in comparison with those expressing Src(G2A) in Western blot. Expression levels in both cells were significantly higher in that expressing control vector. However, expression levels of myristoylated protein at 60 kDa in DU145 cells expressing Src(G2A) were similar to that in DU145 cells expressing control vector in the cell lysate fraction, and were barely detected in the the exosomes fraction. In contrast, higher expression levels of myristoylated proteins at ~60 kDa corresponding to Src kinase were detected in both the cell lysate and exosomes (Figure 3.3). The results suggest that the presence of Src kinase in exosomes was the myristoylated .

Src kinase activity elevates the enrichment of Src kinase in exosomes

Src kinase contains a negative-regulatory tyrosine residue with Tyr 527, 529 and 530 in chicken, mouse, and human, respectively[43]. The Src(Y529F), a mutant that tyrosine is replaced by phenylalanine at position 529 (Figure 3.4A), is dephosphorylated and constitutively active. Similar to the exosomal enrichment of Src(WT) in comparison with Src(G2A), expression levels of Src protein were significantly elevated in exosomes derived from cells expressing Src(Y529F) in comparison with cells expressing Src(Y529F/G2A) in both DU145 and SYF1 cells (Figure 3.4B-E). Furthermore, the ratio of the expression levels of Src kinase in exosomes versus the cell lysate was further elevated in cells expressing Src(Y529F) compared to Src(WT) in both DU145 and SYF1 cells (Figure 3.4B and 3.4C). Coomassie blue staining confirmed that the same

amount of protein was loaded for both cellular lysates and exosomal proteins, respectively (Figure 3.4D).

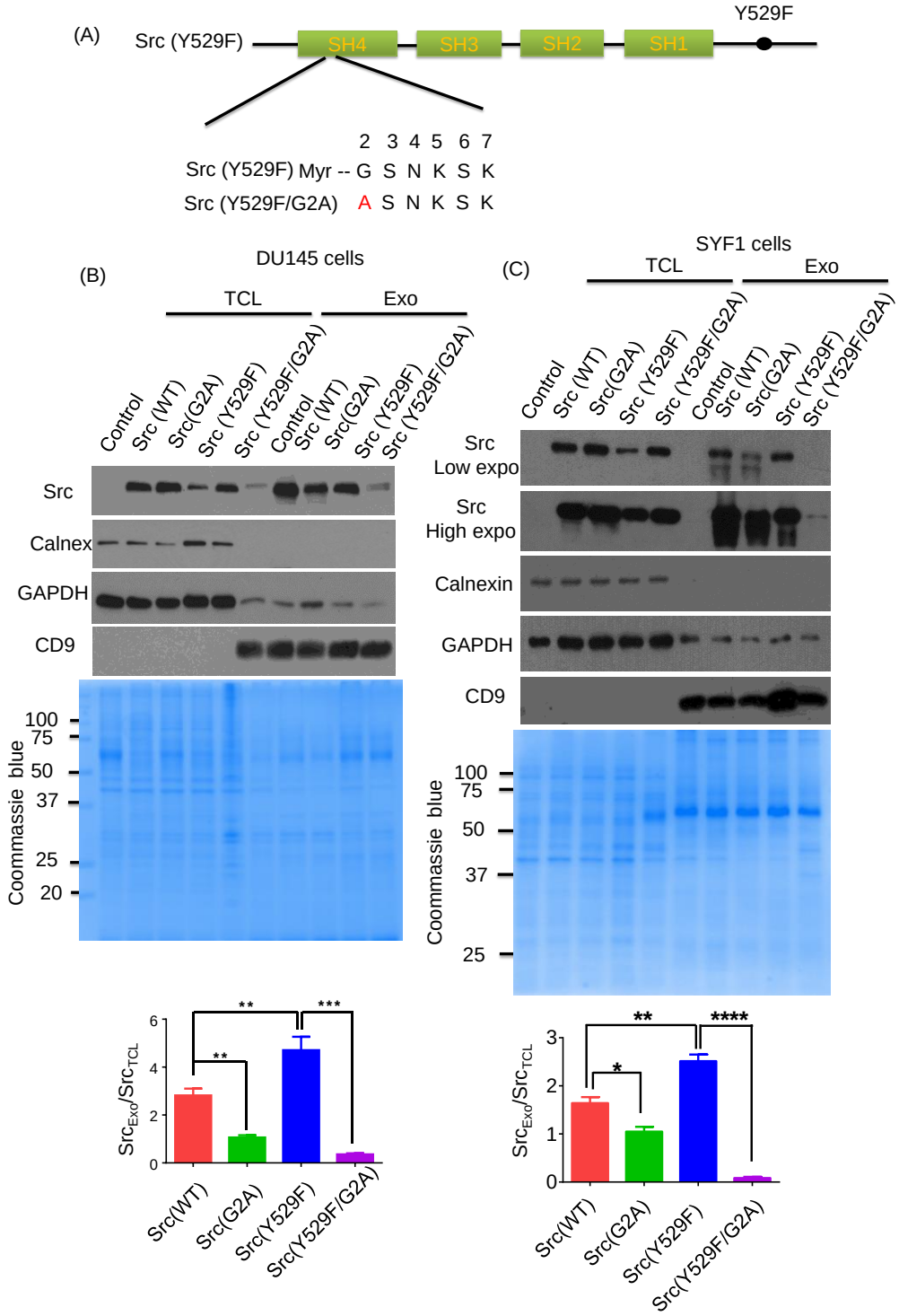

Figure 3.4 Src kinase activity promotes Src encapsulation into exosomes. (A) Schematic diagram of Src(Y529F) and Src(Y529F/G2A) constructs. (B-C). SYF1 and DU145 cells were

transduced with Src(WT), Src(G2A), Src(Y529F), and Src(Y529F/G2A) by lentiviral infection. Exosomes were collected from conditioned medium and isolated by ultracentrifuge method. Exosomes (Exo) and total cell lysate (TCL) were lysed in RIPA buffer. Expression levels of Src, calnexin, GAPDH and CD9 in exosomes and cell lysates derived from (B) DU145 (C) SYF1. Ten µg of Exo or TCL was loaded for analysis. Coomassie blue staining of SYF1 and DU145 cells and their corresponding mutants are loading control. The Src expression level was quantified by Image J software. Data were expressed as mean±S.E.M, * $p < 0.05$; ** $p < 0.01$; *** $p < 0.001$.

Palmitoylation status inhibits encapsulation of Fyn kinase in exosomes

SFKs members such as Fyn are dually acylated by both myristic and palmitic acids at the N-terminal glycine and cysteine residues, respectively[44]. Our previous data suggest that Fyn kinase was not encapsulated into exosomes when compared to expression levels between exosomes and cell lysates (Figure 3.1C). We set out to address the role of palmitoylation in regulation exosome encapsulation. We introduced palmitoylation sites in Src(S3C/S6C) mutant, or removal of palmitoylation sites in Fyn(C3S/C6S) mutant (Figure 3.5A). The palmitoylation was further confirmed in SYF1 cells expressing control vector, Fyn(WT), or Fyn(C3S/C6S) (Figure 3.5B). Similarly, palmitoylation was detected cells expressing a fusion protein of Fyn(8)-RFP, but not Src(8)-RFP (Figure S3.3).

As expected, expression levels of Src in the DU145 cells expressing Src(G2A) with the decreasing ratio of $Src_{exosomes}/Src_{cell\text{-}lysate}$ was significantly inhibited compared to that expressing Src(WT). Similarly, expression level of Src in the cells expressing Src(S3C/S6C) was also significantly inhibited compared to that expressing Src(WT) (Figure 3.5C). In a similar manner, as for the gain of palmitoylation in Src mutant, the ratio of $Fyn_{exosomes}/Fyn_{cell\text{-}lysate}$ in the cells expressing Fyn(C3S/C6S) was significantly increased compared to that expressing Fyn(WT), indicating the downregulation of Fyn expression in exosomes. In addition, the expression levels of Fyn in the cells expressing Fyn(G2A) were significantly inhibited compared to that expressing Fyn(WT), suggesting the important role of myristoylation in the cells over-expressing Fyn.

Collectively, these results indicate that myristoylation promoted the SFK kinases encapsulation into exosomes, whereas palmitoylation inhibited the encapsulation of Fyn kinase into exosomes.

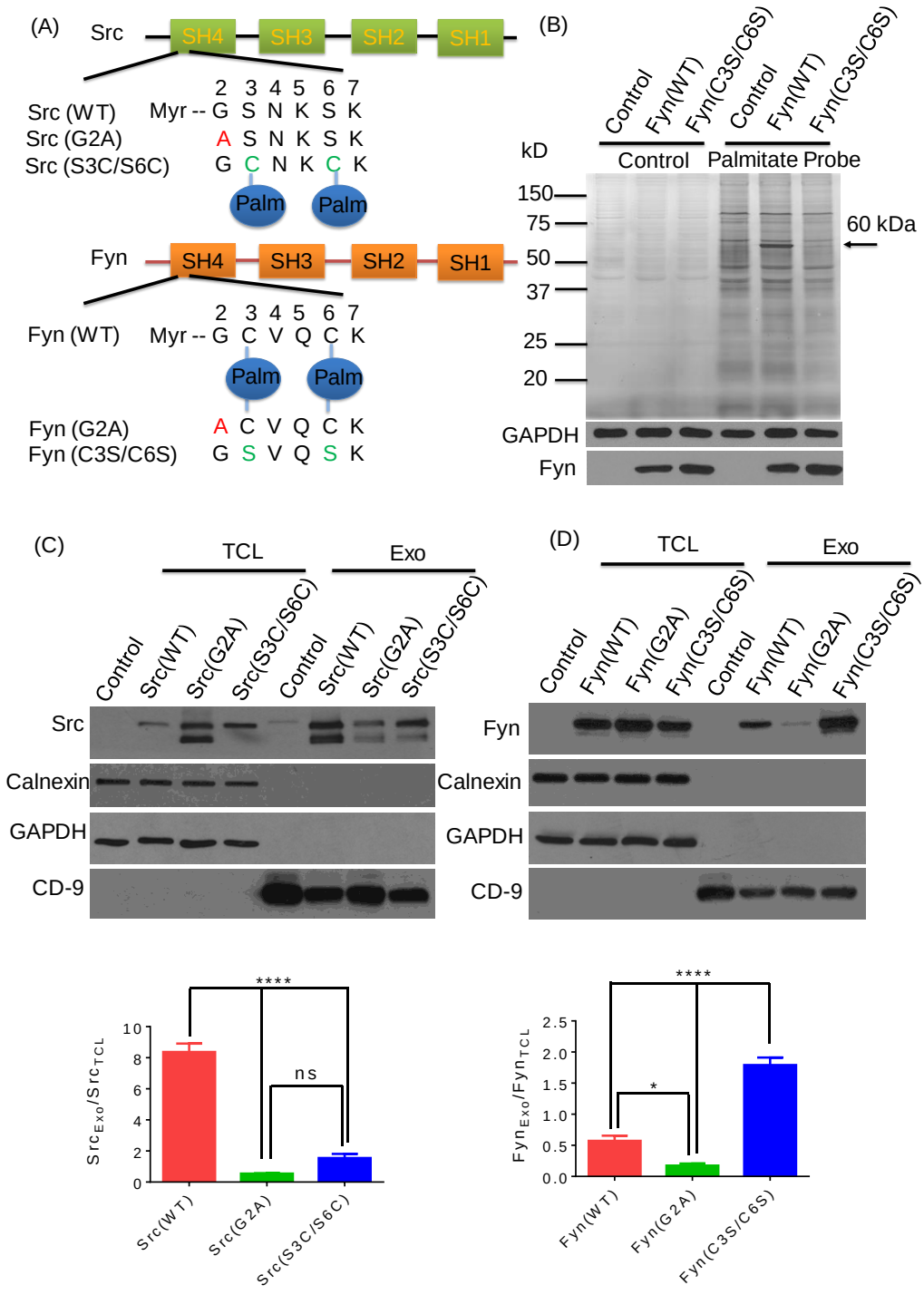

Figure 3.5 Palmitoylation inhibits the encapsulation of Fyn kinase into exosomes. (A) Schematic diagram of Src(WT), Src(G2A), Src(S3C/S6C), Fyn(WT), Fyn(G2A) and

Fyn(C3S/C6S). (B) Detection of palmitoylation in cells expressing Fyn(WT). SYF1 cells were transduced with Fyn(WT) and Fyn(C3S/C6S) by lentiviral infection. The transduced cells were incubated with 17-octadecynoic acid-azide. The cell lysates were subjected to Click Chemistry through azide-alkyne reaction, and detected with streptavidin-HRP by immunoblotting. (C) Gain of palmitoylation sites in Src kinase inhibits Src encapsulation into exosomes. DU145 cells were transduced with Src(WT), Src(G2A), and Src(S3S6) by lentiviral infection for 2 days. The stable cell lines were grown in exosome-free medium for 24 h at 37ºC in 5% CO_2. Exosomes were isolated from the conditioned medium by ultracentrifugation method. Expression levels of Src, calnexin, GAPDH and CD9 in Exo and TCL were analyzed by Western blot. (D) Loss of palmitoylation sites in Fyn kinase enhances Fyn encapsulation into exosomes. DU145 cells were transduced with Fyn(WT), Fyn(G2A), and Fyn(C3C6) by lentiviral infection. Conditioned medium was collected after 24 h incubation in exosome-free medium at 37ºC in 5% CO_2. Exosomes were isolated by ultracentrifugation method. Expression levels of Fyn, calnexin, GAPDH, and CD9 in exosome (Exo) or total cell lysates (TCL) were measured by immunoblotting. Ten µg (with respect to protein) of exosome (Exo) and total cell lysates (TCL) were loaded for protein analysis. The Src protein level was quantified by Image J. Data were expressed as mean±S.E.M, * $p < 0.05$; **** $p < 0.0001$; ns-non significant.

ESCRT is involved in Src kinase encapsulation into exosomes

Lipid-rafts are membrane-associated microdomains enriched with cholesterol and saturated phospholipids like sphingolipids participating in exosome secretion[45, 46]. Lipid-raft pathway modulates the incorporation of proteins into extracellular vesicles through binding proteins such as GPI-anchored proteins, transmembrane proteins, and Src family tyrosine kinases[47-49]. Neuronal Src with 6-amino acid inserted in the SH3 domain is situated in lipid raft in the brain both *in vitro* and *in vivo*[50]. Thus, we speculated if lipid-raft mediates Src encapsulation into exosomes. To test this hypothesis, a disrupting agent, Filipin III, was used to examine whether Src kinase encapsulation into exosomes was dependent on lipid-raft pathway. The cells were treated with Filipin III to disrupt the lipid raft, and cholesterol level was significantly decreased with the observation of reduced fluorescence signal (Figure S3.4A), but the treatment did not affect the Src protein encapsulation into exosomes (Figure S3.4B).

The ESCRT-I protein complex binds to ubiquitinated endosomal cargo, and ESCRT-I associated protein human tumor susceptibility gene 101 (TSG101) is essential for HIV budding process through binding with p6 late domain and regulates the localization of Src kinase[51-53].

Therefore, we further studied the ESCRT pathway in regulation of Src encapsulation by knocking down the TSG101. Both cellular and exosomal levels of TSG101 were decreased when both PC3 and 22Rv1 cells expressing shRNA-TSG101. shRNA-TSG101 did not change the cellular level of Src protein, but significantly reduced the exosomal Src level in both 22Rv1 and PC-3 cells (Figure 3.6A and 3.6B). The Coomassie blue staining confirmed the same protein loading in cellular or exosomal lysates (Figure 3.6A and Figure 3.6B).

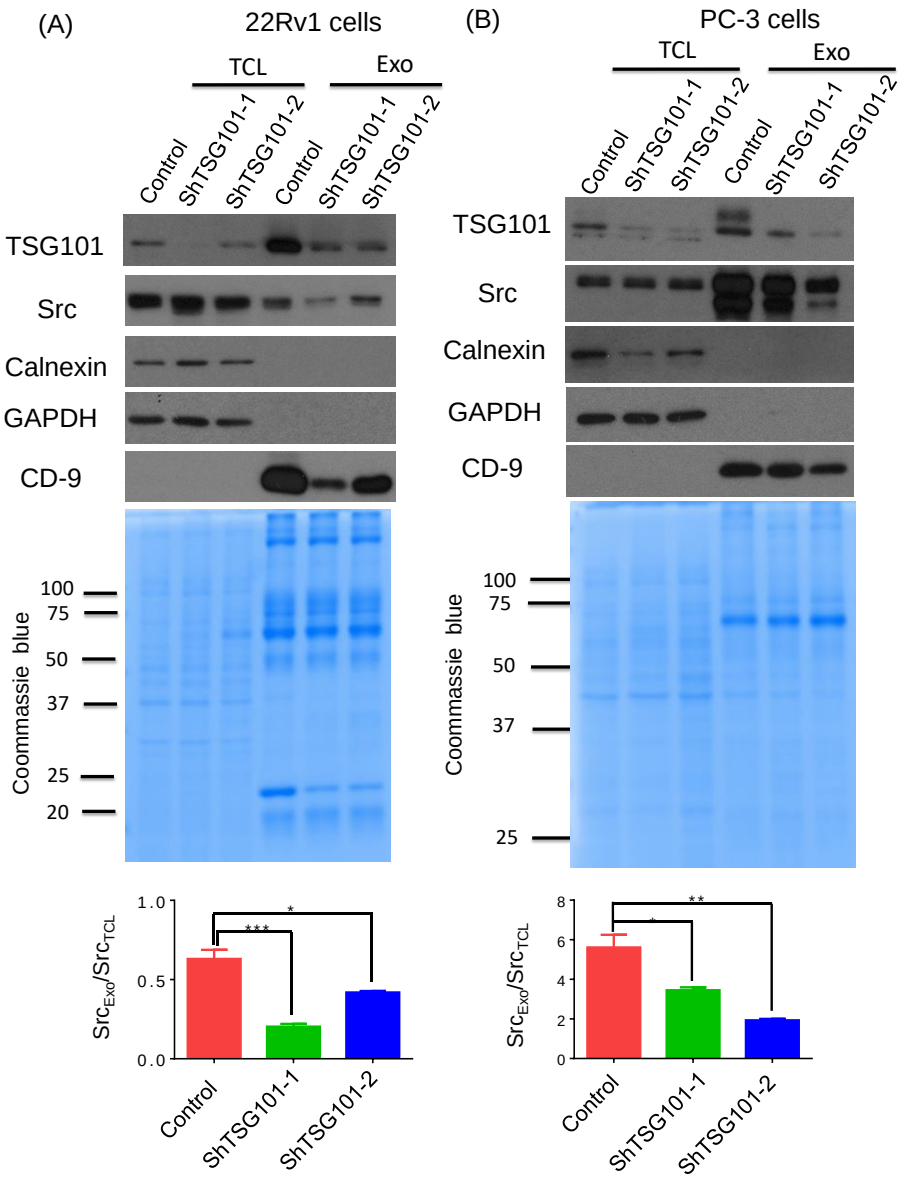

Figure 3.6 Suppression of TSG101 inhibits encapsulation of Src kinase into exosomes. Expression levels of TSG101, Src, Calnexin, GAPDH, CD9 and the corresponding ratio of Src in

exosomes relative to total cell lysates in (A) 22Rv1 (B) PC-3. Coomassie blue staining was used to confirm the equal loading of total protein. 22Rv1 and PC-3 cells were transfected by shRNA-TSG101 via lentiviral infection. 22Rv1 and PC-3 cells expressing shRNA-TSG101 were incubated in exosome-free medium at 37ºC in 5% CO_2 for 48 h. Exosomes were isolated from cell culture medium at day 5 by ultracentrifugation method. Same amounts (10 μg) of exosome (Exo) or total cell lysates (TCL) were loaded as determined by DC protein assay. ShTSG101-1 targets the sequence of 5'-CGGACTGGACACATACCCATATAACTCGAGTTATATGGGTATGTGTCCAGTTTTTTG-3'. ShTSG101-2 targets the sequence of 5'-CCGGGCCTTATAGAGGTAATACATACTCGAGTATGTATTACCTCTATAAGGCTTTTG-3'.

Src is reported to interact with syntenin during exosome biogenesis and budding. Src directly phosphorylates syntenin and promtes syntenin-mediated exosomal biogenesis [54]. Thus, we further investigated whether Src expression levels and its activity regulate the exosome biogenesis. High expression levels of pSrc(Y416) were correlated the number of exosomal particles (Figure 3.1D and Figure 3.7A). Knockdown of Src expression in PC-3 cells significantly decreased the syntenin expression levels in exosomes (Figure 3.7B), suggesting a reduction of exosomes biogenesis. In addition, both DU145 and SYF1 cells overexpressing Src(Y529F) significantly enhanced expression levels of exosomal syntenin (Figure 3.7C-D). In contrast, syntenin levels in the exosomes from DU145 or SYF1 cells expressing Src(Y529F/G2A) mutant, which inhibited Src kinase activity, were significantly inhibited in comparison with those expressing Src(Y529F) (Figure 3.7C and 3.7D). These data suggest that Src expression level and its kinase activity are essential for exosomal biogenesis. Src encapsulation is regulated through syntenin-mediated pathway.

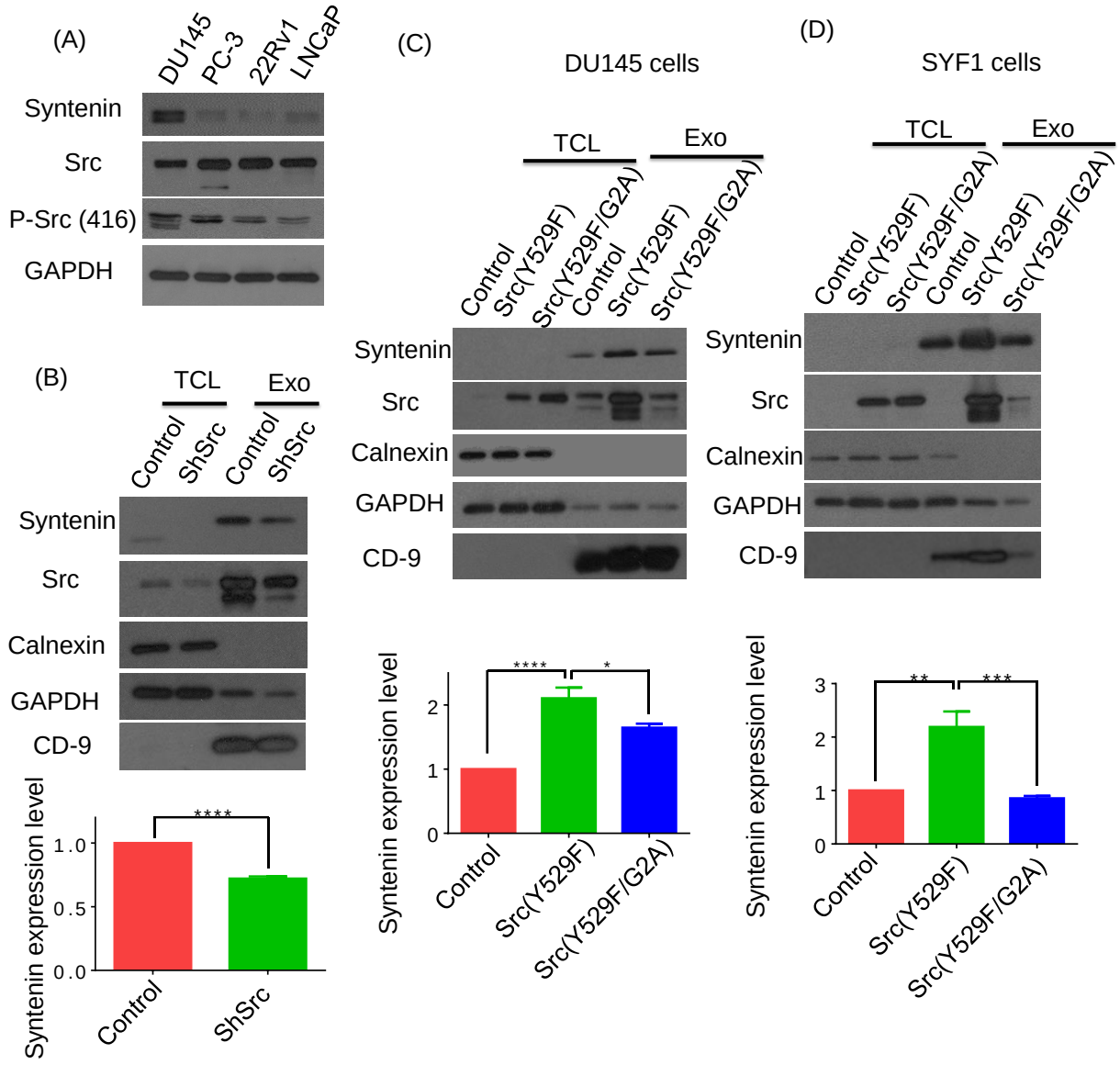

Figure 3.7 Src activity and expression levels promote syntenin mediated exosomes biogenesis. (A) Expression levels of syntenin, Src, pSrc(Y416), and GAPHD in four prostate cancer cell lines DU145, PC-3, LNCaP, and 22Rv1. (B) PC-3 cells were transfected by shRNA-Src or shRNA-Control via lentiviral infection. The cells were incubated in exosome-free medium at 37ºC in 5% CO_2 for 48 h and exosomes were isolated from the conditioned medium at day 5 by ultracentrifugation method. Expression levels of syntenin, Src, calnexin, GAPDH, and CD9 in exosomes and total cell lysates derived from PC-3 expressing shRNA-Src or control were detected by immunoblotting. Expression levels of syntenin in exosomes derived from PC-3 cells expressing shRNA-control or shRNA- Src were quantified. (C-D) DU145 (C) or SYF1 cells (D) were transduced with control, Src(Y529F), or Src(Y529F/G2A) cells. Expression levels of syntenin, Src, calnexin, GAPHD, and CD9 in exosomes and TCL were analyzed by immunoblotting. Syntenin expression levels in exosomes derived from DU145 expressing control, Src(Y529F), or Src(Y529F/G2A) were quatified. The same amounts (10 µg) of exosome (Exo) or total cell lysates (TCL) were loaded as determined by DC protein assay.

Tumor derived exosomes induces apoptosis, and loss of myristoylation suppresses exosomal Src(Y529F) induced apoptosis in the recipient cells

The translocation of Src protein is possibly shuttled from cells to cells through exosomes [55]. Myristylation was demonstrated to promote the encapsulation of Src into exosomes (Figure 3.2B-D). We further evaluated the role of myristoylation to mediate exosomal Src in cell-cell communication. Figure 3.8A illustrates the experimental process that DU145 or its mutant derived exosomes were delivered to SYF1 recipient cells. The exosomes were internalized into SYF1 cells in a time-dependent manner as seen with increased green fluorescence signal upon time (Figure S3.5). Expression levels of Src kinase were increased in response to incubation time (Figure 3.8B), and much higher in SYF1 cells treated with exosomes derived from DU145 cells expressing Src(WT) than those expressing Src(G2A) or control (Figure 3.8C). The different expression levels of Src kinase were attributed to the corresponding expression levels of exosomal Src protein (Figure 3.2B).

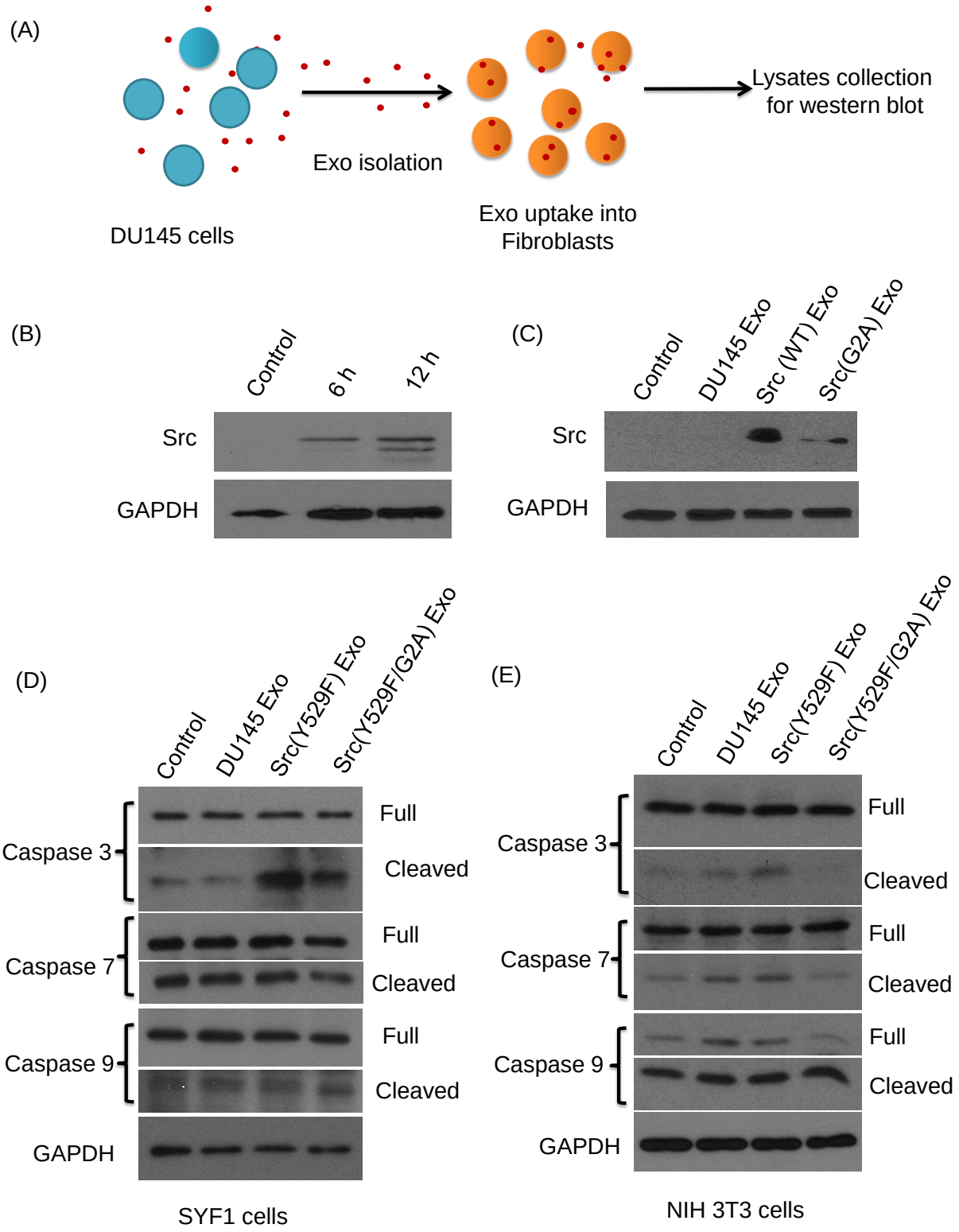

Figure 3.8 The Src kinase is transferred to recipient cells through exosomes and induces apoptotic signaling. (A) Schematic diagram of a process that DU145 derived exosomes were internalized into SYF1 recipient cells. (B) DU145 derived exosomes were incubated with SYF1 recipient cells for 6 and 12 h, the expression levels of Src and GAPDH proteins in SYF1 cells

were evaluated. (C) DU145 cells were transfected with Src(WT) and Src(G2A) by lentiviral infection. Exosomes derived from DU145 cells expressing control, Src(WT), and Src(G2A) were incubated with SYF1 recipient cells for 12 h. Expression levels of Src and GAPDH proteins in SYF1 cells were evaluated. (D-E) DU145 cells were transfected with Src(Y529F) and Src(Y529F/G2A) by lentiviral infection. DU145 cellls expressing Src(Y529F), Src(Y529F/G2A) cells were incubated in exosome-free medium at 37ºC in 5% CO_2 for 24 h and exosomes were isolated from cell culture medium by ultracentrifugation method. Exosomes derived from DU145 control or expressing Src(Y529F), Src(Y529F/G2A) were incubated with SYF1 (D) and NIH 3T3 cells (E) for 24 h. The expression levels of caspase 3, 7, and 9 were determined by immunoblotting. The same amounts (30 µg) of SYF1 and NIH 3T3 cell lysates were loaded as determined by DC protein assay.

We further examined the apoptosis signaling of the recipient cells treated with exosomes from DU145, Src(Y529F) and Src(Y529F/G2A) cells. Expression levels of cleaved caspase 3 were significantly elevated in SYF1 cells treated with Src(Y529F)-Exo, and this effect was attenuated by Src(Y529F/G2A)-Exo. The exosomes treatment did not affect expression levels of caspase 7 and 9 in SYF1 cells (Figure 3.8D). Morphological change was also observed in SYF1 cells treated with exosomes derived from DU145-Src(Y529F), but not Src(Y529F/G2A) (Figure S3.6).

Expression levels of cleaved caspase 3, and 7 were increased in 3T3 cells treated with exosomes derived from DU145 cells in comparison with the control. The expression levels of cleaved caspase 3, and 7 were further elevated in 3T3 cells treated with exosomes from DU145 cells expressing Src(Y529F), but not with exosomes from those expressing Src(Y529F/G2A) (Figure 3.8E). These results suggest a mechanism of exosomes derived from tumors might potentially regulate the surrounding host cells. This might be essential for tumor cells in regulation of host immuno-response.

Myristoylation contributes to exosomal Src protein in plasma

The *in vitro* studies on myristoylation facilitating Src protein encapsulation into exosomes prompted *in vivo* studies to demonstrate this concept. The size and weight of tumors were significantly increased in xenograft tumors expressing Src(Y529F) in comparison with these

from control vector or Src(Y529F/G2A). No significant changes of size (~55 nm) and zeta potential (~-25 mV) were observed from serum exosomes derived xenograft tumors expressing control, vector, Src(Y529F), Src(Y529F/G2A) (Figure 3.9A). The xenograft tumors expressing Src(Y529F) showed much larger tumor size and significantly elevated expression level of Src in the serum exosomes than xenograft tumors expressing vector and Src(Y529F/G2A) (Figure 3.9B and 3.9C), suggesting that myritoylation is essential to falicitate Src protein encapsulation into exosomes. Serum HSP90 is reported to be a potential biomarker for prostate cancer [56]. Thus, we further evaluated the level of HSP90 in the serum, similar to Src, expression levels of HSP90 was found to be much higher in serum exosomes derived from Src(Y529F) compared to control, or mutant Src(Y529F/G2A). The protein TSG101 was used as exosomal markers and was detected in serum exosomes. The same protein loading for all samples was confirmed by Coomassie Blue staining (Figure 3.9D).

There is possibility that high amount of exosomal Src in serum was due to the difference in tumor size other than Src myristoylation. This impedes us to conduct another set of experiment by generating similar size of tumors between Src (Y529F/G2A) and Src(Y529F). We implanted ten times more cells for DU145 cells or DU145 expressing Src(Y529F/G2A) groups than that in DU145 expressing Src(Y529F) group. Similar tumor size was observed in both Src(Y529F) and Src(Y529F/G2A) (Figure 3.10A and 3.10B). Expression levels of Src, HSP90 and non-P-Src(Y529) in the serum exosomes from the Src(Y529F) group were elevated in comparison with those in Src(Y529F/G2A) or vector controls groups (Figure 3.10C). The same amount of exosome protein loading was confirmed by Coomassie blue staining (3.10D). H&E staining and IHC staining of tissue samples confirmed the elevated expression levels of Src and RFP (Figure

3.11). These data suggest that myristoylation is essential for the encapsulation of Src kinase into exosomes from xenograft tumors.

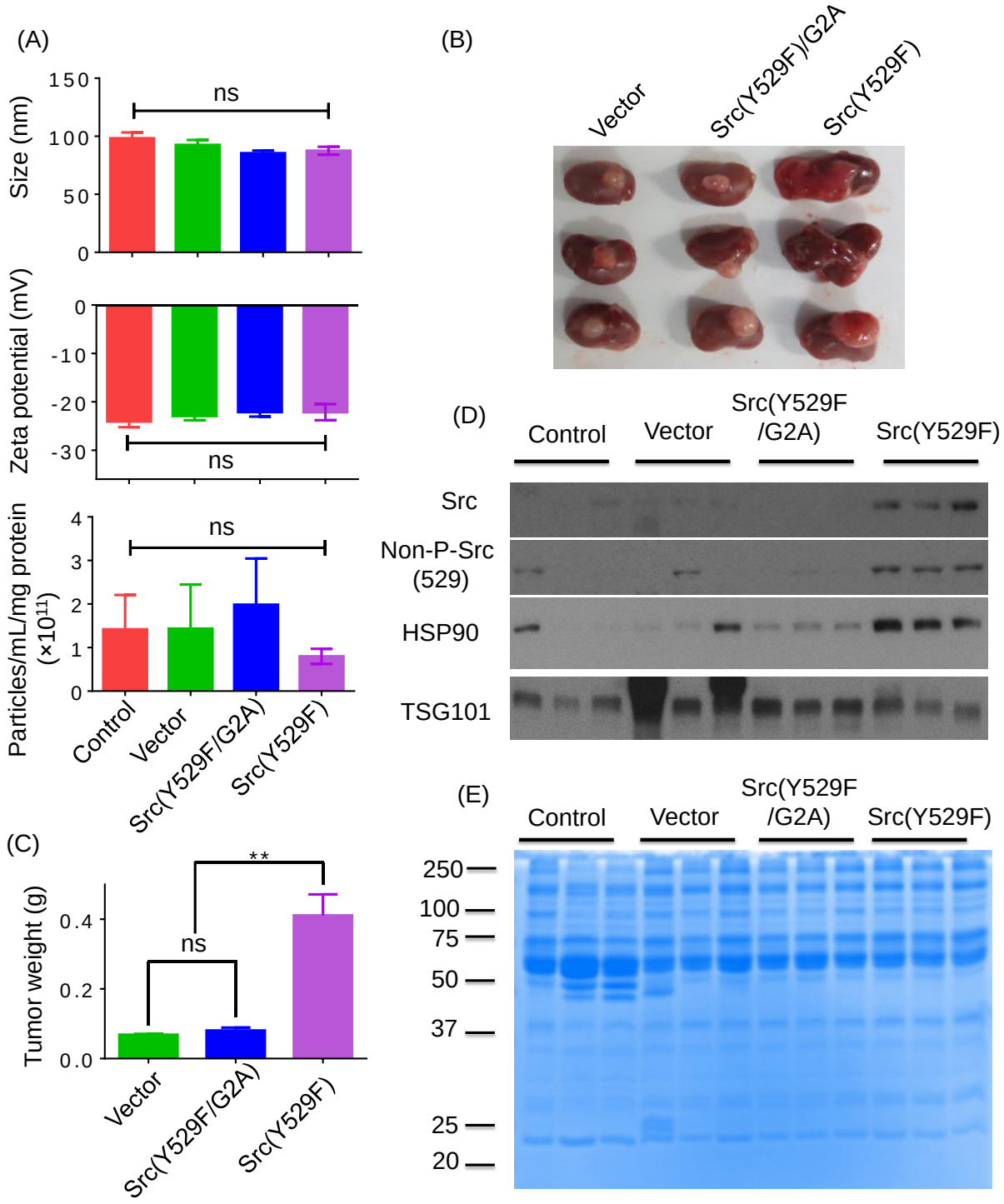

Figure 3.9 Loss of myristoylation inhibits the encapsulation of Src kinase in plasma. DU145 cells were transduced with Src(Y529F) or Src(Y529F/G2A) by lentiviral infection. DU145 cells,

or DU145 cells overexpressing Src(Y529F) or Src(Y529F/G2A) were implanted into sub-renal of SCID mice. After 5 weeks, the mice were sacrificed, tumors and serum samples were harvested. (A) Plasma-derived exosomes were isolated by ExoQuick kit and characterized by size, zeta potential and particle concentration. (B) Representative tumor image and (C) weight of xenograft tumors derived from DU145 vector or cells expressing Src(Y529F) and Src(Y529F/G2A). (D) Expression levels of Src, non-P-Src(Y529), HSP90, and TSG101 of plasma-derived exosomes were evaluated by western blotting analysis. An equivalent amount of exosomes (50 µg with respect to protein) were loaded. The total amount of protein measured by Coomassie Blue staining was used as the equal loading control. Data were expressed as mean ± S.E.M. *** $p < 0.001$; ns, non-significant.

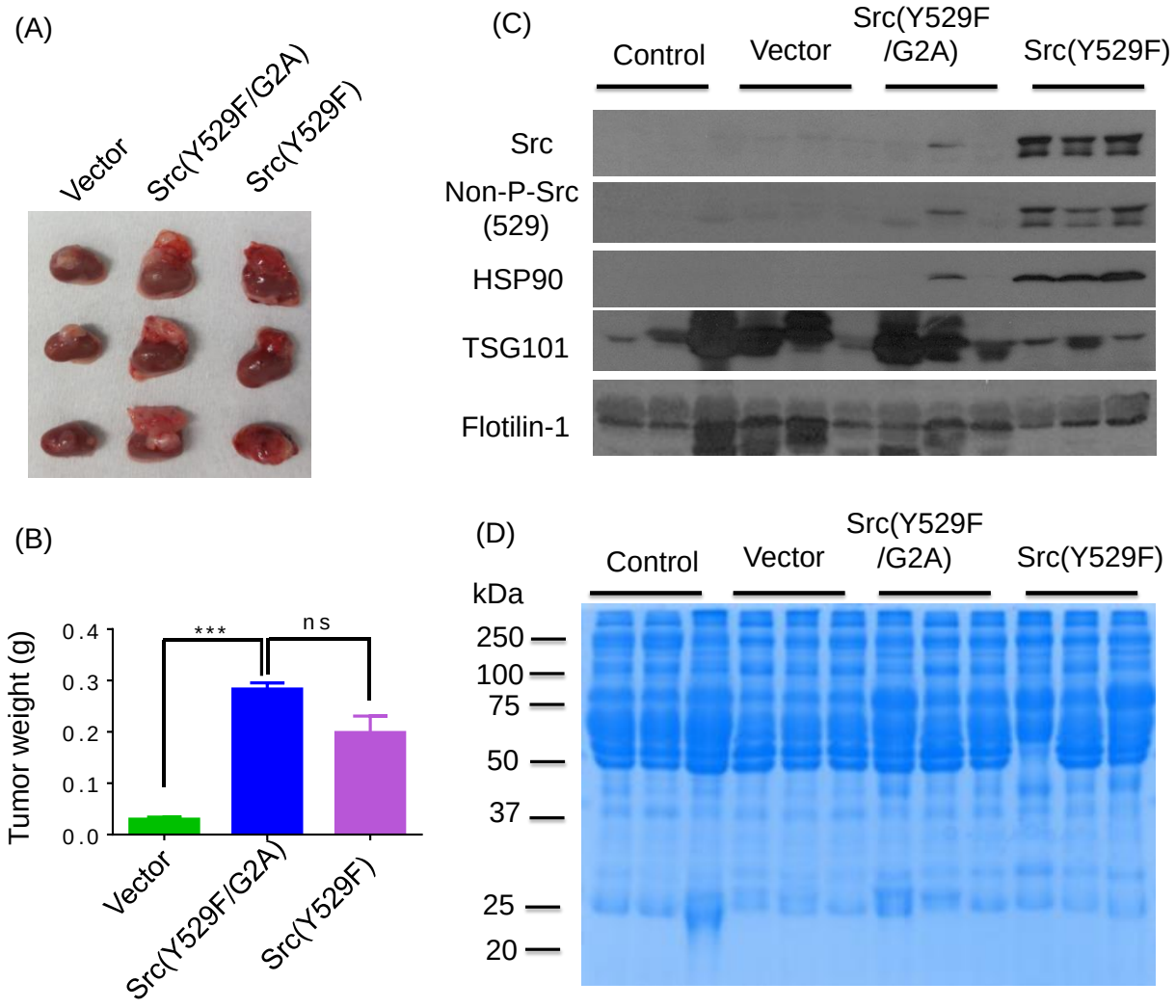

Figure 3.10 Myristoylation promotes the encapsulation of Src kinase in serum exosomes *in vivo*. DU145 cells were transduced with Src(Y529F) or Src(Y529F/G2A) by lentiviral infection. DU145 cells (150,000 cells/graft), or DU145 cells overexpressing Src(Y529F) (150,000

cells/graft) or Src(Y529F/G2A) (15,000 cells/graft) were implanted into sub-renal of SCID mice. After 4 weeks, the mice were sacrificed, tumors and serum samples were harvested. (A) Representative tumor image and (B) weight of xenograft tumors derived from DU145 vector or cells expressing Src(Y529F) and Src(Y529F/G2A). (D) Expression levels of Src, non-P-Src(Y529), HSP90, TSG101, and flotillin-1 of serum exosomes were determined by western blotting analysis. (D) Coomassie Blue staining of serum exosomes. 50 µg of exosomes were loaded. Data were expressed as mean ± S.E.M. *** $p < 0.001$; ns, non-significant.

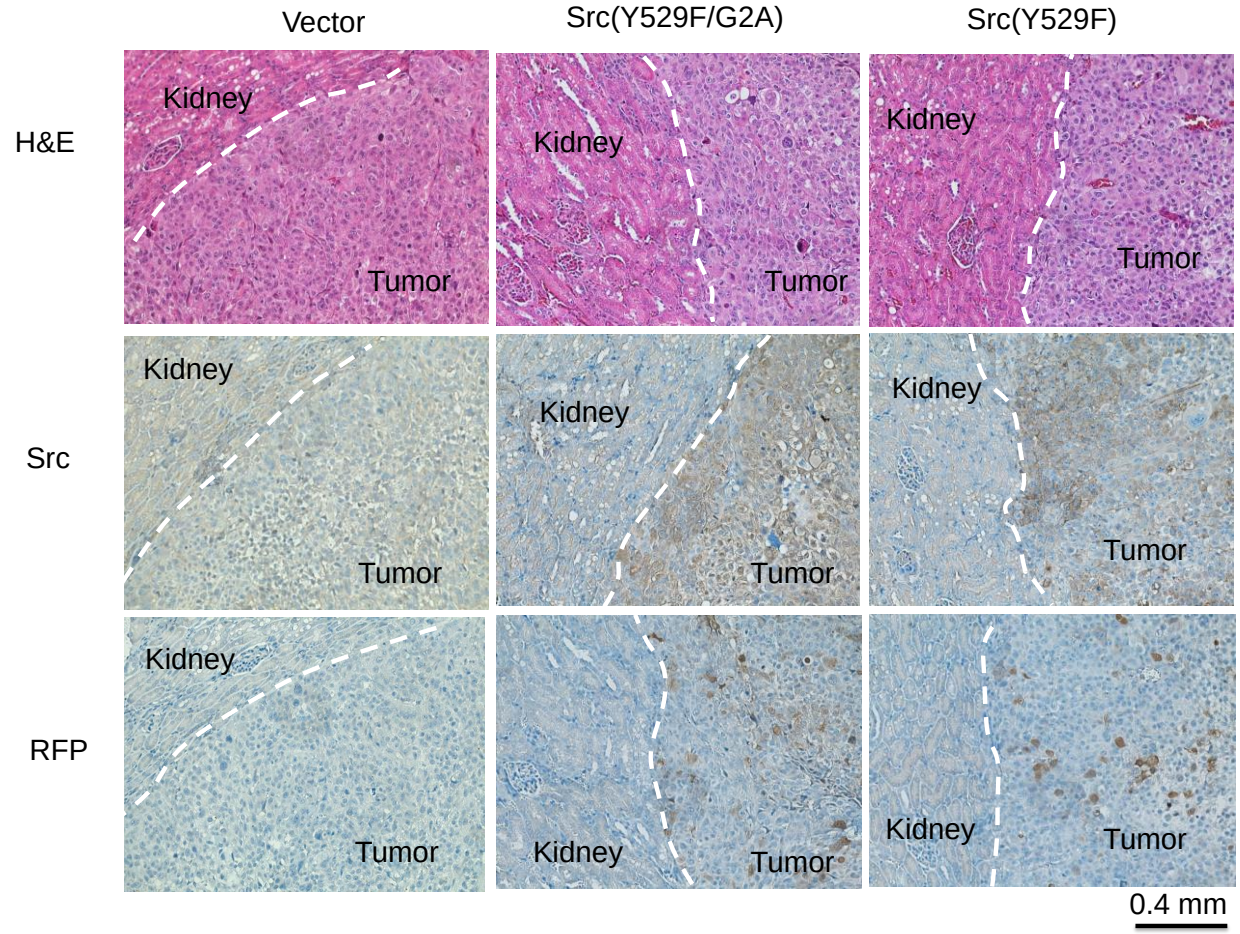

Figure 3.11 Haemotoxylin and Eosin (H&E) staining and immunohistochemistry (IHC) staining of tissue samples from vector, Src(Y529F) and Src(Y529F/G2A) in regards to RFP and Src staining. DU145 cells were transduced with Src(Y529F) or Src(Y529F/G2A) by lentiviral infection.

3.4 DISCUSSION

Myristoylation promotes the Src protein encapsulation into exosomes through its cell membrane association

Src is reported to be enriched in exosomes derived from PC-3, C4-2B, and DU145 cells[35]. Consistently, we have demonstrated that Src was enriched in exosomes compared to cell lysates

in DU145 and PC-3 prostate cancer cells (Figure 3.1B). Myristoylation was found to promote the encapsulation of oncogenic Src kinase into exosomes. Loss of myristoylation by Src(G2A) mutant could reduce the exosomal Src accumulation (Figure 3.2). These may be attributed to the membrane association of Src kinase mediated by myristoylation. The analysis of various cell lines suggested that the promoting role of myristoylation for exosomal accumulation of Src kinase is not cell-specific in prostate cancer (Figure 3.2A and 3.2B) and could be applied to other type of cells as well. Our result is consistent with the literature reported by Shen et al. that myristoylation participated in the secretion of TyA-GFP in exosomes/microvesicles. The loss of myristoylation in Acyl(G2A)TyA-GFP and HIV Gag(G2A)TyA-GFP did not target proteins into the secreted vesicles or HIV virus[24].

Palmitoylation inhibits the SFKs encapsulation into exosomes

We identified that palmitoylation inhibited the accumulation of SFKs into exosomes. The introduction of palmitoylation in Src(S3C/S6C) inhibited the Src incorporation into exosomes, and removal of palmitoylated site in Fyn(C3S/C6S) increased the Fyn encapsulation in the exosomes (Figure 3.5B and 3.5C). Both myristoylation and palmitoylation are involved in SFKs trafficking to membranes[57], but they are different in specific localization of SFKs in the membrane and palmitoylation preferably brings proteins into caveolae of the plasma membrane[32]. The dual acylation by myristoylation and palmitoylation is reported to partially target α-subunit of G-protein into caveolin-containing membrane fractions[58]. Palmitoylation is reported to significantly enhance the localization of Gi1 alpha proteins to caveolae (e.g., 4-fold higher) compared to myristoylation[59]. Thus, the palmitoylated inhibition of SFKs encapsulation into exosomes is possibly attributed to the more concentrated caveolae localization which blocks the exosomal protein encapsulation.

Myristoylation promotes encapsulation of constitutively active form of Src kinase into exosomes

We found that the constitutively active form of Src(Y529F) mutant enhanced the exosomal level of Src kinase compared to inactive Src(WT) (Figure 3.4B and 3.4C). Membrane localization of Src is critical to dephosphorylate Tyr529 for activation of Src kinase possibly attributed to the presence of membrane-bound phosphatase[60]. It is reported that Src-WT-GFP and Src-Y527F-GFP mutants had two-fold of Src kinase in membrane fraction more than cytosol fraction in COS-7 cells, and Src-Y527F-GFP accumulated more of Src kinase in the membrane compared to Src-WT-GFP construct attributed to Src kinase activity and SH2 domain binding, reflecting interactions with lower diffusion membrane-associated protein structures (e.g., focal adhesions) and peripheral membranes [61]. Thus, Src(Y529F) mutant induces more exosomal incorporation of Src kinase possibly due to a higher level of membrane-associated Src protein for subsequent exosomal protein sorting.

Mechanism of Src protein sorting to exosomes

We show that the sorting of Src kinase into exosomes was associated with ESCRT pathway and knockdown of TSG101 reduced the Src enrichment in exosomes (Figure 3.6B and 3.6C). Endosomal sorting complexes required for transport (ESCRT) is a classic pathway for protein sorting into extracellular vesicles like exosomes and identified as the major pathway for virus budding[62, 63], which is composed of ESCRT-0, I, II, III and vacuolar protein-associated sorting (Vsp) 4[64]. The ESCRT pathway is reported to regulate the activity of Src in endosome compartment and is involved in Src-mediated cell migration and associated downstream signaling. The knockdown of TSG101, an ESCRT protein, interrupted the activation of STAT3 and focal adhesion kinase (FAK) by modulating the active formulation of Src protein with the initial elevated level of active Src and attenuated active Src level when TSG101 was fully depleted[53]. The Src is reported to mediate syntenin-syndecans endosomal budding through

acting at the upstream of ARNO/ARF6/PLD2 and directly phosphorylating syndecan DEGSY motif cytosolic domain and tyrosine 46 of syntenin. The Src phosphorylation provides the tyrosine residues for syndecans-syntenin and enhances the endosomal budding[54]. In addition to membrane favorite by myristoylation, the association of Src with ESCRT and syntenin-syndecans pathway possibly explains the Src encapsulation into exosomes.

Syntenin is essential for function of Src kinase and exosomes derived from syntenin-null cells did not show any promigratory properties[54]. Our data clearly indicate that DU145 and PC-3 cells had much higher Src enrichment in exosomes compared to 22Rv1 and LNCaP cells and this is possibly attributed to the much high expression level of syntenin in DU145 and P-Src expression level in DU145 and PC-3 cells (Figure 3.1D and 3.7A). Our finding that active Src facilitates the exosomal syntenin biogenesis is consistent with the literature report (Figure 3.7B-F)[54], and we demonstrate that loss of myristoylation decreases the syntenin sorting into exosomes, this opens up new strategies to block the syntenin-mediated exosome biogenesis. In addition, we provide insight into the events mediated by myristoylation of Src at exosomal budding pathway (Figure 3.11).

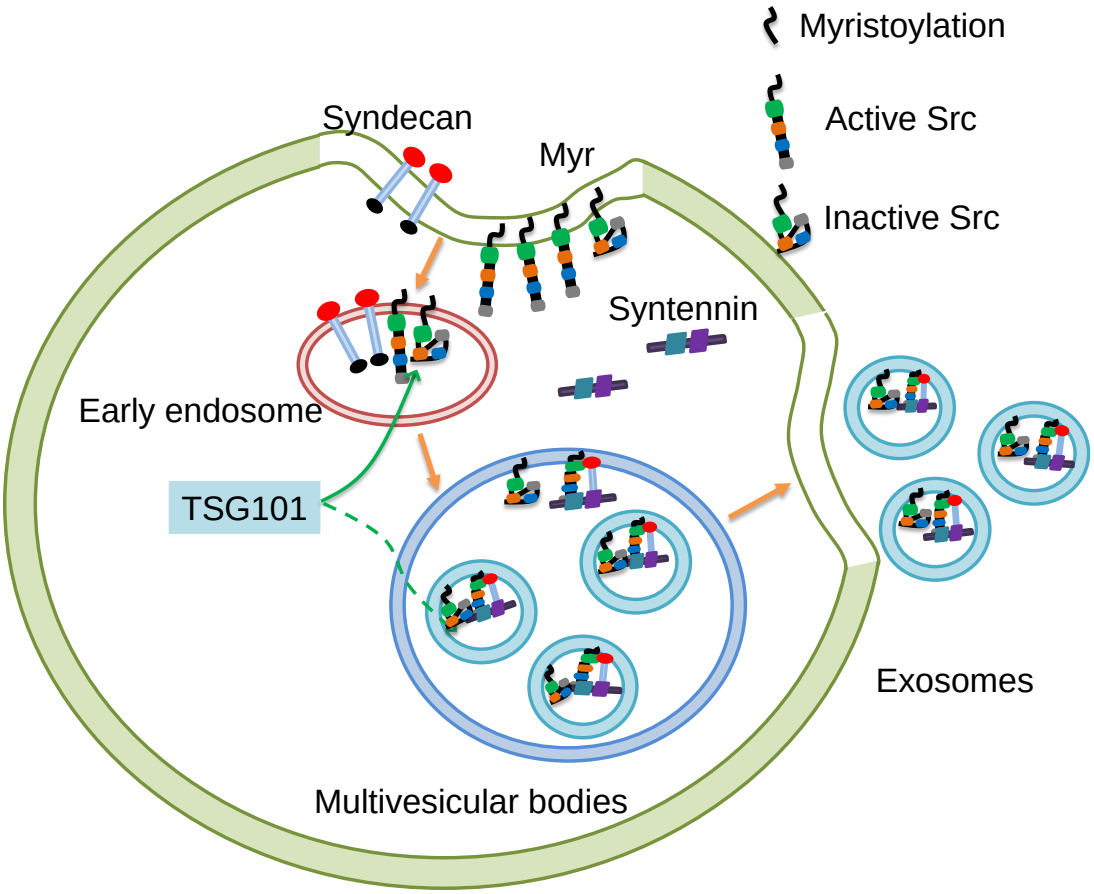

Figure 3.12 Schematic model illustrating the role of myristoylation in Src-mediated exosome secretion pathway. Myristoylated protein is preferably encapsulated and secreted into exosomes. Myristoylated active Src kinase favors syntenin endosomal budding. TSG101 mediates the Src encapsulation process.

Myristoylation mediates the translocation of tumor-derived Src kinase to recipient cells for inducing apoptosis

We found that Src expression level in Src(WT) was much higher compared to Src(G2A) in various cells (Figure 3.2B). Expectedly, higher expression level of Src was observed in SYF1 cells treated with Src(WT) exosomes compared to treatment by Src(G2A) exosomes. These data indicate that myristoylation facilitates the Src transfer by exosomes in responses to the high expression level of exosomal Src, and disruption of myristoylation dramatically reduces the Src accumulation in recipient fibroblasts (Figure 3.8C). Analysis of apoptosis signals revealed that Src(Y529F) derived exosomes substantially increased cleavage of caspase 3/7 *in vitro*.

Overexpression of c-Src is reported to induce the apoptosis of 3Y1 rat fibroblasts through caspase 3 mediated pathway and 3Y1 expressing c-Src cells showed substantial cleavage of the PKC δ and PARP[65]. Downregulation of protein kinase C δ or activating Phospholipase D (PLD) (PLD1 or PLD2) can prevent PKC δ and PARP cleavage by mediating the survival signaling[65, 66]. Thus, the Src activity in fibroblasts produced from exosomes is responsible for apoptotic signals possibly through upregulating protein kinase C δ or downregulating the PLD activity. Further investigations may be needed to fully understand the mechanism of exosomal Src kinase inducing apoptosis.

In vivo demonstration of myristoylation promoting the Src encapsulation into exosomes

In vivo studies demonstrate that Src(Y529F) induced overexpression of Src protein in serum exosomes, which is consistent with *in vitro* investigation that myristoylation promotes the encapsulation of Src into exosomes (Figure 3.2, 3.9, 3.10). The Src plays oncogenic roles in tumor growth, progression, and metastasis of prostate cancer[17]. The overexpressed level of c-Src was found in serum exosomes derived from TRAMP mice with tumor implantation[35]. The overexpression of Src kinase observed in our study further confirms the concept of circulating Src in serum exosomes being used as a potential biomarker for prostate cancer. Src kinase inhibition is identified as an important therapeutic strategy against cancer through preventing the direct function on host cells by down-stream signals[22]. The serum HSP90 is reported to be overexpressed and be a potential biomarker for cancer[67, 68]. Our observation of high expression level of HSP90 in serum exosomes suggests that exosomal Src were generated from DU145 Src(Y529F) tumor cells (Figure 3.9D and 3.10C).

We found that myristoylation promoted Src incorporation into exosomes and oncogenic Src proteins could be taken up by fibroblasts such as SYF1 and NIH 3T3 cells through cancer-derived exosomes in a time-dependent manner and induced cellular apoptosis via caspase

pathway (Figure 3.7D and 3.7E). Thus, it is important to block the Src accumulation into exosomes to prevent apoptosis in neighboring or distal healthy cells (e.g., fibroblasts) through inhibiting myristoylation process. Besides, myristoylation could also be a potential target for cancer therapy to prevent other cellular processes such as angiogenesis for tumor survival and growth caused by oncogenic Src protein shuttled by exosomes. The chronic myeloid leukemia cell-derived K562 exosomes are reported to promote angiogenesis in human umbilical vein endothelial cells (HUVECs) by stimulating Src phosphorylation and activating the corresponding downstream signalings[55].

3.5 CONCLUSIONS

We demonstrate that myristoylation promotes the oncogenic Src kinase incorporation into exosomes, and palmitoylation inhibits this process to extracellular vesicles. The removal of palmitoylation in dual acylated Fyn kinase enhances Fyn accumulation in exosomes and loss of myristoylation significantly reduces the Src kinase encapsulation into exosomes. The exosomal Src kinase secretion is involved in ESCRT machinery regulated by TSG101. *In vivo* studies demonstrate that myristoylation remarkably promotes the circulation of Src protein in serum exosomes originated from tumor cells. This provides new insights into a novel target of inhibiting myristoylation to block the Src translocation and prevent the apoptotic signaling through exosome communication from cell-to-cell.

3.6 SUPPORTING INFORMATION

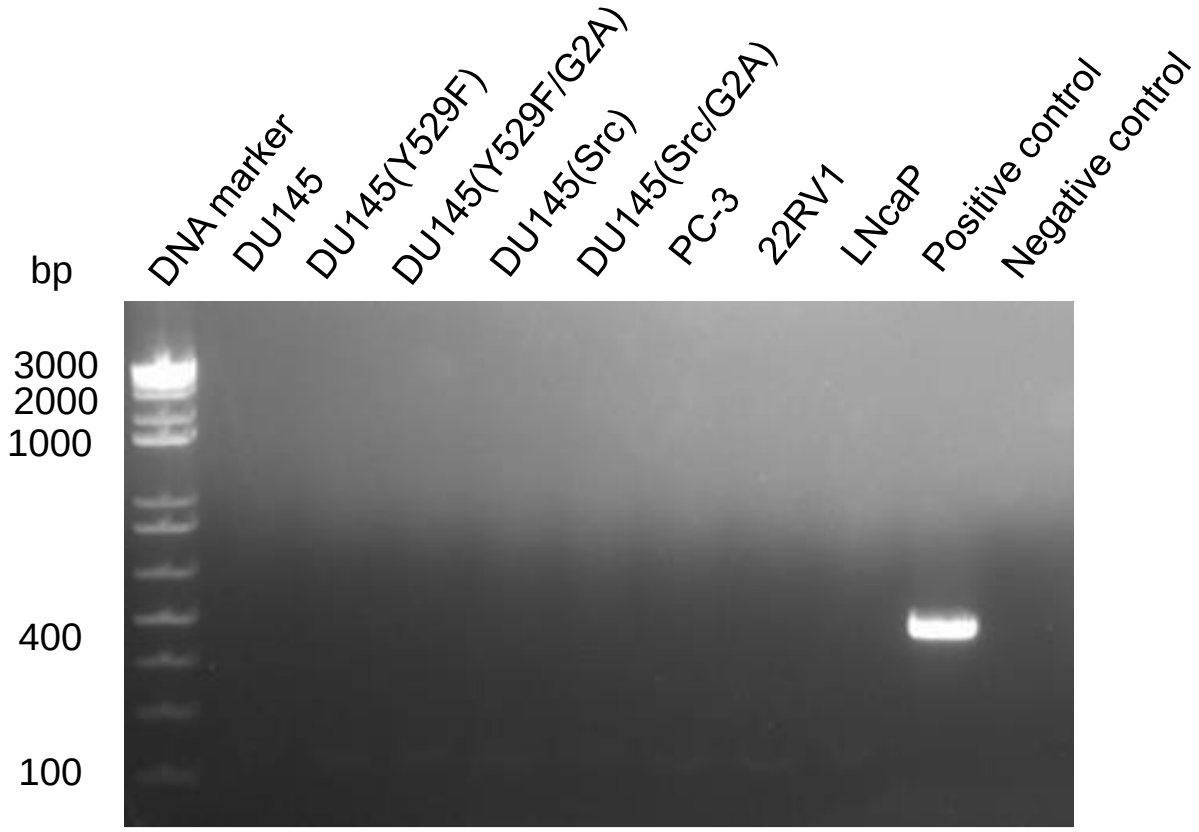

Figure S3.1 Mycoplasma analysis of various cell lines.

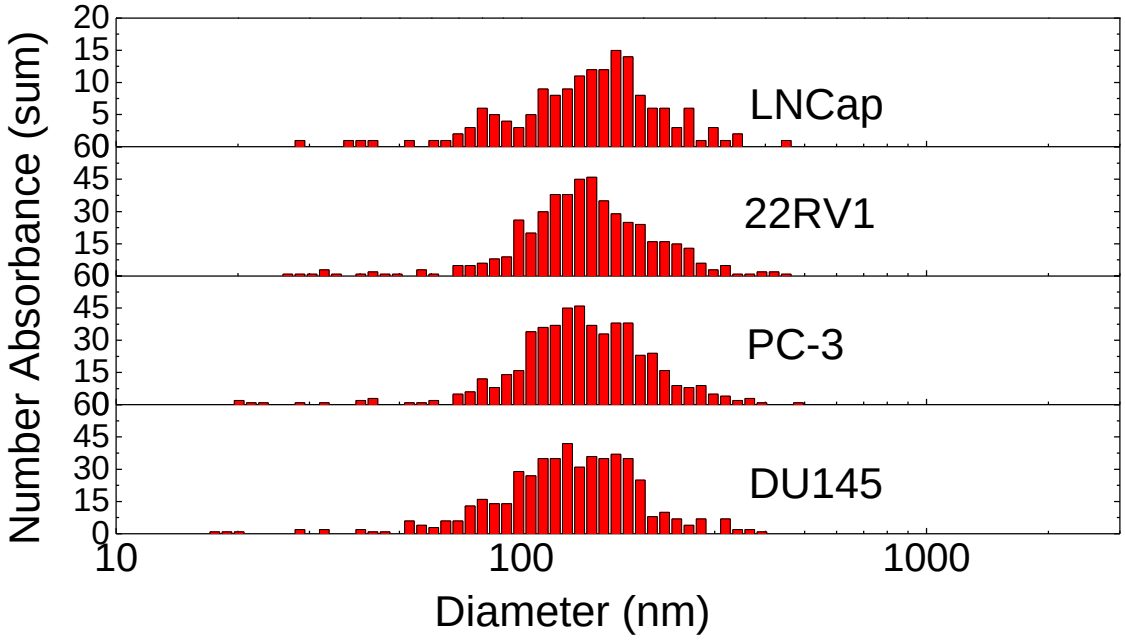

Figure S3.2 Size distribution histogram of exosomes derived from four cell lines.

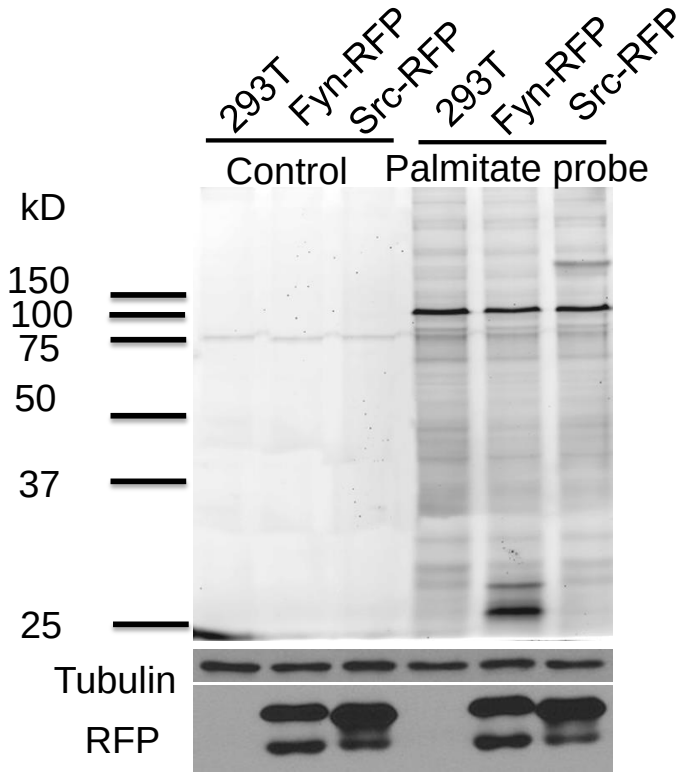

Figure S3.3 Palmitoylation evaluation in Fyn-RFP and Src-RFP in 293T cells. 293T cells were transduced with Fyn-RFP and Src-RFP by lentiviral infection. The transduced cells were labelled with palmitoylated probe 17-octadecynoic acid. The cell lysates were conjugated to biotin using Click Chemistry through azide-alkyne interaction and detected with streptavidin-HRP by immunoblot. Fyn-RFP and Src-RFP was constructed by conjugating a short sequence containing eight amino acids in Fyn (MGCVQCKD) and Src (MGSNKSKP) with RFP fusion peptide.

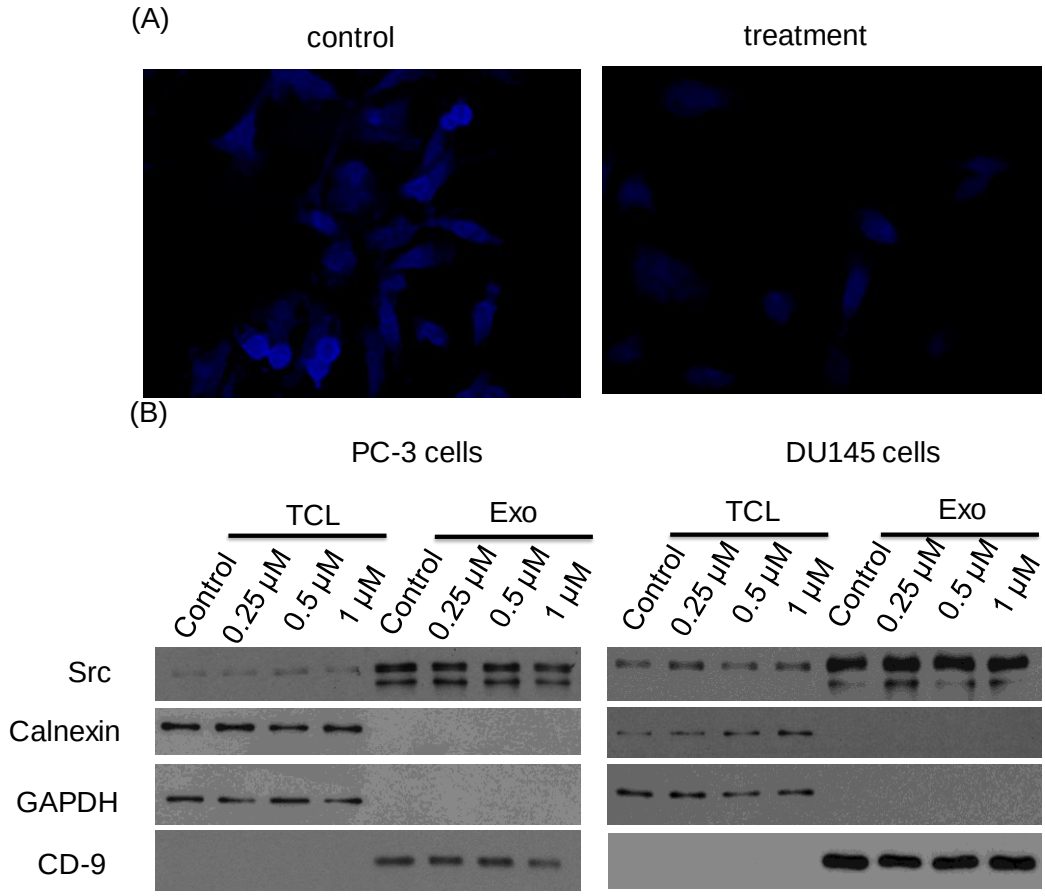

Figure S3.4 (A) The cholesterol level of PC-3 cells when treated with filipin III at a concentration of 1 μM for 24 h. (B) The expression level of Src protein in exosomes when PC-3 and DU145 cells were treated by lipid-raft disrupting agent Filipin III at various concentrations up to 1 μM for 24 h derived from both PC-3 and DU145 cells. PC-3 and DU145 cells were incubated in exosome-free medium at 37ºC in 5% CO_2 for 24 h and exosomes were isolated from cell culture medium by ultracentrifugation method.

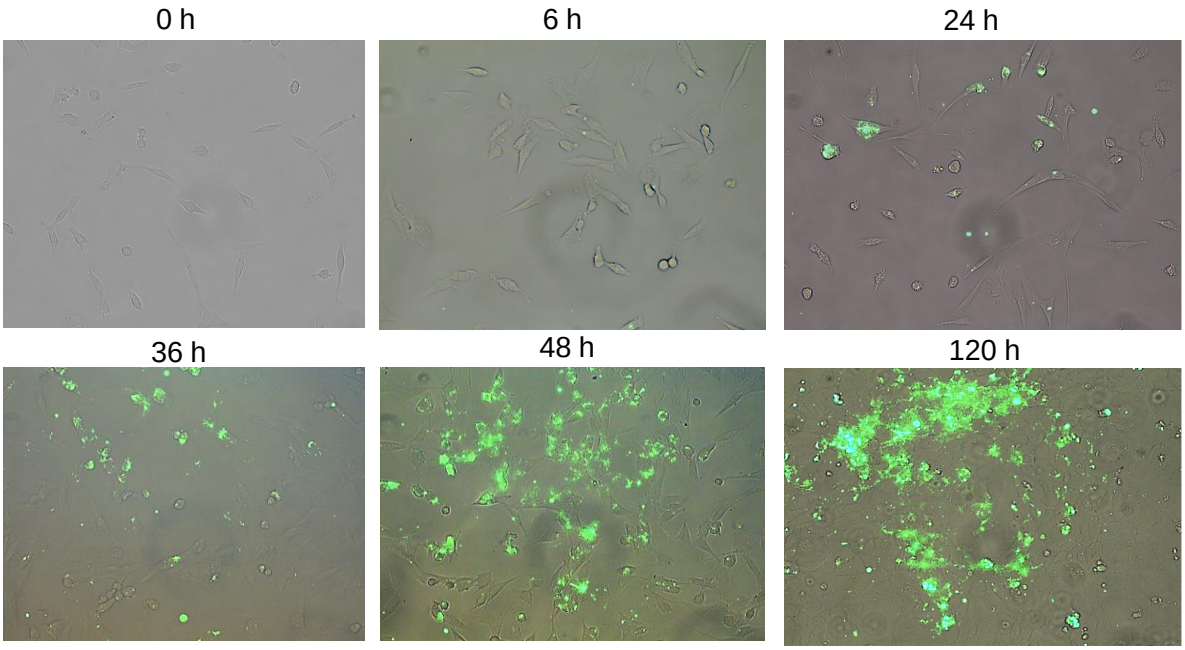

Figure S3.5 DU145 derived exosomes were incubated with SYF1 cells up to 120 h. DU145 derived exosomes were isolated from cell culture medium by ultracentrifugation method and exosomes were labelled with PKH-67 dye.

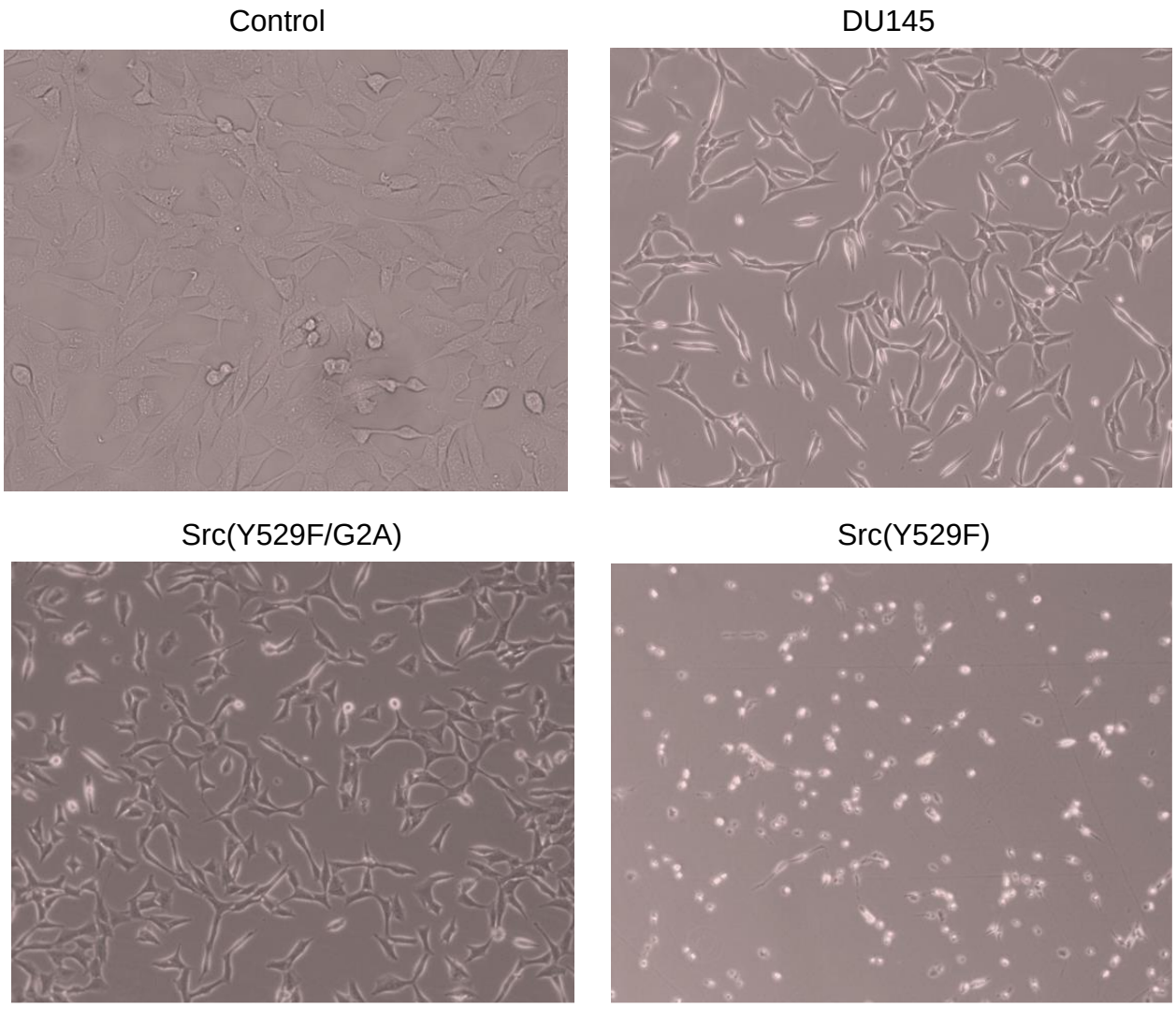

Figure S3.6 SYF1 cells were treated with DU145, DU145 Src(Y529F), DU145 Src(Y529F/G2A) exosomes for 24 h and imaged under microscope. DU145 cells were transduced with Src(Y529F) and Src(Y529F/G2A) by lentiviral infection for 2 days.

Table S3.1 Myristoylated protein of NCI-60 cell lines[37]

Protein ID	Gene Name	Sequence	Appearance frequency in NCI-60
P84077	ARF1	MGNIFANLFKGLFGKKEMRILMVGLDAAGK	60
P18085	ARF4 ARF2	MGLTISSLFSRLFGKKQMRILMVGLDAAGK	60
P62330	ARF6	MGKVLSKIFGNKEMWILMLGLDAAGKTTIL	60
P04899	GNAI2 GNAI2B	MGCTVSAEDKAAAERSKMIDKNLREDGEKA	60
P08754	GNAI3	MGCTLSAEDKAAVERSKMIDRNLREDGEKA	60
P62241	RPS8 OK/SW-cl.83	MGISRDNWHKRRKTGGKRKPYHKKRKYELG	60
Q96TA1	FAM129B C9orf88	MGDVLSTHLDDARRQHIAEKTGKILTEFLQ	58
Q6IAA8	LAMTOR1 C11orf59 PDRO PP7157	MGCCYSSENEDSDQDREERKLLLDPSSPPT	57
Q14254	FLOT2 ESA1 M17S1	MGNCHTVGPNEALVVSGGCCGSDYKQYVFG	56
P84085	ARF5	MGLTVSALFSRIFGKKQMRILMVGLDAAGK	54
P61313	RPL15 EC45 TCBAP0781	MGAYKYIQELWRKKQSDVMRFLLRVRCWQY	54
P07947	YES1 YES	MGCIKSKENKSPAIKYRPENTPEPVSTSVS	54
Q9NUQ9	FAM49B BM-009	MGNLLKVLTCTDLEQGPNFFLDFENAQPTE	52
Q9H4G4	GLIPR2 C9orf19 GAPR1	MGKSASKQFHNEVLKAHNEYRQKHGVPPLK	52
P63096	GNAI1	MGCTLSAEDKAAVERSKMIDRNLREDGEKA	52
P36405	ARL3 ARFL3	MGLLSILRKLKSAPDQEVRILLLGLDNAGK	51
P36404	ARL2	MGLLTILKKMKQKERELRLLMLGLDNAGKT	50
Q96FZ7	CHMP6 VPS20	MGNLFGRKKQSRVTEQDKAILQLKQQRDKL	50
Q99653	CHP1 CHP	MGSRASTLLRDEELEEIKKETGFSHSQITR	50
Q8WWI5	SLC44A1 CD92 CDW92 CTL1	MGCCSSASSAAQSSKREWKPLEDRSCTDIP	49
P07948	LYN JTK8	MGCIKSKGKDSLSDDGVDLKTQPVRNTERT	47
P49006	MARCKSL1 MLP MRP	MGSQSSKAPRGDVTAEEAAGASPAKANGQE	47
O75695	RP2	MGCFFSKRRKADKESRPENEEERPKQYSWD	47
P29966	MARCKS MACS PRKCSL	MGAQFSKTAAKGEAAAERPGEAAVASSPSK	46
Q8N9N7	LRRC57	MGNSALRAHVETAQKTGVFQLKDRGLTEFP	45
P37235	HPCAL1 BDR1	MGKQNSKLRPEVLQDLRENTEFTDHELQEW	44
P00387	CYB5R3 DIA1	MGAQLSTLGHMVLFPVWFLYSLLMKLFQRS	43
Q9NRX5	SERINC1 KIAA1253	MGSVLGLCSMASWIPCLCGSAPCLLCRCCP	42

	TDE1L TDE2 UNQ396/PRO732		
P12931	SRC SRC1	MGSNKSKPKDASQRRRSLEPAENVHGAGGG	42
P40616	ARL1	MGGFFSSIFSSLFGTREMRILILGLDGAGK	40
P80723	BASP1 NAP22	MGGKLSKKKKGYNVNDEKAKEKDKKAEGAA	40
Q9NX63	CHCHD3 MIC19 MINOS3	MGGTTSTRRVTFEADENENITVVKGIRLSE	39
Q96PY5	FMNL2 FHOD2 KIAA1902	MGNAGSMDSQQTDFRAHNVPLKLPMPEPGE	38
P62166	NCS1 FLUP FREQ	MGKSNSKLKPEVVEELTRKTYFTEKEVQQW	38
Q9BZQ8	FAM129A C1orf24 NIBAN GIG39	MGGSASSQLDEGKCAYIRGKTEAAIKNFSP	37
Q8NHG7	SVIP	MGLCFPCPGESAPPTPDLEEKRAKLAEAAE	37
Q9Y3E7	CHMP3 CGI149 NEDF VPS24 CGI-149	MGLFGKTQEKPPKELVNEWSLKIRKEMRVV	35
Q99828	CIB1 CIB KIP PRKDCIP	MGGSGSRLSKELLAEYQDLTFLTKQEILLA	32
P17612	PRKACA PKACA	MGNAAAAKKGSEQESVKEFLAKAKEDFLKK	31
Q8ND76	CCNY C10orf9 CBCP1 CFP1	MGNTTSCCVSSSPKLRRNAHSRLESYRPDT	30
Q9H8Y8	GORASP2 GOLPH6	MGSSQSVEIPGGGTEGYHVLRVQENSPGHR	29
Q99570	PIK3R4 VPS15	MGNQLAGIAPSQILSVESYFSDIHDFEYDK	28
Q14699	RFTN1 KIAA0084 MIG2	MGCGLNKLEKRDEKRPGNIYSTLKRPQVET	25
Q7L014	DDX46 KIAA0801	MGRESRHYRKRSASRGRSGSRSRSRSPSDK	24
O60936	NOL3 ARC NOP	MGNAQERPSETIDRERKRLVETLQADSGLL	24
P08473	MME EPN	MGKSESQMDITDINTPKPKKKQRWTPLEIS	22
P22694	PRKACB	MGNAATAKKGSEVESVKEFLAKAKEDFLKK	22
Q8IV36	HID1 C17orf28 DMC1	MGSTDSKLNFRKAVIQLTTKTQPVEATDDA	21
Q8IVF7	FMNL3 FHOD3 FRL2 KIAA2014 WBP3	MGNLESAEGVPGEPPSVPLLLPPGKMPMPE	19
O15355	PPM1G PPM1C	MGAYLSQPNTVKCSGDGVGAPRLPLPYGFS	19
Q9NUM4	TMEM106B	MGKSLSHLPLHSSKEDAYDGVTSENMRNGL	19
P09471	GNAO1	MGCTLSAEERAALERSKAIEKNLKEDGISA	17
O75896	TUSC2 C3orf11 FUS1 LGCC PDAP2	MGASGSKARGLWPFASAAGGGGSEAAGAEQ	16

Q9NS886	LANCL2 GPR69B TASP	MGETMSKRLKLHLGGEAEMEERAFVNPFPD	15
Q02952	AKAP12 AKAP250	MGAGSSTEQRSPEQPPEGSSTPAEPEPSGG	13
P06239	LCK	MGCGCSSHPEDDWMENIDVCENCHYPIVPL	11
P27216	ANXA13 ANX13	MGNRHAKASSPQGFDVDRDAKKLNKACKGM	10
P06241	FYN	MGCVQCKDKEATKLTEERDGSLNQSSGYRY	10
O00461	GOLIM4 GIMPC GOLPH4 GPP130	MGNGMCSRKQKRIFQTLLLLTVVFGFLYGA	9
P63098	PPP3R1 CNA2 CNB	MGNEASYPLEMCSHFDADEIKRLGKRFKKL	9
P62760	VSNL1 VISL1	MGKQNSKLAPEVMEDLVKSTEFNEHELKQW	9
Q8IWE4	DCUN1D3 SCCRO3	MGQCVTKCKNPSSTLGSKNGDREPSNKSHS	8
P29728	OAS2	MGNGESQLSSVPAQKLGWFIQEYLKPYEEC	8
O75688	PPM1B PP2CB	MGAFLDKPKTEKHNAHGAGNGLRYGLSSMQ	7
P56559	ARL4C ARL7	MGNISSNISAFQSLHIVMLGLDSAGKTTVL	6
Q86UY6	NAA40 NAT11 PATT1	MGRKSSKAKEKKQKRLEERAAMDAVCAKVD	6
Q9ULE6	PALD1 KIAA1274 PALD	MGTTASTAQQTVSAGTPFEGLQGSGTMDSR	6
O43149	ZZEF1 KIAA0399	MGNAPSHSSEDEAAAAGGEGWGPHQDWAAV	6
Q9BRQ8	AIFM2 AMID PRG3	MGSQVSVESGALHVVIVGGGFGGIAAASQL	5
Q9YNA8	ERVK-19	MGQTKSKIKSKYASYLSFIKILLKRGGVKV	5
Q9C0E8	LNPK KIAA1715 LNP	MGGLFSRWRTKPSTVEVLESIDKEIQALEE	5
Q96BS2	TESC CHP3	MGAAHSASEEVRELEGKTGFSSDQIEQLHR	5
Q9Y250	LZTS1 FEZ1	MGSVSSLISGHSFHSKHCRASQYKLRKSSH	4
Q969G9	NKD1 NKD PP7246	MGKLHSKPAAVCKRRESPEGDSFAVSAAWA	4
Q9Y3C5	RNF11 CGI-123	MGNCLKSPTSDDISLLHESQSDRASFGEGT	4
Q8NHG8	ZNRF2 RNF202	MGAKQSGPAAANGRTRAYSGSDLPSSSSGG	4
O15121	DEGS1 DES1 MLD MIG15	MGSRVSREDFEWVYTDQPHADRRREILAKY	3
Q8WU20	FRS2	MGSCCSCPDKDTVPDNHRNKFKVINVDDDG	3
P08631	HCK	MGGRSSCEDPGCPRDEERAPRMGCMKSKFL	3
Q9P032	NDUFAF4 C6orf66 HRPAP20 HSPC125 My013	MGALVIRGIRNFNLENRAEREISKMKPSVA	3
P17568	NDUFB7	MGAHLVRRYLGDASVEPDPLQMPTFPPDYG	3
P40617	ARL4A ARL4	MGNGLSDQTSILSNLPSFQSFHIVILGLDC	2

Q9H0F7	ARL6 BBS3	MGLLDRLSVLLGLKKKEVHVLCLGLDNSGK	2
Q9BSF0	C2orf88	MGCMKSKQTFPFPTIYEGEKQHESEEPFMP	2
Q9BRQ6	CHCHD6 CHCM1 MIC25	MGSTESSEGRRVSFGVDEEERVRVLQGVRL	2
Q7L9B9	EEPD1 KIAA1706	MGSTLGCHRSIPRDPSDLSHSRKFSAACNF	2
P63130	ERVK-7	MGQTKSKIKSKYASYLSFIKILLKRGGVKV	2
P19086	GNAZ	MGCRQSSEEKEAARRSRRIDRHLRSESQRQ	2
Q9Y6M0	PSMC1	MGARGALLLALLLARAGLRKPESQEAAPLS	2
P19087	GNAT2 GNATC	MGSGASAEDKELAKRSKELEKKLQEDADKE	1
A8MTJ3	GNAT3	MGSGISSESKESAKRSKELEKKLQEDAERD	1
O60291	MGRN1 KIAA0544 RNF156	MGSILSRRIAGVEDIDIQANSAYRYPPKSG	1
Q6BDI9	REP15	MGQKASQQLALKDSKEVPVVCEVVSEAIVH	1
Q52LD8	RFTN2 C2orf11	MGCGLRKLEDPDDSSPGKIFSTLKRPQVET	1
Q8IZE3	SCYL3 PACE1	MGSENSALKSYTLREPPFTLPSGLAVYPAV	1
Q9H6Q3	SLA2 C20orf156 SLAP2	MGSLPSRRKSLPSPSLSSSVQGQGPVTMEA	1
O75716	STK16 MPSK1 PKL12 TSF1	MGHALCVCSRGTVIIDNKRYLFIQKLGEGG	1
Q99487	PAFAH2	MGVNQSVGFPPVTGPHLVGCGDVMEGQNLQ	0
P42684	ABL2 ABLL ARG	MGQQVGRVGEAPGLQQPQPRGIRGSSAARP	0
O43687	AKAP7 AKAP15 AKAP18	MGQLCCFPFSRDEGKISELESSSSAVLQRY	0
Q9P2G1	ANKIB1 KIAA1386	MGNTTTKFRKALINGDENLACQIYENNPQL	0
P61204	ARF3	MGNIFGNLLKSLIGKKEMRILMVGLDAAGK	0
Q969Q4	ARL11 ARLTS1	MGSVNSRGHKAEAQVVMMGLDSAGKTTLLY	0
Q8N4G2	ARL14 ARF7	MGSLGSKNPQTKQAQVLLLGLDSAGKSTLL	0
Q8IVW1	ARL17A ARL17P1; ARL17B ARF1P2 ARL17A PRO2667	MGNIFEKLFKSLLGKKKMRILILSLDTAG	0
P49703	ARL4D ARF4L	MGNHLTEMAPTASSFLPHFQALHVVVIGLD	0
Q9Y689	ARL5A ARFLP5 ARL5	MGILFTRIWRLFNHQEHKVIIVGLDNAGKT	0
Q96KC2	ARL5B ARL8	MGLIFAKLWSLFCNQEHKVIIVGLDNAGKT	0
A6NH57	ARL5C ARL12	MGQLIAKLMSIFGNQEHTVIIVGLDNEGKT	0
Q8WXS3	BAALC	MGCGGSRADAIEPRYYESWTRETESTWLTY	0
P51451	BLK	MGLVSSKKPDKEKPIKEKDKGQWSPLKVSA	0
Q969J3	BORCS5 LOH12CR1	MGSEQSSEAESRPNDLNSSVTPSPAKHRAK	0

Q9UPA5	BSN KIAA0434 ZNF231	MGNEVSLEGGAGDGPLPPGGAGPGPGPGPG	0
Q9P203	BTBD7 KIAA1525	MGANASNYPHSCSPRVGGNSQAQQTFIGTS	0
A6NGG8	C2orf71	MGCTPSHSDLVNSVAKSGIQFLKKPKAIRP	0
Q9NZU7	CABP1	MGGGDGAAFKRPGDGARLQRVLGLGSRREP	0
Q9NPB3	CABP2	MGNCAKRPWRRGPKDPLQWLGSPPRGSCPS	0
A6NI79	CCDC69	MGCRHSRLSSCKPPKKKRQEPEPEQPPRPE	0
Q15078	CDK5R1 CDK5R NCK5A	MGTVLSLSPSYRKATLFEDGAATVGHYTAV	0
Q13319	CDK5R2 NCK5AI	MGTVLSLSPASSAKGRRPGGLPEEKKKAPP	0
O43745	CHP2 HCA520	MGSRSSHAAVIPDGDSIRRETGFSQASLLR	0
Q717R9	CYS1	MGSGSSRSSRTLRRRRSPESLPAGPGAAAL	0
Q6QHC5	DEGS2 C14orf66	MGNSASRSDFEWVYTDQPHTQRRKEILAKY	0
Q9NRW4	DUSP22 JSP1 LMWDSP2 MKPX	MGNGMNKILPGLYIGNFKDARDAEQLSKNK	0
Q7RTS9	DYM	MGSNSSRIGDLPKNEYLKKLSGTESISEND	0
P16452	EPB42 E42P	MGQALGIKSCDFQAARNNEEHHTKALSSRR	0
P87889	ERVK-10	MGQTKSKIKSKYASYLSFIKILLKRGGVKV	0
P62683	ERVK-21	MGQTKSKIKSKYASYLSFIKILLKRGGVKV	0
P63145	ERVK-24	MGQTKSKIKSKYASYLSFIKILLKRGGVKV	0
Q9HDB9	ERVK-5 ERVK5	MGQTKSKTKSKYASYLSFIKILLKRGGVRV	0
Q7LDI9	ERVK-6 ERVK6	MGQTKSKIKSKYASYLSFIKILLKRGGVKV	0
P62685	ERVK-8	MGQTKSKIKSKYASYLSFIKILLKRGGVKV	0
P63126	ERVK-9	MGQTKSKIKSKYASYLSFIKILLKRGGVKV	0
P63128	ERVK-9	MGQTKSKIKSKYASYLSFIKILLKRGGVKV	0
P09769	FGR SRC2	MGCVFCKKLEPVATAKEDAGLEGDFRSYGA	0
O95466	FMNL1 C17orf1 C17orf1B FMNL FRL1	MGNAAGSAEQPAGPAAPPPKQPAPPKQPMP	0
O43559	FRS3	MGSCCSCLNRDSVPDNHPTKFKVTNVDDEG	0
P11488	GNAT1 GNATR	MGCTLSAEDKAAVERSKMIDRNLREDGEKA	0
Q9BQQ3	GORASP1 GOLPH5 GRASP65	MGLGVSAEQPAGGAEGFHLHGVQENSPAQQ	0
P43080	GUCA1A C6orf131 GCAP GCAP1 GUCA1	MGNVMEGKSVEELSSTECHQWYKKFMTECP	0
Q9UMX6	GUCA1B GCAP2	MGQEFSWEEAEAAGEIDVAELQEWYKKFVM	0
O95843	GUCA1C GCAP3	MGNGKSIAGDQKAVPTQETHVWYRTFMMEY	0
P53701	HCCS CCHL	MGLSPSAPAVAVQASNASASPPSGCPMHEG	0

P62684	HERVK_113	MGQTKSKIKSKYASYLSFIKILLKRGGVKV	0
Q8TB92	HMGCLL1	MGNVPSAVKHCLSYQQLLREHLWIGDSVAG	0
P84074	HPCA BDR2	MGKQNSKLRPEMLQDLRENTEFSELELQEW	0
Q9UM19	HPCAL4	MGKTNSKLAPEVLEDLVQNTEFSEQELKQW	0
P63252	KCNJ2 IRK1	MGSVRTNRYSIVSSEEDGMKLATMAVANGF	0
Q6VT66	MARC1 MOSC1	MGAAGSSALARFVLLAQSRPGWLGVAALGL	0
P61601	NCALD	MGKQNSKLRPEVMQDLLESTDFTEHEIQEW	0
O76050	NEURL1 NEURL NEURL1A RNF67	MGNNFSSIPSLPRGNPSRAPRGHPQNLKDS	0
Q969F2	NKD2	MGKLQSKHAAAARKRRESPEGDSFVASAYA	0
P29474	NOS3	MGNLKSVAQEPGPPCGLGLGLGLGLCGKQG	0
Q7Z494	NPHP3 KIAA2000	MGTASSLVSPAGGEVIEDTYGAGGGEACEI	0
Q6X4W1	NSMF NELF	LRSEAMSSVAAKVRAARAFG	0
Q96MG8	PCMTD1	MGGAVSAGEDNDDLIDNLKEAQYIRTERVE	0
Q9NV79	PCMTD2 C20orf36	MGGAVSAGEDNDELIDNLKEAQYIRTELVE	0
O00408	PDE2A	MGQACGHSILCRSQQYPAARPAEPRGQQVF	0
Q9UPV7	PHF24 KIAA1045	MGVLMSKRQTVEQVQKVSLAVSAFKDGLRD	0
Q494U1	PLEKHN1	MGNSHCVPQAPRRLRASFSRKPSLKGNRED	0
P35813	PPM1A PPPM1A	MGAFLDKPKMEKHNAQGQGNGLRYGLSSMQ	0
Q96LZ3	PPP3R2 CBLP PPP3RL	MGNEASYPAEMCSHFDNDEIKRLGRRFKKL	0
Q9Y478	PRKAB1 AMPK	MGNTSSERAALERHGGHKTPRRDSSGGTKD	0
P22612	PRKACG	MGNAPAKKDTEQEESVNEFLAKARGDFLYR	0
Q13237	PRKG2 PRKGR2	MGNGSVKPKHSKHPDGHSGNLTTDALRNKV	0
Q9NR22	PRMT8 HRMT1L3 HRMT1L4	MGMKHSSRCLLLRRKMAENAAESTEVNSPP	0
P11801	PSKH1	MGCGTSKVLPEPPKDVQLDLVKKVEPFSGT	0
Q13702	RAPSN RNF205	MGQDQTKQQIEKGLQLYQSNQTEKALQVWT	0
P35243	RCVRN RCV1	MGNSKSGALSKEILEELQLNTKFSEEELCS	0
Q96EQ8	RNF125	MGSVLSTDSGKSAPASATARALERRRDPEL	0
Q8WVD5	RNF141 ZNF230	MGQQISDQTQLVINKLPEKVAKHVTLVRES	0
Q96PX1	RNF157 KIAA1917	MGALTSRQHAGVEEVDIPSNSVYRYPPKSG	0
Q13239	SLA SLAP SLAP1	MGNSMKSTPAPAERPLPNPEGLDSDFLAVL	0
Q8WU08	STK32A YANK1	MGANTSRKPPVFDENEDVNFDHFEILRAIG	0
H3BQB6	STMND1	MGCGPSQPAEDRRRVRAPKKGWKEEFKADV	0
Q13009	TIAM1	MGNAESQHVEHEFYGEKHASLGRKHTSRSL	0
Q81VF5	TIAM2 KIAA2016 STEF	MGNSDSQYTLQGSKNHSNTITGAKQIPCSL	0

Q86XR7	TICAM2 TIRAP3 TIRP TRAM	MGIGKSKINSCPLSLSWGKRHSVDTSPGYH	0
Q6P9B6	TLDC1 KIAA1609	MGNSRSRVGRSFCSQFLPEEQAEIDQLFDA	0
Q9BVX2	TMEM106C EMOC	MGSQHSAAARPSSCRRKQEDDRDGLLAERE	0
P98073	TMPRSS15 ENTK PRSS7	MGSKRGISSRHHSLSSYEIMFAALFAILVV	0
Q8ND25	ZNRF1 NIN283	MGGKQSTAARSRGPFPGVSTDDSAVPPPGG	0

Table S3.2 Myristoylated protein in human thymic exosomes[42]

Protein ID	Gene Name	Sequence
Q02952	AKAP12 AKAP250	MGAGSSTEQRSPEQPPEGSSTPAEPEPSGG
P84077	ARF1	MGNIFANLFKGLFGKKEMRILMVGLDAAGK
P18085	ARF4 ARF2	MGLTISSLFSRLFGKKQMRILMVGLDAAGK
P84085	ARF5	MGLTVSALFSRIFGKKQMRILMVGLDAAGK
P62330	ARF6	MGKVLSKIFGNKEMWILMLGLDAAGKTTIL
P40616	ARL1	MGGFFSSIFSSLFGTREMRILILGLDGAGK
P36405	ARL3 ARFL3	MGLLSILRKLKSAPDQEVRILLLGLDNAGK
P80723	BASP1 NAP22	MGGKLSKKKKGYNVNDEKAKEKDKKAEGAA
Q96FZ7	CHMP6 VPS20	MGNLFGRKKQSRVTEQDKAILQLKQQRDKL
P00387	CYB5R3 DIA1	MGAQLSTLGHMVLFPVWFLYSLLMKLFQRS
Q7L014	DDX46 KIAA0801	MGRESRHYRKRSASRGRSGSRSRSRSPSDK
Q9BZQ8	FAM129A C1orf24 NIBAN GIG39	MGGSASSQLDEGKCAYIRGKTEAAIKNFSP
Q96TA1	FAM129B C9orf88	MGDVLSTHLDDARRQHIAEKTGKILTEFLQ
Q9NUQ9	FAM49B BM-009	MGNLLKVLTCTDLEQGPNFFLDFENAQPTE
Q14254	FLOT2 ESA1 M17S1	MGNCHTVGPNEALVVSGGCCGSDYKQYVFG
Q96PY5	FMNL2 FHOD2 KIAA1902	MGNAGSMDSQQTDFRAHNVPLKLPMPEPGE
P06241	FYN	MGCVQCKDKEATKLTEERDGSLNQSSGYRY
Q9H4G4	GLIPR2 C9orf19 GAPR1	MGKSASKQFHNEVLKAHNEYRQKHGVPPLK
P63096	GNAI1	MGCTLSAEDKAAVERSKMIDRNLREDGEKA
P04899	GNAI2 GNAI2B	MGCTVSAEDKAAAERSKMIDKNLREDGEKA
P08754	GNAI3	MGCTLSAEDKAAVERSKMIDRNLREDGEKA
Q9H8Y8	GORASP2 GOLPH6	MGSSQSVEIPGGGTEGYHVLRVQENSPGHR
P08631	HCK	MGGRSSCEDPGCPRDEERAPRMGCMKSKFL
P37235	HPCAL1 BDR1	MGKQNSKLRPEVLQDLRENTEFTDHELQEW
P06239	LCK	MGCGCSSHPEDDWMENIDVCENCHYPIVPL
Q8N9N7	LRRC57	MGNSALRAHVETAQKTGVFQLKDRGLTEFP
P07948	LYN JTK8	MGCIKSKGKDSLSDDGVDLKTQPVRNTERT
P29966	MARCKS MACS PRKCSL	MGAQFSKTAAKGEAAAERPGEAAVASSPSK
P49006	MARCKSL1 MLP MRP	MGSQSSKAPRGDVTAEEAAGASPAKANGQE
P08473	MME EPN	MGKSESQMDITDINTPKPKKKQRWTPLEIS

P29728	OAS2	MGNGESQLSSVPAQKLGWFIQEYLKPYEEC
Q99570	PIK3R4 VPS15	MGNQLAGIAPSQILSVESYFSDIHDFEYDK
P17612	PRKACA PKACA	MGNAAAAKKGSEQESVKEFLAKAKEDFLKK
P22694	PRKACB	MGNAATAKKGSEVESVKEFLAKAKEDFLKK
Q14699	RFTN1 KIAA0084 MIG2	MGCGLNKLEKRDEKRPGNIYSTLKRPQVET
O75695	RP2	MGCFFSKRRKADKESRPENEEERPKQYSWD
P61313	RPL15 EC45 TCBAP0781	MGAYKYIQELWRKKQSDVMRFLLRVRCWQY
P62241	RPS8 OK/SW-cl.83	MGISRDNWHKRRKTGGKRKPYHKKRKYELG
Q8WWI5	SLC44A1 CD92 CDW92 CTL1	MGCCSSASSAAQSSKREWKPLEDRSCTDIP
P12931	SRC SRC1	MGSNKSKPKDASQRRRSLEPAENVHGAGGG
P07947	YES1 YES	MGCIKSKENKSPAIKYRPENTPEPVSTSVS
O43149	ZZEF1 KIAA0399	MGNAPSHSSEDEAAAAGGEGWGPHQDWAAV
P61204	ARF3	MGNIFGNLLKSLIGKKEMRILMVGLDAAGK
O95466	FMNL1 C17orf1 C17orf1B FMNL FRL1	MGNAAGSAEQPAGPAAPPPKQPAPPKQPMP
P11488	GNAT1 GNATR	MGCTLSAEDKAAVERSKMIDRNLREDGEKA
P61601	NCALD	MGKQNSKLRPEVMQDLLESTDFTEHEIQEW
O00408	PDE2A	MGQACGHSILCRSQQYPAARPAEPRGQQVF
Q9NR22	PRMT8 HRMT1L3 HRMT1L4	MGMKHSSRCLLLRRKMAENAAESTEVNSPP

Table S3.3 Myristoylated proteins in breast milk exosomes[41]

Protein ID	Gene Name	Sequence
P18085	ARF4 ARF2	MGLTISSLFSRLFGKKQMRILMVGLDAAGK
P62330	ARF6	MGKVLSKIFGNKEMWILMLGLDAAGKTTIL
P04899	GNAI2 GNAI2B	MGCTVSAEDKAAAERSKMIDKNLREDGEKA
P08754	GNAI3	MGCTLSAEDKAAVERSKMIDRNLREDGEKA
Q96TA1	FAM129B C9orf88	MGDVLSTHLDDARRQHIAEKTGKILTEFLQ
Q6IAA8	LAMTOR1 C11orf59 PDRO PP7157	MGCCYSSENEDSDQDREERKLLLDPSSPPT
Q14254	FLOT2 ESA1 M17S1	MGNCHTVGPNEALVVSGGCCGSDYKQYVFG
P84085	ARF5	MGLTVSALFSRIFGKKQMRILMVGLDAAGK
P61313	RPL15 EC45 TCBAP0781	MGAYKYIQELWRKKQSDVMRFLLRVRCWQY
P07947	YES1 YES	MGCIKSKENKSPAIKYRPENTPEPVSTSVS
Q9NUQ9	FAM49B BM-009	MGNLLKVLTCTDLEQGPNFFLDFENAQPTE
Q9H4G4	GLIPR2 C9orf19 GAPR1	MGKSASKQFHNEVLKAHNEYRQKHGVPPLK
P63096	GNAI1	MGCTLSAEDKAAVERSKMIDRNLREDGEKA
P36405	ARL3 ARFL3	MGLLSILRKLKSAPDQEVRILLLGLDNAGK
Q96FZ7	CHMP6 VPS20	MGNLFGRKKQSRVTEQDKAILQLKQQRDKL
Q99653	CHP1 CHP	MGSRASTLLRDEELEEIKKETGFSHSQITR
Q8WWI5	SLC44A1 CD92 CDW92 CTL1	MGCCSSASSAAQSSKREWKPLEDRSCTDIP
P07948	LYN JTK8	MGCIKSKGKDSLSDDGVDLKTQPVRNTERT
P49006	MARCKSL1 MLP MRP	MGSQSSKAPRGDVTAEEAAGASPAKANGQE
O75695	RP2	MGCFFSKRRKADKESRPENEEERPKQYSWD
P29966	MARCKS MACS PRKCSL	MGAQFSKTAAKGEAAAERPGEAAVASSPSK
Q8N9N7	LRRC57	MGNSALRAHVETAQKTGVFQLKDRGLTEFP
P37235	HPCAL1 BDR1	MGKQNSKLRPEVLQDLRENTEFTDHELQEW
Q9NRX5	SERINC1 KIAA1253 TDE1L TDE2 UNQ396/PRO732	MGSVLGLCSMASWIPCLCGSAPCLLCRCCP
P40616	ARL1	MGGFFSSIFSSLFGTREMRILILGLDGAGK
P80723	BASP1 NAP22	MGGKLSKKKKGYNVNDEKAKEKDKKAEGAA
Q96PY5	FMNL2 FHOD2 KIAA1902	MGNAGSMDSQQTDFRAHNVPLKLPMPEPGE
Q9BZQ8	FAM129A C1orf24 NIBAN GIG39	MGGSASSQLDEGKCAYIRGKTEAAIKNFSP
Q8NHG7	SVIP	MGLCFPCPGESAPPTPDLEEKRAKLAEAAE
Q9Y3E7	CHMP3 CGI149 NEDF VPS24 CGI-149	MGLFGKTQEKPPKELVNEWSLKIRKEMRVV
Q99828	CIB1 CIB KIP PRKDCIP	MGGSGSRLSKELLAEYQDLTFLTKQEILLA
P17612	PRKACA PKACA	MGNAAAAKKGSEQESVKEFLAKAKEDFLKK
Q8ND76	CCNY C10orf9 CBCP1 CFP1	MGNTTSCCVSSSPKLRRNAHSRLESYRPDT

O00461	GOLIM4 GIMPC GOLPH4 GPP130	MGNGMCSRKQKRIFQTLLLLTVVFGFLYGA
Q8NHG8	ZNRF2 RNF202	MGAKQSGPAAANGRTRAYSGSDLPSSSSGG
P40617	ARL4A ARL4	MGNGLSDQTSILSNLPSFQSFHIVILGLDC
O60291	MGRN1 KIAA0544 RNF156	MGSILSRRIAGVEDIDIQANSAYRYPPKSG
Q9P2G1	ANKIB1 KIAA1386	MGNTTTKFRKALINGDENLACQIYENNPQL
P61204	ARF3	MGNIFGNLLKSLIGKKEMRILMVGLDAAGK
P35813	PPM1A PPPM1A	MGAFLDKPKMEKHNAQGQGNGLRYGLSSMQ
Q9Y478	PRKAB1 AMPK	MGNTSSERAALERHGGHKTPRRDSSGGTKD

Table S3.4 Myristoylated proteins in urine exosomes[40]

Protein ID	Gene Name	Sequence
Q9BRQ8	AIFM2 AMID PRG3	MGSQVSVESGALHVVIVGGGFGGIAAASQL
Q02952	AKAP12 AKAP250	MGAGSSTEQRSPEQPPEGSSTPAEPEPSGG
P27216	ANXA13 ANX13	MGNRHAKASSPQGFDVDRDAKKLNKACKGM
P84077	ARF1	MGNIFANLFKGLFGKKEMRILMVGLDAAGK
P18085	ARF4 ARF2	MGLTISSLFSRLFGKKQMRILMVGLDAAGK
P84085	ARF5	MGLTVSALFSRIFGKKQMRILMVGLDAAGK
P62330	ARF6	MGKVLSKIFGNKEMWILMLGLDAAGKTTIL
P36405	ARL3 ARFL3	MGLLSILRKLKSAPDQEVRILLLGLDNAGK
Q9H0F7	ARL6 BBS3	MGLLDRLSVLLGLKKKEVHVLCLGLDNSGK
P80723	BASP1 NAP22	MGGKLSKKKKGYNVNDEKAKEKDKKAEGAA
Q8ND76	CCNY C10orf9 CBCP1 CFP1	MGNTTSCCVSSSPKLRRNAHSRLESYRPDT
Q9Y3E7	CHMP3 CGI149 NEDF VPS24 CGI-149	MGLFGKTQEKPPKELVNEWSLKIRKEMRVV
Q96FZ7	CHMP6 VPS20	MGNLFGRKKQSRVTEQDKAILQLKQQRDKL
Q99653	CHP1 CHP	MGSRASTLLRDEELEEIKKETGFSHSQITR
Q99828	CIB1 CIB KIP PRKDCIP	MGGSGSRLSKELLAEYQDLTFLTKQEILLA
P00387	CYB5R3 DIA1	MGAQLSTLGHMVLFPVWFLYSLLMKLFQRS
Q9BZQ8	FAM129A C1orf24 NIBAN GIG39	MGGSASSQLDEGKCAYIRGKTEAAIKNFSP
Q96TA1	FAM129B C9orf88	MGDVLSTHLDDARRQHIAEKTGKILTEFLQ
Q9NUQ9	FAM49B BM-009	MGNLLKVLTCTDLEQGPNFFLDFENAQPTE
Q14254	FLOT2 ESA1 M17S1	MGNCHTVGPNEALVVSGGCCGSDYKQYVFG
P06241	FYN	MGCVQCKDKEATKLTEERDGSLNQSSGYRY
Q9H4G4	GLIPR2 C9orf19 GAPR1	MGKSASKQFHNEVLKAHNEYRQKHGVPPLK
P63096	GNAI1	MGCTLSAEDKAAVERSKMIDRNLREDGEKA
P04899	GNAI2 GNAI2B	MGCTVSAEDKAAAERSKMIDKNLREDGEKA
P08754	GNAI3	MGCTLSAEDKAAVERSKMIDRNLREDGEKA
P09471	GNAO1	MGCTLSAEERAALERSKAIEKNLKEDGISA
P19086	GNAZ	MGCRQSSEEKEAARRSRRIDRHLRSESQRQ
O00461	GOLIM4 GIMPC GOLPH4 GPP130	MGNGMCSRKQKRIFQTLLLLTVVFGFLYGA
P08631	HCK	MGGRSSCEDPGCPRDEERAPRMGCMKSKFL
Q8IV36	HID1 C17orf28 DMC1	MGSTDSKLNFRKAVIQLTTKTQPVEATDDA
P37235	HPCAL1 BDR1	MGKQNSKLRPEVLQDLRENTEFTDHELQEW
Q6IAA8	LAMTOR1 C11orf59 PDRO PP7157	MGCCYSSENEDSDQDREERKLLLDPSSPPT
P06239	LCK	MGCGCSSHPEDDWMENIDVCENCHYPIVPL
Q8N9N7	LRRC57	MGNSALRAHVETAQKTGVFQLKDRGLTEFP

P29966	MARCKS MACS PRKCSL	MGAQFSKTAAKGEAAAERPGEAAVASSPSK
P49006	MARCKSL1 MLP MRP	MGSQSSKAPRGDVTAEEAAGASPAKANGQE
O60291	MGRN1 KIAA0544 RNF156	MGSILSRRIAGVEDIDIQANSAYRYPPKSG
P08473	MME EPN	MGKSESQMDITDINTPKPKKKQRWTPLEIS
O75688	PPM1B PP2CB	MGAFLDKPKTEKHNAHGAGNGLRYGLSSMQ
P17612	PRKACA PKACA	MGNAAAAKKGSEQESVKEFLAKAKEDFLKK
P22694	PRKACB	MGNAATAKKGSEVESVKEFLAKAKEDFLKK
Q14699	RFTN1 KIAA0084 MIG2	MGCGLNKLEKRDEKRPGNIYSTLKRPQVET
O75695	RP2	MGCFFSKRRKADKESRPENEEERPKQYSWD
P62241	RPS8 OK/SW-cl.83	MGISRDNWHKRRKTGGKRKPYHKKRKYELG
Q9NRX5	SERINC1 KIAA1253 TDE1L TDE2 UNQ396/PRO732	MGSVLGLCSMASWIPCLCGSAPCLLCRCCP
Q8WWI5	SLC44A1 CD92 CDW92 CTL1	MGCCSSASSAAQSSKREWKPLEDRSCTDIP
P12931	SRC SRC1	MGSNKSKPKDASQRRRSLEPAENVHGAGGG
Q8NHG7	SVIP	MGLCFPCPGESAPPTPDLEEKRAKLAEAAE
P07947	YES1 YES	MGCIKSKENKSPAIKYRPENTPEPVSTSVS
Q9P2G1	ANKIB1 KIAA1386	MGNTTTKFRKALINGDENLACQIYENNPQL
P61204	ARF3	MGNIFGNLLKSLIGKKEMRILMVGLDAAGK
Q9P203	BTBD7 KIAA1525	MGANASNYPHSCSPRVGGNSQAQQTFIGTS
Q717R9	CYS1	MGSGSSRSSRTLRRRRSPESLPAGPGAAAL
Q7Z494	NPHP3 KIAA2000	MGTASSLVSPAGGEVIEDTYGAGGGEACEI
P35813	PPM1A PPPM1A	MGAFLDKPKMEKHNAQGQGNGLRYGLSSMQ
Q9Y478	PRKAB1 AMPK	MGNTSSERAALERHGGHKTPRRDSSGGTKD
Q13237	PRKG2 PRKGR2	MGNGSVKPKHSKHPDGHSGNLTTDALRNKV
P11801	PSKH1	MGCGTSKVLPEPPKDVQLDLVKKVEPFSGT
Q6P9B6	TLDC1 KIAA1609	MGNSRSRVGRSFCSQFLPEEQAEIDQLFDA

3.6 REFERENCES

1. Kowal, J., M. Tkach, and C. Théry, Biogenesis and secretion of exosomes. Curr Opin Cell Biol, 2014. 29: p. 116-125.
2. Thery, C., L. Zitvogel, and S. Amigorena, Exosomes: composition, biogenesis and function. Nat Rev Immunol, 2002. 2(8): p. 569-579.
3. Colombo, M., G. Raposo, and C. Théry, Biogenesis, secretion, and intercellular interactions of exosomes and other extracellular vesicles. Annu Rev Cell Dev Biol, 2014. 30: p. 255-289.
4. Keller, S., M.P. Sanderson, A. Stoeck, and P. Altevogt, Exosomes: From biogenesis and secretion to biological function. Immunol Lett, 2006. 107(2): p. 102-108.
5. Villarroya-Beltri, C., F. Baixauli, C. Gutiérrez-Vázquez, F. Sánchez-Madrid, and M. Mittelbrunn, Sorting it out: Regulation of exosome loading. Sem Cell Biol, 2014. 28: p. 3-13.
6. Simons, M. and G. Raposo, Exosomes–vesicular carriers for intercellular communication. Curr Opin Cell Biol, 2009. 21(4): p. 575-581.
7. Kahlert, C. and R. Kalluri, Exosomes in tumor microenvironment influence cancer progression and metastasis. J Mol Med, 2013. 91(4): p. 431-437.
8. Skog, J., T. Würdinger, S. Van Rijn, D.H. Meijer, L. Gainche, W.T. Curry, B.S. Carter, A.M. Krichevsky, and X.O. Breakefield, Glioblastoma microvesicles transport RNA and proteins that promote tumour growth and provide diagnostic biomarkers. Nat Cell Biol, 2008. 10(12): p. 1470-1476.
9. Abusamra, A.J., Z. Zhong, X. Zheng, M. Li, T.E. Ichim, J.L. Chin, and W.-P. Min, Tumor exosomes expressing Fas ligand mediate CD8+ T-cell apoptosis. Blood Cells Mol Dis, 2005. 35(2): p. 169-173.
10. Fizazi, K., The role of Src in prostate cancer. Ann Oncol, 2007. 18(11): p. 1765-1773.
11. Erpel, T. and S.A. Courtneidge, Src family protein tyrosine kinases and cellular signal transduction pathways. Curr Opin Cell Biol, 1995. 7(2): p. 176-182.
12. Parsons, J.T. and S.J. Parsons, Src family protein tyrosine kinases: cooperating with growth factor and adhesion signaling pathways. Curr Opin Cell Biol, 1997. 9(2): p. 187-192.
13. Xu, W., S.C. Harrison, and M.J. Eck, Three-dimensional structure of the tyrosine kinase c-Src. Nature, 1997. 385(6617): p. 595.
14. Sicheri, F., I. Moarefi, and J. Kuriyan, Crystal structure of the Src family tyrosine kinase Hck. Nature, 1997. 385(6617): p. 602.
15. Sicheri, F. and J. Kuriyan, Structures of Src-family tyrosine kinases. Curr Opin Cell Biol, 1997. 7(6): p. 777-785.
16. Tatarov, O., T.J. Mitchell, M. Seywright, H.Y. Leung, V.G. Brunton, and J. Edwards, SRC family kinase activity is up-regulated in hormone-refractory prostate cancer. Clin Cancer Res, 2009. 15(10): p. 3540-3549.
17. Irby, R.B. and T.J. Yeatman, Role of Src expression and activation in human cancer. Oncogene, 2000. 19(49): p. 5636.
18. Vlaeminck-Guillem, V., G. Gillet, and R. Rimokh, SRC: marker or actor in prostate cancer aggressiveness. Front Oncol, 2014. 4.
19. Ishizawar, R. and S.J. Parsons, c-Src and cooperating partners in human cancer. Cancer cell, 2004. 6(3): p. 209-214.

20. Lara Jr, P.N., J. Longmate, C.P. Evans, D.I. Quinn, P. Twardowski, G. Chatta, E. Posadas, W. Stadler, and D.R. Gandara, A phase II trial of the Src-kinase inhibitor AZD0530 in patients with advanced castration-resistant prostate cancer: a California Cancer Consortium study. Anti-cancer drugs, 2009. 20(3): p. 179.
21. Park, S.I., J. Zhang, K.A. Phillips, J.C. Araujo, A.M. Najjar, A.Y. Volgin, J.G. Gelovani, S.-J. Kim, Z. Wang, and G.E. Gallick, Targeting SRC family kinases inhibits growth and lymph node metastases of prostate cancer in an orthotopic nude mouse model. Cancer Res, 2008. 68(9): p. 3323-3333.
22. Kim, L.C., L. Song, and E.B. Haura, Src kinases as therapeutic targets for cancer. Nat Rev Clin Oncol, 2009. 6(10): p. 587-595.
23. Casey, P.J., Protein lipidation in cell signaling. Science, 1995. 268(5208): p. 221.
24. Shen, B., N. Wu, J.-M. Yang, and S.J. Gould, Protein targeting to exosomes/microvesicles by plasma membrane anchors. J Biol Chem, 2011. 286(16): p. 14383-14395.
25. Wright, M.H., W.P. Heal, D.J. Mann, and E.W. Tate, Protein myristoylation in health and disease. J Chem Biol, 2010. 3(1): p. 19-35.
26. Resh, M.D., Myristylation and palmitylation of Src family members: the fats of the matter. Cell, 1994. 76(3): p. 411-413.
27. Flaumenhaft, R. and D.S. Sim, Protein palmitoylation in signal transduction of hematopoietic cells. Hematology, 2005. 10(6): p. 511-519.
28. Milligan, G., M. Parenti, and A.I. Magee, The dynamic role of palmitoylation in signal transduction. Trends Biochem Sci, 1995. 20(5): p. 181-186.
29. Resh, M.D., Membrane targeting of lipid modified signal transduction proteins, in Membrane Dynamics and Domains. 2004, Springer. p. 217-232.
30. Resh, M.D., Fatty acylation of proteins: new insights into membrane targeting of myristoylated and palmitoylated proteins. BBA Mol Cell Res, 1999. 1451(1): p. 1-16.
31. Robbins, S.M., N.A. Quintrell, and J.M. Bishop, Myristoylation and differential palmitoylation of the HCK protein-tyrosine kinases govern their attachment to membranes and association with caveolae. Mol Cell Biol, 1995. 15(7): p. 3507-3515.
32. Shenoy-Scaria, A.M., D.J. Dietzen, J. Kwong, D.C. Link, and D.M. Lublin, Cysteine 3 of Src family protein tyrosine kinases determines palmitoylation and localization in caveolae. J Cell Biol, 1994. 126(2): p. 353-364.
33. Kim, S., X. Yang, Q. Li, M. Wu, L. Costyn, Z. Beharry, M.G. Bartlett, and H. Cai, Myristoylation of Src kinase mediates Src-induced and high-fat diet–accelerated prostate tumor progression in mice. J Biol Chem, 2017. 292(45): p. 18422-18433.
34. Kim, S., O.A. Alsaidan, O. Goodwin, Q. Li, E. Sulejmani, Z. Han, A. Bai, T. Albers, Z. Beharry, and Y.G. Zheng, Blocking myristoylation of Src inhibits its kinase activity and suppresses prostate cancer progression. Cancer Res, 2017. 77(24): p. 6950-6962.
35. DeRita, R.M., B. Zerlanko, A. Singh, H. Lu, R.V. Iozzo, J.L. Benovic, and L.R. Languino, c-Src, Insulin-Like Growth Factor I Receptor, G-Protein-Coupled Receptor Kinases and Focal Adhesion Kinase are Enriched Into Prostate Cancer Cell Exosomes. J Cell Biochem, 2017. 118(1): p. 66-73.
36. Cai, H., I. Babic, X. Wei, J. Huang, and O.N. Witte, Invasive prostate carcinoma driven by c-Src and androgen receptor synergy. Cancer Res, 2010.

37. Hurwitz, S.N., M.A. Rider, J.L. Bundy, X. Liu, R.K. Singh, and D.G. Meckes Jr, Proteomic profiling of NCI-60 extracellular vesicles uncovers common protein cargo and cancer type-specific biomarkers. Oncotarget, 2016. 7(52): p. 86999.
38. Khoury, G.A., R.C. Baliban, and C.A. Floudas, Proteome-wide post-translational modification statistics: frequency analysis and curation of the swiss-prot database. Sci Rep, 2011. 1: p. 90.
39. Consortium, U., UniProt: the universal protein knowledgebase. Nucleic Acids Res, 2016. 45(D1): p. D158-D169.
40. Wang, Z., S. Hill, J.M. Luther, D.L. Hachey, and K.L. Schey, Proteomic analysis of urine exosomes by multidimensional protein identification technology (MudPIT). Proteomics, 2012. 12(2): p. 329-338.
41. van Herwijnen, M.J., M.I. Zonneveld, S. Goerdayal, E.N. Nolte, J. Garssen, B. Stahl, A.M. Altelaar, F.A. Redegeld, and M.H. Wauben, Comprehensive proteomic analysis of human milk-derived extracellular vesicles unveils a novel functional proteome distinct from other milk components. Mol Cell Proteomics, 2016. 15(11): p. 3412-3423.
42. Skogberg, G., J. Gudmundsdottir, S. van der Post, K. Sandström, S. Bruhn, M. Benson, L. Mincheva-Nilsson, V. Baranov, E. Telemo, and O. Ekwall, Characterization of human thymic exosomes. PloS one, 2013. 8(7): p. e67554.
43. Brown, M.T. and J.A. Cooper, Regulation, substrates and functions of src. BBA Rev Cancer, 1996. 1287(2-3): p. 121-149.
44. Aicart-Ramos, C., R.A. Valero, and I. Rodriguez-Crespo, Protein palmitoylation and subcellular trafficking. BBA Biomembranes, 2011. 1808(12): p. 2981-2994.
45. Tan, S.S., Y. Yin, T. Lee, R.C. Lai, R.W.Y. Yeo, B. Zhang, A. Choo, and S.K. Lim, Therapeutic MSC exosomes are derived from lipid raft microdomains in the plasma membrane. J Extracell Vesicles, 2013. 2(1): p. 22614.
46. Trajkovic, K., C. Hsu, S. Chiantia, L. Rajendran, D. Wenzel, F. Wieland, P. Schwille, B. Brügger, and M. Simons, Ceramide triggers budding of exosome vesicles into multivesicular endosomes. Science, 2008. 319(5867): p. 1244-1247.
47. Simons, K. and E. Ikonen, Functional rafts in cell membranes. nature, 1997. 387(6633): p. 569.
48. Mayor, S. and H. Riezman, Sorting GPI-anchored proteins. Nat Rev Mol Cell Biol, 2004. 5(2): p. 110-120.
49. de Gassart, A., C. Géminard, B. Février, G. Raposo, and M. Vidal, Lipid raft-associated protein sorting in exosomes. Blood, 2003. 102(13): p. 4336-4344.
50. Mukherjee, A., L. Arnaud, and J.A. Cooper, Lipid-dependent recruitment of neuronal Src to lipid rafts in the brain. J Biol Chem, 2003. 278(42): p. 40806-40814.
51. Babst, M., D.J. Katzmann, W.B. Snyder, B. Wendland, and S.D. Emr, Endosome-associated complex, ESCRT-II, recruits transport machinery for protein sorting at the multivesicular body. Dev Cell, 2002. 3(2): p. 283-289.
52. Garrus, J.E., U.K. Von Schwedler, O.W. Pornillos, S.G. Morham, K.H. Zavitz, H.E. Wang, D.A. Wettstein, K.M. Stray, M. Côté, and R.L. Rich, Tsg101 and the vacuolar protein sorting pathway are essential for HIV-1 budding. Cell, 2001. 107(1): p. 55-65.
53. Tu, C., C.F. Ortega-Cava, P. Winograd, M.J. Stanton, A.L. Reddi, I. Dodge, R. Arya, M. Dimri, R.J. Clubb, and M. Naramura, Endosomal-sorting complexes required for transport (ESCRT) pathway-dependent endosomal traffic regulates the localization of active Src at focal adhesions. Proc Natl Acad Sci, 2010. 107(37): p. 16107-16112.

54. Imjeti, N.S., K. Menck, A.L. Egea-Jimenez, C. Lecointre, F. Lembo, H. Bouguenina, A. Badache, R. Ghossoub, G. David, and S. Roche, Syntenin mediates SRC function in exosomal cell-to-cell communication. Proc Natl Acad Sci, 2017. 114(47): p. 12495-12500.
55. Mineo, M., S.H. Garfield, S. Taverna, A. Flugy, G. De Leo, R. Alessandro, and E.C. Kohn, Exosomes released by K562 chronic myeloid leukemia cells promote angiogenesis in a Src-dependent fashion. Angiogenesis, 2012. 15(1): p. 33-45.
56. Burgess, E.F., A.J.L. Ham, D.L. Tabb, D. Billheimer, B.J. Roth, S.S. Chang, M.S. Cookson, T.J. Hinton, K.L. Cheek, and S. Hill, Prostate cancer serum biomarker discovery through proteomic analysis of alpha-2 macroglobulin protein complexes. Proteomics Clin Appl, 2008. 2(9): p. 1223-1233.
57. Sandilands, E., V.G. Brunton, and M.C. Frame, The membrane targeting and spatial activation of Src, Yes and Fyn is influenced by palmitoylation and distinct RhoB/RhoD endosome requirements. J Cell Sci, 2007. 120(15): p. 2555-2564.
58. GUZZI, F., D. ZANCHETTA, B. CHINI, and M. PARENTI, Thioacylation is required for targeting G-protein subunit Go1α to detergent-insoluble caveolin-containing membrane domains. Biochem J, 2001. 355(2): p. 323-331.
59. Song, K., M. Sargiacomo, F. Galbiati, M. Parenti, and M. Lisanti, Targeting of a G alpha subunit (Gi1 alpha) and c-Src tyrosine kinase to caveolae membranes: clarifying the role of N-myristoylation. Cell Mol Biol, 1997. 43(3): p. 293-303.
60. Patwardhan, P. and M.D. Resh, Myristoylation and membrane binding regulate c-Src stability and kinase activity. Mol Cell Biol, 2010. 30(17): p. 4094-4107.
61. Shvartsman, D.E., J.C. Donaldson, B. Diaz, O. Gutman, G.S. Martin, and Y.I. Henis, Src kinase activity and SH2 domain regulate the dynamics of Src association with lipid and protein targets. J Cell Biol, 2007. 178(4): p. 675-686.
62. Raiborg, C. and H. Stenmark, The ESCRT machinery in endosomal sorting of ubiquitylated membrane proteins. Nature, 2009. 458(7237): p. 445-452.
63. Votteler, J. and W.I. Sundquist, Virus budding and the ESCRT pathway. Cell Host Microbe, 2013. 14(3): p. 232-241.
64. Christ, L., C. Raiborg, E.M. Wenzel, C. Campsteijn, and H. Stenmark, Cellular functions and molecular mechanisms of the ESCRT membrane-scission machinery. Trends Biochem Sci, 2017. 42(1): p. 42-56.
65. Zhong, M., Z. Lu, and D.A. Foster, Downregulating PKC δ provides a PI3K/Akt-independent survival signal that overcomes apoptotic signals generated by c-Src overexpression. Oncogene, 2002. 21(7): p. 1071.
66. Zhong, M., Y. Shen, Y. Zheng, T. Joseph, D. Jackson, and D.A. Foster, Phospholipase D prevents apoptosis in v-Src-transformed rat fibroblasts and MDA-MB-231 breast cancer cells. Biochem Biophys Res Commun, 2003. 302(3): p. 615-619.
67. Yu, K.H., C.G. Barry, D. Austin, C.M. Busch, V. Sangar, A.K. Rustgi, and I.A. Blair, Stable isotope dilution multidimensional liquid chromatography-tandem mass spectrometry for pancreatic cancer serum biomarker discovery. J Proteome Res, 2009. 8(3): p. 1565-1576.
68. Rong, B., C. Zhao, H. Liu, Z. Ming, X. Cai, W. Gao, and S. Yang, Identification and verification of Hsp90-beta as a potential serum biomarker for lung cancer. Am J Cancer Res, 2014. 4(6): p. 874.

4. TURN UP THE CELLULAR POWER GENERATOR WITH VITAMIN E ANALOGUE FORMULATION*

*Wen, R. and Dhar S. 2016.*Chem Sci*. 7(8): p. 5559-5567.
Reprinted here with permission of the Royal Society of Chemistry.

ABSTRACT

The down regulation of the cellular power generator, adenosine triphosphate (ATP) synthase, in cancer cells limits electron flux in the mitochondrial respiratory chain and prevents mitochondria-mediated cell death. Cancer cells up-regulate ATPase inhibitory factor 1 (IF1) and down-regulate β-F1-ATPase of ATP synthase to enhance aerobic glycolysis for tumor growth via inhibiting total ATP synthase activity in the oxidative phosphorylation (OXPHOS) pathway. Alpha-tocopheryl succinate (α-TOS), one of the most bioactive derivatives of vitamin E, can selectively induce apoptosis in numerous cancer cells. The cancer cell selective apoptosis inducing property of α-TOS is correlated to: mitochondrial destabilization, inhibition of anti-apoptotic B cell lymphoma 2 (Bcl2) and protein kinase C (PKC), caspase 3 activation, production of mitochondrial reactive oxygen species (ROS), inhibition of succinate dehydrogenase activity of mitochondrial complex II, and complexes I and III to some extent. There is no report which elucidates the effects of α-TOS on the cellular power generator, complex V or ATP synthase. Here, we report, for the first time, cancer cell selective activation of mitochondrial ATP synthase using a suitably designed chemical formulation of α-TOS. A mitochondria targeted α-TOS nanoparticle formulation demonstrated enhanced cytotoxicity and mitochondrial activities in cancer cells by inhibiting of Bcl2 protein and activating ATP synthase. The modulation of severely compromised ATP synthase in cancer cells by the engineered formulation of α-TOS, with further development, is a promising means of transforming the acute crisis of solid cancers with down-regulated β subunit of ATP synthase to chronic disease.

4.1 INTRODUCTION

Down-regulation of the cellular power generator, ATP synthase, is a signature bioenergetic phenomenon of several tumors such as cancers of liver, kidney, colon, lung, and breast[1-4]. Dysfunctional mitochondrial bioenergetics related to the down regulation of ATP synthase in cancer cells limits electron flux in the respiratory chain due to coupling between mitochondrial respiration and oxidative phosphorylation (OXPHOS), and results in resistance towards mitochondria-mediated cancer cell death. Mitochondrial ATP synthase, or F1F0-ATP synthase, is a unique complex of 16 subunits of $\alpha 3\beta 3\gamma\delta$ and ε forming the F1 component: a, b, c, d, e, f, g, A6L, oligomycin sensitivity-conferring protein (OSCP), and coupling factor 6, and forming the F0 component: the stator, and an intrinsic inhibitor protein, ATPase inhibitory factor 1 (IF1). Decreased activity of ATP synthase in cancer cells arises from a combination of up-regulated expression of IF1 and down-regulation of β-F1-ATPase, resulting in enhanced aerobic glycolysis (Scheme 1)[5]. ATP synthase activity and protein expression in colon cancer cells were reported to be down regulated under 5-fluorouracil (5-FU) resistance[4]. The suppression of ATP synthase subunits is dependent on cancer cell lines. Clinical studies demonstrated that patients possessed a longer life expectancy when there is higher tumor expression level of β-F1-ATPase[6]. Thus, ATP synthase activity enhancement in cancer cells can modulate the mitochondrial bioenergetic functions to cause cancer cell death in unique ways. However, there are not many therapeutic agents that can enhance the activity of ATP synthase in a therapeutically beneficial way. Defects in ATP synthase are involved in extremely severe and difficult to treat tumors. Given that this ATP generator is located in the inner membrane of mitochondria and in a highly concentrated manner in inner membrane cristae as a part of the

ATP synthasome and in association with inorganic phosphate carrier and the adenine nucleotide translocase[4], it is extremely difficult to access ATP synthase for therapeutic modulation.

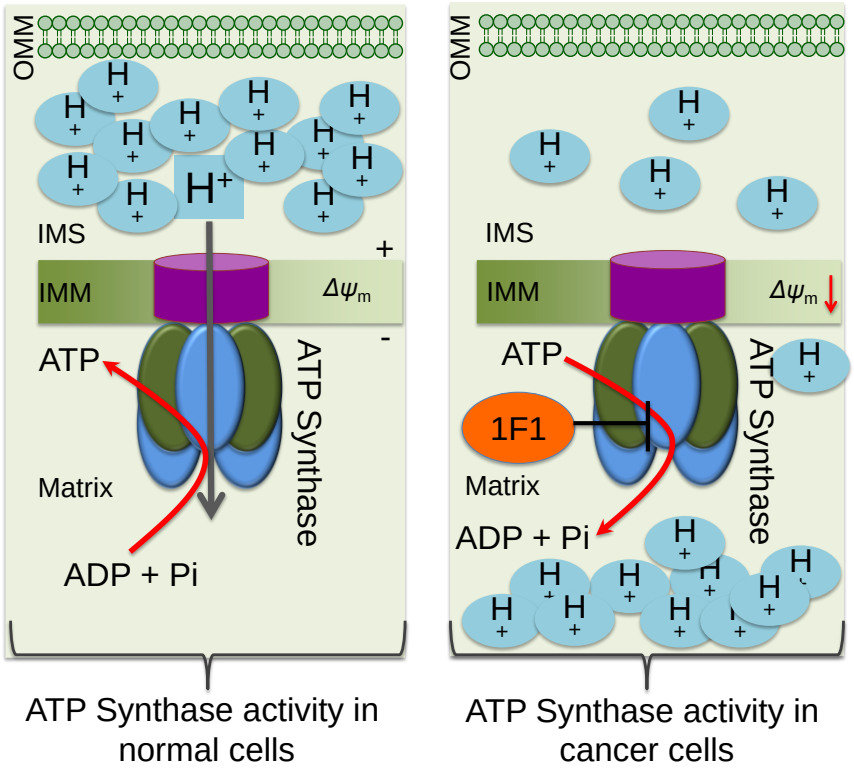

Scheme 1. Schematic representation of differences in ATP synthase in normal and cancer cell mitochondria. OMM: outer mitochondrial membrane; IMS: intermembrane space; IMM: inner mitochondrial membrane.

Alpha-tocopheryl succinate (α-TOS) is the most bioactive vitamin E analogue, among α-tocopherol, α-tocopheryl acetate, and α-tocopheryl nicotinate, that participates in selective apoptosis induction in cancer cells[7]. α-TOS selectively inhibits proliferation and induces apoptosis in various cancer cells, such as leukemia, breast, colorectal, and prostate cancer cells over normal cells[8]. The pro-apoptotic and anti-neoplastic properties of α-TOS are related to mitochondrial destabilization accessing several targets located in this complex organelle.[9] A brief list of biological actions and targets of α-TOS includes: mitochondrial destabilization, inhibition of anti-apoptotic B cell lymphoma 2 (Bcl2)[10], protein kinase C (PKC),5 and

mitochondrial complex II, caspase 3 activation, generation of mitochondrial reactive oxygen species (ROS)[11], and inhibition of mitochondrial complexes I and III to some extent[12-14]. A mitochondria targeted α-TOS formulation, MitoVES, was developed by conjugating α-TOS with mitochondria-targeting triphenylphosphonium (TPP) cation[15, 16]. However, no work thus far has looked into the activity of α-TOS on mitochondrial complex V or ATP synthase. In this work, we aimed to investigate the effects of this vitamin E analogue on ATP synthase by developing a chemical formulation with abilities to associate α-TOS with the mitochondrial space. We developed a chemical formulation of α-TOS to access ATP synthase in cancer cells for therapeutic benefits. Here, we report the unexplored activity of α-TOS when it is delivered to the mitochondria using a biodegradable controlled release polymeric nanoparticle (NP). The mitochondria targeted α-TOS-NPs demonstrated activation of ATP synthase. Given that the down-expression of β subunit of ATP synthase is associated with the mitochondrial bioenergetics dysfunctions of various cancers such as cancers of liver, kidney, colon, lung, and breast[2-4, 17], we believe that the ATP synthase activation property of mitochondria targeted NP formulation of α-TOS can be important when explored further under in vivo settings.

4.2 EXPERIMENTAL DETAILS

Materials

All chemicals were used without further purification unless otherwise noted. N, N'-dicyclohexylcarbodiimide (DCC), hydrogen peroxide solution (30 wt.% in H_2O), camptothecin, carbonyl cyanide 4-(trifluoromethoxy) phenylhydrazone (FCCP), oligomycin, antimycin A, rotenone, *α*-tocopheryl succinate (*α*-TOS), 3-(4,5-dimethylthiazol-2-yl)-2,5-diphenyltetrazolium bromide (MTT), OH-polyethylene glycol-OH (OH-PEG-OH) of molecular weight 3350, 6-bromohexanoic acid, sodium bicarbonate ($NaHCO_3$), triphenylphosphine, glucose, sodium

hydroxide, and tris(hydroxymethyl)aminomethane (Tris) were purchased from Sigma-Aldrich. XF24-well cell culture microplates were purchased from Seahorse Biosciences. 4-dimethylaminopyridine (DMAP) (catalog No. 1122-58-3) was purchased from Alfa Aesar Inc. Poly(DL-lactide-co-glycolide) (PLGA-COOH) with inherent viscosity of 0.15-0.25 dL/g, was purchased from Durect LACTEL® Absorbable Polymers. Bicinchoninic acid (BCA) protein assay kit (Pierce 23227), RIPA buffer (catalog No. 89900), and nitrocellulose membrane (catalog No. 88018) were purchased from Thermo Scientific. Glutamine, penicillin/streptomycin, trypsin-EDTA solution, HEPES buffer (1 M), and sodium pyruvate were purchased from Sigma Life Sciences. Roswell Park Memorial Institute (RPMI) medium, Dulbecco's Modified Eagle's Medium (DMEM), fetal bovine serum (FBS), 5,5',6,6'-tetrachloro-1,1,3,3-tetraethylbenzimidazolylcarbocyanine iodide (JC-1) dye were purchased from Life Technologies. Annexin V-FITC-propidium iodide (PI) (catalog number 556547) apoptosis detection kit was purchased from BD Biosciences Pharmingen™. Tween 20 was purchased from Fisher Bio-reagent. $CDCl_3$ was purchased from Cambridge Isotope Laboratories Inc. Regenerative cellulose membrane Amicon ultra centrifugal 100 kDa filters (Catalog number UFC910096) were purchased from Merck Millipore Ltd. ATP quantification kit (Catalog number G7570) was purchased from CellTiter-Glo® Promega. Cell-Tak solution for cell and tissue adhesive properties was purchased from Corning® Cell-Tak™ (catalog number. 354240). MitoTox™ Complex V OXPHOS activity microplate assay kit (Catalog number. ab109907), anti-Bcl-2 antibody (Catalog number. ab32124), anti-beta actin antibody (Catalog number. ab8227), and goat anti-rabbit IgG H&L (HRP) preadsorbed (Catalog number. ab97080) were purchased from Abcam Inc. OxiSelect™ Intracellular reactive oxygen species (ROS) assay kit was purchased by Cell Biolabs (Catalog number. STA-342). Amplex® Red hydrogen peroxide/peroxidase assay kit

(Catalog number. A22188) was purchased from Thermo Life Technology. Apoptosis inducing factor (AIF) H-300 antibody (Catalog number. sc-5586) was purchased from Santa Cruz Biotechnology. Lactate assay kit (Catalog number. K627-100) was purchased from BioVision Inc. Ammonium persulfate (Catalog number. 161-0180), tris/glycine/SDS buffer (Catalog number. 161-0732), SDS-PAGE gel preparation kit TGX stain-free™ fast cast™ acrylamine 10% (Catalog number. 161-0182), and Clarity™ western ECL substrate (Catalog number. 170-5060) were purchased from Bio-Rad Inc.

Instruments

Nanopure water was purified by a 0.22 μm filter Millipore Milli-Q Biocel water purification system (18.2 MΩ). Slide-A-Lyzer MINI dialysis tubes were obtained from Thermo Scientific. Proton NMR analyses were carried out on a 400 MHz Varian NMR spectrometer. High-performance liquid chromatography (HPLC) experiments were conducted using an Agilent 1200 LC series instrument equipped with automated injector, and UV and fluorescence detectors. Dynamic light scattering (DLS) measurements were performed on a Malvern Zetasizer Nano ZS system. Transmission electron microscopy (TEM) images were carried out by Philips/FEI Tecnai 20 microscope. Gel permeation chromatographic (GPC) analyses were performed on Shimadzu LC20-AD prominence liquid chromatographer equipped with RI detector. Flow cytometry analyses were performed on Beckman Coulter CyAn™ ADP Analyzer. Cells were counted using a Countess® automated cell counter (Invitrogen Life Technology). Plate reader analyses were performed on a Bio-Tek Synergy HT microplate reader. Mitochondrial bioenergetics assay was performed on a Seahorse XF24 (Agilent Seahorse Biosciences, North Billerica, MA, USA) analyzer. Western blots were imaged on a FluorChem HD2 system from Alpha Innotech (Protein Simple, Santa Clara, CA, USA).

Cell Line and Cell Culture

Human breast cancer cell line MCF-7, human prostate cancer cell line PC-3, Bcl2 Jurkat, and Neo Jurkat cell line were obtained from the American type culture collection (ATCC). H9C2 cardiomyocytes were received as a generous gift from Prof. Mark Anderson, University of Iowa. MCF-7, PC-3, Bcl2 Jurkat, and Neo Jurkat cells were grown in RPMI 1640 medium containing 10% FBS, 1% L-glutamine, 1% sodium pyruvate, 1% HEPES, and 1% penicillin/streptomycin at 37 °C in 5% CO_2. H9C2 cell was grown in DMEM with 10% FBS, 1% L-glutamine, 1% sodium pyruvate, 1% HEPES, and 1% penicillin/streptomycin. The cells were passed every 2 to 3 days up to 20 passages and restarted from a new stock.

Preparation and Characterizations of α-TOS-loaded NPs

The targeted and non-targeted α-TOS nanoparticles (T-*α*-TOS-NPs, NT-*α*-TOS-NPs) were prepared using PLGA-*b*-PEG-TPP and PLGA-*b*-PEG-OH polymers, respectively. A stock solution of the polymer was made by dissolving 5 mg of the polymer in 1 mL of dimethylformamide (DMF). *α*-TOS with different percent feed with respect to polymer was added to the polymer solution. This 1 mL stock solution containing polymer and *α*-TOS was then added drop wise into 10 mL of nanopure water. The mixture was stirred for 2 h and then filetered using Amicon centrifugation filtering device and washed three time using water under centrifugal force of 3000 rpm at 4 °C. Finally the freshly prepared NPs were resuspended in 1 mL water and characterized using DLS and TEM. Size and zeta potential were measured by DLS. The DLS and TEM samples were made by 20 times dilution of the prepared NPs. TEM samples were stained with 4% uranyl acetate. The stained samples (5 μL) were then dropped into the copper grid and air dry for overnight. The concentration of α-TOS in NPs was quantified by HPLC. A 50:50 isopropanol: acetonitrile was used as the mobile phase using a wavelength of 292 nm.

Release of α-TOS from NPs

To evaluate the release of α-TOS from the NPs, the prepared NPs were diluted by 4 times with nanopure water. Then, 100 μL of the diluted solution was added to dialysis tubes. These dialysis tubes were then submerged in phosphate buffered saline (PBS) of pH=7.4 and stirred at 37 °C up to 96 h. The PBS was changed every 4 h for the first 12 h and then changed every 12 h. The samples were collected at predetermined time points and analyzed by HPLC for α-TOS concentration.

Cell Viability Evaluation

The cytotoxicity of T-α-TOS-NPs and NT-α-TOS-NPs in various cell line was studied by the (3-(4,5-dimethylthiazol-2-yl)-2,5-diphenyltetrazolium bromide) (MTT) assay. Specifically, MCF-7 (1500 cells/well), PC-3 (3000 cells/well), H9C2 (2000 cells/well) were seeded in a 96 well plate and grown overnight at 37 °C in 5% CO_2. Then, the media was replenished and NPs at various concentrations were added. For Bcl2 Jurkat and Neo Jurkat cells, 10000 cells/well were seeded in a 96 well plate and the NPs were directly added. After 12 h, the media was removed and fresh media was added. After another 60 h of further incubation, MTT reagent (5 mg/mL, 20 μL/well) was added. Upon 5 h incubation, MTT containing media was removed and cells were lysed using 100 μL of DMSO, followed by 5 min gentle shaking at room temperature. The sample absorbance was monitored at 550 nm using a background absorbance at 800 nm. Cytotoxicity was expressed as mean percentage ± standard deviation (S.D.) relative to the untreated control. Cytotoxicity data was fitted by a sigmoidal curve and IC_{50}, the concentration which inhibits 50% cell growth compared to untreated control, was calculated by a four parameters logistic model. All these analyses were performed with GraphPad Prism (San Diego, U.S.A).

Evaluation of Mitochondrial Membrane Potential

Bcl2 Jurkat and Neo Jurkat cells (1×10^6 cells /well) were plated in 12-well plates. NPs with concentration range of 20-45 μM with respect to α-TOS was added and incubated for 12 h. As positive control, FCCP at a concentration of 10 μM was added and incubated for 30 min. 5,5′,6,6′-tetrachloro-1,1′,3,3′-tetraethylbenzimidazolylcarbocyanine iodide or JC-1 was added to each well at a final concentration of 2 μg/mL and incubated for 30 min at 37 °C. The stained samples were harvested by centrifugation at 1500 rpm for 5 min (4 °C) and washed with 1 mL PBS for two times. The cells were then resuspended in 100 μL PBS and fluorescence was read at both 485/528 and 530/590 nm.

Apoptosis Assay

Bcl2 Jurkat and Neo Jurkat cells ($1x10^6$) were plated in 12-well plate and 25 μM NPs with respect to α-TOS or free α-TOS at the same concentration were added and incubated for 12 h. A positive and negative control for early apoptosis and necrosis were also used by adding camptothecin (20 μM for 12h) and H_2O_2 (100 mM for 45 min), respectively. The cell pellets were collected by centrifuge with 1500 rpm for 5 min at 4 °C. After 3 washes with cold PBS, the cells were resuspend in 100 μL 1X annexin-binding buffer stained with Annexin V-FITC and propidium iodide for 15 min at room temperature, then 400 μL 1X annexin-binding buffer was added, and the samples were analyzed by flow cytometry.

Bicinchoninic acid (BCA) assay

The protein quantification was carried out by BCA assay. Albumin was used as standard. Samples were incubated with 200 μL of working solution composed of reagent A: reagent B=50:1 at 37º C for 30 min, and then the absorbance was measured at 562 nm.

Immune Blotting

Bcl2 Jurkat and Neo Jurkat cells (1×10^6 cells/well) were plated into the 24-well plate and treated with α-TOS, NT-α-TOS-NPs, or T-α-TOS-NPs (20 μM with respect to α-TOS) for 12 h. The cells were harvested by centrifugation at 1500 rpm for 5 min at 4 °C and washed with PBS twice. Radioimmunoprecipitation assay (RIPA) buffer was added into the cells and then incubated on ice for 30 min. The supernatants were collected as the samples after centrifugation at 12000 *g* for 10 min at 4 °C. The protein concentrations in the samples were quantified by the BCA assay. Proteins were resolved in a SDS-PAGE gel, transferred onto a nitrocellulose membrane, and incubated with primary antibody (Bcl2, AIF, β-actin) at 4 °C overnight, and then incubated with secondary antibodies at room temperature for 2 h. The membranes were developed with enhanced chemiluminescence (ECL) for imaging. The bands in membranes were quantified by Image J.

ATP Synthase Activity Assay

The mitochondria ATP synthase activity was assessed by the complex V OXPHOS activity assay kit from Abcam. ATP synthase was exposed to reagents by solubilizing the bovine heart mitochondria (BHM). 40 μL of detergent was mixed with 360 μL BHM (5.5 mg/mL) and incubated on ice for 30 min to solubilize the mitochondria. The supernatant solubilized BHM was collected by centrifugation at 12,000xg for 20 min at 4 °C and diluted with 5 mL of 1X Mito-Buffer. The exposed ATP synthase with respect to 0.5 μg/mL protein was treated with either 30 μM of NPs with respect to α-TOS in 200 μL of complex V activity buffer containing ATP, PK, LDH, phosphoenolpyruvate, NADH. As controls, oligomycin (200 nM)-treated and non-treated samples were analyzed. The absorbance was measured at 340 nm.

MitoStresss Assay

Bcl2 Jurkat (1×10^6 cells/well) were plated into the 24-well plate and treated with α-TOS, NT-α-TOS-NPs, or T-α-TOS-NPs (20 μM with respect to α-TOS) for 12 h. The XF cartridge was hydrated with 1 mL calibrant for 12 h in a CO_2 free environment at 37 °C incubator. The coated XF microplate was prepared by 1 h incubation at 37 °C with 50 μL coating solution containing 22.4 μg/mL of Cell-Tak solution in neutral buffer. A volume of 1 M NaOH equal to half the volume of Cell-Tak solution was used to bring the solution to neutral. Then the microplate was washed with tissue culture grade sterile water 3 times and air-dried for 10 min. The cells were collected via centrifugation at 1500 rpm for 5 min at 4 °C and washed with cold PBS twice. Assay medium was prepared by DMEM (pH=7.42) containing 1% L-glutamine, 1% sodium pyruvate, and 1% glucose. After resuspension in 0.5 mL assay medium, the cells (100 μL) were seeded into the coated XF microplate and centrifuged to have the cells adhered to the bottom. The centrifuge speed range was adjusted to low for DEC. Once the centrifuge speed reached to 450 rpm, it was stopped. The coated XF microplate was then rotated 180 °C and centrifugation stopped once the speed reached 650 rpm. After the cells were incubated in a CO_2 free environment at 37 °C for 20 min, 450 μL of assay medium was added, and incubated for another 30 min. Finally, the samples were analyzed by MitoStress assay (Agilent Seahorse Bioscience) with injection of oligomycin (1.0 μM), FCCP (1.0 μM), antimycin-A (1.0 μM), and rotenone (1.0 μM) using A, B, and C ports in hydrated cartridge, respectively.

For H9C2 cells, 20,000 cells/well were plated in a 24-well microplate and grown for overnight. The medium was replenished and cells were treated with α-TOS, NT-α-TOS-NPs, or T-α-TOS-NPs (20 μM with respect to α-TOS) for 12 h. The medium was removed by taking 150 μL out and washed 3 times with adding and removing of 450 μL of assay medium. Finally, 450 μL of

assay medium was added and incubated for 1 h. Finally, the samples were analyzed by MitoStress assay as described before for Bcl2 Jurkat cells.

CellTiter-Glo® Luminescent ATP Quantification

ATP quantification was carried out by CellTiter-Glo® Cell Viability Assay kit. MCF-7 and H9C2 cells (50000 cells/well) were plated in 96-well plates in 100 μL medium and grown for overnight. Then the medium was replenished and cells were treated with α-TOS, NT-α-TOS-NPs, or T-α-TOS-NPs (40 μM with respect to α-TOS) for 5 h at 37 °C in 5% CO_2 atmosphere. As a control, oligomycin (100 μM for MCF-7, 25 μM for H9C2) treatment was performed. The plates were equilibrated at room temperature for 30 min. 100 μL reagent was added into the 96 well plate and mix for 2 min to ensure the cell lysis. The luminescence was recorded with 10 min delay at room temperature.

ROS Assay

Intracellular ROS was assessed by the ROS assay Kit from Cell Biolabs. MCF-7 and H9C2 cells (50000 cells/well) were plated in 96-well plates in 100 μL medium and grown for overnight. Then the medium was replenished and cells were treated with α-TOS, NT-α-TOS-NPs, or T-α-TOS-NPs (40 μM for MCF-7, 60 μM for H9C2 with respect to α-TOS) for 12 h at 37 °C in 5% CO_2 atmosphere. As a control, oligomycin (25 μM) treatment was performed. The media was removed and 100 μL of 1X dichloro-dihydro-fluorescein diacetate (DCFH-DA)/media solution was added to the cells and incubated for 45 min. The solution was removed and washed with PBS twice. Finally, RIPA cell lysis buffer was added and mixed for 2 min. The fluorescence was recorded at 485/530 nm.

Cellular H_2O_2 Production Assay

H_2O_2 production by cells was quantified by Amplex Red-hydrogen peroxide/peroxidase assay kit. MCF-7 (50000 cells/well) were plated in 96-well plates and grown for overnight. The

medium was replenished and the cells were treated with malonate (100 mM), α-TOS, NT-α-TOS-NPs, or T-α-TOS-NPs (40 μM with respect to α-TOS) with or without malonate for 24 h at 37 °C. To each well, 100 μL Amplex Red working substrate containing 100 μM Amplex® Red reagent and 0.2 U/mL horseradish peroxidase was added and incubated for 30 min. A standard curve of H_2O_2 was constructed in medium for quantification. The fluorescence was measured at 530/590 nm.

Cellular Lactate Analyses

Cellular lactate level was analyzed using a BioVison lactate analysis kit. MCF-7 cells (50,000 cells per well) were plated in a 96-well plate and grown for overnight. The medium was replenished and the cells were treated with α-TOS, NT-α-TOS-NPs, or T-α-TOS-NPs at a concentration of 40 μM with respect to α-TOS. Oligomycin (25 μM) was used as a control. Incubation was carried out for 5 h. The medium was removed and 50 μL of RIPA buffer was used to lyse the cells, followed by addition of 50 μL of reaction mix containing 46 μL lactate assay buffer, 2 μL lactate probe, and 2 μL lactate enzyme mix. The absorbance was measured at 450 nm after incubation for 30 min at room temperature in the dark.

Statistics

All data were expressed as mean ± S.D (standard deviation). Statistical analysis was performed using GraphPad Prism® software v. 5.00. Comparisons between two values were performed using an unpaired Student t test. A one-way ANOVA with a post-hoc Tukey test was used to identify significant differences among groups.

4.3 RESULTS AND DISCUSSION

Construction of α-TOS NPs to access ATP synthase

A block copolymer of poly (lactic-co-glycolic acid) (PLGA)-polyethylene glycol (PEG) (PLGA-b-PEG-OH) and a mitochondria targeting ligand triphenylphosphonium (TPP) cation

which utilizes the mitochondrial membrane potential (Δψm), were used to construct a mitochondria targeted polymer PLGA-b-PEG-TPP[18]. Mitochondria-targeted α-TOS encapsulated T-α-TOS-NPs and the control non-targeted NT-α-TOS-NPs were constructed using PLGA-b-PEG-TPP and PLGA-b-PEG-OH polymers, respectively (Figure 4.1A). A library of targeted and non-targeted NPs were prepared using varied percent feed of α-TOS with respect to PLGA-b-PEG-TPP or PLGA-b-PEG-OH for NP property optimization in terms of diameter, charge, and payload loading (Figure 4.1B). Determination of hydrodynamic diameter (Zaverage), zeta potential, and polydispersity index (PDI) of α-TOS loaded NPs by dynamic light scattering (DLS) indicated that a higher α-TOS feed results in larger particles. Increase in size with percent feed of α-TOS was particularly more significant for T-α-TOS-NPs (Figure 4.1B, ESI Figure S4.1). T-α-TOS-NPs demonstrated decreased positive surface charge as the percent α-TOS feed was increased. NT-α-TOS-NPs showed less negatively charged surface with increased α-TOS feed (Figure 4.1B, ESI Figure S4.1). The targeted NPs prepared from 10% α-TOS feed with a diameter of 57.4±5.5 nm and a zeta potential of +35.8±4.1 mV and the non-targeted NPs with diameter of 61.2±5.7 nm and zeta potential of -24.6±4.9 mV were found to be most suitable for our purpose (Figure 4.1B). High performance liquid chromatography (HPLC) analyses indicated that the percent loading of α-TOS in the targeted or non-targeted NPs was ~8% with an encapsulation efficiency (EE) of 80% for 10% α-TOS feed (Figure 4.1B, ESI Figure S4.2). In our studies, NPs with 10% feed of α-TOS with respect to the polymer were used. A homogeneous spherical population of α-TOS-NPs was confirmed by transmission electron microscopy (TEM) analyses (Figure 4.1C). Investigation of α-TOS release from T and NT NPs under physiological conditions of pH 7.4 at 37 °C indicated that both targeted and non-targeted

NPs were able to release α-TOS in a well-controlled manner and there was no significant difference in the extent of α-TOS release between targeted and non-targeted NPs (Figure 4.1D).

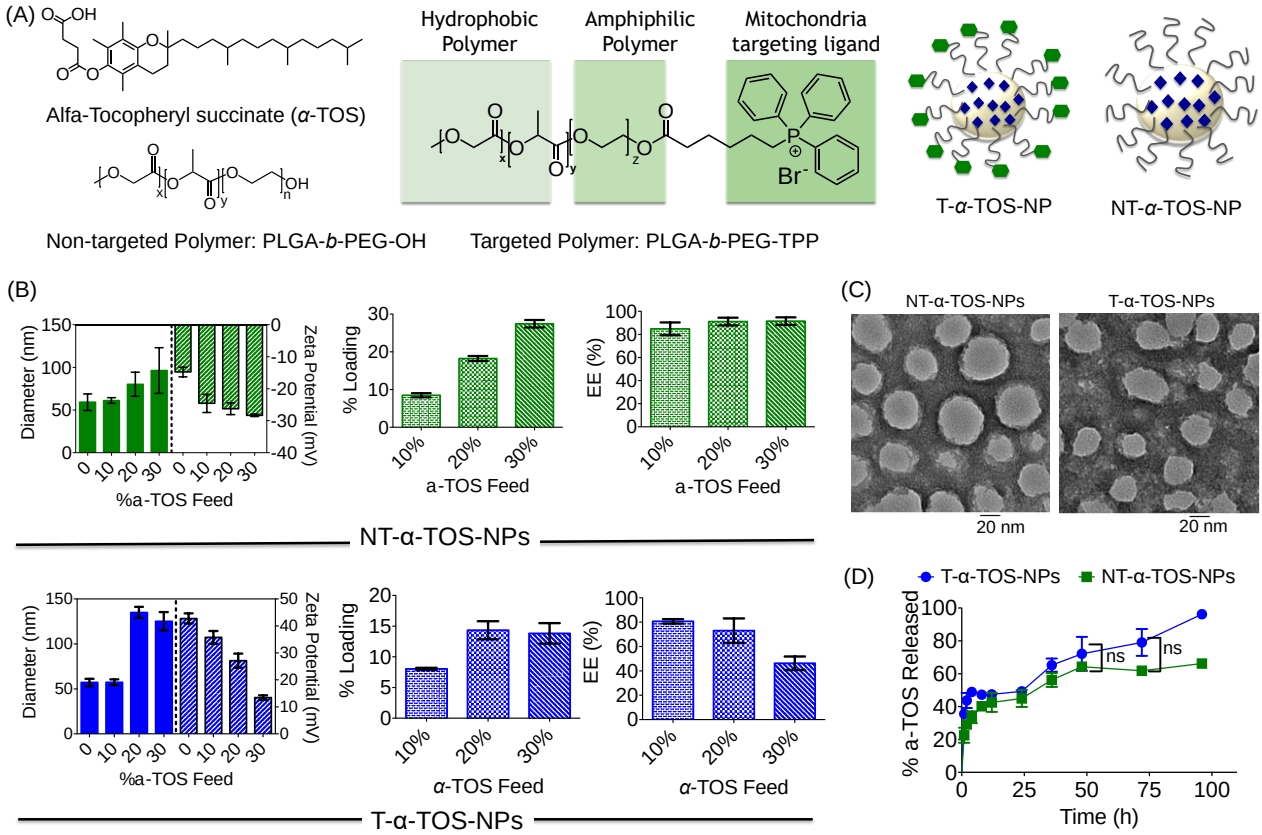

Figure 4.1 (A) Structures of targeted, non-targeted polymers, α-TOS, and schematic representations of targeted-α-TOS-NPs (T-α-TOS-NPs) and non-targeted-α-TOS-NPs (NT-α-TOS-NPs). (B) Comparison of diameter, zeta potential, percent loading and EE of library of T and NT NPs prepared with varied α-TOS feed. (C) TEM of T/NP-α-TOS-NPs prepared with 10% α-TOS feed. (D) Release kinetics of α-TOS from T and NT NPs under physiological conditions of temperature 37 °C, pH 7.4. ns: non-significant.

Unique activities of α-TOS NPs in cancer cells

Cytotoxic activities of NT/T-α-TOS-NPs and α-TOS were evaluated in Bcl2 expressing Bcl2 Jurkat and knock out Neo Jurkat cells. Bcl2 levels in these two cell types were evaluated by Western blot. In both the cancer cell lines, T-α-TOS-NPs demonstrated significantly higher cytotoxic effects compared to free α-TOS (Figure 4.2A and 4.2B). In Bcl2 overexpressing Jurkat cells, when α-TOS was delivered with mitochondria targeted T-α-TOS-NPs, its activity was

significantly increased compared to that of non-targeted NT-α-TOS-NPs; however, their activities were not statistically different in Bcl2 negative Neo Jurkat cells (Figure 4.2). This indicated that in Bcl2 overexpressing cells, delivering α-TOS to the mitochondria is beneficial since the target Bcl2 is located at the OMM. In breast cancer MCF-7 and prostate cancer PC-3 cell lines, the activity of T-α-TOS-NPs was found to be better than free α-TOS or NT-α-TOS-NPs (Figure 4.2). It was particularly interesting to observe that T/NT-α-TOS-NPs were less toxic in normal heart cells; these experiments were carried out on rat cardiomyocyte H9C2 cells (Figure 4.2). This indicated that in Bcl2 overexpressing cells, delivering α-TOS to the mitochondria is beneficial since the target Bcl2 is located at the OMM. In breast cancer MCF-7 and prostate cancer PC-3 cell lines, the activity of T-α-TOS-NPs was found to be better than free α-TOS or NT-α-TOS-NPs (Figure 4.2). It was particularly interesting to observe that T/NT-α-TOS-NPs were less toxic in normal heart cells; these experiments were carried out on rat cardiomyocyte H9C2 cells (Figure 4.2).

Cell death pathways were determined by analyzing the state of mitochondrial membrane potential of Bcl2 and Neo Jurkat cells upon treatment with α-TOS or T/NT-α-TOS-NPs (Figure 4.3A, ESI Figure S4.3). As a control, carbonyl cyanide 4-(trifluoromethoxy)phenylhydrazone (FCCP), which is an uncoupler of mitochondrial membrane was used. These studies indicated that mitochondrial membrane potential collapse is more significant in T-α-TOS NP treated cells compared to α-TOS or NT-α-TOS-NPs. Cellular apoptosis was analyzed by Annexin V/propidium iodide (PI) staining after treatment with α-TOS, T/NT-α-TOS-NPs in Bcl2 and Neo Jurkat cells. These studies indicated increased cell apoptosis by T-α-TOS-NPs compared to α-TOS or NT-α-TOS-NPs in both the cell lines; however the increased apoptotic property of T-α-TOS-NPs was more drastic in Bcl2 Jurkat cells (Figure 4.3B and 4.3C).

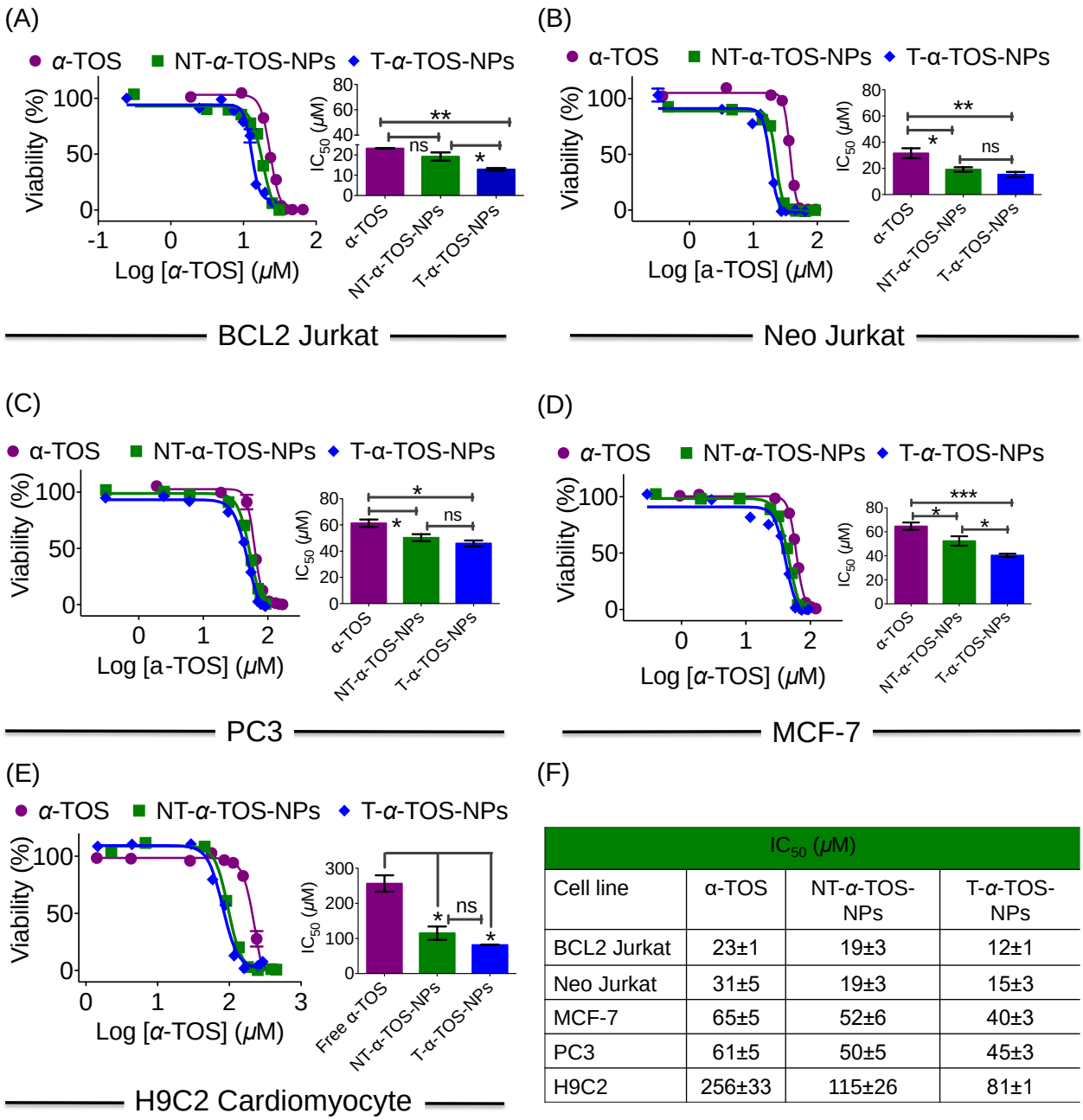

(F)

IC_{50} (μM)			
Cell line	α-TOS	NT-α-TOS-NPs	T-α-TOS-NPs
BCL2 Jurkat	23±1	19±3	12±1
Neo Jurkat	31±5	19±3	15±3
MCF-7	65±5	52±6	40±3
PC3	61±5	50±5	45±3
H9C2	256±33	115±26	81±1

Figure 4.2 (A-D) Cellular toxicity of α-TOS, T-α-TOS-NPs, and NT-α-TOS-NPs in different cancer cell lines. (E) Relatively less cytotoxic effects of α-TOS, T-α-TOS-NPs, and NT-α-TOS-NPs in normal H9C2 cardiomyocytes. (F) A comparison of toxicity of α-TOS, T-α-TOS-NPs, NT-α-TOS-NPs in cancer and normal cells.

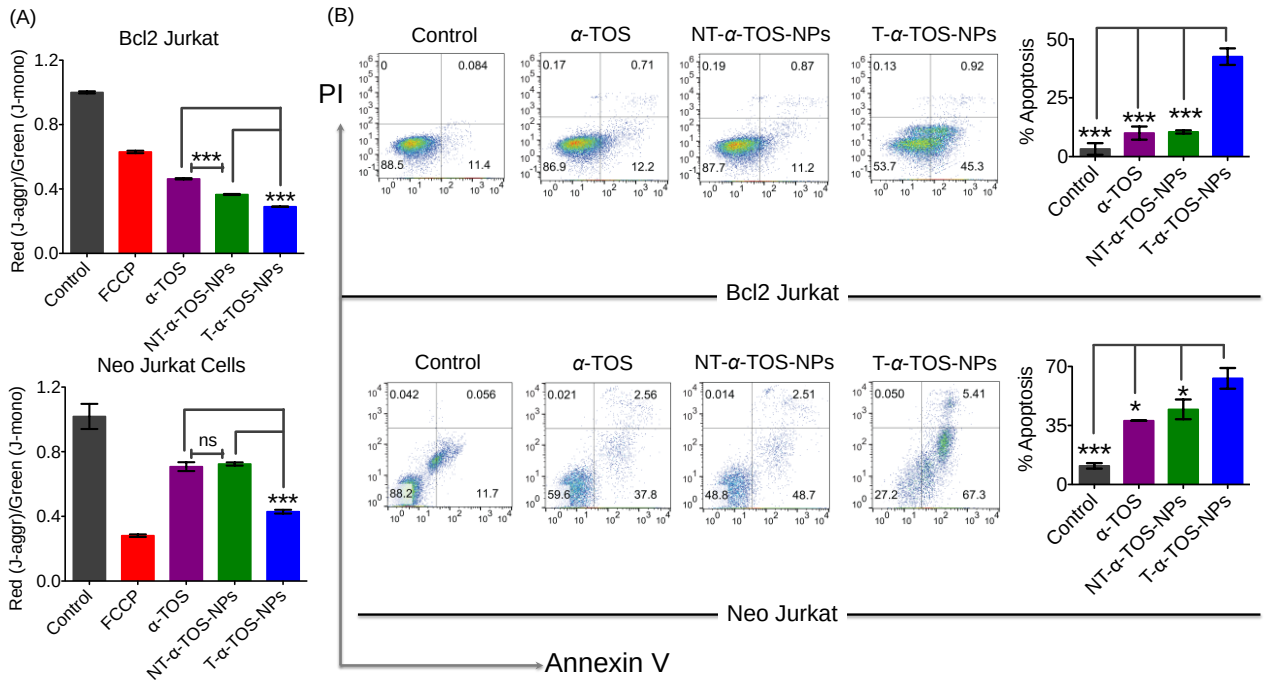

Figure 4.3 (A) Changes in mitochondrial membrane potential in Bcl2 Jurkat and Neo Jurkat cells in presence of α-TOS, T-α-TOS-NPs, and NT-α-TOS-NPs. (B) Comparison of extent of apoptosis in Bcl2 Jurkat and Neo Jurkat cells in presence of α-TOS, T-α-TOS-NPs, NT-α-TOS-NPs by Annexin V-PI assay. ns: non significant. ***P <0.001; **P = 0.001-0.01.

Inhibition of Bcl2 and induction of apoptosis inducing factor

Bcl2, a mitochondrial membrane protein mainly located in the outer mitochondrial membrane (OMM), prevents most types of cell apoptosis[19, 20]. α-TOS induces apoptosis by regulating the Bcl-xL/Bcl2 pathways in which α-TOS disrupts association of Bak Bcl2 homology 3 (BH3) peptide to Bcl-xL and Bcl2 resulting caspase-dependent apoptosis[10, 11]. Apoptosis-inducing factor (AIF) is a mitochondrial intermembrane flavoprotein that induces caspase-independent apoptotic cascade in the presence of death stimuli[21]. Western blot analyses were carried out in Bcl2 and Neo Jurkat cells to investigate whether T/NT-α-TOS-NPs treatment modulate the expression of these key signal proteins (Figure 4.4). We observed ~50% down expression of Bcl2 protein in Bcl2 Jurkat cells when treated with T-α-TOS-NP. Inhibition of Bcl2 in α-TOS or NT-α-TOS-NP treated Bcl2 Jurkat cells was much less compared to that of targeted NPs (Figure 4.4). For T-α-TOS-NP, AIF was up regulated by ~4 and 10 fold in Bcl2 Jurkat and Neo Jurkat

cells, respectively (Figure 4.4). These results indicate that T-α-TOS-NP is able to modulate the mitochondrial proteins Bcl2 and AIF for cellular apoptosis.

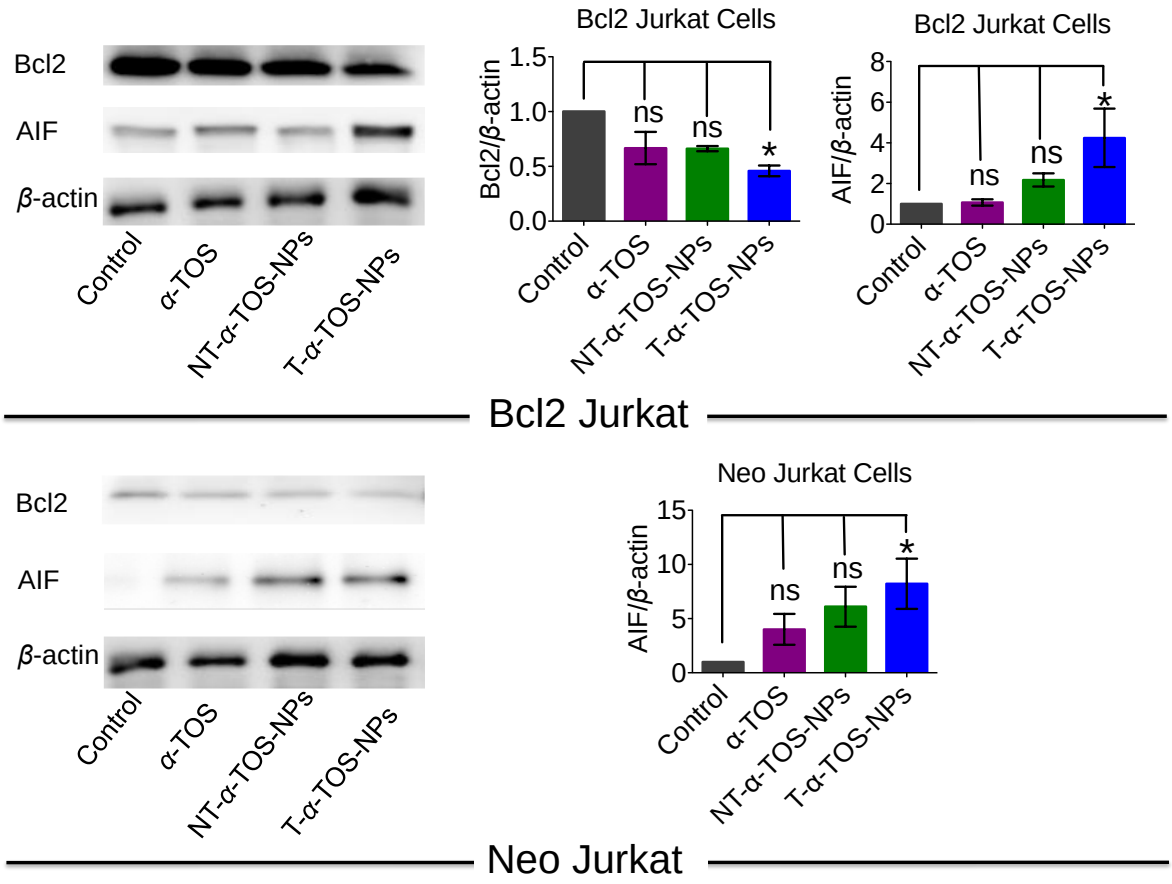

Figure 4.4 Representative western blot images and quantification of Bcl2, AIF proteins in Bcl2 Jurkat and Neo Jurkat cells treated with *α*-TOS and its T/NT NPs.

Effects of T-α-TOS-NP on mitochondrial bioenergetics and respiratory complexes

The effects of T/NT-α-TOS-NPs and α-TOS on bioenergetics of Bcl2 Jurkat cells were evaluated by performing a mitostress assay using XF24 extracellular flux analyzer (Figure 4.5). Free α-TOS treated cells showed similar trends under the influence of ATP synthase inhibitor oligomycin, FCCP which is an uncoupling agent, and a mixture of antimycin A (A), a mitochondrial complex III inhibitor and rotenone (R), a mitochondrial complex I inhibitor as seen with the control cells, demonstrating no significant activity on mitochondrial energetics and respiration at the concentration used (Figure 4.5).

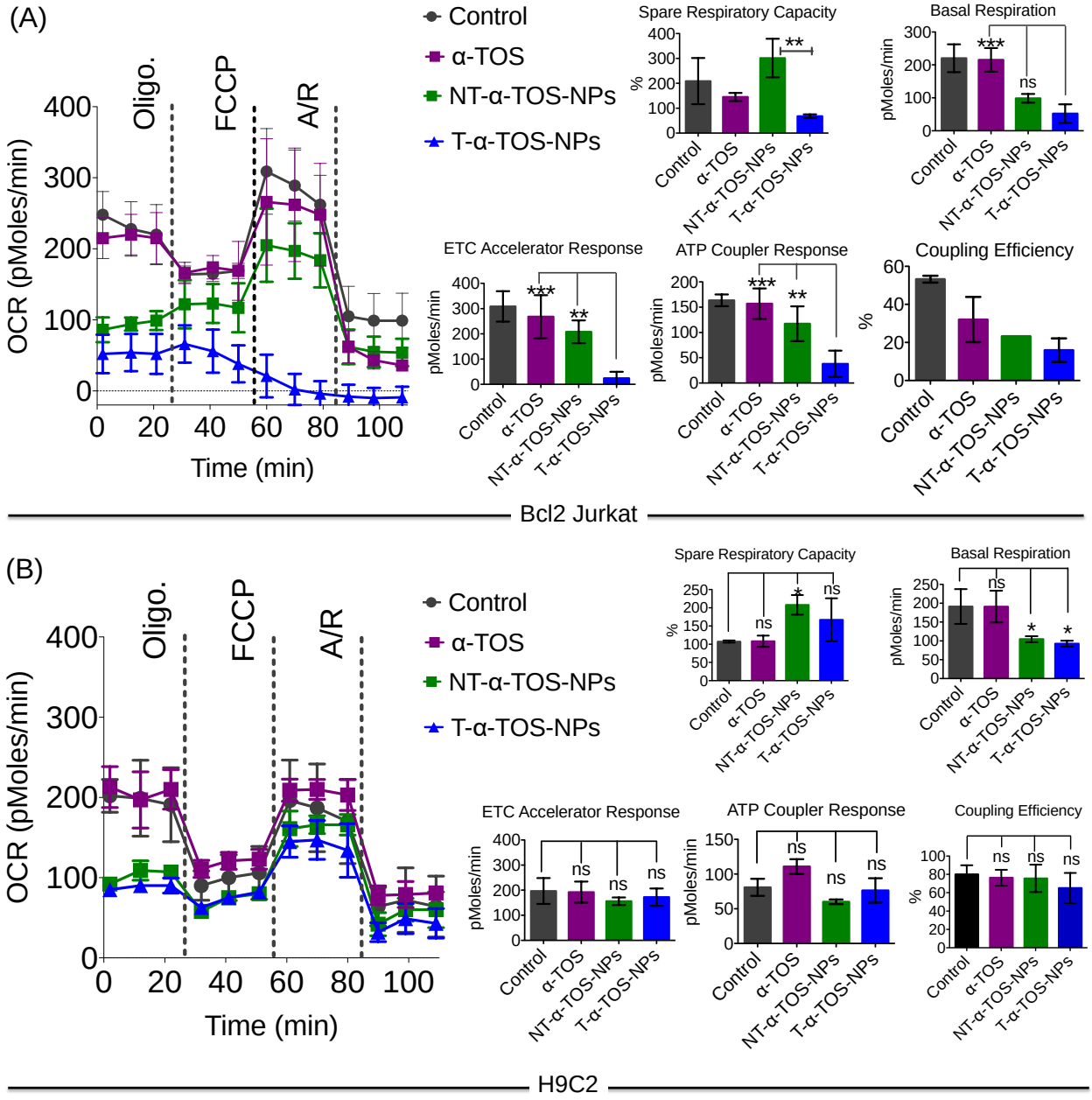

Figure 4.5 Mitochondrial activity of α-TOS, T-α-TOS-NPs, and NT-α-TOS-NPs in (A) Bcl2 Jurkat and (B) H9C2 cells. From these studies, it was found that T-α-TOS-NPs cause stimulation of ATP synthase upon injection of oligomycin only in cancer cells but not in normal cells. ns: non significant. ***P <0.001; **P = 0.001-0.01. A: Antimycin A; R: Rotenone.

At the same α-TOS concentration, after oligomycin injection, the oxygen consumption rates (OCRs) in presence of T-α-TOS-NPs and NT-α-TOS-NPs did not experience reduction

compared to OCR prior to oligomycin addition which, one would predict, is due to ATP synthase inhibition (Figure 4.5). This suggested that when delivered with a NP, α-TOS is either participating in ATP synthase activation or prohibiting oligomycin to inhibit ATP synthase. When FCCP was injected, an increase in OCR was observed for NT-α-TOS-NP treated cells; OCR levels in T-α-TOS-NP treated cells, however, declined indicating that $\Delta\psi m$ was collapsed for this treatment. Compared to free α-TOS, NT-α-TOS-NP treatment had more effects on the mitochondrial respiration of these cells. The injection of a mixture of A and R resulted in shut down of mitochondrial respiration for every group (Figure 4.5A).

In normal H9C2 cells, α-TOS, NT/T-α-TOS-NPs showed similar trends as the control when mitochondrial stress indu cers, oligomycin, FCCP, and A/R were injected (Figure 4.5B). In particular, unlike cancer cells, NT/T-α-TOS-NPs treated H9C2 cells did not experience an increase in OCR when oligomycin was injected. This indicated that the activity of NT/T-α-TOS-NPs on ATP synthase is cancer cell specific.

T-α-TOS-NP-induced activation of the power generator ATP synthase

The observation that T/NT-α-TOS-NPs promote ATP synthase activity either by enhancing its action or by inhibiting oligomycin prompted us to investigate the effects these NPs on ATP synthase. Detailed ATP synthase activity assays were carried out to shed light on this observation. ATP synthase activity was determined using an in vitro assay on isolated bovine heart mitochondria in presence of substrates for ATP synthesis. Mitochondrial ATP synthase activity was monitored by following ATP hydrolysis[22-24]. ATP synthase was exposed to the substrate buffer by solubilizing isolated bovine heart mitochondria. Regeneration of ADP coupled with the oxidative reaction of NADH to NAD+ in the presence of the pyruvate kinase (PK) and lactate dehydrogenase (LDH) were used in this experiment (Figure 4.6A). ATP

synthase activity enhancement was found to be highest when T-α-TOS-NPs were used (Figure 4.6B). There was no significant difference between free α-TOS and the control. When oligomycin was used as an inhibitor of ATP synthase, it was possible to protect activity of this enzyme in the presence of α-TOS or T/NT-α-TOS-NPs (Figure 4.6C). Any possibility of complex formation between oligomycin and α-TOS was ruled out by performing HPLC analyses (ESI Figure S4.4). This study demonstrated that α-TOS does not interact with oligomycin. Thus, α-TOS recovers the ATP synthases activity in a different pathway rather than just reacting with oligomycin. It was possible to recover oligomycin inhibited ATP synthase activity by either free α-TOS or T/NT-α-TOS-NPs (Figure 4.6C).

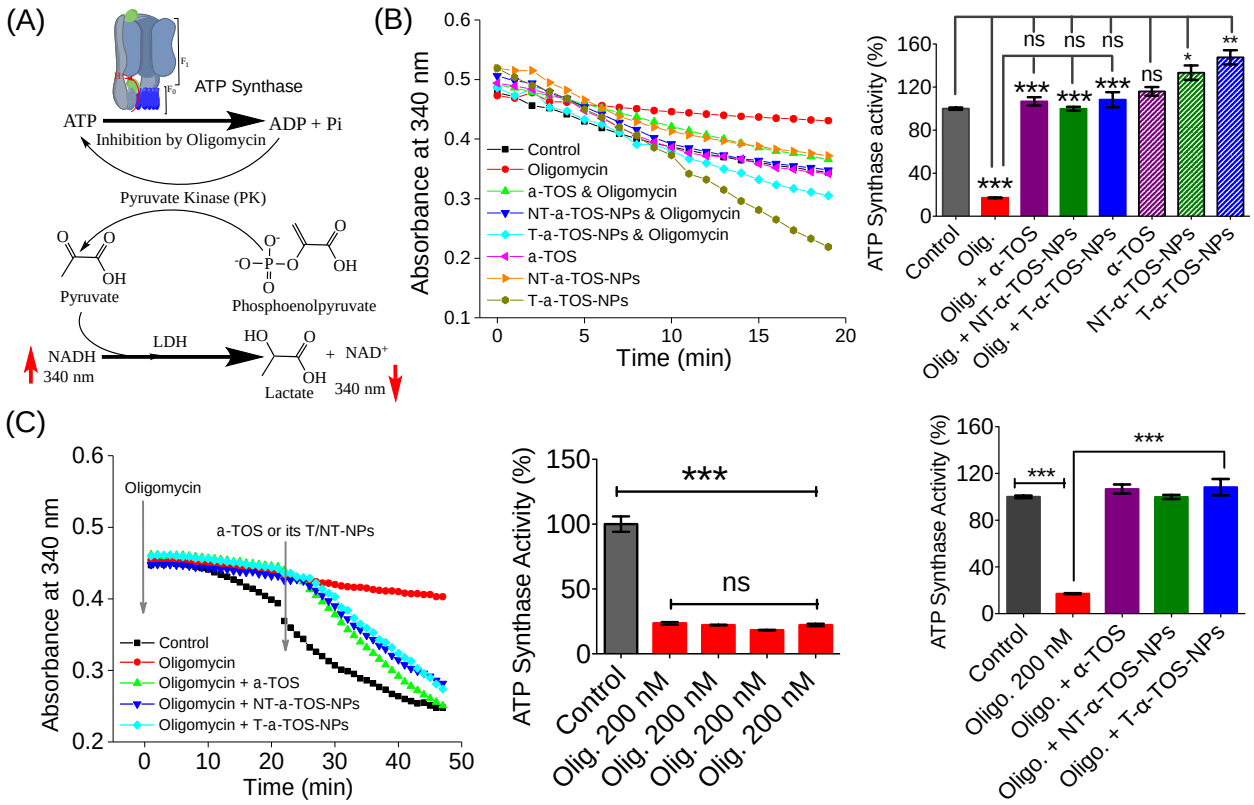

Figure 4.6 (A) Schematic representation of ATP synthase activity used in our experiment. (B) Stimulation of ATP synthase activity by *α*-TOS, T-*α*-TOS-NPs, and NT-*α*-TOS-NPs in the presence or absence of ATP synthase inhibitor oligomycin. (C) Recovery of oligomycin inhibited ATP synthase activity by *α*-TOS or T/NT-*α*-TOS-NPs. ns: non-significant. ****P* <0.001; ***P* = 0.001-0.01.

We further investigated whether this ATP synthase activation can be recycled; first by addition of oligomycin or T-α-TOS-NPs, then T-α-TOS-NPs or oligomycin, and then oligomycin or T-α-TOS-NPs. In this fashion, it was possible to modulate ATP synthase activities (Figure 4.7). It was possible for T-α-TOS-NP to recycle ATP synthase activity. ATP synthase recycling activity was also observed with α-TOS and NT-α-TOS-NPs (Figure 4.7A and 4.7B) in presence of oligomycin. However, the extent of ATP synthase activation was less for α-TOS or NT-α-TOS-NPs in contrast to T-α-TOS-NPs. We believe that the enhanced ATP synthase activation by T-α-TOS-NPs is due to close localization of α-TOS in the vicinity of ATP synthase when delivered with a mitochondria targeted NP.

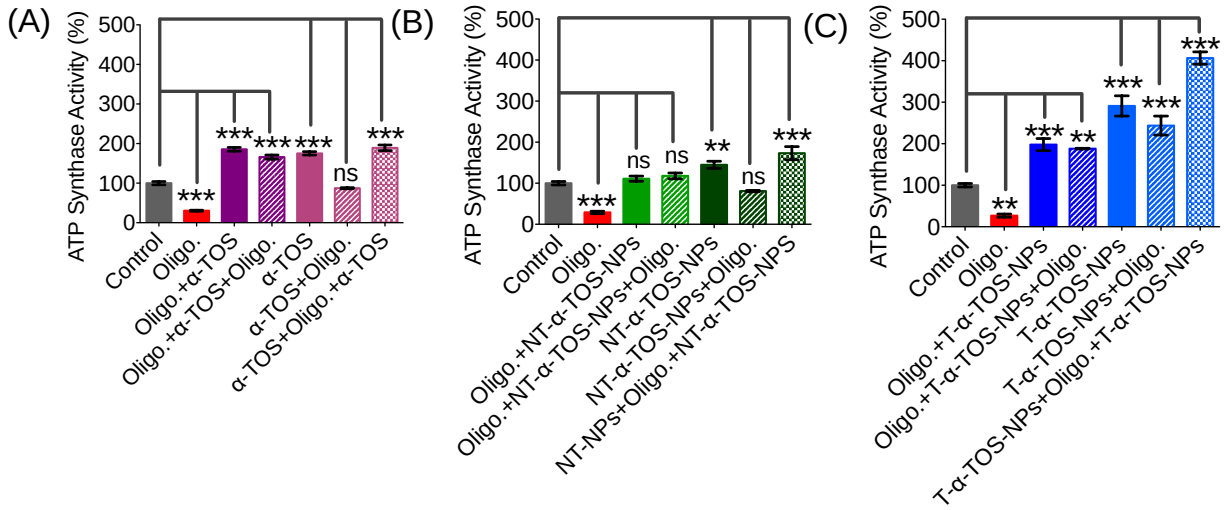

Figure 4.7 Recycled ATP synthase activation by *α*-TOS (A: Left), NT-*α*-TOS-NP (B: Middle), and T-*α*-TOS-NPs (C: Right) in presence of oligomycin. ns: non-significant. ****P* <0.001; ***P* = 0.001-0.01.

ATP and lactate levels in treated cells

The enhanced ATP synthase activity was further confirmed by increased production of ATP in MCF-7 breast cancer cells in the presence of T/NT-α-TOS-NPs; however free α-TOS did not show any significant increase in ATP (Figure 4.8A). This observation further strengthens the claim that T/NT-α-TOS-NP participates in ATP synthase activation. Oligomycin at a concentration of 100 µM did not show inhibition of ATP level in MCF-7 cells. This is most

likely due to the Warburg effect that exists in cancer cells undergoing glycolytic ATP generation[25]. However, there was no significant difference in ATP levels when H9C2 normal cells were treated with α-TOS or T/NT-α-TOS-NPs compared to the control (Figure 4.8A). Oligomycin at a concentration of 25 μM significantly decreased ATP production by H9C2 normal cells (Figure 4.8A).

We then examined whether the activated OXPHOS pathway affected glycolysis in α-TOS or T/NT-α-TOS-NPs treated MCF-7 cells. No significant change in the lactate level was observed when α-TOS or T/NT-α-TOS-NP was used. These results indicated that the T/NT-α-TOS-NP activates ATP synthase activity without affecting the glycolytic pathway (Figure 4.8B).

Cancer cell selective ROS production

Inhibition of mitochondrial respiration chain complexes I and II by α-TOS is well documented[12, 14]. Our current study discovered an additional cellular activity of α-TOS when delivered with a NP formulation. This new pathway uses activation of ATP synthase or complex V. α-TOS is also known to increase Ca^{2+} uptake in the mitochondria[26]. The activity of ATP synthase can be enhanced by intra-mitochondrial Ca^{2+}. This is supported by the fact that when Ca^{2+} blocker, such as ruthenium red, is used, ATP synthase activity can be abolished[27-29]. Further, overload of Ca^{2+} in the mitochondria causes mitochondrial membrane permeability damage and excess ROS production, which eventually leads to apoptotic cell death.[30, 31] ATP synthase mediates efficient execution of apoptosis by ROS generation and down-regulation of ATP synthase is a molecular approach used by cancer cells to escape from ROS related apoptosis[32]. Expression of ATP synthase is known to be suppressed in cancer cells which undergo glycolytic pathway for the energy generation[33]. Up regulated expression of IF1 of ATP synthase is modulated in cancer cells with Warburg phenotype of enhanced aerobic glycolysis[5]. It was also reported that down regulation of ATP synthase activity in colon cancer

cells is observed under chemo-resistance. Thus, activation of ATP synthase provides a strategy to induce cancer cell apoptosis by increasing ROS production.

We conducted ROS production by breast cancer MCF-7 cells in response to α-TOS or T/NT-α-TOS-NPs. These studies indicated that ROS was increased significantly compared to the control cells in presence of α-TOS or its NP formulation. This increase in ROS was more significant for T-α-TOS-NP treated cells (Figure 4.8C). When the same study was conducted in normal H9C2 cardiomyocytes, no enhancement in ROS was observed with α-TOS or its NPs (Figure 4.8C). It is reported that cancer cells is more sensitive to α-TOS and may uptake more α-TOS compared to normal cells[7]. We believe that differences in ROS production in cancer and normal cells is due to less uptake of free α-TOS by normal cells which maintain more alkaline pH favouring deprotonated form of α-TOS and result in less uptake compared to uptake in cancer cells, which have a characteristically acidic cellular milieu. Furthermore, in regards to T-α-TOS-NP, less hydrolysis of α-TOS should occur in normal cells than in cancer cells due to the relative less abundance of esterase.

Previous studies supported that apoptosis of cancer cells by α-TOS is notably via inhibition of complex II. Our findings show contribution of complex V towards α-TOS activity when used a suitably engineered NP. Thus, we investigated the extent of complex V contribution towards enhanced activity of α-TOS when used in a NP platform. We studied the contributions of complex II and V by measuring H_2O_2 release profile from MCF-7 cells. Malonate is reported to inhibit complex II activity towards H_2O_2 production[34], and thus we introduce it to inhibit complex II contribution in the presence of T/NT-α-TOS NPs or free α-TOS. Interestingly, we found that NPs formations of α-TOS (T/NT-α-TOS-NPs) have greater H_2O_2 production attributed to complex V activitycompared to free α-TOS (Figure 4.8D), whereas T-α-TOS-NPs

have the highest inhibition of H2O2 in the absence of malonate, indicating their significant role on complex II inhibition. This indicated that T-α-TOS-NP is most effective in activating complex V.

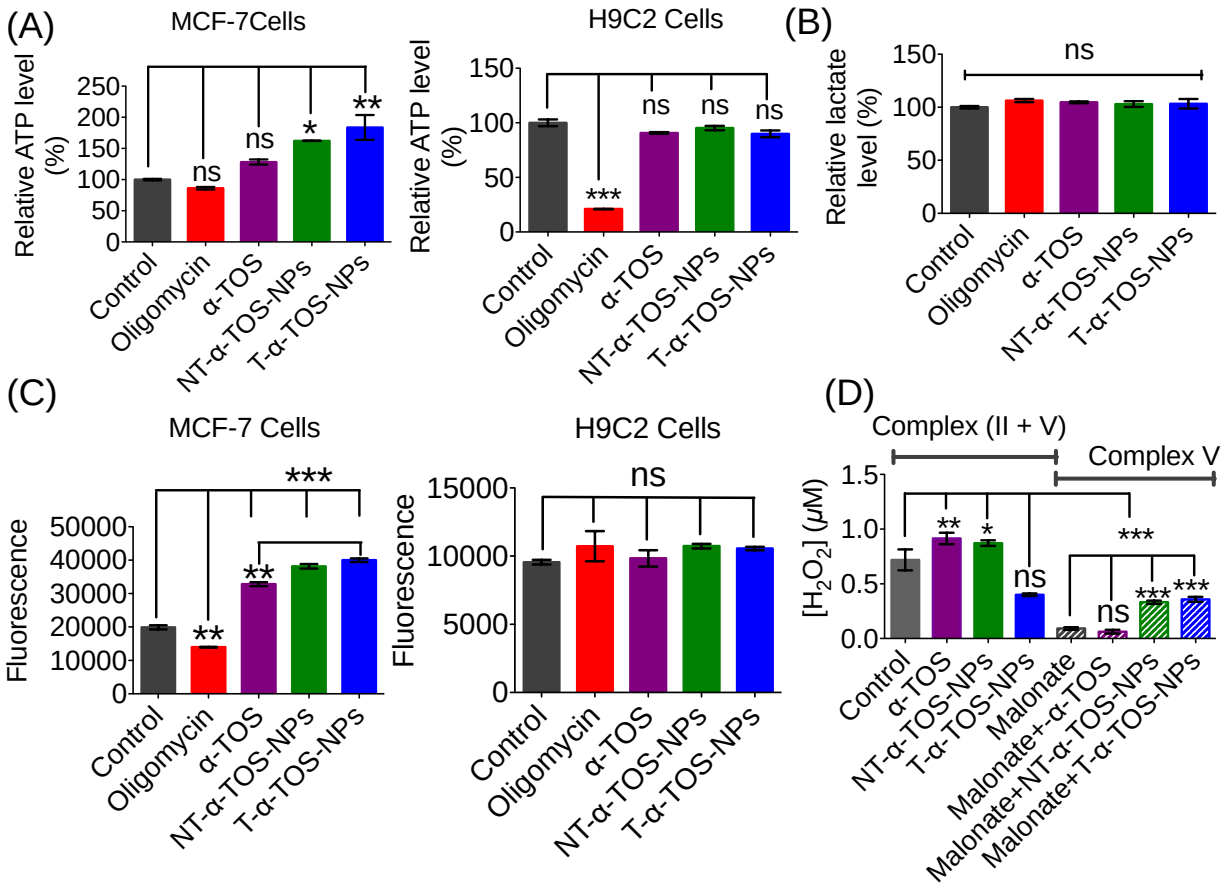

Figure 4.8 (A) Increased production of ATP in MCF-7 breast cancer cells in presence of α-TOS, T-α-TOS-NP, and NT-α-TOS-NP. There was no significant increase in ATP level in normal H9C2 cardiomyocytes in presence of α-TOS, T-α-TOS-NP, and NT-α-TOS-NP. (B) Relative lactate level in MCF-7 cells treated with oligomycin, α-TOS, or T/NT-α-TOS-NP. (C) Increased ROS production in MCF-7 in presence of α-TOS, T-α-TOS-NP, and NT-α-TOS-NP. There was no significant increase in ROS level in normal H9C2 cardiomyocytes in presence of α-TOS, T-α-TOS-NP, and NT-α-TOS-NP. (D) H_2O_2 production in MCF-7 cell by Amplex Red-hydrogen peroxide/peroxidase assay in presence of α-TOS, NT-α-TOS-NPs, or T-α-TOS-NPs (40 μM with respect to α-TOS) without or with 100 mM malonate for 24 h. ns: non-significant. ***P <0.001; **P = 0.001-0.01.

4.4 CONCLUSIONS

Targeted α-TOS-NP was developed to modulate cancer cell function by accessing targets at the mitochondrial membrane. Engineered NP formulations of α-TOS exhibited enhanced

cytotoxicity and mitochondrial activity in cancer cells compared to free α-TOS. The mitochondria-targeted α-TOS NP showed the highest mitochondrial activity related to apoptosis, Bcl2/AIF regulation, and ATP synthase. This was likely due to enhanced apoptosis by ROS generation through increased ATP synthase activity. Therefore, T-α-TOS NP is a promising formulation of vitamin E with abilities to modulate the cellular power generator ATP synthase in cancer cells. T-α-TOS NP may provide a powerful therapeutic tool against solid cancers with down-regulated β subunit of ATP synthase, especially since there is no apparent mechanism of resistance or protection against sudden increases in ROS in these cancer types. Furthermore, application of this formulation of vitamin E has not been thoroughly investigated and should be explored further for new therapeutic gains.

4.5 SUPPORTING INFORMATION

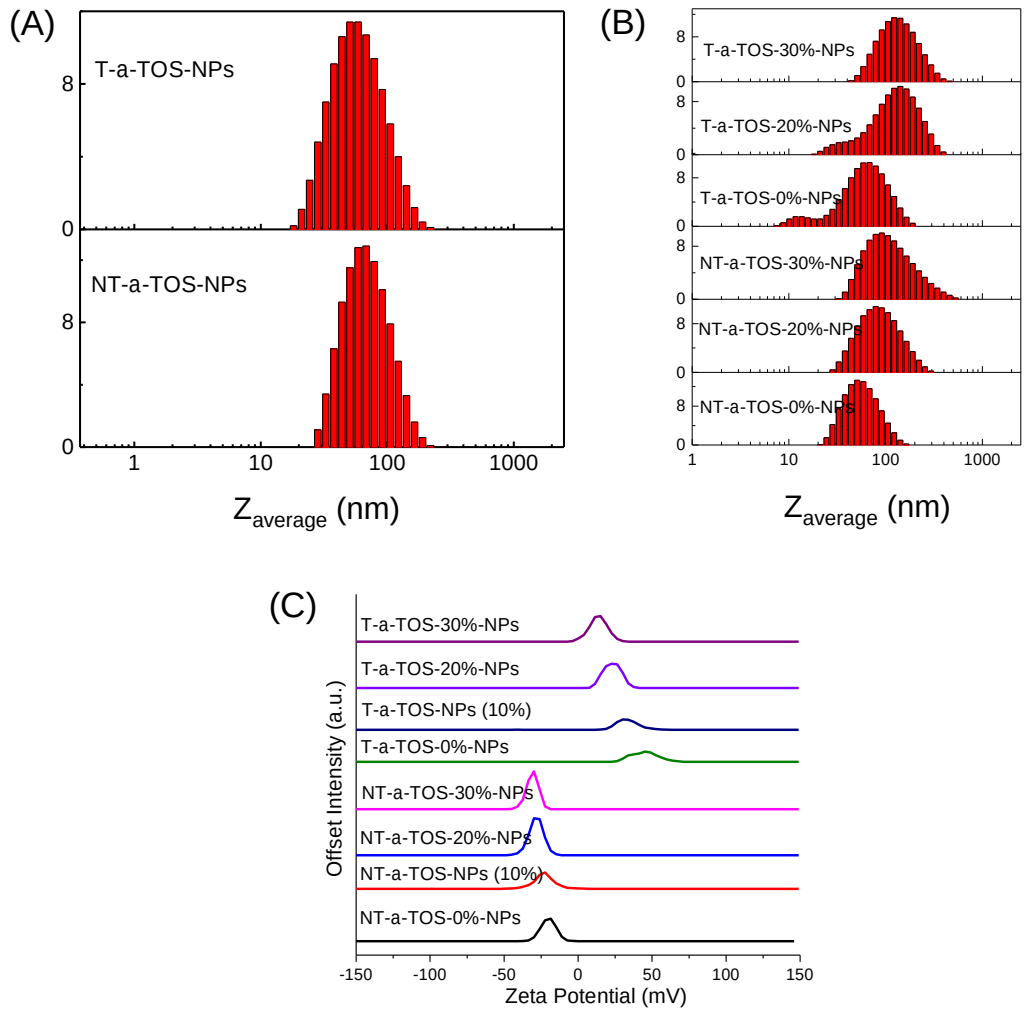

Figure S4.1 (A) Hydrodynamic diameter ($Z_{average}$) of T-α-TOS-NPs and NT-α-TOS-NPs prepared with 10% feed of α-TOS. (B) Hydrodynamic diameter ($Z_{average}$) of T-α-TOS-NPs and NT-α-TOS-NPs prepared with varied feed of α-TOS demonstrating that the NPs with 10% feed have monodisperse population. (C) Zeta potential of T-α-TOS-NPs and NT-α-TOS-NPs prepared with varied feed of α-TOS. T-α-TOS-NPs demonstrated decreased positive surface charge as the percent α-TOS increased and NT-α-TOS-NPs also showed less negatively charged surface as the α-TOS feed was increased.

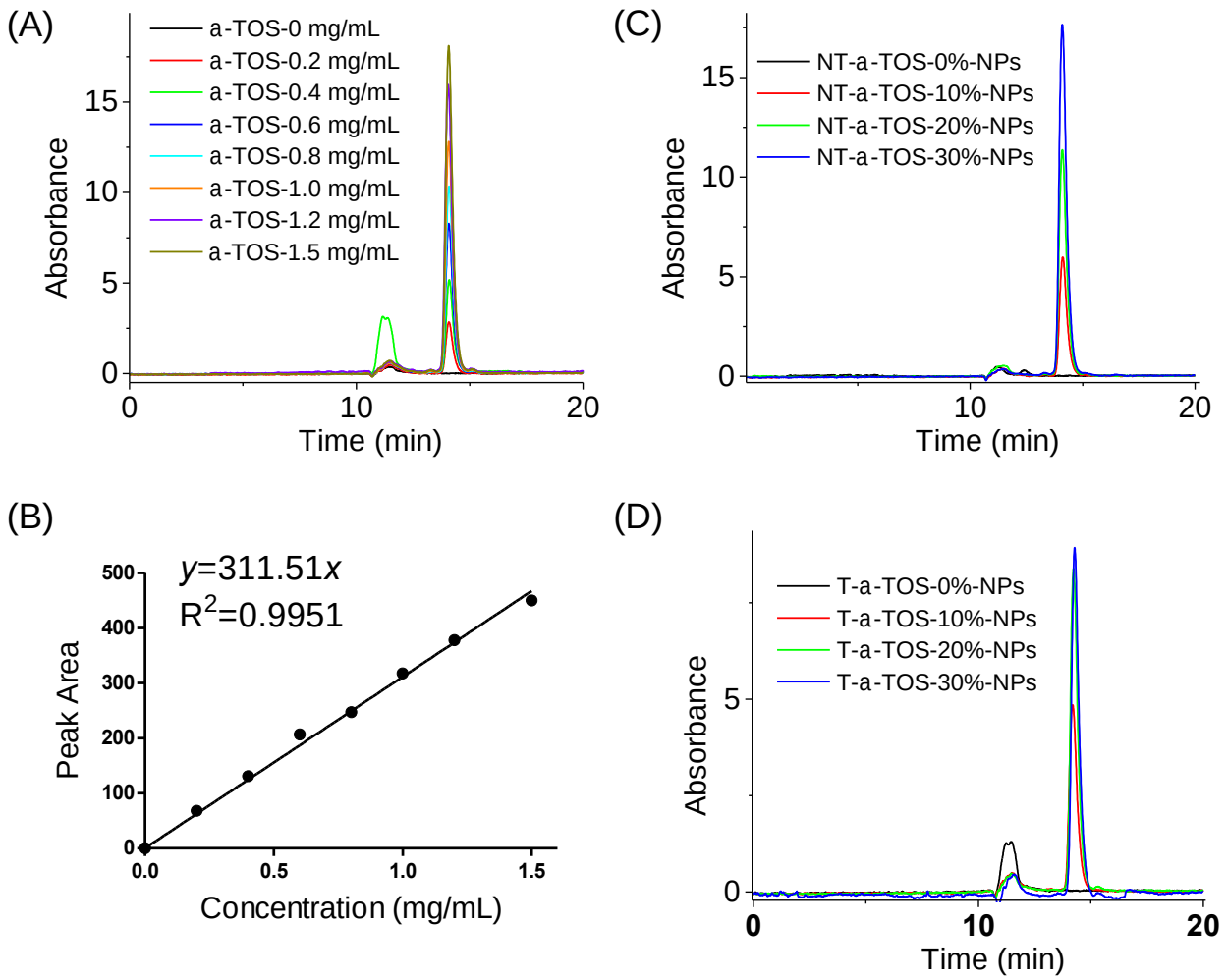

Figure S4.2 (A) Representative high-performance liquid chromatography (HPLC) chromatograms of α-TOS with various concentrations as standard and (B) corresponding calibration curve. Representative HPLC chromatograms of (C) NT-α-TOS-NPs and (D) T-α-TOS-NPs. The peak area with retention time centered at ~14 min was plotted in the calibration curve and the concentration of T/NT-α-TOS-NPs was calculated by using the calibration curve.

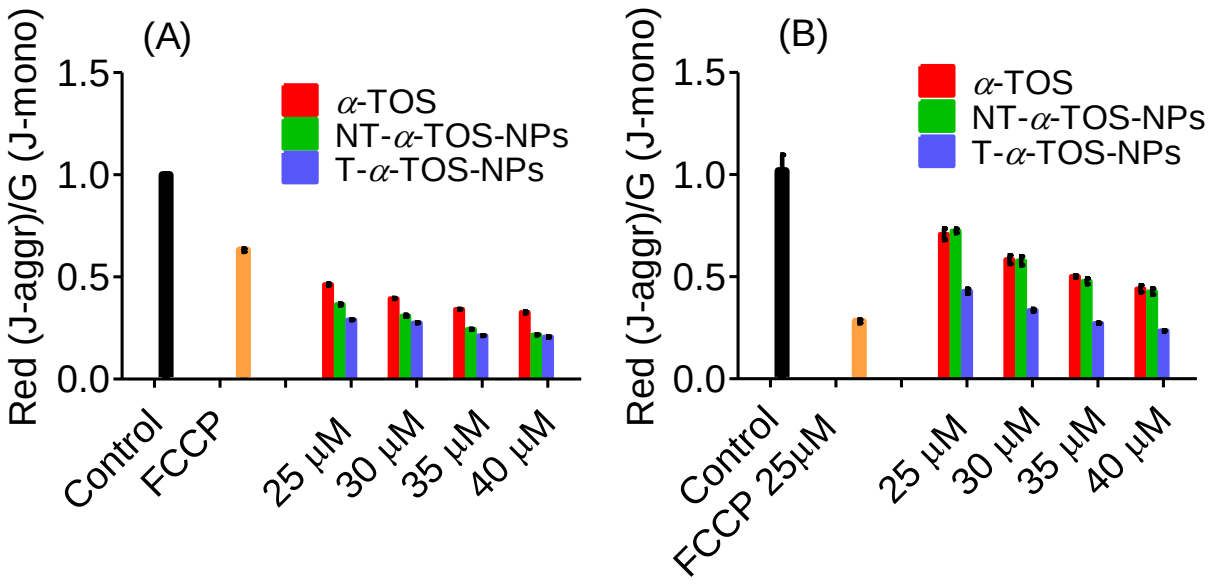

Figure S4.3 Representative JC-1 aggregate to monomer ratio for (A) Bcl2 Jurkat cells (B) Neo Jurkat cells with treatment by α-TOS, T/NT-α-TOS-NPs at varied concentration with respect to α-TOS for mitochondria membrane potential collapse study.

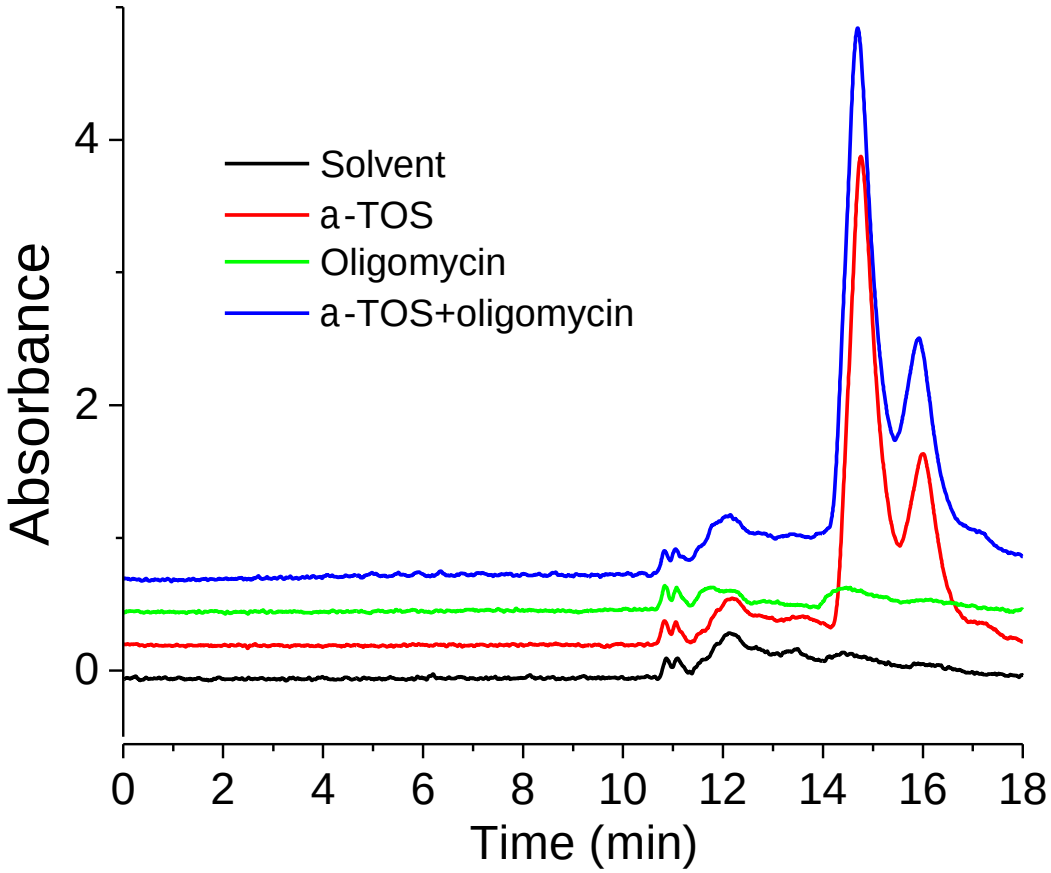

Figure S4.4 Representative HPLC chromatograms of *α*-TOS, oligomycin, *α*-TOS and oligomycin combination ruling out any possibility of complex formation between α-TOS and oligomycin.

4.6 REFERENCES

1. Cuezva, J.M., M. Krajewska, M.L. de Heredia, S. Krajewski, G. Santamaría, H. Kim, J.M. Zapata, H. Marusawa, M. Chamorro, and J.C. Reed, The bioenergetic signature of cancer a marker of tumor progression. Cancer Res, 2002. 62(22): p. 6674-6681.
2. Isidoro, A., M. Martinez, P.L. Fernandez, A.D. Ortega, G. Santamaria, M. Chamorro, J.C. Reed, and J.M. Cuezva, Alteration of the bioenergetic phenotype of mitochondria is a hallmark of breast, gastric, lung and oesophageal cancer. Biochem J, 2004. 378(Pt 1): p. 17-20.
3. Cuezva, J.M., G. Chen, A.M. Alonso, A. Isidoro, D.E. Misek, S.M. Hanash, and D.G. Beer, The bioenergetic signature of lung adenocarcinomas is a molecular marker of cancer diagnosis and prognosis. Carcinogenesis, 2004. 25(7): p. 1157-63.
4. Shin, Y.K., B.C. Yoo, H.J. Chang, E. Jeon, S.H. Hong, M.S. Jung, S.J. Lim, and J.G. Park, Down-regulation of mitochondrial F1F0-ATP synthase in human colon cancer cells with induced 5-fluorouracil resistance. Cancer Res, 2005. 65(8): p. 3162-70.
5. Sánchez-Cenizo, L., L. Formentini, M. Aldea, A.D. Ortega, P. García-Huerta, M. Sánchez-Aragó, and J.M. Cuezva, Up-regulation of the ATPase inhibitory factor 1 (IF1) of the mitochondrial H^+-ATP synthase in human tumors mediates the metabolic shift of cancer cells to a Warburg phenotype. J Biol Chem, 2010. 285(33): p. 25308-25313.
6. López-Ríos, F., M. Sánchez-Aragó, E. García-García, Á.D. Ortega, J.R. Berrendero, F. Pozo-Rodríguez, Á. López-Encuentra, C. Ballestín, and J.M. Cuezva, Loss of the mitochondrial bioenergetic capacity underlies the glucose avidity of carcinomas. Cancer Res, 2007. 67(19): p. 9013-9017.
7. Prasad, K.N., B. Kumar, X.-D. Yan, A.J. Hanson, and W.C. Cole, α-Tocopheryl succinate, the most effective form of vitamin E for adjuvant cancer treatment: a review. J Am Coll Nutr, 2003. 22(2): p. 108-117.
8. Youk, H.-J., E. Lee, M.-K. Choi, Y.-J. Lee, J.H. Chung, S.-H. Kim, C.-H. Lee, and S.-J. Lim, Enhanced anticancer efficacy of α-tocopheryl succinate by conjugation with polyethylene glycol. J Control Rel, 2005. 107(1): p. 43-52.
9. Neuzil, J., I. Svensson, T. Weber, C. Weber, and U.T. Brunk, α-Tocopheryl succinate-induced apoptosis in Jurkat T cells involves caspase-3 activation, and both lysosomal and mitochondrial destabilisation. FEBS Lett., 1999. 445(2): p. 295-300.
10. Shiau, C.-W., J.-W. Huang, D.-S. Wang, J.-R. Weng, C.-C. Yang, C.-H. Lin, C. Li, and C.-S. Chen, α-Tocopheryl succinate induces apoptosis in prostate cancer cells in part through inhibition of Bcl-xL/Bcl-2 function. J Biol Chem, 2006. 281(17): p. 11819-11825.
11. Weber, T., H. Dalen, L. Andera, A. Nègre-Salvayre, N. Augé, M. Sticha, A. Lloret, A. Terman, P.K. Witting, and M. Higuchi, Mitochondria play a central role in apoptosis induced by α-tocopheryl succinate, an agent with antineoplastic activity: comparison with receptor-mediated pro-apoptotic signaling. Biochemistry, 2003. 42(14): p. 4277-4291.
12. Dos Santos, G., R.A. e Lima, C. Pestana, A. Lima, P. Scheucher, C. Thomé, H. Gimenes-Teixeira, B. Santana-Lemos, A. Lucena-Araujo, and F. Rodrigues, α-Tocopheryl succinate inhibits the mitochondrial respiratory chain complex I and is as effective as arsenic trioxide or ATRA against acute promyelocytic leukemia in vivo. Leukemia, 2012. 26(3): p. 451-460.

13. Dong, L.-F., V.J. Jameson, D. Tilly, J. Cerny, E. Mahdavian, A. Marín-Hernández, L. Hernández-Esquivel, S. Rodríguez-Enríquez, J. Stursa, and P.K. Witting, Mitochondrial targeting of vitamin E succinate enhances its pro-apoptotic and anti-cancer activity via mitochondrial complex II. J Biol Chem, 2011. 286(5): p. 3717-3728.
14. Dong, L.-F., P. Low, J.C. Dyason, X.-F. Wang, L. Prochazka, P.K. Witting, R. Freeman, E. Swettenham, K. Valis, and J. Liu, α-Tocopheryl succinate induces apoptosis by targeting ubiquinone-binding sites in mitochondrial respiratory complex II. Oncogene, 2008. 27(31): p. 4324-4335.
15. Dong, L.-F., V.J. Jameson, D. Tilly, L. Prochazka, J. Rohlena, K. Valis, J. Truksa, R. Zobalova, E. Mahdavian, and K. Kluckova, Mitochondrial targeting of α-tocopheryl succinate enhances its pro-apoptotic efficacy: a new paradigm for effective cancer therapy. Free Radic Biol Med, 2011. 50(11): p. 1546-1555.
16. Rohlena, J., L.-F. Dong, K. Kluckova, R. Zobalova, J. Goodwin, D. Tilly, J. Stursa, A. Pecinova, A. Philimonenko, and P. Hozak, Mitochondrially targeted α-tocopheryl succinate is antiangiogenic: potential benefit against tumor angiogenesis but caution against wound healing. Antioxid Redox Signal, 2011. 15(12): p. 2923-2935.
17. Cuezva, J.M., M. Krajewska, M.L. de Heredia, S. Krajewski, G. Santamaria, H. Kim, J.M. Zapata, H. Marusawa, M. Chamorro, and J.C. Reed, The bioenergetic signature of cancer: a marker of tumor progression. Cancer Res, 2002. 62(22): p. 6674-81.
18. Marrache, S. and S. Dhar, Engineering of blended nanoparticle platform for delivery of mitochondria-acting therapeutics. Proc Natl Acad Sci, 2012. 109(40): p. 16288-16293.
19. Hockenbery, D.M., Z.N. Oltvai, X.-M. Yin, C.L. Milliman, and S.J. Korsmeyer, Bcl-2 functions in an antioxidant pathway to prevent apoptosis. Cell, 1993. 75(2): p. 241-251.
20. Yang, J., X. Liu, K. Bhalla, C.N. Kim, A.M. Ibrado, J. Cai, T.-I. Peng, D.P. Jones, and X. Wang, Prevention of Apoptosis by Bcl-2: Release of Cytochrome c from Mitochondria Blocked. Science, 1997. 275(5303): p. 1129-1132.
21. Candé, C., I. Cohen, E. Daugas, L. Ravagnan, N. Larochette, N. Zamzami, and G. Kroemer, Apoptosis-inducing factor (AIF): a novel caspase-independent death effector released from mitochondria. Biochimie, 2002. 84(2–3): p. 215-222.
22. McEnery, M.W. and P. Pedersen, Diethylstilbestrol. A novel F_0-directed probe of the mitochondrial proton ATPase. J Biol Chem, 1986. 261(4): p. 1745-1752.
23. Bosetti, F., G. Yu, R. Zucchi, S. Ronca-Testoni, and G. Solaini, Myocardial ischemic preconditioning and mitochondrial F_1F_0-ATPase activity. Mol Cell Biochem, 2000. 215(1): p. 31-38.
24. Zheng, J. and V.D. Ramirez, Rapid inhibition of rat brain mitochondrial proton F_0F_1-ATPase activity by estrogens: comparison with Na^+, K^+-ATPase of porcine cortex. Eur J Pharmacol, 1999. 368(1): p. 95-102.
25. Gatenby, R.A. and R.J. Gillies, Why do cancers have high aerobic glycolysis? Nat Rev Cancer, 2004. 4(11): p. 891-899.
26. Gogvadze, V., E. Norberg, S. Orrenius, and B. Zhivotovsky, Involvement of Ca^{2+} and ROS in α-tocopheryl succinate-induced mitochondrial permeabilization. Int J Cancer, 2010. 127(8): p. 1823-1832.
27. Das, A.M. and D.A. Harris, Control of mitochondrial ATP synthase in rat cardiomyocytes: effects of thyroid hormone. BBA-Mol Basis Dis, 1991. 1096(4): p. 284-290.

28. Das, A.M. and D.A. Harris, Control of mitochondrial ATP synthase in heart cells: inactive to active transitions caused by beating or positive inotropic agents. Cardiovasc Res, 1990. 24(5): p. 411-417.
29. Territo, P.R., V.K. Mootha, S.A. French, and R.S. Balaban, Ca^{2+} activation of heart mitochondrial oxidative phosphorylation: role of the F_0/F_1-ATPase. Am J Physiol 2000. 278(2): p. C423-C435.
30. Adam-Vizi, V. and A.A. Starkov, Calcium and mitochondrial reactive oxygen species generation: how to read the facts. J Alzheimers Dis, 2010. 20(Suppl 2): p. S413.
31. Votyakova, T.V. and I.J. Reynolds, Ca^{2+} induced permeabilization promotes free radical release from rat brain mitochondria with partially inhibited complex I. J Neurosci, 2005. 93(3): p. 526-537.
32. Santamaría, G., M. Martínez-Diez, I. Fabregat, and J.M. Cuezva, Efficient execution of cell death in non-glycolytic cells requires the generation of ROS controlled by the activity of mitochondrial H^+-ATP synthase. Carcinogenesis, 2006. 27(5): p. 925-935.
33. Cuezva, J.M., M. Sánchez-Aragó, S. Sala, A. Blanco-Rivero, and Á.D. Ortega, A message emerging from development: the repression of mitochondrial β-F_1-ATPase expression in cancer. J Bioenerg Biomembr, 2007. 39(3): p. 259-265.
34. Siebels, I. and S. Drose, Q-site inhibitor induced ROS production of mitochondrial complex II is attenuated by TCA cycle dicarboxylates. Biochim Biophys Acta, 2013. 1827(10): p. 1156-64.

5. CONCLUSIONS AND PERSPECTIVES

Exosomes are secreted by almost all type of cells through various pathways such as ESCRT pathway, lipid-raft regulation, syntenin-syndecan interaction, and Rab family protein modulation. The exosomes could be taken up by recipient cells through several pathways including endocytosis, membrane fusion, micropinocytosis and phagocytosis, depending on the type of exosome origin and recipient cells. However, mechanisms of exosomes secretion and exosome-cell interactions are not yet fully understood, and extensive investigations are needed to reveal the exosome cargos (e.g., proteins and RNAs) sorting mechanism and their translocation into distant sites. Some types of compositions are highly expressed in tumor derived exosomes and thus may be used as potential biomarkers for cancer detection and diagnosis.

Protein acylation modulates the protein sorting pathway into exosomes in a manner that myristoylation promotes the oncogenic Src kinase incorporation into exosomes. The gain of myristoylation site only by removing palmitoylated site in Fyn kinase significantly increased its accumulation into exosomes, and cells transfected by Src(G2A) mutant depleting myristoylation reduced the Src kinase secretion into exosomes. Mechanistic investigations suggest that ESCRT pathway, but not lipid-raft pathway was involved in the sorting of Src kinase into exosomes, and knockdown of TSG101 by shRNA transfection inhibited Src kinase incorporation into exosomes. The activity of Src mediate the syntenin trafficking and secretion into exosomes. *In vivo* mouse studies demonstrate that myristoylation remarkably enhanced Src encapsulation and circulation in serum exosomes, which potentiates Src as diagnostic biomarker for prostate cancer. These provide insights by identifying myristoylation as a potential target to block the exosomal transfer

of oncogenic proteins from cell to cell and thus prevent the oncogenic proteins associated mutations/changes.

The detection of myristoylated protein is reported by myristic acid analog 12-azidododecanoic acid (12-ADA) for fluorescent imaging *in vitro* and zebrafish model[1], and we have also confirmed the myristoylated protein *in vitro*. However, there is still not yet report on the detection of myristoylated protein *in vivo* mice model. Further studies are necessary to evaluate myristoylated protein *in vivo* and thus will benefit the subsequent investigation of therapeutic intervention and diagnostic biomarker for cancer.

The oncogenic Src proteins could be translocated into healthy fibroblasts causing pathological signaling through exosomes when fibroblast cells were treated with active form of Src(Y529F) derived tumor cell exosomes. Further intensive studies are necessary to answer (1) what is mechanism of tumor derived exosomal Src kinase induces pathological changes of healthy cells? (2) What factors would influence the uptake of tumor exosomes enriched with Src kinase into healthy cells? (3) Is oncogenic proteins inducing pathological signaling/mutation to other type of normal cells such as B and T immune cells, or does myristoylation play any role in this process? The removal of myristoylation may prevent pathological mutation of neighboring and/or distant healthy cells when blocking the Src protein accumulation into exosomes and thus prevent cancer cascade pathologies of healthy tissues/cells. Exosome derived from chronic myeloid leukemia cells is reported to induce the angiogenesis by Src-mediated activating downstream signaling[2], and future direction may focus on the role of myristoylation in promoting tumorigenesis/angiogenesis by upregulating the Src kinase expression through exosome communication.

Exosomes are critical in cellular crosstalk or communication. Besides Src kinase protein, other components such as RNA in the exosomes may also be important for the cellular function and communication. Several studies have been made on mechanistic pathways of exosome RNA regulating the cancer cellular function. Stromal cells interacts with cancer cells through transferring RNA and noncoding transcripts/transposable segments via exosomes to activate STAT1-mediated antiviral signaling and NOTCH3 pathway when inducing recognition receptor RIG-I, eventually generating resistance to chemotherapeutics[3]. Tumor-derived exosomes can transfer activated epidermal growth factor receptor (EGFR) to macrophages and inhibit innate immunity by reducing type I interferons[4]. Despite these efforts, there still needs extensive studies to reveal the mechanism of cell-cell interaction or communication by using exosome tools. Various types of exosome parent cells or recipient cells may affect the cellular uptake of exosomes differently due to the unique properties of exosomes and cells. In addition to EGFR, other oncogenic proteins such as Ras may also influence the immune cells such as T cells, and future studies may focus on this direction to fully understand the role of tumor-derived exosomes in immune systems.

Fibroblast growth factor (FGF) participates in various cellular processes including stemness, proliferation, and angiogenesis through binding to FGF receptors (FGFRs) for transducing signals[5]. FGFRs have been associated with several types of cancer regarding mutations, splicing, and gene amplification[6]. FGFR2 plays pivotal role in cellular survival and growth in gastric cancer[7]. We conducted a preliminary study of FGFR2 by using three gastric cell lines (AGS, SNU 16 and KATA III cells). The FGFR2 was detected in exosomes derived from both SNU 16 and KATO III cells (Figure 5.1A) but not from AGS, which did not express FGFR2 in the cell. Cell viability assay indicates that all three kinds of cancer cell exosomes were toxic to

fibroblast NIH/3T3 cells, and AGS cell-derived exosomes were the most lethal to fibroblast with IC50 of 0.3 μg/mL compared to KATO III exosomes (IC50=0.7 μg/mL) and SNU 16 (IC50=2.2 μg/mL) (Figure 5.1B). The internalization of exosomes to fibroblasts was confirmed by appearance of green fluorescence (Figure 5.1C). The mechanism of how these various types of exosomes have different effects on fibroblasts are not yet cleared. Given that EGFR2 expression level in the exosomes was the highest in KATO III, the EGFR2 would not be the main factor that is related to the toxicity of exosomes to fibroblast. The expression of miRNA level may be responsible, and more studies are required to validate this assumption and identify specific miRNA.

These limited preliminary data show that FGFR2 could be encapsulated into the exosomes and may affect the cellular processes through exosomes communication from cell to cell. However, more studies are required to reveal the translocation of FGFR2 from tumor cells to normal cells by exosomes and the mechanisms of how gastric cancer exosomes inhibit the growth and survival of normal recipient cells. Exosomes possess the capabilities to alter cellular function in normal cells. While more studies are needed to understand and ultimately reverse the effect of cancer exosomes on normal cells. The use of nanoparticles for altering cancer cellular function and metabolism provides a much needed starting point for potential therapeutics that reverse the effect of cancer exosomes.

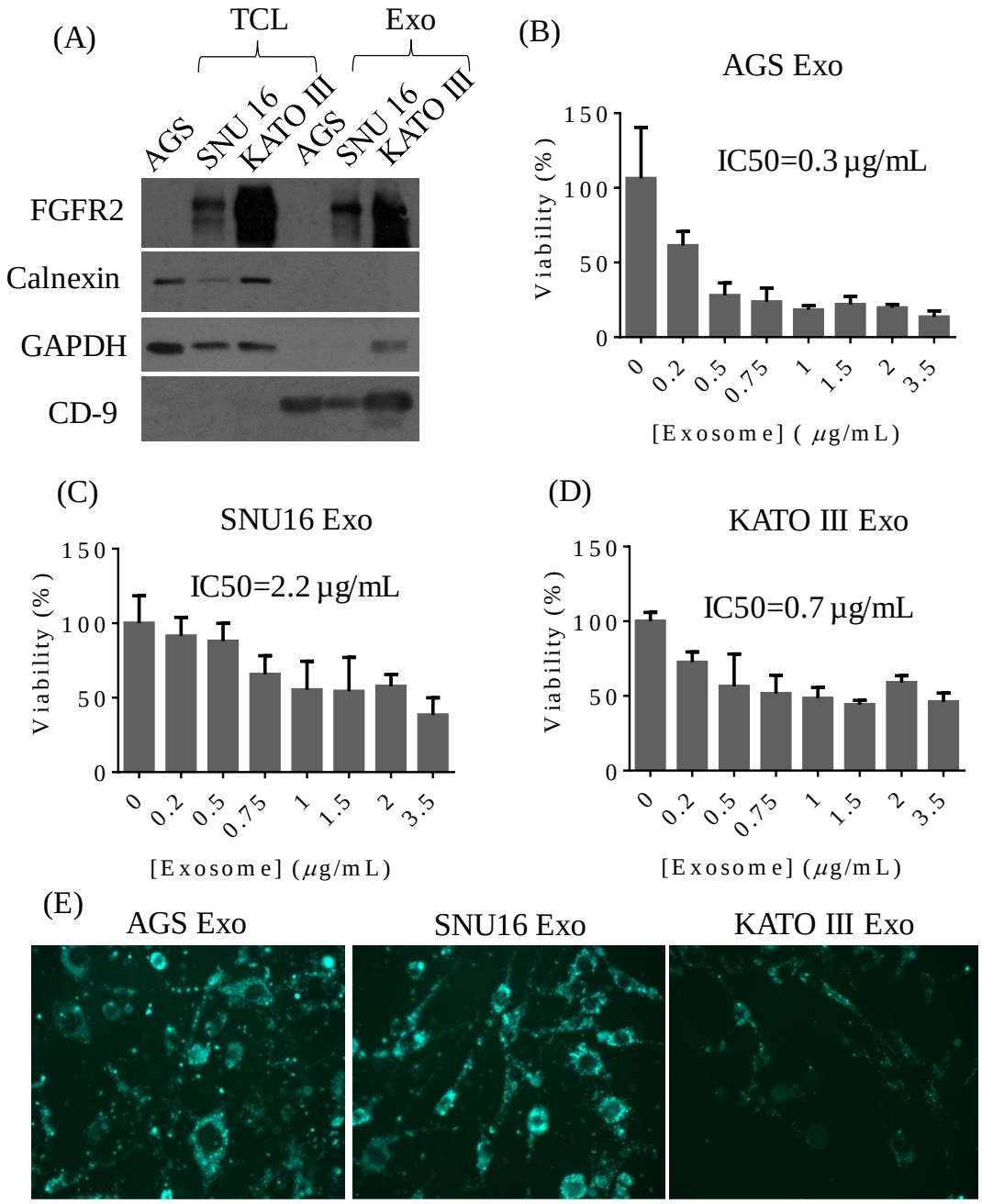

Figure 5.1 (A) Immunoblotting analysis of expression levels of EGFR, calnexin, GAPDH, and CD-9 in AGS, SNU16, KATO III total cell lysates (TCL) and exosomes (Exo) collected from cell culture medium by ultracentrifuge method. NIH 3T3 cells were plated in 96-well plate and various concentrations of exosomes prepared by ultracentrifugation of cell culture medium derived from (B) AGS (C) SNU16 (D) KAT III, was added into the NIH 3T3 cells and incubated for 72 h. The cell viability was evaluated by MTT assay. (E) Cellular uptake of exosomes derived from AGS, SUN16, KATO III cells determined by fluorescence microscope. The exosomes were labelled with PKH67 green fluorescence marker and added into fibroblast NIH 3T3 cells for 24 h incubation.

The α-TOS-loaded polymeric nanoparticles were constructed to modulate cancer cell function through mitochondria-mediated apoptotic machinery. Nanoparticle formulations with α-TOS showed enhanced cytotoxicity and mitochondrial activity in various cancer cells compared to free α-TOS compound. The α-TOS nanoparticles were much more toxic to cancer cells over normal cells, suggesting the potential of therapeutic intervention when using a concentration with normal cells remaining intact. The mitochondria-targeted α-TOS polymeric nanoparticles showed the highest mitochondrial toxicity and activity as evidenced by mitochondria membrane potential collapse, apoptosis, Bcl2/AIF inhibition, and activated complex V activity. The significantly enhanced apoptosis by targeted nanoparticles was stimulated by increased ROS produced through upregulated ATP synthase activity. Hence, α-TOS nanoparticle is a promising approach to modulate the cellular power generator ATP synthase in cancer cells. *In vivo* studies are needed to explore the therapeutic efficacy and molecular mechanistic pathways of complex V activity. Currently, there is no apparent mechanism of resistance or protection against sudden increases in ROS in solid tumors, targeted α-TOS nanoparticle may be a powerful therapeutic tool against solid cancers by downregulating ATP synthase activity. The identification of novel complex V mediated mechanism suggests a potential role of nanoparticle vector to investigate the cellular function of compounds/drugs of their therapeutic intervention in cancer.

5.1 REFERENCES

1. Witten, A.J., K.F. Ejendal, L.M. Gengelbach, M.A. Traore, X. Wang, D.M. Umulis, S. Calve, and T.L. Kinzer-Ursem, Fluorescent imaging of protein myristoylation during cellular differentiation and development. J Lipid Res, 2017. 58(10): p. 2061-2070.
2. Mineo, M., S.H. Garfield, S. Taverna, A. Flugy, G. De Leo, R. Alessandro, and E.C. Kohn, Exosomes released by K562 chronic myeloid leukemia cells promote angiogenesis in a Src-dependent fashion. Angiogenesis, 2012. 15(1): p. 33-45.
3. Boelens, M.C., T.J. Wu, B.Y. Nabet, B. Xu, Y. Qiu, T. Yoon, D.J. Azzam, C. Twyman-Saint Victor, B.Z. Wiemann, and H. Ishwaran, Exosome transfer from stromal to breast cancer cells regulates therapy resistance pathways. Cell, 2014. 159(3): p. 499-513.
4. Gao, L., L. Wang, T. Dai, K. Jin, Z. Zhang, S. Wang, F. Xie, P. Fang, B. Yang, and H. Huang, Tumor-derived exosomes antagonize innate antiviral immunity. Nat Immunol, 2018: p. 1.
5. Katoh, M. and H. Nakagama, FGF receptors: cancer biology and therapeutics. Med Res Rev, 2014. 34(2): p. 280-300.
6. Touat, M., E. Ileana, S. Postel-Vinay, F. André, and J.-C. Soria, Targeting FGFR signaling in cancer. Clin Cancer Res, 2015. 21(12): p. 2684-2694.
7. Kunii, K., L. Davis, J. Gorenstein, H. Hatch, M. Yashiro, A. Di Bacco, C. Elbi, and B. Lutterbach, FGFR2-amplified gastric cancer cell lines require FGFR2 and Erbb3 signaling for growth and survival. Cancer Res, 2008. 68(7): p. 2340-2348.